Jean P. Ometto
Rostyslav Bun
Matthias Jonas
Zbigniew Nahorski
Editors

Uncertainties in Greenhouse Gas Inventories

Expanding Our Perspective

Springer

Uncertainties in Greenhouse Gas Inventories

Jean P. Ometto • Rostyslav Bun • Matthias Jonas
Zbigniew Nahorski
Editors

Uncertainties in Greenhouse Gas Inventories

Expanding Our Perspective

Previously published in *Climatic Change*
Volume 124, issue 3, 2014
Special Issue: Third International Workshop on
Uncertainty in Greenhouse Gas Inventories

Springer

Editors
Jean P. Ometto
Earth System Science Center
National Institute for Space Research
São José dos Campos
São Paulo, Brazil

Matthias Jonas
Advanced Systems Analysis
International Institute for Applied Systems Analysis
Laxenbourg, Austria

Rostyslav Bun
Department of Applied Mathematics
Lviv Polytechnic National University
Lviv, Ukraine

Zbigniew Nahorski
Systems Research Institute
Polish Academy of Sciences
Warszawa, Poland

ISBN 978-3-319-15900-3 ISBN 978-3-319-15901-0 (eBook)
DOI 10.1007/978-3-319-15901-0

Library of Congress Control Number: 2015936604

Springer Cham Heidelberg New York Dordrecht London
© Springer International Publishing Switzerland 2015
This work is subject to copyright. All rights are reserved by the Publisher, whether the whole or part of the material is concerned, specifically the rights of translation, reprinting, reuse of illustrations, recitation, broadcasting, reproduction on microfilms or in any other physical way, and transmission or information storage and retrieval, electronic adaptation, computer software, or by similar or dissimilar methodology now known or hereafter developed.
The use of general descriptive names, registered names, trademarks, service marks, etc. in this publication does not imply, even in the absence of a specific statement, that such names are exempt from the relevant protective laws and regulations and therefore free for general use.
The publisher, the authors and the editors are safe to assume that the advice and information in this book are believed to be true and accurate at the date of publication. Neither the publisher nor the authors or the editors give a warranty, express or implied, with respect to the material contained herein or for any errors or omissions that may have been made.

Printed on acid-free paper

Springer International Publishing AG Switzerland is part of Springer Science+Business Media (www.springer.com)

Preface

This book has been written to enhance understanding of the uncertainty encountered in estimating greenhouse gas (GHG) emissions and in dealing with the challenges resulting from those estimates. Such challenges include, but are not limited to i) monitoring emissions; ii) adhering to emission commitments; iii) securing the proper functioning of emission trading markets; and iv) meeting low-carbon or low-GHG futures in the long term.

The title of the book, *Uncertainties in Greenhouse Gas Inventories: Expanding Our Perspective*, indicates that researching uncertainty is not a quick exercise but involves a fairly painstaking long-term commitment. Moreover, proper treatment of uncertainty is costly in terms of both time and effort because it forces us to make the step from "simple" to "complex" in order to grasp a wider and more holistic systems view and, only after that, to discuss any simplifications that may be warranted.

This book is a reprint of the 2014 Special Issue 124(3) of *Climatic Change*. Like its predecessors, it is intended for readers who prefer hardcover books to the paperback format of special journal issues. It brings together 16 key papers presented at, or produced subsequent to, the 2010 (3rd) International Workshop on Uncertainty in Greenhouse Gas Inventories. The Workshop was jointly organized by the Lviv Polytechnic National University (http://www.lp.edu.ua/en), Ukraine; the Systems Research Institute of the Polish Academy of Sciences (http://www.ibspan.waw.pl/glowna/en); and the International Institute for Applied Systems Analysis (http://www.iiasa.ac.at/), Austria.

This book follows on from *Accounting for Climate Change: Uncertainty in Greenhouse Gas Inventories – Verification, Compliance, and Trading* (Lieberman et al. 2007); and *Greenhouse Gas Inventories: Dealing with Uncertainty* (White et al. 2011), two books that reflect the outcome of the 2004 (1st) and 2007 (2nd) Workshops on Uncertainty in Greenhouse Gas Inventories held in Poland and Austria, respectively.

The issues of concern at the 3rd Uncertainty Workshop continue to be rooted in the level of confidence with which national emission inventories can be performed. They also go beyond this, bringing new approaches, as explained below. The topics addressed by the 16 key papers in this book follow a structure based on the Workshop sessions:

- *Introduction* (written in retrospect): see paper by Ometto et al. 2014a
- *General & Policy*: see papers by Jonas et al. 2014; Rafaj et al. 2013; Lesiv et al. 2014; and Hryniewicz et al. 2014
- *Energy*: see paper by Uvarova et al. 2014;
- *Land Use, Land-Use Change, and Forestry*: see paper by Ometto et al. 2014b
- *Spatial Inventories*: see papers by Boychuk and Bun 2014; Horabik and Nahorski 2014; and Verstraete 2014;
- *Non-CO_2 / Waste*: see papers by Joerss 2013;
- *Economy and Climate Change*: see papers by Xu et al. 2014; Ermolieva et al. 2013; Nahorski et al. 2014; Dolgopolova et al. 2014; and Nijnik and Pajot 2014.

Unsurprisingly, the most important take-home message from the 3rd Uncertainty Workshop is that the existing rationale for improving and conducting uncertainty analyses (see Box 1) is still considered to hold true. The alternative, the past policy approach of ignoring inventory uncertainty altogether (inventory uncertainty was monitored, but not regulated, under the Kyoto Protocol) at the country, sector, corporate, or other level, is problematical. Emission reductions are activity- and gas-dependent and can be wide-ranging. Biases (discrepancies between true and reported emissions) are not uniform across space and time and can discredit flux-difference schemes which tacitly assume that biases cancel out. Human impact on nature is not necessarily constant and/or negligible and can jeopardize a partial GHG accounting approach that is not a logical subset of, and safeguarded by, a full GHG accounting approach. Thus, the legitimate concern was, and still is, that policy agreements are trying to tie down a system that, while considered certain, is not truly controlled. Being aware of the uncertainties involved will help to strengthen future political decision making, for example, the UNFCCC negotiations toward a new universal climate agreement in 2015.

This leads to the important question as to the advances made at the 3rd Uncertainty Workshop. Box 2 provides a summary of the status quo of uncertainty research as it unfolded after the 2007 (2nd) Uncertainty Workshop. Six interdependent key insights materialized at the time which, according to experts, would require further attention. These insights center around (abridged)

1. Verification: reconciling bottom-up and top-down GHG emission analyses;
2. Avoiding systemic surprises: distinguishing between subsystems with fundamentally different emission-dynamic and uncertainty characteristics before superimposing them;
3. Making uncertainty analysis a key component of national GHG inventory analysis to support the development of informed policy in the framing of international environmental agreements: providing advanced guidance, beyond the methodologies offered by the IPCC, to ensureuncertainty is dealt with appropriately in an internationally consistent way across countries, subsystems, sources and sinks, GHGs, and sectors;
4. Minimizing the impact of uncertainty to support the design of advanced policy agreements: providing approaches that allow subsystems to be treated individually and differently rather than collectively (in terms of CO_2-equivalence) and equally (not distinguishing between emissions and removals).

5. Full GHG accounting: ensuring that any differentiated approach to accounting forms a logical subset of a full GHG accounting approach;
6. Compliance versus reporting (bifurcation of agreements) but in a complementary manner: providing options that allow for smarter treatment of subsystems, for example, individually and differently, while at the same time following full GHG accounting.

BOX 1 Rationale for improving and conducting uncertainty analyses. Source: White et al. (2011: 3–18)

- Calculations of greenhouse gas (GHG) emissions contain uncertainty for a variety of reasons such as the lack of availability of sufficient and appropriate data and the techniques for processing them.
- Understanding the basic science of GHG gas sources and sinks requires an understanding of the uncertainty in their estimates.
- Schemes to reduce human-induced global climate impact rely on confidence that inventories of GHG emissions allow the accurate assessment of emissions and emission changes. To ensure such confidence, it is vital that the uncertainty present in emissions estimates is transparent. Clearer communication of the forces underlying inventory uncertainty may be needed so that the implications are better understood.
- Uncertainty estimates are not necessarily intended to dispute the validity of national GHG inventories, but they can help improve them.
- Uncertainty is higher for some aspects of a GHG inventory than for others. For example, past experience shows that, in general, methods used to estimate nitrous oxide (N_2O) emissions are more uncertain than methane (CH_4) and much more uncertain than carbon dioxide (CO_2). If uncertainty analysis is to play a role in cross-sectoral or international comparison or in trading systems or compliance mechanisms, then approaches to uncertainty analysis need to be robust and standardized across sectors and gases, as well as among countries.
- Uncertainty analysis helps to understand uncertainties: better science helps to reduce them. Better science needs support, encouragement, and greater investment. Full carbon accounting (FCA), or full accounting of emissions and removals, including all GHGs, in national GHG inventories is important for advancing the science.
- FCA is a prerequisite for reducing uncertainties in our understanding of the global climate system. From a policy viewpoint, FCA could be encouraged by including it in reporting commitments, but it might be separated from negotiation of reduction targets. Future climate agreements will be made more robust, explicitly accounting for the uncertainties associated with emission estimates.

We give here a brief overview of how the 15 core papers of this book contribute to the key insights mentioned in Box 2—or of the likely consequences should insights not be heeded. Ometto et al. 2014a provide an in-depth look at the papers in their *Introduction*.

Together, all the papers confirm or advance key insights 1–4.

Jonas et al. and Rafaj et al. advance key insights 2 and 3, respectively. Jonas et al. broaden our thinking on emissions accounting systems by stepping out of the "here and now" of national emission inventories. They provide a framework that i) allows a

country to be consistently embedded in a global emissions and long-term warming context; ii) enables a country's performance—past as well as projected achievements—in complying with a future warming target to be monitored, while at the same time iii) considering uncertainty in historic and projected emissions and quantifying the associated risks of missing target and/or pledged emissions. It is the combination of uncertainty and risk that postulates the need for even stricter emission reductions so as to limit the increase in global mean surface temperature until 2050 and beyond, as currently broadly discussed in the wake of the 5th Assessment Report of the Intergovernmental Panel on Climate Change (IPCC 2013: SPM). The paper by Rafaj et al., which identifies the principal determinants of the changes in SO_2, NO_x, and CO_2 emissions in Europe from 1960 to 2010, is interesting from two perspectives: i) it also includes ozone precursors; and ii) it does not, ostensibly, focus on uncertainty. However, the authors' methodology is important, as it allows a better understanding of uncertainty in projecting emission changes through isolation and quantification of the main factors that are most influential in reducing emissions.

The three papers by Lesiv et al., Hryniewicz et al., and Uvarova et al. also center on key insight 3, but more from a methodological perspective. Lesiv et al. and Hryniewicz et al. advance our knowledge by studying two important, though rather neglected, issues. Lesiv et al. seek to shed light on changes in the uncertainty of emission estimates due to learning (change in knowledge) and/or structural change in emissions. Hryniewicz et al. provide an answer to a vexing problemthat arises in comparing two parties (e.g., countries), A and B, whose uncertainties encompass the same emissions target—party A manages to just comply with the target but reveals a much greater uncertainty than that of party B, which slightly misses the target. Which party should we consider more credible in terms of meeting this emission target? Finally, Uvarova et al. illustrate the impact of learning, thus confirming Lesiv et al. The authors show how accuracy improves and relative uncertainty decreases through the use of more appropriate (higher-tier) accounting methods where these are available.

The paper by Ometto et al. 2014b centers on key insight 1. They are the only authors in the book to confirm the importance of full GHG accounting. With the focus on bottom-up accounting, the authors show how notable differences among existing biomass maps for the Brazilian Amazon, which combine remote sensing and field data analyses, lead to a wide spread in the estimated carbon emissions from deforestation. The general understanding among all Workshop participants was that it will take carbon-monitoring satellites such as NASA's OCO-2 (Orbiting Carbon Observatory), successfully relaunched in the meantime (Nature: http://blogs.nature.com/news/2014/07/nasa-launches-carbon-monitoring-satellite.html), to take the global carbon cycle and the issue of verification to new levels.

BOX 2 Lessons learned from uncertainty treatment: Conclusions drawn after the 2007 (2nd) International Workshop on Uncertainty in Greenhouse Gas Inventories. Source: White et al. (2011: 339–343)

1. The currently used bottom-up approach to accounting for greenhouse gas (GHG) emissions is incomplete in itself, as it cannot deal with the issue of accuracy. Bottom-up accounting for emissions is important in the sense that it shows which activities and actors are responsible for emissions. However, the ultimate accounting must be directed top-down, and reductions in emissions must be reflected in reductions in atmospheric GHG concentrations.

There are two immediate consequences of this: i) bottom-up accounting will be subject to continued revision in the future and must remain flexible; ii) this perception of emissions accounting runs counter to the ways in which emission trading schemes have been set up to date. To produce the desired results, these trading schemes need to be anchored, not least legally, within a reliable reference system, and this is not the case with current bottom-up accounting. Emission permits by country, which countries can sell at a given point in time but the number of which change because of continuous revisions in the estimates, fall outside conventional economic thinking. As a consequence, anything that raises doubt about the integrity of emission reductions is excluded because such doubt could potentially damage the market.

2. Earth's ecology acts as a complex and nonlinear system that is in a constant state of change. This system can be best understood over a long-term perspective; one should not expect to utilize nature to reduce anthropogenic GHG emissions in the same way that we use technological opportunities. By anticipating some accounting pitfalls, we can state that, to avoid surprises, we need to exercise caution in superposing subsystems with different emission-dynamic and uncertainty characteristics.
3. Uncertainty analysis should be used to develop clear understanding and informed policy in the framing of international environmental agreements. To ensure that uncertainty analysis becomes a key component of national GHG inventory analysis in support of international environmental policy, advanced guidance is needed so that uncertainty can be dealt with appropriately in an internationally consistent way across countries, subsystems, sources and sinks, GHGs, and sectors. This guidance goes beyond the methodologies offered by the Intergovernmental Panel on Climate Change (IPCC) to conduct and execute uncertainty analyses.
4. Uncertainty is higher for some GHGs and some sectors of an inventory than for others. Nature-related emissions and removals (e.g., in the land use, land-use change, and forestry (LULUCF) and the landfill sector) have greater uncertainty than technospheric emissions (e.g., in the fossil-fuel sector); and current estimates of nitrous oxide (N_2O) emissions are more uncertain than those of methane (CH_4) and carbon dioxide (CO_2). This raises the option that in designing future policy agreements, some components of a GHG inventory could be treated differently from others. The approach of treating subsystems individually and differently would allow emissions and uncertainty to be looked at simultaneously and would thus allow for differentiated emission reduction policies. This approach could have an advantage over treating all GHG emissions and removals collectively (in terms of CO_2-equivalence) and equally (not distinguishing between emissions and removals), which usually leads to increased uncertainty, with potentially important scientific and policy implications (e.g., in cases where countries claim fulfillment of their commitments to reduce or limit emissions). To recall, under the Kyoto Protocol the agreed emission changes for most countries were of the same order of magnitude as the uncertainty that underlay their combined emission estimates.
5. Any differentiated approach to accounting must form a logical subset of a full GHG accounting approach. Full accounting is the only way to reach a proper understanding of the global climate system and is a prerequisite for reducing the uncertainties in that understanding. Providing reliable and comprehensive estimates of uncertainty cannot necessarily be achieved by applying the approach favored under the UN Framework Convention on Climate Change (UNFCCC) and the Kyoto Protocol, which provided only for partial accounting of GHG fluxes to and from the atmosphere. It is virtually impossible to estimate the reliability of any system output if only part of the system is considered.

6. The option of treating subsystems individually and differently, while at the same time following full GHG accounting, forces us to deal with subsystems more skillfully than we have in the past. The maxim to follow would be to treat the technosphere, our built environment, and the biosphere individually but also holistically. Dealing with the technosphere and biosphere individually and differently, but not independently, although leading to agreement bifurcation, has clear advantages for emission inventories. First, it does not jeopardize verification—atmospheric measurements can discriminate between fossil fuel, terrestrial biosphere, and ocean carbon by means of their carbon isotope fingerprints in combination with measurement of atmospheric O_2; but they cannot identify individual fluxes within any of these categories. Second, differentiated accounting offers the option of i) placing emissions from the technosphere, where uncertainty is believed to be lowest, under stringent compliance with clear rules for dealing with uncertainty; while ii) putting biospheric emissions and removals, with their greater uncertainties, under consistent reporting by means of a global monitoring framework.

The three papers by Boychuk and Bun, Horabik and Nahorski and Verstraete are all unique in their own way. However, they should be seen collectively as advancing key insight 3 from the perspective of accounting for emissions of GHGs and air pollutants consistently across spatial (from local/regional to national) scales as well as from the methodological standpoint—a perspective that has not been given adequate importance in the context of insight 3.

The paper by Joerss advances key insight 4. By applying Monte Carlo simulation, it expands the issue of statistical dependence in input data for the overall uncertainty of a country's (here: Germany's) emission inventory from GHGs to particulate matter (PM_{10} and $PM_{2.5}$) and ozone precursors (SO_2, NO_x, NH_3, and NMVOV). This research paves the way for a better, that is, differentiated, understanding of uncertainty in emissions by gas or pollutant and sector.

Finally, the last five papers by Xu et al., Ermolieva et al., Nahorski et al., Dolgopolova et al., and Nijnik and Pajot can also be looked at *en bloc*. They advance our knowledge of emissions trading under uncertainty—and thus of key insight 1 (emissions trading is considered under verification; cf. Box 2)—in various specific ways pertaining to

- the impact of uncertainty on the price of certified emission reductions by examining a gas and sector specific example (Xu et al.);
- the impact of robustness on achieving emission reductions in a multi-country setting by considering decentralized bilateral trade and constraining the probability-based risk that emissions in combination with their uncertainty exceed a priori agreed emissions targets (Ermolieva et al.);
- the impact of uncertainty on trading rules in a multi-country setting by simulating bilateral trade and simple, reverse sealed auction mimicking the Kyoto Protocol with modified, uncertainty dependent rules and with learning versus non-learning agents (Nahorski et al.);
- the impact of economic, institutional and technological uncertainties on trading carbon emissions both at national and business levels by conducting simulations with the help of two systems dynamics models (Dolgopolova et al.);
- and, last but not least, the impact of varying discounting rates for carbon uptake specifically and economic cost-benefit analyses and the policy-making process in general (Nijnik and Pajot).

However, none of these approaches advance key insight 1 from a more fundamental perspective, the reason being that they are still subject to a bottom-up emissions accounting bias and are not yet anchored in a two-sided (bottom-up versus top-down) or verified emissions accounting framework. This means that the approaches cannot handle inaccuracy (at least, not beyond a certain magnitude), only imprecision. Thus, it remains to be seen how economists face up to the challenge of shaping emissions trading under conditions of a changing reference system—until bottom-up/top-down accounting is in place and conducted.

To conclude, it is noted that the challenges of addressing key insights 5 and 6 still exist; they were not tackled at the Workshop. However, on a general note, the approaches to addressing uncertainty discussed by all authors attempt to improve national inventories, not only for their own sake but also from a wider, systems analytical perspective that seeks to strengthen their usefulness under a compliance and/or global monitoring and reporting framework. They thus show the challenges and benefits of including inventory uncertainty in policy analysis, and where advances are being made. The issues that are raised by the authors and featured in their papers, and the role that uncertainty analysis plays in many of their arguments, highlight the importance of such efforts. The general understanding among all Workshop participants was unanimous: uncertainty analysis is needed for developing clear understanding and informed policy. Uncertainty matters, and it is key to many issues related to inventorying and reducing emissions. Dealing proactively with uncertainty allows useful knowledge to be generated that the international community should have to hand before negotiating international successor agreements to the Kyoto Protocol.

M. Jonas
International Institute for Applied Systems Analysis (IIASA), Schlossplatz 1, 2361 Laxenburg, Austria
e-mail: jonas@iiasa.ac.at

J. P. Ometto
Earth System Science Centre, National Institute for Space Research (CCST/INPE), Av dos Astronautas, 1758, 12227-010 São José dos Campos, SP, Brazil
e-mail: jean.ometto@inpe.br

R. Bun
Lviv Polytechnic National University, Bandery str., 12, Lviv 79013, Ukraine
e-mail: rbun@org.lviv.net

Z. Nahorski
Systems Research Institute, Polish Academy of Sciences, Newelska 6, 01-447 Warsaw, Poland
e-mail: Zbigniew.Nahorski@ibspan.waw.pl

Acknowledgment

The book was made possible through the generous financial support of the Systems Research Institute of the Polish Academy of Sciences.

References

IPCC 2013 Summary for policymakers, In: Stocker TF et al (eds) Climate change 2013: the physical science basis. Cambridge University Press, Cambridge, United Kingdom and New York, NY, United States of America, pp 3–29

Lieberman, D et al (eds) (2007) Accounting for climate change. Uncertainty in greenhouse gas inventories – verification, compliance, and trading. Springer, Netherlands

White, T et al (eds) (2011) Greenhouse gas inventories: dealing with Uncertainty. Springer, Netherlands

Contents

About the Editors

The Editors **Jean Pierre Ometto**, **Rostyslav Bun**, **Matthias Jonas** and **Zbigniew Nahorski** are senior scientists coming from different backgrounds. They work for Brazil's National Institute for Space Research, the Lviv Polytechnic National University in the Ukraine, the International Institute for Applied Systems Analysis in Austria, and the Systems Research Institute of the Polish Academy of Sciences. Their book shows that uncertainty matters and it is key to many issues related to inventorying and reducing emissions. Dealing proactively with uncertainty allows useful knowledge to be generated that the international community should have to hand before negotiating international successor agreements to the Kyoto Protocol.

DOI 10.1007/978-3-319-15901-0_1
Reprinted from *Climatic Change* Journal, DOI 10.1007/s10584-014-1149-5

INTRODUCTION

Uncertainties in greenhouse gases inventories – expanding our perspective

Jean P. Ometto · Rostyslav Bun · Matthias Jonas · Zbigniew Nahorski · Mykola I. Gusti

Received: 9 April 2014 / Accepted: 5 May 2014 / Published online: 24 May 2014
© Springer Science+Business Media Dordrecht 2014

Strategies for mitigating global climate change require accurate estimates of the emissions of greenhouse gases (GHGs). A strong consensus in the global scientific community states that efforts to control climate change require stabilization of the atmospheric concentration of GHGs (as per a recent compilation; (IPCC 2013)). Estimates of the amounts of carbon dioxide and other GHGs emitted to the atmosphere, as well as the amounts absorbed by terrestrial and aquatic systems, are crucial for planning, analyzing, validating and at global scale verifying mitigation efforts and for analyzing scenarios of future emissions. The magnitude and distribution of current emissions and the path of future emissions are both of considerable importance. It is critical that we have estimates of emissions and that we acknowledge and deal with the uncertainty in our best estimates. The range of issues that derive from uncertainty in emissions estimates was the subject of the 3rd International Uncertainty Workshop held in Lviv, Ukraine, 2010, and is the subject of this special issue.

Resolving national or regional contributions to changes in atmospheric GHG concentrations involves international agreements and national inventories of emissions. Countries, cities, companies, and individuals are now commonly calculating their GHG emissions, and markets

This article is part of a Special Issue on "Third International Workshop on Uncertainty in Greenhouse Gas Inventories" edited by Jean Ometto and Rostyslav Bun.

J. P. Ometto (✉)
Earth System Science Centre, National Institute for Space Research (CCST/INPE), Av dos Astronautas, 1758, 12227-010 São José dos Campos, SP, Brazil
e-mail: jean.ometto@inpe.br

R. Bun
Department of Applied Mathematics, Lviv Polytechnic National University, P.O.Box 5446, Lviv 79031, Ukraine

M. Jonas · M. I. Gusti
Advance Systems Analysis Program, International Institute for Applied Systems Analysis (IIASA), Schlossplatz 1, A 2361 Laxenburg, Austria

Z. Nahorski
Systems Research Institute, Polish Academy of Sciences, Newelska 6, 01-447 Warsaw, Poland

M. I. Gusti
Department of International Information, Lviv Polytechnic National University, 1 Sviatoho Yura Square, Lviv 79031, Ukraine

exist that allow trading emissions permits of carbon. Companies report corporate-level emissions or even the carbon footprint of products. But GHG emissions are seldom measured directly. For instance, it may be considered important that total, and trend, uncertainty in national emissions estimates is smaller than the reductions to which countries agree to under an international compliance regime, as well that emissions mitigation strategies, and trade, be based on accurate knowledge of the magnitudes and sources of emissions.

The 2010 United Nations Framework Convention on Climate Change (UNFCCC-COP 16; Cancun, Mexico) produced an agreement with the desire to limit global average surface temperature to 2°C above the pre-industrial level. To achieve this objective, the total amount of greenhouse gas emissions emitted to the atmosphere in 2020 has to be targeted at around 44 Pg CO_2-eq, from the current estimated value of 48 Pg CO_2-eq [assuming a linear target path]. However the current emissions trajectories follow the most carbon intensive path of the recently published scenarios of the Intergovernmental Panel on Climate Change Fifth Assessment Report (IPCC 2013) (based on Representative Concentration Pathways; www.globalcarbonproject.org/). Experience with the Kyoto Protocol shows that quantitative estimation of uncertainty increases the value of the inventory provided by reporting authorities. Yet, only a few Annex I Parties report full uncertainty analysis, although default methods and underlying data are available for all countries.

UNFCCC reporting should be improved as Parties report comprehensive uncertainty analysis of the GHG inventory estimates and provide validation reports (for data and models used). The Intergovernmental Panel on Climate Change (IPCC) has proposed standardized methodologies for adequate accounting of national, natural and human-induced GHG sources and sinks. The methods, applied to national scales, have guided the production of emissions assessments at the country level for several years. Comparable methodologies have been developed within countries and trade groups. The constant evolution of the IPCC scientific review, associated with increasing international concerns over anticipated changes in the future climate, has raised a number of issues about compliance and verification, and about proposed and agreed strategies meant to reduce the impact on the global climate associated with human activities.

Because of the accumulation of GHGs in the atmosphere, concern focuses on not just current rates of emissions but on the trend in emissions and in cumulative emissions totals. Cumulative GHG emission budgets (i.e., for 2000–2050) have been shown to be a robust indicator for global temperatures at, and beyond, 2050 (Meinshausen et al., 2009), and are thus well suited to link long-term global warming targets with near and mid-term emissions. Cumulative global emissions targets can be translated into near term national emissions objectives, but uncertainty in both natural and anthropogenic fluxes of GHGs must be incorporated in monitoring and projecting emissions trends.

The international workshop in Lviv, Ukraine, was the third in a series exploring the magnitude and implications of uncertainty in GHG emissions estimates. Papers presented at the workshop and peer reviewed for this Climatic Change Special Issue explore the uncertainty in emissions estimates but also focus on detecting and evaluating changes in emissions; independent monitoring and verification of emissions estimates; and determining how to obtain critical information, and how to proceed without information that cannot be obtained. The papers are presented under general themes such as: Spatial Inventories; Land Use, Land Use Change and Forestry; Energy; Non-CO_2 and Waste emissions; Economy and Climate Change; and General & Policy.

In *General & Policy*, *Jonas* et al. ask how uncertainty over time will affect short-term GHG emission commitments and long-term efforts to meet global temperature targets for 2050 and beyond. The study addresses a fundamental problem: how to combine uncertainty about current and historic emissions (diagnostic uncertainty) with uncertainty about projected future emissions (prognostic uncertainty). Although the authors' mode of bridging uncertainty across

temporal scales still relies on discrete points in time and is not yet continuous, their study takes a valuable first step toward that objective. The proposed emissions-temperature-uncertainty framework assumes that cumulative emissions can be constrained over time by binding international agreements, as well as that emissions can be estimated only imprecisely, and whether or not they will achieve an agreed temperature target is also uncertain. The framework allows policymakers to understand diagnostic and prognostic uncertainty so that they can make more informed (precautionary) decisions for reducing emissions given an agreed future temperature target. The paper by *Rafaj* et al. examines key factors that have driven the observed evolution of SO_2, NO_x, and CO_2 emissions in Europe from 1960 to 2010, contributing to the understanding of the relationship between emissions and economic growth. It has often been suggested that emissions first increase with growing income and social welfare and subsequently decrease once a certain level of wealth has been attained. However, the authors' analysis demonstrates that observed turning points occur for different countries and pollutants at different income levels, and no turning point has yet been identified for CO_2. Although there are factors determined by economic parameters (e.g. energy intensity, fuel mix, technological advances), the results provide little evidence that the emission control measures are directly linked to economic growth, but their adoption is rather driven by enforcement of deliberate mitigation policies. The methodology presented by the authors provides a quantitative basis for investigating uncertainties related to the determinants of emission projections. Their exemplary decomposition analysis allows for identifying those parameters that are most relevant in assessing the uncertainty of GHG emission inventories. Under the same theme, *Lesiv* et al. deal with the change in the uncertainty of emission estimates which, in general, results from both learning (improvement of knowledge) and the structural change in emissions (change in emitters). Understanding the change in uncertainty due to the two processes and being able to distinguish between them becomes particularly important under a compliance regime when countries claim fulfillment of their commitments to reduce or limit emissions, or for trading emission quotas under such a regime. In the first part of their study, focusing on the individual Member States of the former EU-15, the historical change in the total uncertainty of CO_2 emissions from stationary sources is analyzed. In the second part of their study, the authors present examples of changes in total uncertainty considering scenarios of structural changes in the emitters consistent with the EU's "20–20–20" targets. This exercise shows that the increased knowledge of inventory processes has determined the change in total uncertainty in the past and should also be considered as the driving factor in the prospective future. In the final contribution within *General & Policy*, Hryniewicz et al. return to the problem of checking compliance of uncertain GHG inventories with agreed emission targets. That is, why a direct comparison of emissions with targets is not scientifically robust. The starting point of this study is the IPPC Good Practice Guidelines statement that reporting of inventories should be consistent, comparable and transparent. Thus, there exists the need to explain why inventoried emissions satisfy a target or are closer to it in one case than in another. This idea led the authors to look at a compliance procedure via comparison of uncertain alternatives. Traditionally, probabilistic methods have been used, in which emissions are treated as a random variable. Comparison rules based on moments, such as mean values and variances, are not suitable for the comparison of emissions. More appropriate methods use percentiles and critical values, like a so-called undershooting technique which was discussed earlier, e.g. by Nahorski et al. (Nahorski et al. 2007) and Nahorski and Horabik (Nahorski and Horabik 2010). However, emissions are inventoried usually only once per year, and they are typically not random, so it is difficult to treat them as probabilistic variables. This is why possibility theory, which has grown out of the fuzzy sets, is more suitable to the problem. A possibility distribution is not based on frequencies of observations, but may be constructed, e.g., by experts. Despite the

differences in the probability/possibility paradigms, the methods behind both approaches show similarities and the checking rules are often alike. Taking uncertainty into account, additional parameters are proposed to be included in a checking rule: how stringent do we understand compliance; or to which extent is the target met. Such a rule allows for classifying inventories: how credible are these in satisfying the target? This information can be used in elaborating advanced decision rules, which would allow for taking a more or less conservative position.

The evolution in reducing uncertainty in emissions estimates reflects: (1) improvements in knowledge within the scientific community (e.g., more precisely known emission factors and improvements in energy data); and (2) structural changes in the emissions (e.g., an increasing fraction of emissions from the sectors where data can be estimated with smaller uncertainty, such as energy). Within the *Energy* category of the contribution to this Special Issue volume, *Uvarova* et al. focus on a prime emitter – emissions from oil operations in the Russian Federation. The authors provide a good example to illustrate the impact of learning. They investigate improvement in accuracy of emission estimates under a shift of accounting methods: from the production-based IPCC (IPCC 2000) Tier 1 to the mass-balance-based IPCC (IPCC 2006) Tier 2. The authors' comparison shows that the estimates in accordance with the higher-tier method result in a greater accuracy and lower relative uncertainty (26 % under Tier 2 versus 54 % under Tier 1). The authors suggest that this uncertainty can be reduced further, e.g., by improving the accuracy of the parameters, including the use of more geographically explicit emission factors, employed in the emissions calculations.

Furthermore, in the session dedicated to emissions associated with Land Use, Land Use Change and Forestry, *Ometto* et al., explore uncertainties associated with emissions related to land use change in the tropics, focusing on deforestation. As reported by Le Quéré et al. (Le Quéré et al. 2013), net emissions from deforestation are decreasing, although this issue is far from resolved. The carbon stock in the terrestrial biosphere is enormous and the pressure for land use and agricultural expansion is constant, especially in tropical systems (Dalla-Nora et al. 2014). The methods currently adopted to estimate the spatial variation of above- and below-ground biomass in tropical forests are usually based on remote sensing analyses coupled with field datasets. Field measurements in tropical forests are, typically, relatively scarce and often limited in their spatial distribution. Thus, lack of data is one major step to be overcome concerning reducing uncertainty in estimating GHG emissions from land use change, in particular in tropical regions. In this paper, the authors do a comparative analysis of recently published biomass maps of the Amazon region, including the official data used by the Brazilian government for its report to the UNFCCC Secretariat. Among the outcomes of their analysis, the evolvement to higher resolved, spatially distributed forest biomass data is key to reduce uncertainty in emissions estimates in tropical regions. Establishing national systems of GHG emissions estimation and reporting in Land Use, Land Use Change, and Forestry (LULUCF) is under continuous improvement, with key features given by the availability of datasets and in-country improving capacity of data generation. However, regional harmonization of methods involved in national GHG estimation systems is rather poor. There are also necessary within-country steps toward better coordination of the research effort supporting GHG estimation, reporting and accounting under UNFCCC requirements. As well, the increase of data availability for external evaluation is an important step further toward better estimates of uncertainty.

The spatial distribution and estimates of emissions are further explored in the *Spatial Inventories Section*. Emission inventories with high spatial and temporal resolution can be related to a process-level understanding of emissions sources and yield many advantages in the realm of designing and evaluating emission control strategies; and they would be very helpful for climate models and for monitoring emissions and checking emissions commitments in

greater detail where necessary. *Boychuk and Bun*, also referring to the *Energy Section* of this Special Issue, present a Geographical Information System (GIS) approach to the spatial inventory of GHG emissions in the energy sector. It includes the mathematical background for creating the spatial inventories of point-, line-, and area-type emission sources, caused by fossil-fuel use for power and heat production, the residential sector, industrial and agricultural sectors, and transport. The approach is based on the IPCC guidelines, official statistics on fuel consumption, and digital maps of the region under investigation. As an example, the western Ukraine region with an area of 110.6^{th} km^2 was used for experiments. The uncertainty of inventory results is calculated, and the results of sensitivity analysis are investigated. The approach proposes that allocating emissions to the places where they actually occur helps to improve the inventory process and to reduce the overall uncertainty. Such methodology is useful for large countries with uneven distribution of emission sources. Spatial inventories support decision making in reducing emissions at the regional level. Such mathematical tools and algorithms can also be used in climate models, for the analysis and prediction of the emission processes and their structure for a variety of scenarios. In a similar vein, *Horabik and Nahorski* present an original approach to allocating spatially correlated data, such as GHG emission inventories, to finer spatial scales, based on covariate information observable in a fine grid. This approach is useful for data disaggregation, like activity data in some categories of human activity, during GHG spatial inventory. Dependences are modeled with the conditional autoregressive structure introduced into a linear model as a random effect. The maximum likelihood approach to inference is employed, and the optimal predictors are developed to assess missing values in a fine grid. The authors propose a relevant disaggregation model and illustrate the approach using a real dataset of ammonia emission inventory in a region of Poland in 15 km, 10 km, and 5 km grids. For the considered inventory, the fourfold allocation benefits greatly from the incorporation of the spatial component, while for the ninefold allocation, this advantage is limited, but still evident. Also, the proposed method is found to be particularly useful in correcting the prediction bias encountered for upper range emissions in the linear regression models. In this case study, the authors use the original data in a fine grid to assess the quality of resulting predictions, but for the purpose of potential applications, they also developed a relevant measure of prediction error. It is an important step to quantify the prediction error in situations, where original emissions in a fine grid are not known. The method of improving resolution opens the door to uncertainty reduction of spatially explicit GHG emission inventories.

Processing spatial data, such as GHG inventories, poses several problems, as the data are represented as grids. *Verstraete* proposes an approach to optimize the mapping of values in mismatched grids. When data that are represented using different grids need to be combined, the main problem is that the underlying distribution of activity data or any other parameter is not known, and thus a remapping from one grid onto another grid is difficult. Traditional methods work by making simple assumptions regarding the underlying distribution, but as those often do not match reality, it decreases the accuracy of the data. However, often there is knowledge available that can help with better estimating the real distribution. In the article, the author presents a new method, which allows additional data to be used. The method presented uses techniques from artificial intelligence (fuzzy sets, inference systems, etc.) to determine how one grid can be remapped onto another grid. Even with additional data, this is not straightforward, as data may not match exactly or may be incomplete. The article describes the concept of the approach, and discusses the results of experiments on artificial datasets.

Joerss, contributing to the *Non-CO_2 / Waste Section*, compares results of air pollutant inventories from several European countries with the results of the PArticle REduction Strategies (PAREST) research project in Germany. The author uses a Monte-Carlo simulation

for assessing the uncertainties in emissions of particulate matter (PM10 & PM2.5) and aerosol precursors (SO_2, NO_x, NH_3 and NMVOC). The methodology and analysis for uncertainty assessment in the emissions inventories is successful for particulate matter and aerosol precursors. The uncertainty of the pollutant species analyses is determined and falls in the range of recent uncertainty assessments of European countries. The analysis by *Xu* et al, also part of this section, reveals a link between *Non-CO_2* emissions and economy, where the authors tackle the problem of uncertainty assessment in coal mine methane emissions projects, and estimation of its impact on a negotiated Certified Emission Reduction (CER) price. They use the Rubinstein-Ståhl bargaining model to fill the gaps in the database and to simulate negotiations concerning CER price, assuming that a buyer's willingness to negotiate a CER depends on the uncertainty associated with the emission reduction. The bargaining model is broadened by introducing dependence of some parameters on the probability of a contracted CER amount not to be realized. To quantify this probability, the authors develop a conditional distribution given information on the point estimate of methane emissions for the project under consideration, and on the distribution of available estimates from coalmines having similar characteristics. The proposed methodology is applied to a coalmine methane project implemented in the Huainan coalmine, the Anhui Province in Eastern China. The parameters of uncertainty distribution of the methane content are estimated using data, which are gathered from 25 Chinese coalmines with similar geological conditions. The results indicate that the uncertainty influence on price is significant, particularly when the credibility of a seller increases, and the probability of a failure to fulfill the project decreases.

The aggregated impact of climate change on society, economy and ecosystems, comprises the total impact across regions. Producing results of aggregated impact involves the challenge of discerning how adaptation will occur in society and ecosystems (what is the resilience of natural systems) and what are the paths that future development (economic and social) will follow (IPCC AR5). The section dedicated to the *Economy & Climate Change* brings some of these elements to the discussion. *Ermolieva* et al. develop a novel trading-market model which mimics decentralized bilateral trade of emission permits under uncertainty. In contrast to existing emissions markets, the proposed model allows for addressing long-term socio-economic and environmental consequences of trade, irreversibility, and inherent uncertainty including asymmetric information of agents (countries). The model relies on an anonymous computerized optimization system (computerized market system) that can be viewed as "cloud computing". Trading between both countries and regions is shown to be robust. The trading process converges to the core solution and the trading parties create the stable (core) solution without incentives to leave the trading coalition. Numerical results show that the explicit treatment of uncertainty may significantly change the trading process by turning sellers of emission permits into buyers.

Looking at the carbon market under the Kyoto Protocol, *Nahorski* et al. present a simulation system that mimics trading of GHG emissions among parties, according to the Protocol's rules. It is admitted that the emissions are uncertain and this knowledge affects the trading rules, as presented in earlier studies by Nahorski et al. (Nahorski et al. 2007) and Nahorski and Horabik (Nahorski and Horabik 2010). These rules lead to more uncertain emissions that are less expensive on the market. The simulation does not assume an ideal market: the equilibrium prices are not known during the trade. Bilateral negotiations and sealed bid reverse auctions are considered for pricing the traded emissions. Only transactions profitable for both participants are accepted. A multi-agent approach is used as a tool for simulating the trading process. Non-learning and learning agents are considered. The former use fixed probability distributions for placing orders, while the latter learn to modify the distribution according to the success/lack

of success in winning transactions. Negotiation examples present phenomena similar to those spotted in real markets.

Following up on carbon trading, and on the influence of uncertainty on driving the market and defining prices, *Dolgopolova* et al. employ system dynamics models to analyze the impact of different uncertainties on emission trading - both on national and business levels. Economic, institutional and technological uncertainties determine the benefits from trading emissions permits. For any country participating in an international trading market, the uncertainty in the price range becomes crucial. In the case of business investment decisions for implementing resource-saving technologies, the proposed system dynamics model shows that the first-mover investor will obtain significantly fewer advantages than his followers, which leads to a delay in primary investments.

Nijnik & Pajot analyze the social function of forests and the opportunity for mitigation through maintaining and replanting trees, and discuss the economic impact of dealing with uncertainties in using forests to mitigate climatic change. Limiting the analysis of uncertainty to discounting, the authors challenge the traditional cost-benefit analysis. Different settings of discounting are tested for carbon sequestration of the forestry sector in Scotland and Ukraine. The policy consequences of the exercise are also investigated. The choices of discounting protocols are shown to have a major influence on both the economic analysis and the decision-making process, which directly affect the climate change mitigation strategies in these countries. The authors highlight the implications on the policy decisions when uncertainty is considered in mitigating climate change through forestry.

Changes in relative uncertainty over time and scientific understanding of the main determinants of that change have obvious implications, e.g., for assessing the uncertainty of emissions with regard to compliance with emission reduction commitments and for trading emission quotas under the Kyoto Protocol or REDD+ mechanisms. Advances in methodology and mathematical modelling to constrain uncertainties associated with ecosystems and some carbon pools, are observed. However, investments in methodology-oriented research are particularly important for a full-system uncertainty estimate. In terrestrial systems, historical patterns and long-term datasets are important to draw a more accurate picture of the carbon pools evolution. In this respect we see the following scientific advances evolving from the workshop that should be considered in future studies: (i) combining diagnostic and prognostic uncertainty in a (e.g.) emissions-temperature setting that seeks to constrain global warming and linking uncertainty consistently across temporal scales; (ii) developing methodologies and information technologies that allow estimating GHG emissions and sinks with lower uncertainties, e.g., spatial GHG cadastres, and higher level tier methods; (iii) evaluating the influence of uncertainty on GHG emission markets aiming at robust and efficient emission trading; (iv) studying issues that influence the dynamics of GHG emissions estimates, e.g., learning curves and structural changes in emitters, as well as social, political and economic drivers, etc.; (v) constraining uncertainties in land use change emissions, as having great potential for reduction, and per its influence on ecosystem services and social aspects; and developing marked strategies for making emissions reduction economically attractive.

References

Dalla-Nora EL, de Aguiar APD, Lapola DM et al. (2014) Why have land use change models for the Amazon failed to capture the amount of deforestation over the last decade? Land Use Policy (http://dx.doi.org/10.1016/j.landusepol.2014.02.004).

IPCC (2000) Good practice guidance and uncertainty management in national greenhouse gas inventories. IPCC National Greenhouse Gas Inventories Programme. IGES/OECD/IEA, 2000

IPCC (2006) In: Eggleston HS, Buendia L, Miwa K, Ngara T, Tanabe K (eds) 2006 IPCC Guidelines for National Greenhouse Gas Inventories, Prepared by the National Greenhouse Gas Inventories Programme. IGES, Japan

IPCC (2013) The Physical Science Basis. Contribution of Working Group I to the Fifth Assessment Report of the Intergovernmental Panel on Climate Change [Stocker TF, Qin D, Plattner GK, Tignor M, Allen SK, Boschung J, Nauels A, Xia Y, Bex V and Midgley PM (eds.)]. Cambridge University Press, Cambridge, United Kingdom and New York, NY, USA, 1535 pp

Le Quéré C, Peters GP, Andres RJ (2013) Global carbon budget 2013. Earth Syst Sci Data Discus 6:689–760. doi:10.5194/essdd-6-689-2013

Nahorski Z, Horabik J (2010) Compliance and emission trading rules for asymmetric emission uncertainty estimates. Clim Chang 103(1–2):303–325

Nahorski Z, Horabik J, Jonas M (2007) Compliance and emission trading under the Kyoto Protocol: Rules for uncertain inventories. Water Air Soil Pollut Focus 7(4–5):539–558

DOI 10.1007/978-3-319-15901-0_2
Reprinted from *Climatic Change* Journal, DOI 10.1007/s10584-014-1103-6

Uncertainty in an emissions-constrained world

Matthias Jonas · Gregg Marland · Volker Krey · Fabian Wagner · Zbigniew Nahorski

Received: 28 December 2012 / Accepted: 27 February 2014 / Published online: 1 April 2014
© Springer Science+Business Media Dordrecht 2014

Abstract Our study focuses on uncertainty in greenhouse gas (GHG) emissions from anthropogenic sources, including land use and land-use change activities. We aim to understand the relevance of diagnostic (retrospective) and prognostic (prospective) uncertainty in an emissions-temperature setting that seeks to constrain global warming and to link uncertainty consistently across temporal scales. We discuss diagnostic and prognostic uncertainty in a systems setting that allows any country to understand its national and near-term mitigation and adaptation efforts in a globally consistent and long-term context. Cumulative emissions are not only constrained and globally binding but exhibit quantitative uncertainty; and whether or not compliance with an agreed temperature target will be achieved is also uncertain. To facilitate discussions, we focus on two countries, the USA and China. While our study addresses whether or not future increase in global temperature can be kept below 2, 3, or 4 °C targets, its primary aim is to use those targets to demonstrate the relevance of both diagnostic and prognostic uncertainty. We show how to combine diagnostic and prognostic uncertainty to take more educated (precautionary) decisions for reducing emissions toward an agreed temperature target; and how to perceive combined diagnostic and prognostic uncertainty-related risk. Diagnostic uncertainty is the uncertainty contained in inventoried emission estimates and relates to the risk that true GHG emissions are greater than inventoried emission estimates reported in a specified year; prognostic uncertainty refers to cumulative emissions between a start year and a future target year, and relates to the risk that an agreed temperature target is exceeded.

This article is part of a Special Issue on "Third International Workshop on Uncertainty in Greenhouse Gas Inventories" edited by Jean Ometto and Rostyslav Bun.

Electronic supplementary material The online version of this article (doi:10.1007/s10584-014-1103-6) contains supplementary material, which is available to authorized users.

M. Jonas (✉) · V. Krey · F. Wagner
International Institute for Applied Systems Analysis (IIASA), Schlossplatz 1, 2361 Laxenburg, Austria
e-mail: jonas@iiasa.ac.at

G. Marland
Appalachian State University, Boone, NC, USA

Z. Nahorski
Systems Research Institute, Polish Academy of Sciences, Warsaw, Poland

1 Introduction

This study focuses on the uncertainty in estimates of anthropogenic greenhouse gas (GHG) emissions, including land use and land-use change activities. It aims to provide an overview of how to perceive uncertainty in a systems context seeking to constrain global warming.

It focuses on understanding uncertainty across temporal scales and on reconciling short-term GHG emission commitments with long-term efforts to meet average global temperature targets in 2050 and beyond. The discussion is a legacy of the 2nd International Workshop on Uncertainty in Greenhouse Gas Inventories, which concluded:

> the consequence of including inventory uncertainty in policy analysis has not been quantified to date. The benefit would be both short-term and long-term, for example, an improved understanding of compliance … or of the sensitivity of climate stabilization goals to the range of possible emissions, given a single reported emissions inventory" (Jonas et al. 2010a).

It addresses a fundamental problem: how to combine diagnostic (retrospective) and prognostic (prospective) uncertainty. Current (and historic) GHG emission inventories contain uncertainty in relation to our ability to estimate emissions (Lieberman et al. 2007; White et al. 2011). Diagnostic uncertainty results from grasping emissions accurately but imprecisely (our initial assumption). It can be related to the risk that true GHG emissions are greater than inventoried estimates reported at a given time point (Jonas et al. 2010b: Tab. 3). (The opposite case, true emissions being smaller than inventoried estimates, is not relevant from a precautionary perspective.)

Diagnostic uncertainty, our ability to estimate current emissions, stays with us also in the future. Assuming that compliance with an agreed emissions target is met in a target year allows prognostic uncertainty to be eliminated entirely. How this target was reached is irrelevant; only our real diagnostic capabilities of estimating emissions in the target year matter. This is how experts proceeded, e.g., when they evaluated ex ante the impact of uncertainty in the case of compliance with the Kyoto Protocol (KP) in 2008–2012, the Protocol's commitment period (Jonas et al. 2010b).

Emissions accounting in a target year can involve constant, increased or decreased uncertainty compared with the start (reference) year, depending on whether or not our knowledge of emission-generating activities and emission factors becomes more precise. The typical approach to date has been to assume that, in relative terms, our knowledge of uncertainty in the target year will be the same as it was in the start year.

However, uncertainty under a prognostic scenario always increases with time. The further we look into the future, the greater the uncertainty. This important difference suggests that diagnostic and prognostic uncertainty are independent. This differs from how prognostic modelers usually argue. A prevalent approach is to realize a number of scenarios and grasp prognostic uncertainty by means of the spread in these scenarios over time—which increases with increasing uncertainty in the starting conditions built into their models. However, this approach nullifies diagnostic uncertainty once a target (future) is reached.

To stabilize Earth's climate within 2 °C of historic levels, treaty negotiations have pursued mechanisms that reduce GHG emissions globally and lead to sustainable management of the atmosphere at a "safe," steady-state level. In recent years, international climate policy has increasingly focused on limiting temperature rise as opposed to achieving GHG concentration–related objectives (Rogelj et al. 2011). A promising and robust methodology for adhering to a long-term global warming target appears to be to constrain cumulative GHG emissions in the future (WBGU 2009; Allen et al. 2009; Matthews et al. 2009; Meinshausen et al. 2009; Zickfeld

et al. (2009); Raupach et al. 2011). Cumulative emissions, defined by the area under an emissions scenario path, are a good predictor for the expected temperature rise. The concept of cumulative emissions began influencing climate policymaking after the 2009 climate conference in Copenhagen, where it was first discussed broadly and publicly. The emission reductions required from the fossil-fuel and land-use sectors to comply with the concept of constraining cumulative emissions until 2050 to limit global warming to 2 °C in 2050 and beyond are daunting: 50–85 % below the 1990 global annual emissions, with even greater reductions for industrialized countries (Fisher et al. 2007; Jonas et al. 2010a).

The cumulative emissions concept is particularly suited to linking diagnostic and prognostic uncertainty because it allows compliance with both emissions and temperature targets to be investigated at a selected future time point. Here, we employ Meinshausen et al.'s (2009) global-scale research, which centers on limiting the increase in average global temperature to 2 °C from its pre-industrial level. Meinshausen et al. express compliance with this temperature target in terms of constraining cumulative CO_2 or CO_2 equivalent (CO_2-eq) emissions between 2000 and 2049 while accounting for a multitude of model-based, forward-looking emission-climate change scenarios. Thus, the relationship between cumulative emissions and the risk of exceeding the 2 °C target—an S-shaped curve broadening between its end points (see Fig. 3 and S1a in Meinshausen et al.)—is not unequivocal. For a given cumulative emissions value, multiple emission pathways per modeling exercise are conceivable that comply, or not, with the 2 °C target, thus allowing the risk of exceedance pertinent to this cumulative emissions value to be defined. The risk value translates into an interval, if many modeling exercises are considered.

The broadened S-curve shows that a sharp cumulative emissions value translates into a risk interval for exceeding 2 °C; vice versa, a sharp risk value translates into a cumulative emissions interval. The latter interval comprises all cumulative emissions allowing at least one emissions pathway that exhibits this risk. These intervals can be interpreted in terms of (prognostic) uncertainty, subsuming our lack of knowledge in toto (from the climate system and its key characteristics through to model representation). Here, we employ the two extreme alternatives—sharp cumulative emissions versus uncertain risk, and uncertain cumulative emissions versus sharp risk—without further investigating the two uncertainties' interdependence.

We discuss diagnostic and prognostic uncertainty in an emissions-temperature setting that allows any country to understand its national and near-term mitigation and adaptation efforts in a globally consistent and long-term context. In this systems context, cumulative emissions are constrained and globally binding but exhibit quantitative uncertainty (i.e., they can be estimated only imprecisely); and whether or not compliance with an agreed temperature target will be achieved is also uncertain. Because more data are available, we focus on the 2 °C temperature target, disregarding the current dispute about the achievability of this target (Victor 2009). Later in the analysis we consider higher temperature targets (3 and 4 °C), our objective being to understand the relevance of diagnostic and prognostic uncertainty in a global emissions-temperature context and across temporal scales. Although our mode of bridging uncertainty across temporal scales still relies on discrete points in time and is not yet continuous, it provides a valuable first step toward that objective.

Our study is structured as follows: Section 2 links to the data, techniques, and models we employ; it provides the methodological overview and describes the steps taken to establish the systems context. It prepares the basis for addressing our objective—in Section 3—where we present uncertainty in the elaborated emissions-temperature context for selected countries. Findings and conclusions are summarized in Section 4.

2 Methodology

We use publicly available emission and other data (Supplementary Information [henceforth "SI"]: Tab. S1). The time period 1990–2008/09 is the diagnostic part (D) of our study (although some data to 2008/09 are lacking). The time period 2008/09 and beyond is its prognostic part (P).

In establishing the emissions-temperature-uncertainty context for countries, we also employ a number of techniques and models that are publicly available and/or described in the scientific literature. Table S2 in SI provides an overview of the techniques and models, their mode of application, and how their output is used.

2.1 Global emission constraints

The notion of constraining cumulative emissions gained momentum with a number of publications in 2009, among them Meinshausen et al. and the German Advisory Council on Global Change (WBGU). WBGU in 1995 raised the idea of determining an upper limit for the tolerable increase of the mean global temperature and deriving a global CO_2 reduction target through an inverse approach (i.e., a backward calculation [WBGU 1995]). The budget concept (WBGU 2009) is the further development of this idea.

To limit atmospheric warming, total anthropogenic CO_2 emitted to the atmosphere must be constrained. Concerning 2 °C, WBGU (2009) proposed adoption of a binding upper limit for the total CO_2 emitted from fossil-fuel sources up to 2050 and allocation of the defined amount of emissions among countries, subject to negotiation but based on various principles, among them "polluter-pays," precautionary principle, and the principle of equality.

WBGU thus separated the global emissions budget into national emissions budgets based on an equal per capita (p/c) basis. The budget concept contains four political (i.e., negotiable) parameters: (i) the start year and (ii) end year for the total budget period; (iii) the cumulative emissions constraint or, equivalently, the probability of exceeding the 2 °C temperature target; and (iv) the reference year for global population. Our choices for the four parameters—(i) 1990 (to conform with the KP) and 2000 (to study the impact of a different start year on national emission budgets); (ii) 2050; (iii) alternative combinations of uncertainty in both cumulative emissions and risk of exceeding temperature targets ranging from 2 to 4 °C; and (iv) 2050—differ from the options investigated by WBGU.[1] We also assess both alternative and imperative global emission reduction concepts. These are linked, e.g., to reducing emission intensity for technospheric emissions and to achieving sustainability across total land use and land-use change (LU) activities. Costs of mitigation measures (and the uncertainty in costs resulting from emissions uncertainty) can be expressed as marginal costs and p/c costs. Here we refer to p/c costs.

2.2 From global to national: per capita emissions equity in 2050

We apply a "contraction & convergence" approach as an initial reference approach (GCI 2012). This allows establishment of global linear target paths for 1990–2050 (from 36.8 Pg CO_2-eq in 1990 to 25.9 Pg CO_2-eq in 2050) and for 2000–2050 (from 39.5 Pg CO_2-eq in 2000 to 20.5 Pg CO_2-eq in 2050), and derivation of global emission targets for 2050 (Fig. 1 and SI:

[1] The four parameters in WBGU's "historical responsibility" approach are (i) 1990, (ii) 2050, (iii) 25 %, and (iv) 1990; and (i) 2010, (ii) 2050, (iii) 33 %, and (iv) 2010 in its "future responsibility" approach. In both approaches, the probability of exceeding the 2 °C temperature target refers to cumulative emission constraints for 2000–2049.

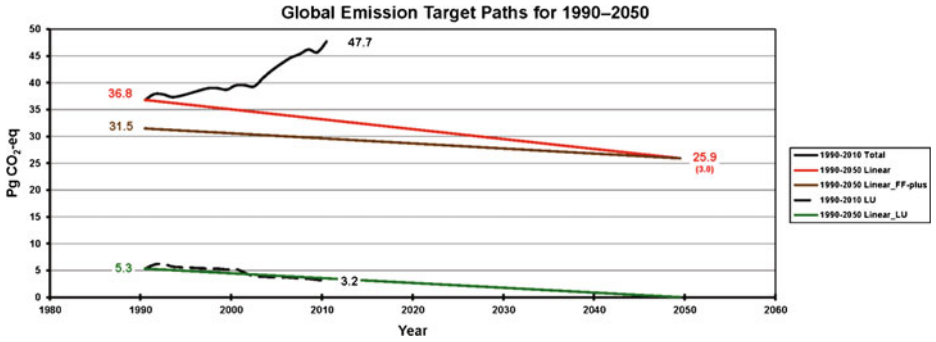

Fig. 1 Global linear emission target paths for 1990–2050 and global emission targets (global emissions equity, GEE, in parentheses) for 2050 (see also SI: Tab. S3). Emissions between 2000 and 2050 are constrained by 1500 Pg CO_2-eq. Emissions are in Pg CO_2-eq (GEE in t CO_2-eq/cap). The global target paths are for (i) total GHG emissions (*solid red line*); (ii) total emission excluding emissions from land use and land-use change (LU), i.e., emissions from fossil-fuel burning and cement production and for technospheric GHGs other than CO_2 ("FF-plus": *solid brown line*); and (iii) emissions from LU (*solid green line*). The 2050 global targets for total GHG emissions and FF-plus emissions are identical (25.9 Pg CO_2-eq and 3.0 t CO_2-eq/cap, respectively) because the 2050 global target for LU emissions is set to zero. The *solid black and dashed black curves* show actual estimates of total GHG emissions and LU emissions

Tab. S3). In conformity with Meinshausen et al. (2009) we apply an emissions constraint of 1500 Pg CO_2-eq for the period 2000–2049 (2050 is hereafter the "end year") to which we add the CO_2-eq emissions emitted cumulatively between 1990 and 1999 if we choose 1990 as start year. We also stipulate that the emission targets derived for 2050 are exclusively available for technospheric emissions. The imperative we follow for net emissions from LU activities is that these will be reduced linearly to zero by 2050; that is, we assume that deforestation and other LU mismanagement will cease and that net emissions balance. Our underlying assumptions are that (i) the remainder of the biosphere (including oceans) stays in or returns to an emissions balance—which must be questioned (Canadell et al. 2007); (ii) this return, which refers to CO_2-C, implies in turn that emissions and removals of CH_4, N_2O, etc. also return to an emissions balance; and (iii) these returns happen without systemic surprises of the terrestrial biosphere.

To achieve universally applicable global emissions equity (GEE) by 2050, we divide the aforementioned global emission targets by the global population we expect by 2050—estimated as ranging between 7.5 and 10.2 10^9 with a best estimate of 8.8 10^9 and a confidence interval (CI) of 95 %.[2] We find 2050 GEE values of 3.0 and 2.3 t CO_2-eq/cap for 1990–2050 and 2000–2050, respectively (Fig. 1 and SI: Tab. S3).

2.3 Uncertainty in cumulative emissions and risk of exceeding 2 °C in 2050

Figure 3 of Meinshausen et al. (2009) and Figure S1a in their supplementary information show that a sharp cumulative CO_2 (or CO_2-eq) emissions value for 2000–2050 translates into a risk interval of exceeding 2 °C in 2050 and beyond; vice versa, a sharp risk value translates into a cumulative emissions interval. We interpret these intervals in terms of prognostic uncertainty and apply the 2 °C Check Tool of Meinshausen et al. (SI: Tab. S2) to derive the two extreme alternatives: sharp cumulative emissions versus uncertain risk (min/max) and uncertain cumulative emissions versus sharp risk (max/min). If we choose 1990 as start year, the cumulative

[2] IIASA's World Population Program reports 7.8 and 9.9 for the 10th and 90th percentiles.

CO_2-eq emissions for 1990–1999 are added to the cumulative CO_2-eq emissions for 2000–2050, but the risk and the uncertainty in the risk do not change.

The 2000–2050 constraint of 1500 Pg CO_2-eq entails a risk ranging from 10 to 43 % of exceeding 2 °C, with its center at 26 % (SI: Tab. S4; see also Tab. 1 in Meinshausen et al.). For comparison, we ran the 2 °C Check Tool (in a repetitive, trial-and-error mode) to determine the upper and lower CO_2-eq constraints for keeping the risk of exceeding 2 °C constant at 26 %, we found 1189 and 1945 Pg CO_2-eq cumulative emissions, respectively; acknowledging that the 2 °C Check Tool does not allow insertion of cumulative constraints for 2000–2050 below 1189 Pg CO_2-eq (see also Fig. S1a in Meinshausen et al.).

The uncertainty in cumulative emissions of 1189–1945 Pg CO_2-eq for 2000–2050 translates into an uncertainty in GEE values in 2050 that depends on start year choice (1990 or 2000). For 1990, we find a GEE interval of 1.8–4.7 with its center at 3.0 t CO_2-eq/cap; for 2000, we find a GEE interval of 0.9–4.4 with its center at 2.3 t CO_2-eq/cap. Considering, in addition, the uncertainty in the 2050 population estimate, we find 1.5–5.4 t CO_2-eq/cap for 1990–2050 and 0.8–5.1 t CO_2-eq/cap for 2000–2050 (Table 1: column "1500 Pg CO_2-eq").

Finally, we tweak the min-max uncertainty combination. The case of no uncertainty in the cumulative emissions constraint (1500 Pg CO_2-eq) is impacted, if expressed on a p/c basis, by the uncertainty in the population estimate. The respective GEE intervals are 2.5–3.5 t CO_2-eq/cap for 1990–2050 and 2.0–2.7 t CO_2-eq/cap for 2000–2050 (these adjusted GEE intervals are reported in Table 1). We did not reapply the 2 °C Check Tool to adjust the uncertainty in the risk of exceeding 2 °C.

2.4 Uncertainty in cumulative emissions and risk of exceeding 3 and 4 °C in 2050

In this section we translate the min/max and max/min uncertainty combinations for cumulative emissions and risk from 2 to 3 and 4 °C. This translation is graphically based and approximate but sufficient for present purposes. The stepwise release of the global temperature target for 2050 and beyond from 2 to 4 °C translates into a stepwise increase of the 2050 GEE values. The crucial question is whether these values can still be distinguished from each other given the underlying uncertainties in cumulative emissions and risk.

The translation is realized with the help of Figures 33 and 34 in Meinshausen (2005), which quantify the risk of overshooting global mean equilibrium warming ranging from 1.5 to 4 °C for different stabilization levels of CO_2-eq concentration. The details are outlined in SI (Note 5).

With this translation to hand and supported by the 2 °C Check Tool, we can explore the min/max and max/min uncertainty combinations investigated in Section 2.3 for: (i) cumulative emission constraints for 2000–2050 other than 1500 Pg CO_2-eq and (ii) temperature targets for 2050 and beyond other than 2 °C. In the first step, we keep the temperature target at 2 °C and expand our investigation of the min/max and max/min uncertainty combinations over a range of cumulative emission constraints that is well covered by the 2 °C Check Tool, here to constraints of 1800, 2100, and 2400 Pg CO_2-eq. In the next step we translate the risk contained in these min/max and max/min uncertainty combinations into the risk of exceeding 3 and 4 °C. Table 1 summarizes the expansion and translation process.

Prudence is needed, however. The assumptions underlying this expansion and translation process are that (i) the risk of overshooting is comparatively stable and independent of the particular warming situation, equilibrium or transient, when going from, e.g., 2 to 3 °C; and (ii) deviations from this assumption are minor compared to the considerable change in risk when going from 2 to 3 °C under either warming, equilibrium or transient.

Table 1 should be read as follows: the cumulative GHG emissions constraint for 2000–2050 of 1800 Gt CO_2-eq with reference to start year 1990 (Table 1a) results in a risk of between 20 and 58 % of exceeding the 2 °C temperature target if the p/c emissions (GEE) in 2050 center at 4.1 t CO_2-eq within the interval from 3.5 to 4.8 t CO_2-eq. If the latter interval is increased to 2.1–6.3 t CO_2-eq, the risk interval of exceeding the 2 °C temperature target decreases to about 38 %.[3] The two examples result in lower risks ranging between 5 and 26 % and 12–17 %, respectively, if the 1800 Gt CO_2-eq constraint is interpreted with regard to exceeding the 3 °C temperature target.

The comparison of the min/max uncertainty combinations—i.e., minimal uncertainty in GEE in 2050 and maximal uncertainty in the risk of exceeding 2, 3, or 4 °C in 2050 and beyond—across cumulative emission constraints for 2000–2050 ranging from 1500 to 2400 Pg CO_2-eq (or for GEE in 2050 ranging from 3.0 to 6.4 t CO_2-eq/cap) shows that the GEE values increasingly overlap. That is, distinguishing GEE values from each other for the various cumulative emission constraints becomes increasingly difficult. For example, with regard to exceeding the 4 °C temperature target: for the cumulative emissions constraint of 2100 Gt CO_2-eq the GEE uncertainty range goes from 4.5 to 6.1 t CO_2-eq/cap (with its center at 5.2 t CO_2-eq/cap). For comparison, for the cumulative emissions constraint of 2400 Gt CO_2-eq the GEE uncertainty range goes from 5.5 to 7.4 t CO_2-eq/cap (with its center at 6.4 t CO_2-eq/cap) (columns "2100 Pg CO_2-eq" and "2400 Pg CO_2-eq" in Table 1a).

Comparison of Table 1a (start year 1990) with Table 1b (start year 2000) also indicates uncertainty becoming too large for cumulative emission constraints for 2000–2050 above ~2100 Gt CO_2-eq. GEE values in 2050 can no longer be properly distinguished. We are at the limits in resolution terms of our graphical-based approach. Uncertainty overshadows differences in the GEE values resulting from differences in both cumulative emissions and start year.

2.5 Uncertainty in inventoried emissions

In this section we introduce diagnostic uncertainty which is related to the risk that true GHG emissions are greater than inventoried emission estimates reported at given time points. We are interested in the order of magnitude involved in correcting cumulative emission constraints so that this diagnostic uncertainty-related risk vanishes.

Analyzing uncertainty is an important tool for improving emission inventories containing uncertainty for various reasons (Lieberman et al. 2007, White et al. 2011). Jonas et al. (2010b) describe six techniques to analyze uncertain emission changes (signals) and we apply two of those techniques here: the undershooting (Und) and the combined undershooting and verification time concept (Und&VT). The two techniques differ, but common to them is that they apply undershooting to limit, or even reduce, the risk that true emissions are greater than agreed emissions in a target year—from 50 % (no undershooting: ignoring uncertainty altogether) to 0 % (with undershooting: the undershooting needed to make the diagnostic uncertainty-related risk vanish can be calculated).

The Und concept accounts for the trend uncertainty in the emission estimates between any two time points, e.g., start year and target year, and correlates uncertainty between these. The Und&VT concept also allows undershooting but accounts for the linear dynamics of the emission signal between start and target year, and the total uncertainty in the latter.

[3] Note that applying the 2 °C Check Tool as described in Section 2.3 but to a cumulative emissions constraint for 2000–2050 of 1800, instead of 1500 Pg CO_2-eq, does not encounter any limitations, which is why the risk interval is minimal for maximal uncertainty in p/c emissions and consists of a single value only.

Table 1 Interpreting the global cumulative GHG emission constraints for 2000–2050 of 1500 to 2400 Pg CO_2-eq with reference to start year **a**) 1990 and **b**) 2000; and in terms of uncertainty in both p/c emissions (GEE) in 2050 and risk of exceeding a temperature target in 2050 and beyond ranging between 2 and 4 °C. The table lists min/max and max/min combinations of these two uncertainties

a) Start year 1990 (1990–2050):

T	Uncertainty	in 2050 under a cumulative GHG emissions constraint for 2000–2050 of			
	min/max – max/min	1500 Pg CO_2-eq	1800 Pg CO_2-eq	2100 Pg CO_2-eq	2400 Pg CO_2-eq
°C	Uncertainty in emissions	t CO_2-eq/cap	t CO_2-eq/cap	t CO_2-eq/cap	t CO_2-eq/cap
	Uncertainty in risk	%	%	%	%
2	in emissions	3.0 [2.5 – 3.5]	4.1 [3.5 – 4.8]		
	in risk of exceeding 2 °C	10 – 43	20 – 58		
	in emissions	1.5 – 5.4	2.1 – 6.3		
	in risk of exceeding 2 °C	26 – 31	38		
3	in emissions		4.1 [3.5 – 4.8]	5.2 [4.5 – 6.1]	
	in risk of exceeding 3 °C		5 – 26	11 – 40	
	in emissions		2.1 – 6.3	3.5 – 7.8	
	in risk of exceeding 3 °C		12 – 17	21 – 26	
4	in emissions			5.2 [4.5 – 6.1]	6.4 [5.5 – 7.4]
	in risk of exceeding 4 °C			4 – 21	8 – 36
	in emissions			3.5 – 7.8	4.5 – 9.5
	in risk of exceeding 4 °C			9 – 13	17 – 21

b) Start year 2000 (2000–2050):

T	Uncertainty	in 2050 under a cumulative GHG emissions constraint for 2000–2050 of			
	min/max – max/min	1500 Pg CO_2-eq	1800 Pg CO_2-eq	2100 Pg CO_2-eq	2400 Pg CO_2-eq
°C	Uncertainty in emissions	t CO_2-eq/cap	t CO_2-eq/cap	t CO_2-eq/cap	t CO_2-eq/cap
	Uncertainty in risk	%	%	%	%
2	in emissions	2.3 [2.0 – 2.7]	3.7 [3.2 – 4.3]		
	in risk of exceeding 2 °C	10 – 43	20 – 58		
	in emissions	0.8 – 5.1	1.5 – 6.2		
	in risk of exceeding 2 °C	26 – 31	38		
3	in emissions		3.7 [3.2 – 4.3]	5.1 [4.4 – 5.9]	
	in risk of exceeding 3 °C		5 – 26	11 – 40	
	in emissions		1.5 – 6.2	3.2 – 7.9	
	in risk of exceeding 3 °C		12 – 17	21 – 26	
4	in emissions			5.1 [4.4 – 5.9]	6.5 [5.5 – 7.5]
	in risk of exceeding 4 °C			4 – 21	8 – 36
	in emissions			3.2 – 7.9	4.4 – 10.0
	in risk of exceeding 4 °C			9 – 13	17 – 21

SI (Note 6) illustrates the combining of diagnostic and prognostic uncertainty graphically. We find a downward shift for representative values of both diagnostic uncertainty (10 % constant in relative terms) and correlation in diagnostic uncertainty (0.75) of global emissions between start and target year, from 36.8 to 24.6 Pg CO_2-eq (Und technique) and from 36.8 to 23.5 Pg CO_2-eq

(Und&VT technique), respectively, between 1990 and 2050 (see also Fig. 1). This translates into a downward shift of about 2–5 % of the 1500 Pg CO_2-eq cumulative constraint for 2000–2050. GEE in 2050 are then 2.8 and 2.7 t CO_2-eq/cap, respectively. That is, to nullify the diagnostic uncertainty-related risk, the GEE intervals listed in the column "1500 Pg CO_2-eq" of Table 1a would need to be shifted downward by an additional 0.2 or 0.3 t CO_2-eq/cap, while the prognostic uncertainty-related risk of exceeding 2 °C is unimpaired.

2.6 Land use and land-use change until 2050

In this section we explain how we deal with emissions from LU activities, which are included in the model-based, global emission-climate change scenarios of Meinshausen et al. (2009). The cumulative CO_2 emissions from land-use activities range from -35 to 248 Pg CO_2 (80 % interval range) over the 2007–2050 period, with a median of 24 Pg CO_2. Cumulative emissions of 24 Pg CO_2 translate into an average of 0.56 Pg CO_2/yr.

Net emissions from LU activities are the least certain in our current understanding of anthropogenic changes in the global carbon cycle (Peters et al. 2011a). They are about 3.3±2.6 Pg CO_2 in 2010 and have apparently declined on average, from 5.5 Pg CO_2/yr during 1990–1999 to 4.0 Pg CO_2/yr during 2000–2009 (http://www.globalcarbonproject.org/carbonbudget/10/hl-full.htm, available via archive-org.com; and Pan et al. 2011). The net atmospheric carbon flux from 1850 to 2010 is modeled as a function of documented land-use change and changes in above- and belowground carbon from land-use change, with unmanaged ecosystems not considered (Houghton 2008).

Country-level LU emissions are equally difficult to deal with (IIASA 2007; Jonas et al. 2010c, 2011; Salk et al. 2013) and have at least comparable uncertainty.

As no fundamental analysis of the future state of terrestrial biospheric carbon stocks exists, we consider the case that the emission targets derived for 2050 are exclusively available for technospheric emissions and that deforestation and other LU mismanagement will cease by 2050, when we require net emissions from LU activities to balance at zero.

We consider this case unrealistic; however, it does allow us to evaluate the challenge of reducing technospheric GHG emissions globally under the assumption that the terrestrial biosphere behaves deterministically (without surprises and unknown feedbacks).

2.7 Accounting for known CO_2 emission transfers

Accounting for emissions can be viewed from both production and consumption perspectives. Historical emission estimates from a consumption perspective are becoming available, but not their uncertainties.

Under the KP, mitigation policy takes place at the country level and applies only to GHG emissions and removals within the country's national or offshore territorial jurisdiction. This territorial-based approach (production perspective) does not consider emission transfers between countries from international trade and may give a misleading interpretation of factors driving emission trends and therefore mitigation policies (EC 2011). To account for international CO_2 transfers, we employ the trade-linked global database for CO_2 emissions of Peters et al. (2011b). This covers 113 countries and/or regions and 57 economic sectors through time (1990–2008; see also Tab. S1 in the SI: the Global Carbon Project (GCP) provides updated data up to 2010) while excluding emissions from LU.

Grasping the spatial disconnect between biomass production and consumption is less advanced. Erb et al. (2009b) use the concept of embodied human appropriation of net primary production (HANPP) to map the global pattern of net-producing and net-consuming regions in

2000 (see also Haberl et al. 2007; Erb et al. 2009a). HANPP measures the extent to which "human activities affect NPP (net primary production) and its availability in the ecosystem as a source of nutritional energy and other ecosystem processes."[4] In contrast, embodied HANPP (eHANPP) is defined as "the NPP appropriated in the course of biomass production, encompassing losses along the production chain as well as productivity changes induced through land conversion or harvest. By making the pressure exerted on ecosystems associated with imports and exports visible, eHANPP allows for the analysis of teleconnections between producing and consuming regions" (Haberl et al. 2009: 119, 121). According to Erb et al. (2009b), international net transfers of eHANPP amount to 6.2 Pg CO_2 in 2000 and are thus of global significance.

Reducing emissions from LU to zero requires discussion of the state of sustainability (including the uncertainties involved) that the terrestrial biosphere will assumedly attain in 2050 under a 2, 3 or 4 °C temperature target. Although the intention behind developing the HANPP concept was different at the time, we consider it useful for tracking sustainability (SI: Note 7).

We employ HANPP embodied in biomass trade to estimate the fraction of global LU emissions traded. This side-step is necessary given the current problematic situation of LU data. Net emissions from LU for 1850–2010 (GCP's carbon budget 2010; Peters et al. 2011a), currently resolve only large regions/continents, not large countries. We preserve GCP's previous set of global LU emission data because, although it only lists emissions until 2005, it does resolve a small number of large countries or units of countries (Canada, China, the USA, and Europe as a whole). Their emission estimates can show considerable discrepancies when compared to the land use, land-use change, and forestry (LULUCF) emission estimates reported by these countries under the UNFCCC (United Nations Framework Convention on Climate Change). These discrepancies are also noted by the World Resources Institute, whose Climate Analysis Indicators Tool (CAIT) employs additional land-use change and forestry data from the 2010 *World Development Report* to resolve the 25 largest emissions contributors for 1990–2005 (WRI 2011).

We consider LU and LULUCF emissions data—which typically disagree with each other and also underestimate real emissions as observed top-down by the "atmosphere"—as sufficiently good to indicate whether the directly human-impacted part of a country's terrestrial biosphere is a net source or net sink. We also use HANPP embodied in biomass trade ($eTrade_{NPP}$=ImpNPP−ExpNPP) to indicate whether a country is a net importer or net exporter of biomass (SI: Note 8).

We apply a globally averaged approach to link $eTrade_{NPP}$ with national LU emissions. This assumes that HANPP and LU emissions refer to the same directly human-impacted part of the terrestrial biosphere. A direct consequence of our approach is that the human appropriation of biomass results in a positive flux to the atmosphere. We use the ratio of net transfer of embodied HANPP to total HANPP to specify the fraction of global LU emissions traded ($eTrade_{LU}$) by country.[5] Traded LU emissions are added to a country's national LU (or LULUCF) emissions, thereby switching from a production to a consumption perspective. Net transfers of LU emissions balance when globally summed. This approach is simple and straightforward, and the calculation of national plus traded emissions is unambiguous.

[4] Ito (2011) provides a historical meta-analysis of global NPP (1860s–2000s) which allows Haberl and Erb's HANPP concept with reference to 2000 to be put into a long-term temporal perspective.

[5] Haberl et al. (2007: Tab. 1) estimate total HANPP in 2000 to be 57.2 Pg CO_2 (including human-induced fires), of which about 6.2 Pg CO_2 is internationally transferred (net transfer) according to Erb et al. (2009b: Tab. 2) (about 7.2 Pg CO_2 according to the data communicated to us).

2.8 Additional insights from models

We employ two types of models that are prognostic or run in a prognostic mode to help bridge reference concepts and norms (SI: Tab. S2). The first type encompasses IIASA's GAINS (Greenhouse gas – Air pollution INteractions and Synergies) model. GAINS allows broadening of the applied contraction & convergence approach by making the step from emissions p/c to costs p/c in the context of discussing Annex I countries' mitigation pledges for 2020.[6]

The second model type encompasses the class of large-scale, energy-economic, and integrated assessment models, from which we selected three illustrative scenarios to 2100 that stabilize atmospheric GHG concentrations at low levels. The scenarios help us deviate from the contraction & convergence reference approach by making the step from emissions p/c to emission intensities measured as emissions per GDP (gross domestic product) in the context of discussing emission reduction scenarios to 2100. We discuss the models in SI (Note 3). In Section 3 below we apply them with the focus on technospheric emissions and exclude CO_2 emissions from land use and land-use change.

3 Results

For illustration, we present uncertainty in the elaborated emissions-temperature systems context for two selected countries, the USA and China. A third example, Austria, is included in SI (Note 9). We select 1990 as start year.

3.1 USA, a data-rich country with high total and p/c emissions

Figure **2**a (see also Table 2) shows that to meet global cumulative emission constraints between 1500 and 2400 Pg CO_2-eq for 2000–2050, each individual within the USA must reduce his/her production-based GHG emissions on average by between 88 % and 74 % from 1990 to 2050. The dark- and light-gray lines (solid and broken) indicate the target paths emissions must follow to achieve universal p/c targets between 3.0 and 6.4 t CO_2-eq. Countries currently emitting p/c quantities above these lines will need to compensate by emitting below the gray lines before 2050 to ensure targets are reached.

As explained in Sections 2.3 and 2.4, the emission target paths can be interpreted in terms of min/max and max/min combinations of uncertainty in both p/c emissions in 2050 and risk of exceeding a specified temperature target in the 2–4 °C range in 2050 and beyond. Table 1a reproduces these min/max uncertainty combinations (see below).

The thick solid black curve in Fig. **2**a shows the technosperic emissions of the six Kyoto GHGs (CO_2, CH_4, N_2O, HFCs, PFCs, and SF_6[7]; excluding CO_2 emissions from land use and land-use change) between 1990 and 2009 as reported by the USA to the UNFCCC; the thin solid black curve additionally considers fossil-fuel emissions embodied in trade, indicating that the USA turned from net exporter to net importer between 1994 and 1998. Comparison with the aforementioned emission target paths shows the USA to be operating beyond a 4 °C global warming. The USA's technospheric emissions are far above the uppermost emission target path, which satisfies a cumulative emissions constraint of 2400 Pg CO_2-eq for 2000–2050 and

[6] See http://unfccc.int/parties_and_observers/parties/annex_i/items/2774.php for Annex I countries to the UNFCCC.

[7] Respectively, carbon dioxide, methane, nitrous oxide, hydrofluorocarbon, sulfur hexafluoride, perfluorocarbon

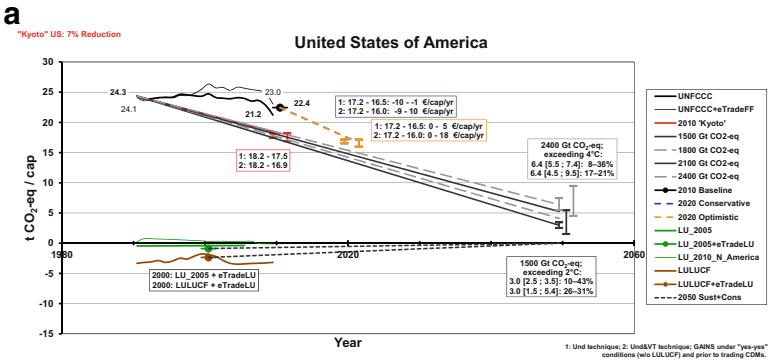
a
"Kyoto" US: 7% Reduction
United States of America
t CO2-eq / cap
Year
1: 17.2 - 16.5: -10 - -1 €/cap/yr
2: 17.2 - 16.0: -9 - 10 €/cap/yr
1: 17.2 - 16.5: 0 - 5 €/cap/yr
2: 17.2 - 16.0: 0 - 18 €/cap/yr
1: 18.2 - 17.5
2: 18.2 - 16.9
2400 Gt CO2-eq; exceeding 4°C: 6.4 [5.5 ; 7.4]: 8–36% 6.4 [4.5 ; 9.5]: 17–21%
1500 Gt CO2-eq; exceeding 2°C: 3.0 [2.5 ; 3.5]: 10–43% 3.0 [1.5 ; 5.4]: 26–31%
2000: LU_2005 + eTradeLU
2000: LULUCF + eTradeLU
UNFCCC
UNFCCC+eTradeFF
2010 'Kyoto'
1500 Gt CO2-eq
1800 Gt CO2-eq
2100 Gt CO2-eq
2400 Gt CO2-eq
2010 Baseline
2020 Conservative
2020 Optimistic
LU_2005
LU_2005+eTradeLU
LU_2010_N_America
LULUCF
LULUCF+eTradeLU
2050 Sust+Cons
1: Und technique; 2: Und&VT technique; GAINS under "yes-yes" conditions (w/o LULUCF) and prior to trading CDMs.

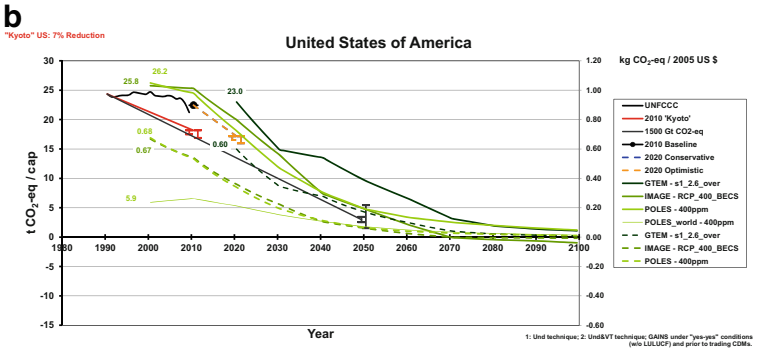
b
"Kyoto" US: 7% Reduction
United States of America
t CO2-eq / cap
kg CO2-eq / 2005 US $
Year
UNFCCC
2010 'Kyoto'
1500 Gt CO2-eq
2010 Baseline
2020 Conservative
2020 Optimistic
GTEM - s1_2.6_over
IMAGE - RCP_400_BECS
POLES - 400ppm
POLES_world - 400ppm
GTEM - s1_2.6_over
IMAGE - RCP_400_BECS
POLES - 400ppm
1: Und technique; 2: Und&VT technique; GAINS under "yes-yes" conditions (w/o LULUCF) and prior to trading CDMs.

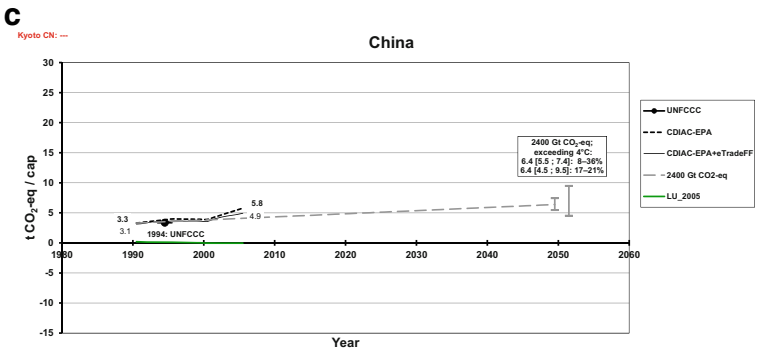
c
Kyoto CN: ---
China
t CO2-eq / cap
Year
2400 Gt CO2-eq; exceeding 4°C: 6.4 [5.5 ; 7.4]: 8–36% 6.4 [4.5 ; 9.5]: 17–21%
1994: UNFCCC
UNFCCC
CDIAC-EPA
CDIAC-EPA+eTradeFF
2400 Gt CO2-eq
LU_2005

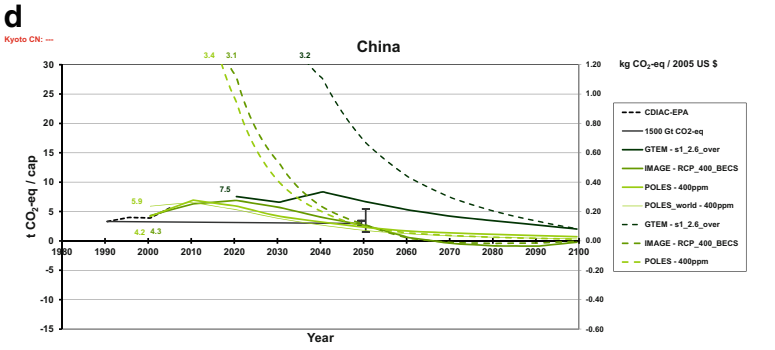
d
Kyoto CN: ---
China
t CO2-eq / cap
kg CO2-eq / 2005 US $
Year
CDIAC-EPA
1500 Gt CO2-eq
GTEM - s1_2.6_over
IMAGE - RCP_400_BECS
POLES - 400ppm
POLES_world - 400ppm
GTEM - s1_2.6_over
IMAGE - RCP_400_BECS
POLES - 400ppm

◀ **Fig. 2** **a** USA (1990–2050): National GHG emissions and removals and near-term mitigation policies and measures in a globally consistent and long-term GHG emissions-temperature-uncertainty context. Technospheric emissions are budget-constrained globally for 2000–2050 but exhibit quantitative uncertainty; while emissions from land use and land-use change (LU and LULUCF) reduce to zero, global temperature targets for 2050 and beyond range between 2 and 4 °C, and compliance with an agreed temperature target is uncertain and entails a risk of exceedance. For further explanations see text. **b** USA (1990–2050): The figure takes over relevant technospheric emission entries of Fig. 2a. In addition, the figure shows three globally-embedded, long-term emission reduction scenarios as realized by GTEM, IMAGE and POLES for the USA. They allow switching between emission reduction perspectives, here from emission reduction p/c (*thick solid, dark to light, green lines*; in t CO_2-eq/cap) to emission reduction per GDP (*thick broken, dark to light, green lines*; in kg CO_2-eq per 2005 US $). The additional thin solid, light green line also belongs to POLES. It shows how POLES performs globally (in t CO_2-eq/cap). It allows the effectiveness of the USA s emission reduction to be put into a global perspective. **c** China (1990–2050): See caption to Fig. 2a and text. **d** China (1990–2050): See caption to Fig. 2b and text

which, as Table 1a indicates, must preferably be interpreted with reference to 4 °C (and higher) temperatures in 2050 and beyond.

Underneath, the (hardly visible) red line shows what p/c emission levels the USA would have committed to in 2010 had it ratified the Kyoto Protocol which stipulates a 7 % emission reduction. Per capita emissions would have practically followed the 2400 Pg CO_2-eq constraint.

The solid black dot shows estimated production-based emissions for 2010 according to IIASA's GAINS model.

The broken blue and orange lines (the latter covers the first) show expected p/c emission reductions for 2010–2020 according to the USA's conservative and optimistic pledges in 2010 (the two pledges—17 % reduction until 2020 relative to 2005—are identical in the case of the USA). The costs for achieving these pledges by applying known mitigation techniques are mentioned in the blue- and orange-framed boxes (GAINS output). The conservative and optimistic pledges to reduce emissions until 2020 are not necessarily identical for the other Annex I countries. IIASA's GAINS model is run in a mode that allows emissions exchange among Annex I countries, and between Annex I and developing countries (i.e., "with Annex I trading" and "with CDM measures"). The conservative and optimistic pledges of the other Annex I countries do not affect the USA's pledge to reduce emissions but do impact the costs of achieving these reductions. The costs differ depending on whether GAINS applies conservative or optimistic country pledges. Negative costs mean that implemented emission reduction measures pay back during their lifetime.

The ranges shown numerically in the red, blue, and orange boxes and graphically by the "I" shape at the end of the red, blue, and orange lines reflect the current range of diagnostic uncertainty (0.7–1.3 t CO_2-eq/cap) in estimating emissions; or, alternatively, the undershooting required to reduce the risk from 50 to 0 % that true emissions are greater than agreed targets or pledges. The uncertainty ranges take into account: (i) uncertainty in GHG inventories in both start and target year; and (ii) uncertainty in the GHG inventory in only the target year.[8] They are derived by applying the two emission change-uncertainty analysis techniques mentioned in Section 2.5. Adjusting the pledges of a country for undershooting—in the USA's case from 17.2 to 16.5 t CO_2-eq/cap according to the Und concept and from 17.2 to 16.0 t CO_2-eq/cap according to the Und&VT concept and reapplying GAINS allows the uncertainty in mitigation costs to be specified (see blue and orange boxes).

[8] We employ a total uncertainty in relative terms of 7.5 % (representing the median of the relative uncertainty class 5–10 %) for reporting the emissions of the six Kyoto GHGs excluding emissions from land use and land-use change in both reference and target year; and 0.75 for the correlation in these uncertainties (Jonas et al. 2010b).

Table 2 P/c GHG emissions (excluding CO_2 emissions from land use and land-use change) globally and by country in 1990 and for 2050 required to meet global cumulative emission constraints for 2000–2050 ranging between 1500 and 2400 Pg CO_2-eq. Percentage emission reductions refer to 1990–2050 (negative reduction = increase)

Global / Country	1990 Emissions	2050 GEE target under a cumulative emissions constraint for 2000–2050 of			
		1500 Pg CO_2-eq	1800 Pg CO_2-eq	2100 Pg CO_2-eq	2400 Pg CO_2-eq
	t CO_2-eq/cap	t CO_2-eq/cap	t CO_2-eq/cap	t CO_2-eq/cap	t CO_2-eq/cap
		3.0	4.1	5.2	6.4
		1990–2050 emission reduction			
		% / cap	% / cap	% / cap	% / cap
Global[a]	5.9	50	30	11	−8
USA[b]	24.3	88	83	78	74
China[c]	3.3	11	−24	−59	−93
Austria[b]	10.2	71	60	48	37

[a] POLES

[b] UNFCCC

[c] CDIAC, EPA, and UN POP

Diagnostic uncertainty has not been introduced and combined with the prognostic uncertainties which we show (in gray) for the lowest and highest GEE targets in 2050 (3.0 and 6.4 t CO_2-eq/cap, respectively). Reducing diagnostic uncertainty to 0 % results in a downward shift of the prognostic uncertainty intervals (and the respective target paths). For instance, the min/max interval, [2.5 ; 3.5], around the lowest GEE target (3.0 t CO_2-eq/cap), by an additional 0.2 or 0.3 t CO_2-eq/cap, dependent on emission change-uncertainty analysis technique applied. This downward shift will not impair the prognostic-uncertainty related risk of exceeding the agreed temperature targets (SI: Note 6).

Both the solid green line and the solid brown line show p/c emissions from land use and land-use change within US territory, the first LU emissions for 1990–2005 (from GCP's LU emissions for 1850–2005) and the second LULUCF emissions for 1990–2009 (reported by the USA under the UNFCCC). The difference between the two is considerable. For comparison, the thin solid green line shows LU emissions for 1990–2010 (from GCP's LU emissions for 1850–2010) but for North America as a whole. GCP's LU emissions for 1850–2005 classify the USA as a moderate sink and Canada as a moderate source (the first slightly greater than the second in absolute terms), while North America as a whole only turns from moderate source to moderate sink around 2006/07, according to GCP's LU emissions for 1850–2010.

Both the solid green and solid brown dots correct the USA's p/c emissions from land use and land-use change for biomass embodied in trade ($eTrade_{LU}$) in 2000. The corrections refer to the GCP LU emissions for 1850–2005 and to the UNFCCC LULUCF emissions for 1990–2009. With these corrections we switch the perspective from production to consumption indicating that, while the directly human-impacted part of the USA's terrestrial biosphere acts as a net sink, the country is also a net biomass exporter. It would greatly benefit the USA to switch to reporting that accounts for $eTrade_{LU}$ (SI: Fig. S3 – case 4, solid arrow).

Although only 2000 data are available to study $eTrade_{LU}$, the magnitude of the adjustment involved in switching from a production to consumption perspective is substantial and greater in relative terms than switching perspectives for technospheric emissions. The dotted gray lines acknowledge this finding. They represent the paths to lowering the USA's p/c emissions

from land use and land-use change plus those embodied in $eTrade_{LU}$ to zero, assuming that the terrestrial biosphere as of today (~2000) represents a sustainable state to be reached in 2050.

Figure 2b takes over some, but not all, technospheric emission entries of Fig. 2a. The figure also shows three solid, dark-to-light, green lines. These reflect typical aggressive, long-term emission reduction scenarios (excluding CO_2 emissions from land use and land-use change; in t CO_2-eq/cap) as realized by GTEM, IMAGE, and POLES for the USA and explained in Section 2.8 and SI (Note 4). Even these scenarios fail to meet the condition of equal emissions above and below the gray reference pathway, which reflects the cumulative constraint of 1500 Gt CO_2-eq for 2000–2050 and ensures the 2 °C target will be reached (Table 1a). However, this looks different at the global scale. The additional thin solid light-green line belongs to POLES. It shows how p/c emissions decrease globally. The global emission reduction scenarios behind the other two USA scenarios are not shown. These are very similar to the global POLES scenario shown in the figure. In 2050 the global POLES scenario considerably undershoots the GEE target of 3.0 t CO_2-eq/cap (belonging to the 1500 Gt CO_2-eq constraint; Table 2).

Emission intensity paths (in kg CO_2-eq per 2005 US $) for the USA that correspond to the p/c emission reduction paths (solid, dark-to-light, green lines) are entered with the help of an additional vertical axis (to the right in Fig. 2b). The emission intensity paths correspond in color but are indicated as broken lines. Switching between the two emission reduction scales is straightforward.

3.2 China, a developing country with high total but lower p/c emissions

Figure 2c is similar to Fig. 2a but shows data for China, a country with high total emissions, no KP commitments, and less abundant data on GHG emissions and sinks. We use emission data of the Carbon Dioxide Information Analysis Center (CDIAC) (CO_2) and Environmental Protection Agency (EPA) (non-CO_2) emission data to visualize China's technospheric emissions for 1990–2005 (SI: Tab. S1) because UNFCCC-reported emissions are for one year only (1994). The difference between technospheric emissions in 1994 was about 0.5 CO_2-eq/cap (CDIAC-EPA: 3.9; UNFCCC: 3.4). The UNFCCC emissions value still falls below the highest emission target path which the figure resolves and which reflects the cumulative emissions constraint of 2400 Pg CO_2-eq for 2000–2050 (target path in 1994: 3.5 CO_2-eq/cap). For a better overview we entered only this emission target path. It not only indicates that China's p/c emissions were allowed to increase by 93 % between 1990 and 2050 (Table 2), but shows too that, from about 2000 onward, China's emissions began to exceed this target path and its upper "uncertainty wedge" (determined by the maximal uncertainty in the 2050 GEE value). To recall, the cumulative emissions constraint of 2400 Pg CO_2-eq should preferably be interpreted with reference to 4 °C in 2050 and beyond. However, considering fossil-fuel emissions embodied in trade—China is a net exporter resulting in a reduction of its territorial emissions—brings its emissions back into the wedge-shaped uncertainty range.

GCP's LU emissions for 1850–2005 classify China as a moderate source before 1999/2000 and moderate sink thereafter. However, considering biomass import and export and, thus, embodied LU emissions—China was a net importer of biomass in 2000—appears to nullify this sink and reclassify China as a moderate source.

Figure 2d is similar to Fig. 2b. Regarding the USA, the aggressive, long-term emission reduction scenarios (in t CO_2-eq/cap) of GTEM, IMAGE, and POLES[9] fail to meet the

[9] Respectively, Global Trade and Environment Model; Integrated Model to Assess the Greenhouse Effect; Prospective Outlook on Long-term Energy Systems (model)

condition of equal emissions above and below the gray reference pathway, which belongs to the cumulative constraint of 1500 Gt CO_2-eq for 2000–2050 and ensures the 2 °C target will be reached (Table 1a). However, in contrast to the USA, two of the reduction scenarios (those of IMAGE and Poles) show that, in the long-term, China's p/c emissions closely follow the global average (by POLES) or even fall below.

Another difference is the remarkable decrease of China's emission intensities realized by all three models. This, together with its low p/c emissions and the projected rapid growth of its economy, explains why China's national response strategy to climate change prioritizes improvement of energy conservation, energy intensity reduction, and improved energy-use efficiency (http://www.beconchina.org/energy_saving.htm).

4 Summary and conclusions

Our study focuses on uncertainty in anthropogenic GHG emissions including emissions from land use and land-use change activities. Our aim was to understand the relevance of diagnostic and prognostic uncertainty in an emissions-temperature setting that seeks to constrain global warming and to link uncertainty consistently across temporal scales.

We discuss diagnostic and prognostic uncertainty in a systems setting that allows any country to understand its national and near-term mitigation and adaptation efforts in a globally consistent and long-term context. In this context cumulative emissions are constrained and globally binding but exhibit quantitative uncertainty, and whether or not compliance with an agreed temperature target will be achieved is also uncertain. To facilitate discussions, we focus on two countries, the USA and China, while limiting global temperature rise to 2, 3, or 4 °C. We show:

- That both diagnostic and prognostic uncertainty need to be considered to facilitate more educated (precautionary) decisions on reducing emissions, given an agreed future temperature target.
- How to combine the two uncertainties which we consider independent. We note that our mode of bridging uncertainty across temporal scales still relies on discrete points in time and is not yet continuous.
- How to perceive diagnostic and prognostic uncertainty–related risk in combination. Here, diagnostic uncertainty refers to the uncertainty contained in inventoried emission estimates and is related to the risk that true GHG emissions are greater than inventoried emission estimates reported in a specified year. In contrast, prognostic uncertainty is derived from a multitude of model-based, forward-looking emission-climate change scenarios; it refers to cumulative emissions between a start year and a future target year, and can be related to the risk that an agreed temperature target is exceeded. We find that, to nullify the diagnostic uncertainty-related risk, the GEE intervals listed in the column (e.g.) "1500 Pg CO_2-eq" of Table 1a would need to be shifted downward by an additional 0.2 or 0.3 t CO_2-eq/cap, while the prognostic uncertainty–related risk of exceeding the 2 °C is unimpaired.
- That, as a direct consequence of the not unequivocal relationship between cumulative emissions and risk, a sharp cumulative emissions value translates into a risk interval for exceeding the agreed temperature target and, vice versa, a sharp risk value translates into a cumulative emissions interval. We interpret these intervals in terms of prognostic uncertainty and make use of the two extreme alternatives – sharp cumulative emissions versus uncertain risk (min/max) and uncertain cumulative emissions versus sharp risk (max/min).

- That scientists face difficulties in adequately embedding cumulative emissions from land use and land-use change in this emission-temperature setting because an achievable future state of sustainability for the terrestrial biosphere in toto has not yet been defined.
- That treating diagnostic uncertainty reaches its limits in the case of sparse data as given, in general, for reporting technospheric GHG emissions by non-Annex I countries and for reporting emissions from land use and land-use change by all countries.
- That prognostic uncertainty becomes too large for cumulative emission constraints for 2000–2050 above ~2100 Gt CO_2-eq. Above 2100 Gt CO_2-eq, GEE values in 2050 can no longer be properly distinguished. Uncertainty overshadows differences in the GEE values which result from differences in both cumulative emissions and start year. Thus our approach cannot be used for temperature targets in 2050 and beyond greater than 4 °C.

Acknowledgement This study was financially supported by the Austrian Climate Research Programme (B068706).

References

Allen MR et al (2009) Warming caused by cumulative carbon emissions toward the trillionth tonne. Nature 458(7242):1163–1166

Canadell JG et al (2007) Contributions to accelerating atmospheric CO_2 growth from economic activity, carbon intensity, and efficiency of natural sinks. PNAS 104(47):18866–18870

EC (2011) 2011 literature review archives – policy/mitigation. Environment Canada, Gatineau, http://www.ec.gc.ca/sc-cs/default.asp?lang=En&n=ACF3648C-1 (accessed 25 January 2012)

Erb K-H et al (2009a) Analyzing the global human appropriation of net primary production – processes, trajectories, implications. An introduction. Ecol Econ 69(2):250–259

Erb K-H et al (2009b) Embodied HANPP: mapping the spatial disconnect between global biomass production and consumption. Ecol Econ 69(2):328–334

Fisher BS, Nakicenovic N (lead authors) (2007) Issues related to mitigation in the long-term context. In: Climate Change 2007: Mitigation of Climate Change. Metz B et al. (eds). Cambridge University Press, United Kingdom, 169–250

GCI (2012) Contraction and convergence: climate justice without vengeance. Global Commons Institute (GCI), United Kingdom, http://www.gci.org.uk (accessed 14 March 2012)

Haberl H et al (2007) Quantifying and mapping the human apprpriation of net primary production in earth's terrestrial ecosystems. PNAS 104(31):12942–12947

Haberl H et al (2009) Using embodied HANPP to analyze teleconnections in the global land system: conceptual considerations. Geogr Tidsskr-Dan J Geogr 109(2):119–130, http://rdgs.dk/djg/pdfs/109/2/Pp_119-130_109_2.pdf

Houghton RA (2008) Carbon flux to the atmosphere from land-use changes: 1850–2005. In TRENDS: a compendium of data on global change. Carbon Dioxide Information Analysis Center, Oak Ridge National Laboratory, United States of America. http://cdiac.ornl.gov/trends/landuse/houghton/houghton.html (accessed 09 January 2012)

IIASA (2007) Uncertainty in greenhouse gas inventories. IIASA Policy Brief, #01, International Institute for Applied Systems Analysis, Austria. http://www.iiasa.ac.at/Publications/policy-briefs/pb01-web.pdf

Ito A (2011) A historical meta-analysis of global terrestrial net primary productivity: are estimates converging? Glob Change Biol 17(10):3161–3175

Jonas M et al (2010a) Benefits of dealing with uncertainty in greenhouse gas inventories: introduction. Clim Change 103(1–2):3–18

Jonas M et al (2010b) Comparison of preparatory signal analysis techniques for consideration in the (post-) Kyoto policy process. Clim Change 103(1–2):175–213

Jonas M et al (2010c) Dealing with uncertainty in GHG inventories: how to go about it? In: Marti K, Ermoliev Y, Makowski M (eds) Coping with uncertainty: robust solutions. Springer, Berlin, pp 229–245

Jonas M et al (2011) Lessons to be learned from uncertainty treatment: conclusions regarding greenhouse gas inventories. In: White T et al (eds) Greenhouse gas inventories: dealing with uncertainty. Springer, Netherlands, pp 339–343

Lieberman D et al. (eds.) (2007) Accounting for climate change. Uncertainty in greenhouse gas inventories—verification, compliance, and trading. Springer, Netherlands

Matthews HD et al (2009) The proportionality of global warming to cumulative carbon emissions. Nature 459(7248):829–833

Meinshausen M (2005) Emission & concentration implications of long-term climate targets. Dissertation, DISS. ETH NO. 15946, Swiss Federal Institute of Technology Zurich, Switzerland. http://www.up.ethz.ch/publications/documents/Meinshausen_2005_dissertation.pdf (accessed 30 September 2011)

Meinshausen M et al (2009) Greenhouse-gas emission targets for limiting global warming to 2 °C. Nature 458(7242):1158–1162

Pan Y et al (2011) A large and persistent carbon sink in the world's forests. Science 333(6045):988–993

Peters GP et al (2011a) Rapid growth in CO_2 emissions after the 2008–2009 global financial crisis. Nat Clim Change 2:2–4

Peters GP et al (2011b) Growth in emission transfers via international trade from 1990–2008. PNAS 108(21): 8903–8908

Raupach MR et al (2011) The relationship between peak warming and cumulative CO_2 emissions, and its use to quantify vulnerabilities in the carbon-climate-human system. Tellus 63B(2):145–164

Rogelj J et al (2011) Emission pathways consistent with a 2 °C global temperature limit. Nat Clim Change 1: 413–418

Salk C, Jonas M, Marland G (2013) Strict accounting with flexible implementation: the first order of business in the next climate treaty. Carbon Manag 4(3):253–256

Victor DG (2009) Global warming: why the 2 °C goal is a polticial delusion. Nature 459(7249):909

WBGU (1995) Scenario for the derivation of global CO_2 reduction targets and implementation strategies. Statement at UNFCCC COP1 in Berlin. Special Report, German Advisory Council on Global Change. http://www.wbgu.de/fileadmin/templates/dateien/veroeffentlichungen/sondergutachten/sn1995/wbgu_sn1995_engl.pdf (accessed 17 November 2011)

WBGU (2009) Solving the climate dilemma: the budget approach. Special Report, German Advisory Council on Global Change. http://www.wbgu.de/fileadmin/templates/dateien/veroeffentlichungen/sondergutachten/sn2009/wbgu_sn2009_en.pdf (accessed 28 September 2011)

White T et al (eds) (2011) Greenhouse gas inventories: dealing with uncertainty. Springer, Netherlands

WRI (2011) CAIT: Greenhouse gas sources & methods. Document accompanying the Climate Analysis Indicators Tool (CAIT), v.9.0. World Resources Institute, Washington DC. http://cait.wri.org/downloads/cait_ghgs.pdf (accessed 17 January 2012)

Zickfeld K et al (2009) Setting cumulative emissions targets to reduce the risk of dangerous climate change. PNAS 106(38):16129–16134

DOI 10.1007/978-3-319-15901-0_3
Reprinted from *Climatic Change* Journal, DOI 10.1007/s10584-013-0826-0

Changes in European greenhouse gas and air pollutant emissions 1960–2010: decomposition of determining factors

Peter Rafaj · Markus Amann · José Siri · Henning Wuester

Received: 14 December 2012 / Accepted: 17 June 2013 / Published online: 4 July 2013
© Springer Science+Business Media Dordrecht 2013

Abstract This paper analyses factors that contributed to the evolution of SO_2, NO_x and CO_2 emissions in Europe from 1960 to 2010. Historical energy balances, along with population and economic growth data, are used to quantify the impacts of major determinants of changing emission levels, including energy intensity, conversion efficiency, fuel mix, and pollution control. Time series of emission levels are compared for countries in Western and Eastern Europe, throwing light on differences in the importance of particular emission-driving forces. Three quarters of the decline in SO_2 emissions in Western Europe resulted from a combination of reduced energy intensity and improved fuel mix, while dedicated end-of-pipe abatement measures played a dominant role in the reduction of NO_x emissions. The increase in atmospheric emissions in Eastern Europe through the mid-1990s was associated with the growth of energy-intensive industries, which off-setted the positive impact of better fuel quality and changes in fuel mix. A continuous decrease in energy intensity and higher conversion efficiencies have been the main factors responsible for the moderate rate of growth of European CO_2 emissions.

Abbreviations

Bln	Billion
CAP	Capita, person
CLRTAP	Convention on Long-range Transboundary Air Pollution
CO	Carbon monoxide
CO_2	Carbon dioxide
EEU	Eastern Europe
EKC	Environmental Kuznets curve

This article is part of a Special Issue on "Third International Workshop on Uncertainty in Greenhouse Gas Inventories" edited by Jean Ometto and Rostyslav Bun.

P. Rafaj (✉) · M. Amann · J. Siri
International Institute for Applied Systems Analysis (IIASA), Schlossplatz 1, 2361 Laxenburg, Austria
e-mail: rafaj@iiasa.ac.at

H. Wuester
United Nations Framework Convention on Climate Change (UNFCCC), Martin-Luther-King-Str. 8, 53175 Bonn, Germany

EMEP	European Monitoring and Evaluation Programme
EU	European Union
FGD	Flue gas desulphurisation
GAINS	Greenhouse gas and Air pollution Interactions And Synergies model
GDP	Gross domestic product
GHG	Greenhouse gas
Gt	Giga tonnes
IEA	International Energy Agency
J	Joule (M Mega 10^6, G Giga 10^9, P Peta 10^{15})
Mt	Mega tonnes
NO_x	Nitrogen oxides
PM	Particulate matter
PPP	Purchasing power parity
RAINS	Regional Air pollution Information and Simulation model
SO_2	Sulfur dioxide
UNFCCC	United Nations Framework Convention on Climate Change
US-$	US dollar
VOCs	Volatile organic compounds
WEU	Western Europe

1 Introduction

Over the last century, Europe has experienced a long phase of dynamic growth in emissions of air pollutants and greenhouse gases. However, the 1970's saw a dramatic reduction in Western European SO_2 emissions, followed by a clear decline in emissions of NO_x a decade later. In contrast, the growth rate of CO_2 emissions has not changed.

There are various hypotheses concerning the underlying factors and driving forces responsible for these observed patterns in air pollutant emissions. For instance, economists have proposed the existence of an environmental Kuznets curve (EKC), under which pollution increases at low levels of income up to a turning point beyond which it decreases, in reference to the original Kuznets curve for economic inequality (Kuznets 1955). Reasons for such an inverted U-shaped relationship are hypothesized to include income-driven changes in: (1) the composition of production and/or consumption; (2) consumer preference for environmental quality; (3) institutions that are needed to internalize externalities; and/or (4) increasing returns to scale associated with pollution abatement. Other voices point to the structural changes in energy and industrial systems that resulted from the increase in global energy prices that followed the 1970's oil crisis, which also reduced the consumption of the most-polluting fuels. Environmentalists often emphasize the elaborate national and international frameworks of environmental legislation through which European countries agreed to take dedicated measures to reduce their emissions, *inter alia* by applying advanced end-of-pipe emission control technologies (Hordijk and Amann 2007).

We explore and quantify the impacts of such driving forces on changes in a set of selected emission species (SO_2, NO_x and CO_2) in Europe between 1960 and 2010, developing two identities that explain observed emissions as the product of key factors. In keeping with the hypothesized EKC, the first identity incorporates three terms: population, per capita income, and per capita emissions. The second identity decomposes the latter into macroeconomic changes, changes in the energy system, and dedicated environmental policy interventions. We assess the evolution of these factors between 1960 and 2010 and attempt to associate observed variations with important exogenous events.

We then estimate the combined impacts of these factors on emission trajectories for Western and Eastern Europe, respectively. While specific factors differ from country to country, this analysis should improve understanding of the relative importance of driving forces in European atmospheric pollution trends: economic welfare (as suggested by the EKC), emerging technological and structural factors, and/or awareness of the harmful environmental impacts of pollution, as reflected in pan-European environmental policies.

The following section briefly reviews the literature on the EKC, summarizing some of the motivations for this study. Section 3 describes our methods and data. Section 4 discusses the evolution of driving forces and resulting emissions of SO_2, NO_x and CO_2 from 1960 to 2010; it provides a theoretical basis for the decomposition analysis and highlights the most important empirical results, including detailed findings for selected countries. Section 5 places the quantitative assessment of the main determinants within a broader policy context. The final section presents conclusions and discusses some policy implications of the main findings.

2 The environmental Kuznets curve

The EKC hypothesis emerged from the debate over the fundamental determinants of long-term improvements in the environment, and particularly from a growing literature on the relationship between pollution and economic growth. It suggests that there is an inverted U-shaped relationship between environmental quality and wealth, such that pollution first increases with economic growth, but then decreases once a certain level of wealth has been attained. Most empirical literature has focused on SO_2 emissions, often making use of urban air quality data, with few studies dedicated to other pollutant species. Existing analyses, moreover, rarely account sufficiently for all relevant aspects of the environmental problems under consideration, or address the underlying causes of the hypothesized relationships. A refined examination of the determinants and effects of changes in air pollutant emissions may help to explain to what extent and through what mechanism economic development influences environmental quality, as well as the role of other factors. Thirty years of international atmospheric protection efforts have generated sufficient data to re-examine the EKC hypothesis and draw lessons for future policy (Vestreng et al. 2007). In particular, publicly available databases contain information about both emission control measures implemented in European countries and energy consumption, which can be linked to data on environmental effects and economic development. Such analyses are especially important in a context where it has been argued that economic growth, in and of itself, will eventually reduce environmental degradation (Andreoni and Levinson 2001). Here, we briefly review the theoretical basis and empirical evidence for the EKC.

2.1 Theoretical work

Gruver (1976) developed a neoclassical growth model with optimized investment into either productive capital or pollution control capital. Whereas productive capital can be used for several purposes (to increase consumption or produce more capital of either type), pollution control capital only enters the utility function through environmental improvements. Given this framework and the convex neoclassical utility function, it is optimal to focus on the build-up of productive capital, neglecting the environment, during an initial phase of development and then, with decreasing marginal utility of consumption, switch to investment aimed at reducing pollution. Selden and Song (1995) describe similar optimal growth,

but with only one investment category and with expenditure on pollution abatement decreasing consumption directly. This provides the basis for the "J-curve for abatement," where at low consumption, abatement expenditure is also minimal or zero; it thus directly explains the inverted U-curve for pollution on the basis of the assumed utility function.

Andreoni and Levinson (2001) briefly survey other theoretical efforts to explain the EKC and develop their own simple microeconomic model. They show that the observed income-pollution relationship can be explained by abatement technology with increasing returns to scale, as is the case for technologies requiring large capital investments. In a critical review of the EKC theory, Stern (2004) concludes that classic EKC results may not adequately explain emission pathways, because the underlying statistical analysis is not robust and there is only weak evidence for a coherent relationship between pollution and income. The study suggests that structural factors contribute to declining pollution rates, but are less influential than the time-related effects of targeted emission abatement measures.

2.2 Empirical studies

Early papers often cited in reference to the EKC include Shafik (1994), Selden and Song (1994) and Grossman and Krueger (1995). These studies use panel data for several countries and years in regression analyses; however, they do not explicitly consider the determinants of the relationship between pollution and income. Shafik (1994) makes use of a broad range of environmental data, including ambient PM, SO_2 and CO_2 levels, deforestation, clean water supply, urban sanitation, O_2 and fecal coliforms in rivers, and municipal waste. For these quality indicators, relationships are derived with respect to per capita income; in some cases these fit the EKC hypothesis, but in others, monotonically decreasing or increasing pollution trends predominate. The study also notes a trend toward lower pollution maxima over time (e.g., annual decreases in the maximum ambient values of 2 % for PM and 5 % for SO_2, respectively), which is attributed to technological improvement. The need for research on both structural and policy determinants of changes in environmental quality is emphasized. Selden and Song (1994) study emissions of SO_2, PM, NO_x, and CO and observe a similar pattern, although they find that pollution begins decreasing at higher levels of per capita income. They attribute this to cheaper costs of abatement for urban air pollution, for instance through the installation of high stacks—this is, at least for PM, a questionable assumption, given its dispersion behaviour. They use their model, in conjunction with country growth rates, to forecast global emission levels. Grossman and Krueger (1995) examine urban concentrations of atmospheric SO_2 and PM as well as water quality in river basins, observing a relationship which supports the EKC hypothesis, though they consider only two countries (Canada and the USA) in the high (i.e., > US-$16,000/year) income range.

Kaufmann et al. (1998) find an inverted U-shaped relationship between the spatial intensity of economic activity and atmospheric concentrations of SO_2, whereas for per capita GDP and SO_2 concentrations the relationship appears U-shaped. They argue that per capita GDP acts merely as a proxy for the spatial intensity of economic activity, which dominates the true association, yet fail to provide any convincing argument for this assertion. For instance, they ignore the acidifying properties of SO_2, which were the main driving force for its abatement in Europe after 1980. This factor may largely explain the observed phenomenon: deposition of sulphur compounds will tend to be more harmful (i.e., more likely to exceed critical loads for acidification) if concentrated within a small area.

De Bruyn et al. (1998) criticize the econometrics of earlier studies and re-examine the literature that associates the decline in the material-intensity of GDP with economic growth.

As they lack the data to conduct a decomposition analysis, they estimate a reduced-form regression model for time series of SO_2, NO_x, and CO_2 emissions for Western Germany, Netherlands, the UK and the USA between 1960 and 1993. In contrast with the expectations of the EKC hypothesis, their model suggests that emissions tend to increase with economic growth. Observed reductions result from the structural and technological factors that dominated subsequent to the low growth rates of the early 1970s. To interpret the results in terms of sustainability, they suggest linking the data to critical loads for acidification and eutrophication. Several other studies (e.g., Viguier 1999; Bruvoll and Medin 2003; Markandya et al. 2006) support the hypothesis that the energy- and material-intensity of GDP behave as inverted U-shaped functions of per capita income. Cole (2000) shows that the EKC can be explained by the cleaner composition of manufacturing and falling share of manufacturing output in GDP with income growth.

Stern and Common (2001) survey the empirical literature on the relationship of SO_2 with income. Making use of a longer (1850–1990) time series of global sulphur emissions, they find that the EKC exists only when the sample is limited to high-income countries. For the global sample, SO_2 emissions per capita are a monotonic function of income, and reductions in emissions are time-related rather than income-related. They identify events—such as the adoption of the first sulphur Protocol to the Convention on Long-range Transboundary Air Pollution (CLRTAP) (UN-ECE 1985)—as possible causes of this time-dependency. In more recent work based on the current evolution of emissions in China and elsewhere, Stern (2006) concludes that although air pollutants tend to increase with rising income, they decrease over time as a result of rapid technological change, suggesting that low income levels do not prevent the adoption of abatement technologies.

2.3 Motivation for this study

The picture that emerges from this brief literature survey is that, while there is some evidence that supports the EKC, especially for air pollutants like SO_2, the empirical and theoretical basis for this relationship is rather weak. There is stronger evidence suggesting that some of the underlying factors that determine emissions, energy consumption or structural change follow a Kuznets-type curve, whereas the deployment of dedicated mitigation measures and policies is likely independent of affluence. This study attempts to isolate these factors and relate them to economic growth. The impacts of driving forces behind changes in emissions are expected to be pollutant-specific, therefore we separately consider SO_2 (emitted mainly from large stationary sources), NO_x (primarily from vehicle engines), and CO_2 (the dominant climate forcing agent, for which there were no end-of-pipe controls used in the past). We examine the effects of determining factors on time series for two subregions in Europe that experienced very different levels of wealth, technological advancement and environmental awareness.

3 Methods

The literature describes many alternative methods for carrying out a decomposition analysis of emission trends (Ang and Zhang 2000). Our model for the evaluation of determinants for emission changes is based on a simplified additive form of the index decomposition analysis. Detailed explanation of this method is provided by Hoekstra and van den Bergh (2003). The following sections present our basic assumptions made for the decomposition, and describe the datasets used in calculations.

3.1 Two identities to explain observed emissions

We examine the evolution of European emissions of SO_2, NO_x and CO_2 as the product of the following three determinants:

$$Emissions = Population \cdot \left(\frac{GDP}{Population}\right) \cdot \left(\frac{Emissions}{GDP}\right),$$

where *GDP* is Gross Domestic Product, a standard measure for economic output. Emissions of a given substance are thus a function of population, economic affluence (*GDP/Population*) and the emission intensity of the economy (*Emissions/GDP*). According to the EKC hypothesis, the third term should take the form of an inverse U-shaped curve, emerging as a composite of autonomous technological progress, structural changes in national economies, behavioural changes and dedicated environmental policies.

To evaluate the importance of these individual components, we extend this identity, and decompose the last term into three factors, as follows:

$$Emissions = Population \cdot \left(\frac{GDP}{Population}\right) \cdot \left(\frac{Energy}{GDP}\right) \cdot \sum_i \left(\frac{Fuel_i}{Energy}\right) \cdot \left(\frac{Emissions}{Fuel_i}\right).$$

Resulting emissions are thus further dependent on the energy intensity of the economy (*Energy/GDP*), i.e., the primary energy required per unit of GDP, on the fuel mix in each sector (*i*) (*Fuel*$_i$*/Energy*), and on the emission intensities of different fuels (*Emissions/Fuel*$_i$). The additive form decomposes the difference in emissions between time *t* and *t-1* into three determinant effects:

$$Emissions^{t} - Emissions^{t-1} = Factor(1)effect + Factor(2)effect + Factor(3)effect$$

These factors capture the key drivers that affect emissions, specifically:

1) overarching economic and/or energy intensity changes resulting from industrial sectoral restructuring, technological progress, energy efficiency improvements and behavioural changes;
2) alterations in the structure of the energy system, wherein emissions are critically determined by fuel mix changes due to, e.g., fuel switching in response to variation in relative fuel-prices;
3) dedicated application of end-of-pipe emission control measures in response to environmental legislation.

Our formulation extends the 'Kaya identity' that expresses emissions of CO_2 as the product of four inputs: population, GDP per capita, energy use per unit of GDP and carbon emissions per unit of energy consumed (Kaya and Yokobori 1997; Waggoner and Ausubel 2002). This extension is useful in isolating the impacts of dedicated environmental policy interventions, of particular importance for emissions of the air pollutants SO_2 and NO_x, for which highly effective end-of-pipe measures exist.

We analyse the development of these factors from 1960 to 2010, quantifying their contribution to observed changes in SO_2, NO_x and CO_2 emissions in Europe. These emission species are selected, *inter alia,* for their environmental significance, extensive documentation in the literature, and because of the availability of reliable data, needed for

the decomposition analysis. We compute hypothetical emission scenarios or trajectories for the study period in which we keep one or several of these factors at the level observed for a selected base year (i.e., 1960) while varying others, as follows:

I. First, a hypothetical upper limit for emissions over time is calculated, assuming that the emission intensities of GDP remain unchanged. Such an emission path would follow from income (GDP) growth, given constant energy intensity of GDP, unchanged fuel mix, and no emission control measures beyond those implemented in the base year; thus:

$$\left(\frac{Energy}{GDP}\right)^{t} = \left(\frac{Energy}{GDP}\right)^{t=0}, \sum_{i}\left(\frac{Fuel_i}{Energy}\right)^{t} = \sum_{i}\left(\frac{Fuel_i}{Energy}\right)^{t=0}, \left(\frac{Emissions}{Fuel_i}\right)^{t} = \left(\frac{Emissions}{Fuel_i}\right)^{t=0}$$

This trajectory reflects only changes in real-term GDP using purchasing power parity (PPP), thus constituting a reference against which the effects of other factors can be quantified.

II. In the following step, an emission trajectory is estimated using data on the real development of total energy consumption, but keeping fuel mix and emission factors for each fuel type constant at the base year level. Comparing this to the first trajectory reveals the impact on emissions of decoupling GDP from energy consumption. Changes in the energy intensities of GDP result from shifts in the sectoral composition of GDP as well as from efficiency improvements in energy systems.

III. Third, a hypothetical emissions time trend is calculated that accounts for changes in fuel mix, while keeping emission factors for each fuel type unchanged with respect to the base year value. A corollary condition is that the shares of all fuels must add up to one (i.e., $\sum_{i} Fuel_i/Energy = 1$). Comparison of this scenario with the trajectory II above quantifies the impacts of fuel substitution (e.g., the replacement of coal by natural gas) on emissions. In some cases, fuel substitution came about in response to environmental legislation, but other factors were often involved, e.g., cost minimization, convenience, accessibility of energy grids and infrastructure.

IV. Finally, the contribution of dedicated emission control measures to total emission changes is derived in a similar way from a fourth trajectory, which tracks actual emissions by incorporating all driving factors, including the changes in emission factors for each fuel type in each sector. Emission factors are determined by the removal efficiency (*Eff*) of an abatement measure adopted at a specific rate (*X*):

$$Emission\ factor = \left(\frac{Emissions}{Fuel_i}\right)^{t} \cdot (1 - Eff) \cdot X^{t}$$

A comparison of the differences among these trajectories reveals the impact on emissions, respectively, of overall economic growth, the decoupling between GDP and energy use, changes in the fuel mix of total energy consumption, and the application of dedicated control measures. As reported by Rafaj et al. (2012), this methodology may be applied to the decomposition of emission trends for a range of other air pollutants

(ammonia, fine particles, VOCs)[1] or short-lived greenhouse gases (methane, ozone), not addressed in this study.

3.2 Data sources

This analysis examines emission changes within the 50-year period from 1960 to 2010 at five-year intervals. It distinguishes between two regions: Western Europe (WEU), comprising the 15 EU members prior to 2004, Switzerland and Norway; and Eastern Europe (EEU), including the 12 EU members that joined after 2004, the Balkan countries, Turkey, Belarus, Ukraine and Moldova (Fig. 1).[2]

As SO_2, NO_x and CO_2 emissions originate almost entirely from the combustion of energy carriers, emission estimates are primarily based on statistical energy data and fuel balances. For most countries, energy statistics from the International Energy Agency (IEA 2009a, b, c, d) have been used for 1960–2005. For some countries of the former Soviet Union, missing statistical data for 1960–1990 have been extracted from the databases of two models: GAINS and its predecessor, RAINS (Amann 1990). Energy consumption for 2010 is based on the projections developed for the revision of the National Emission Ceiling Directive as implemented within the GAINS model (Capros et al. 2008). These sources also provided data on factors that contribute to autonomous emission reductions, such as GDP, energy intensity and population growth. However, because data on the efficiency of end-use devices and appliances is not provided, these factors are treated in aggregate. Emissions of SO_2 and NO_x are calculated for nine fuel categories in five economic sectors, as summarized in Table 1.

Emission factors for 1960 and subsequent years are extracted from the databases of the RAINS and GAINS models and, if necessary, adjusted such that resulting emissions match the official national estimates reported to the European Monitoring and Evaluation Programme (EMEP) under CLRTAP[3] (EMEP 2009). Figures reported by Mylona (1996) and Schöpp et al. (2003) are used to fill in missing data points. Emissions for 2010 are abstracted from the GAINS baseline scenario reported by Amann et al. (2008).

CO_2 emissions are calculated on the basis of total primary energy supply according to IEA energy balances (IEA 2009a, b). In contrast to SO_2 and NO_x, international aviation is not included as a source in estimates of CO_2 emissions, but emissions from non-energy use of fossil fuels (e.g., asphalt production or chemical feedstock) are taken into account. Resulting CO_2 emissions have been adjusted to the estimates reported by the IEA (2010).

[1] Ammonia emissions originate mainly from agricultural activities, such that temporal changes are driven by different forces than for more energy-related pollutants. Economic output of the agricultural sector, levels of primary agricultural production (e.g., livestock numbers), and the structural composition of livestock are used in the decomposition analysis.

[2] WEU thus includes 17 countries: Austria, Belgium, Denmark, Finland, France, Germany, Greece, Ireland, Italy, Luxembourg, Netherlands, Norway Portugal, Spain, Sweden, Switzerland and the United Kingdom; EEU comprises 22 countries: Albania, Belarus, Bosnia and Herzegovina, Bulgaria, Croatia, Cyprus, Czech Republic, Estonia, Hungary, Latvia, Lithuania, Macedonia, Malta, Moldova, Montenegro, Poland, Romania, Serbia, Slovakia, Slovenia, Turkey and Ukraine.

[3] SO_2 and NO_x emission data from EMEP comprise gap-filled and gridded data based, for reasons of consistency, on official reported data supplemented by expert estimates for missing and/or low quality measurements.

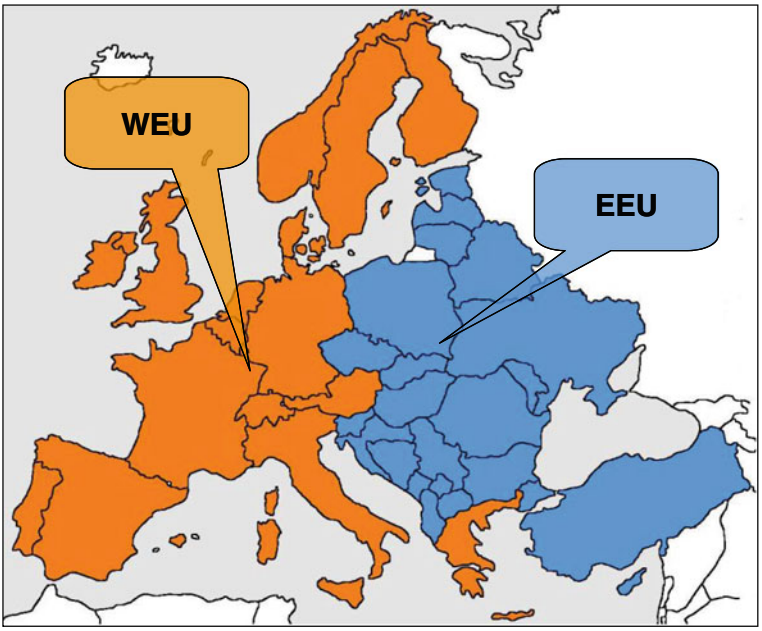

Fig. 1 Geographical coverage of emission calculations

The decomposition analysis of emission changes in this paper addresses only emissions from fuel combustion, excluding fuels for international marine bunkers. Industrial process emissions—the only category of anthropogenic emissions not directly linked to energy consumption—are also not examined here because of a lack of consistent and reliable historical statistics. Sources of such emissions include oil refineries, coke plants, sinter plants, pig iron blast furnaces, non-ferrous metal smelters, sulphuric acid plants, nitric acid plants, cement and lime plants and pulp mills; in 2005 they contributed about 7 % and 5 % to total European SO_2 and NO_x emissions, respectively (EMEP 2009). The share of CO_2 process emissions in Europe, including gas flaring, was about 5 % of total emissions in 2005 (UNFCCC 2009).

Table 1 Sector/fuel combinations applied for emission calculations for SO_2 and NO_x

Sectors	Fuels
Power and heat production	Hard coal
	Lignite
Industry	Coke
	Biomass and waste
Households and services	Gasoline
	Diesel
Transport and aviation	Heavy fuel oil
	Natural gas and derived gases
Energy conversion	Others (renewables, nuclear, electricity, heat)

4 Results

4.1 Emissions in Europe 1960–2010

In WEU, the volume of economic activity increased steadily by about 2.2 %/year between 1960 and 2010, resulting in a quadrupling of GDP (real-term, PPP-adjusted). In the early years of this period, emissions of SO_2, NO_x and CO_2 developed in parallel to the level of economic activity (Fig. 2). However, SO_2 and NO_x emissions later exhibited a distinct

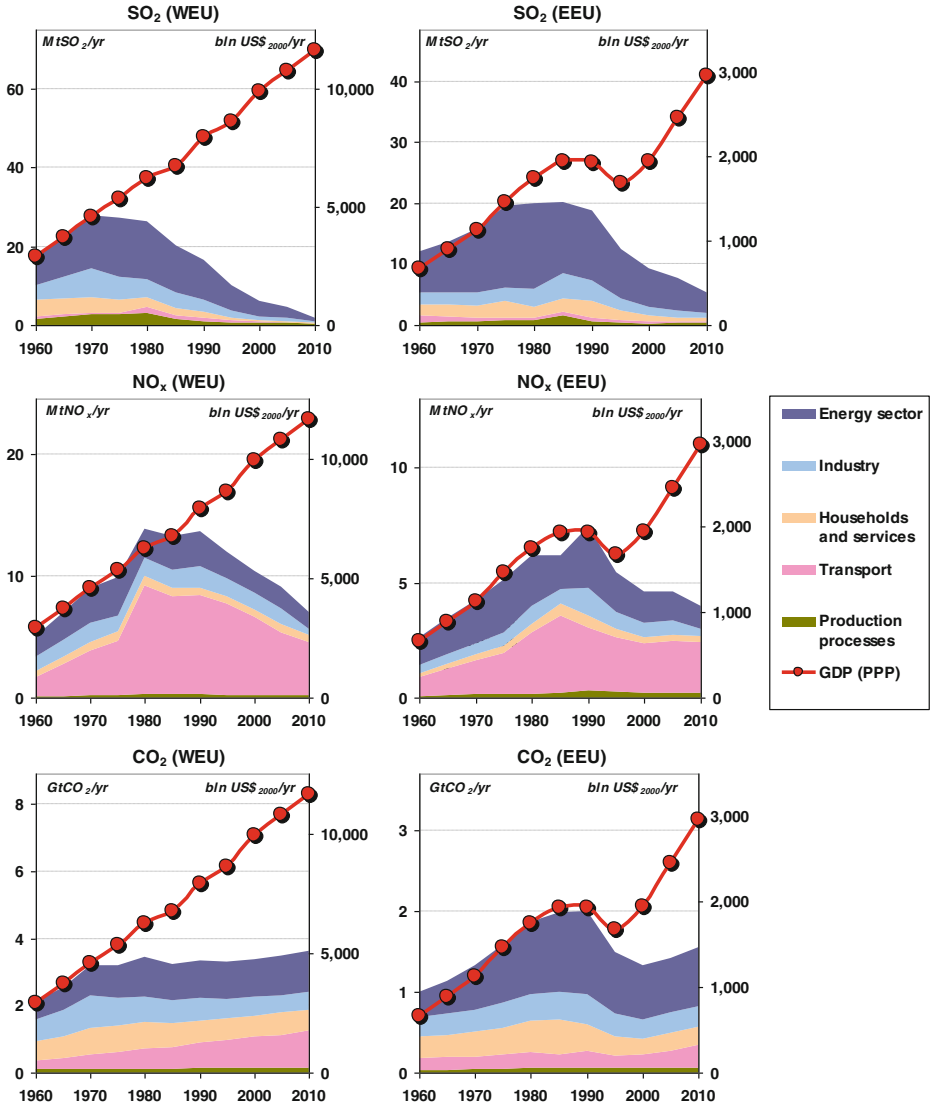

Fig. 2 Evolution of GDP (PPP) and emissions of SO_2, NO_x, and CO_2 by sector in Western Europe (WEU) and Eastern Europe (EEU) between 1960 and 2010; adopted from databases of the RAINS and GAINS models (Amann 1990; Amann et al. 2008; EMEP 2009; IEA 2010)

decoupling from GDP, coinciding with a time when public concerns about their negative environmental impacts (i.e., about 'acid rain' and 'ground-level ozone') emerged. After peaking in the 1970s, SO_2 emissions declined by 90 % through 2010; similarly, NO_x emissions declined by 50 % after a maximum in the 1980s (Schöpp et al. 2003). For CO_2, such a pronounced decoupling effect has not yet been observed.

In EEU, political changes in the 1990s were accompanied by drastic structural changes in national economies. This led to temporary stagnation and a drop in GDP, and to significant alterations in energy systems. From Fig. 2 it is clear that the contributions of individual emission sources are comparable in the WEU and EEU regions; however, the decline in emissions was delayed by about 10 years in EEU compared with WEU. In addition to economic and structural transitions, the implementation of new environmental legislation in EEU contributed substantially to the rapid decrease in emission burden.

Figure 3 shows the share contributed by solid, liquid and gaseous fuels to overall emission levels. While the combustion of coal is the major source of sulphur emissions, oil products used in the transport sector dominate NO_x emission profiles in both the WEU and EEU regions. The increasingly higher share of natural gas in the fuel mix is responsible for its growing contribution to total CO_2 emissions.

4.2 Key factors driving pollutant emissions

4.2.1 Population and income

During the period of interest, population grew at an annual rate of 0.4 % in WEU and 0.6 % in EEU. Whereas a pattern of gradual continued growth was observed in the former, population stabilised and even began to decline during the early 1990s in the latter (Fig. 4). Over the same timeframe, average income more than tripled in WEU and more than doubled in EEU. Even with all other factors held constant, pollutant emissions would be expected to significantly increase as a consequence of observed increases in income.

The EKC hypothesis suggests that, on a per capita basis, emissions will display an inverse U-shaped function with respect to income. Figure 5 shows the trajectories of emissions of SO_2, NO_x and CO_2 plotted against income levels for WEU and EEU countries, respectively. In principle, the EKC hypothesis is consistent with SO_2 emissions in WEU, which increase up to ~13,000 US-$/yr, then decline monotonically with increasing income. For EEU, per capita emissions peaked at an income of ~7,000 US-$/yr, and declined much more rapidly than in WEU. For instance, per capita emissions of about 20 kg SO_2/year were reached in EEU at an income of about 12,000 US-$/yr, while in WEU the same emission level was achieved at about 24,000 US-$/yr. Similar trends apply for NO_x, where emissions in both regions peaked at comparable intensities, but significantly different income levels. Furthermore, the peaks of SO_2 and NO_x emissions coincide for EEU with respect both to time and per capita income, while they are rather different within WEU. For CO_2 emissions, there is no significant income dependency in WEU, while the post-1990 economic restructuring in EEU appears to have set per capita emissions on a new growth path—although at a lower absolute level. In general, all curves for EEU show a distinct break in 1990 at the onset of economic restructuring.

From a broader perspective, data for EEU through 1990 combined with the full range of data for WEU provide only limited support for the existence of universal U-shaped relationships between emissions and per capita income in the ranges considered here. Such relationships are evidently region- and pollutant-specific, peaking at different income levels, and do not indicate a significant decline in CO_2 emissions with increasing prosperity.

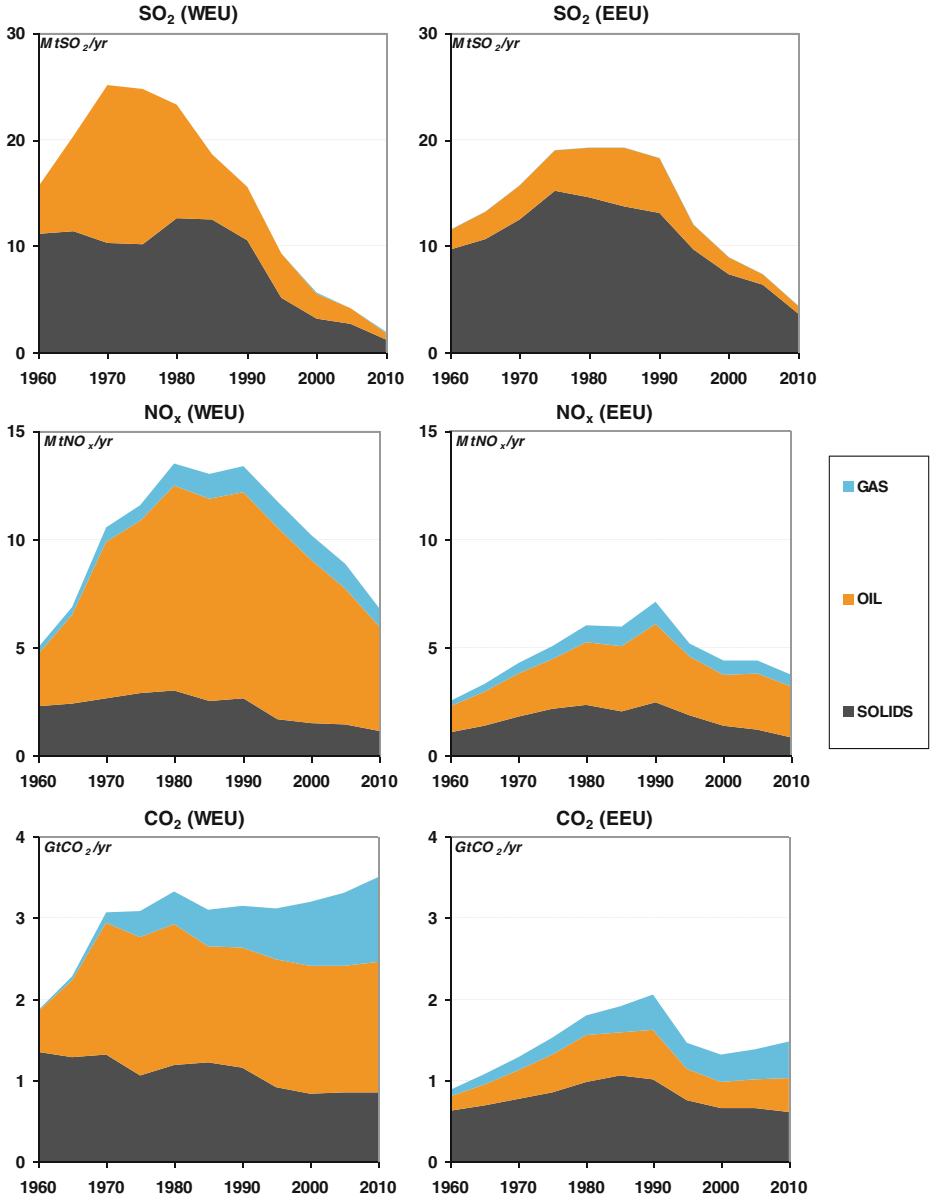

Fig. 3 Evolution of emissions for gas, oil and solid fuels in Western Europe (WEU) and Eastern Europe (EEU) between 1960 and 2010; adopted from databases of the RAINS and GAINS models (Amann 1990; Amann et al. 2008; EMEP 2009; IEA 2010)

However, developments in Eastern Europe after 1990 clearly signal a departure from the status quo, indicating the potential importance of structural changes in emission trends. In sum, historic evidence for SO_2, NO_x and CO_2 emissions in Western and Eastern Europe suggests some income dependency that might be in line with the EKC hypothesis, but this is hardly definitive; in the following sections, we explore alternative factors that could explain the observed changes in pollutants over time.

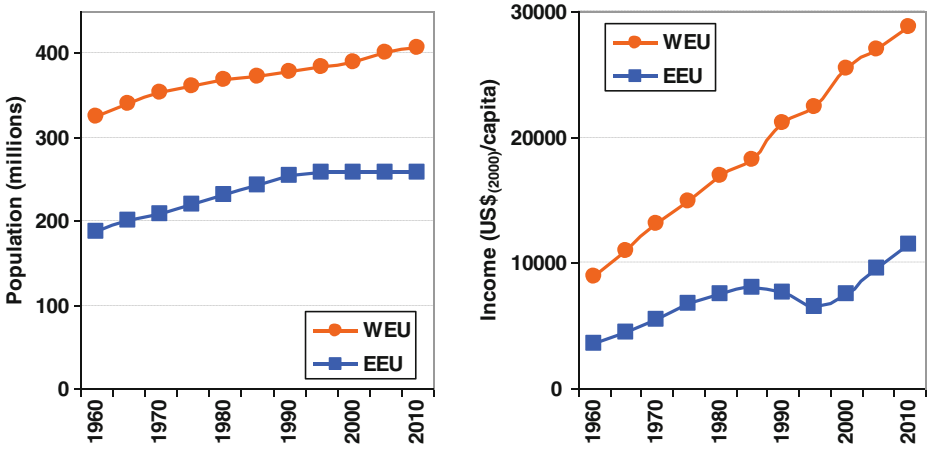

Fig. 4 Evolution of overall population and GDP per capita in Western Europe (WEU) and Eastern Europe (EEU), 1960–2010. Adopted from RAINS (Amann 1990) and IEA (2009a, b)

4.2.2 Energy intensity

Energy intensity, expressed as energy use per unit of GDP produced, has evolved quite differently in WEU and EEU. In the former, after a period of growth, energy intensity

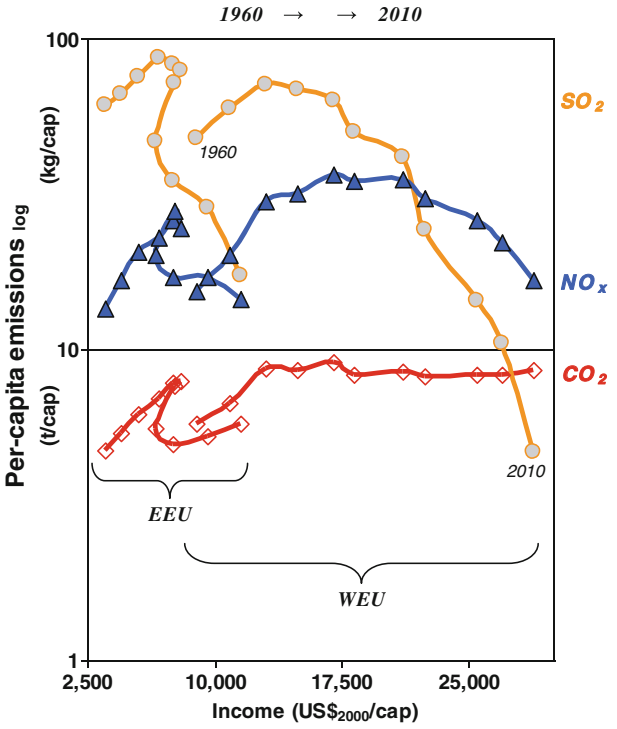

Fig. 5 Trajectories of emissions per capita versus per capita income from 1960–2010 in Western Europe (WEU) and Eastern Europe (EEU). Adopted from RAINS (Amann 1990) and IEA (2009a, b)

gradually decreased, such that present levels are nearly 30 % lower than in 1970 (Fig. 6- Left panel, lower lines), while energy consumption per capita increased steadily (Fig. 6 - Left panel, upper lines). In some WEU countries, oil price shocks affected the level and structure of energy consumption in the mid-1970s and early 1980s. In many WEU countries, energy growth slowed around 1990. Some of these economies managed to decouple energy growth from economic growth. In contrast, energy intensity remained stable or even increased in the EEU region through the 1990s. The strong decline after 1990 is due to the recession in Central and Eastern European countries that underwent a process of economic transition to a market economy. In EEU, energy consumption per capita dropped sharply at the 1990 recession, but increased steadily both before and after.

As explained in Section 3.1, changes in overall energy intensity according to our definition also encompass the contribution of improved conversion efficiency and energy saving measures. Investments in energy conservation during the period of interest were primarily motivated by the pressure of increasing energy prices, on both the supply and demand sides of the energy system. The trajectories of real energy prices (adjusted for inflation) since 1970 (Fig. 6 - Right panel) in WEU evidence very strong fluctuations, however, an increasing trend is observed, especially for oil (gas and oil prices have usually been linked in international markets). The price of coal also increased after the 1970s, though changes have been not as dramatic as for oil and gas. The observed trends suggest a significant correlation between growth in energy costs and reductions in energy intensity. Moreover, the price of energy is one of the decisive components for fuel choice, as discussed in the next paragraph.

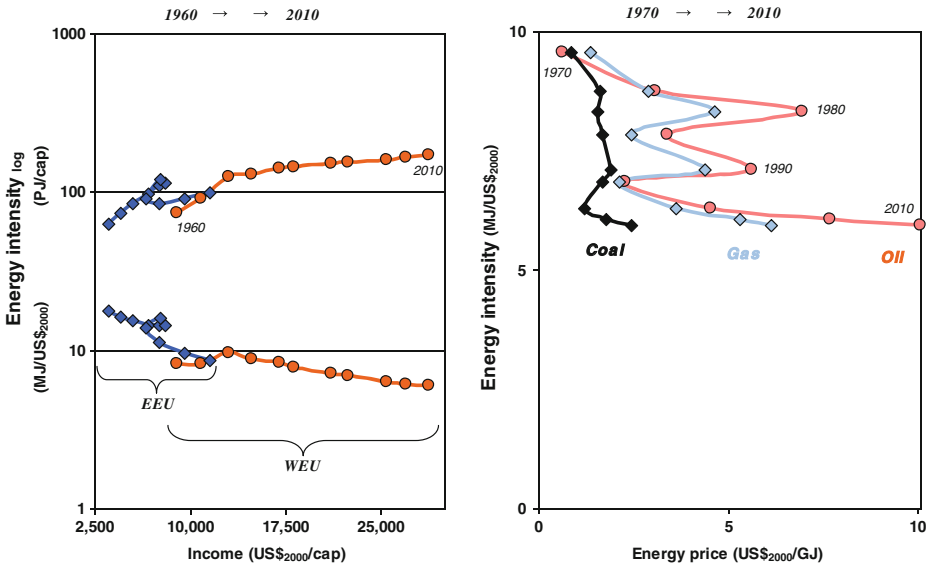

Fig. 6 Left panel—trajectories of energy intensity (ENE/GDP) with respect to economic output (lower lines) and per capita energy consumption (*upper lines*) in Western Europe (WEU) and Eastern Europe (EEU), 1960–2010. Adopted from RAINS (Amann 1990) and IEA (2009a, b). Right panel—evolution of energy intensity (ENE/GDP) in relation to real fuel prices in WEU, 1970–2010. Adopted from BP (2012) and World Bank (2013)

4.2.3 Fuel mix

An important factor driving changes in emissions is the fuel structure of the energy system. Fuel switches have occurred on the supply side since the 1970s, e.g., in the power sector, in the form of expanding nuclear generation capacity, growth in renewables and natural gas use. On the demand side, there has been a shift toward more electricity and heat consumption instead of direct fuel combustion. Figure 7 illustrates the evolution of the overall fuel mix from 1960 to 2010. The share of non-fossil fuels in WEU approached 25 % by 2010, increasing by a factor of six relative to the base year. Similar steep increases are reported for natural gas, which experienced sevenfold growth. The relative importance of coal decreased, while oil usage shifted from heat and power production toward transportation. The transition toward natural gas, nuclear and renewable energies was substantially slower in EEU. Moreover, consumption of coal and oil products increased until 1995 in EEU, making the fuel substitution effect less pronounced in comparison to that in WEU.

4.2.4 Emission intensity

It is clear that ongoing economic and energy sector changes during the period examined had an impact on emission intensity (i.e., the amount of air pollutants released per unit of energy consumed). Of these, the structural changes initiated after the oil price shocks—especially the second shock in 1979 (Kohl 1982)—and during the post-1990 transition period in Central and Eastern Europe are most significant. In addition, changes in emission intensities reflect transitions in the composition of particular economic sectors; for instance, shifts from manufacturing to services, changes in the ratio between passenger and freight transport or improvements in conversion efficiency.

Figure 8 shows trajectories of emission intensity in relation to change in the non-fossil fraction of the overall fuel mix. For both WEU and EEU, emission intensity for SO_2 and NO_x decreased with growing share of carbon-neutral fuels, though this trend for NO_x is only observed after 1980, due to changes in the transport fuel mix. The overall impacts of fuel

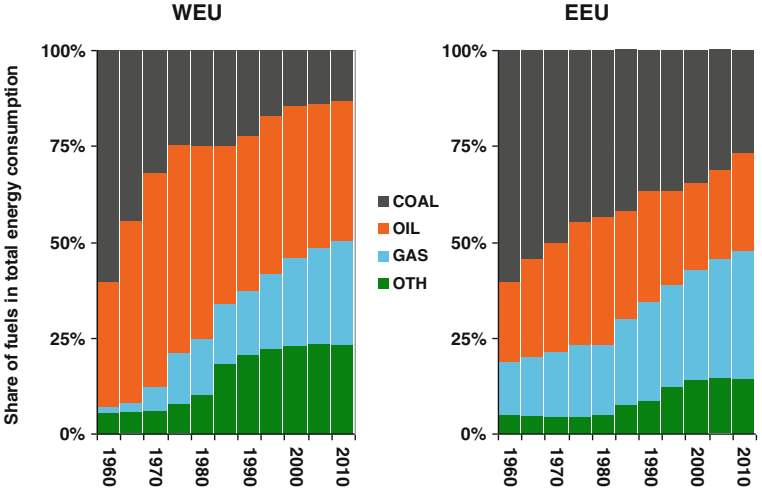

Fig. 7 Evolution of fuel choices in Western Europe (WEU) and Eastern Europe (EEU), 1960–2010. Adopted from RAINS (Amann 1990) and IEA (2009a, b)

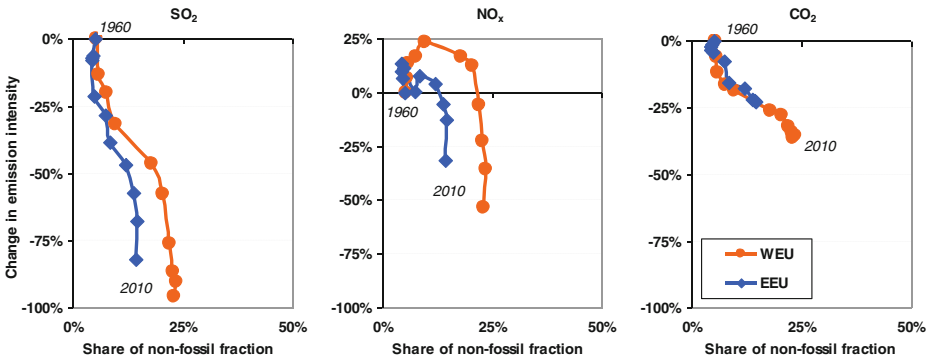

Fig. 8 Evolution of emission intensity for SO_2, NO_x and CO_2 emissions in Western Europe (WEU) and Eastern Europe (EEU) relative to 1960 as a function of the share of non-fossil energy fraction. Adopted from RAINS (Amann 1990) and IEA (2009a, b)

mix changes on SO_2 and NO_x emission intensity reductions are complex, since, over the last two decades, the continuous use of fossil fuels has been accompanied by the adoption of targeted emission control measures and improved fuel quality. For CO_2 emissions, however, changes in fuel mix represent a major mitigation component in the absence of direct end-of-pipe abatement measures. This explains the proportional reduction in aggregated CO_2-emission intensity following the growth in non-fossil fuels.

4.3 Summary of factors leading to emission changes over time

4.3.1 Sulfur dioxide

The decomposition approach discussed in Section 3.1 allows for quantification of emission reductions attributable to particular technological, behavioural or policy-related elements. A simple approach to interpreting these results it to examine how the three main drivers described above (i.e., improved energy intensity, improved fuel mix and end-of-pipe measures) have factored into reductions in emissions over the study period. Figure 9 shows total observed SO_2 emissions in the WEU and EEU regions between 1960 and 2005, projected through 2010. The dark area ("Actual emissions") illustrates the empirical evolution of SO_2 emissions. The red line at the upper margin shows the hypothetical emissions that would have occurred in the absence of any mitigation component; i.e., it represents growth in emissions with growing GDP. Intermediate between these boundaries, different colours represent the contribution of the three drivers to emission reductions: changes in energy intensity and efficiency (blue), changes in energy structure/fuel mix (green), and control measures (yellow).

In WEU, SO_2 emissions have declined monotonically since 1970. Changes in fuel mix combined with reduced energy intensity have offset continued growth in energy consumption, while control measures have further decreased emissions. As of 2010, the reductions in SO_2 emissions attributable to control measures and to energy intensity improvements are of similar moderate magnitude, while fuel mix changes have become the most important abatement element. In EEU, an increase in energy intensity (striped) outweighed the effects of fuel switching and better fuel quality during the first half of the study period, resulting in moderate emission growth through the mid-1980s. After 1990, a decline in total energy consumption brought emissions down, and this process accelerated via efficiency

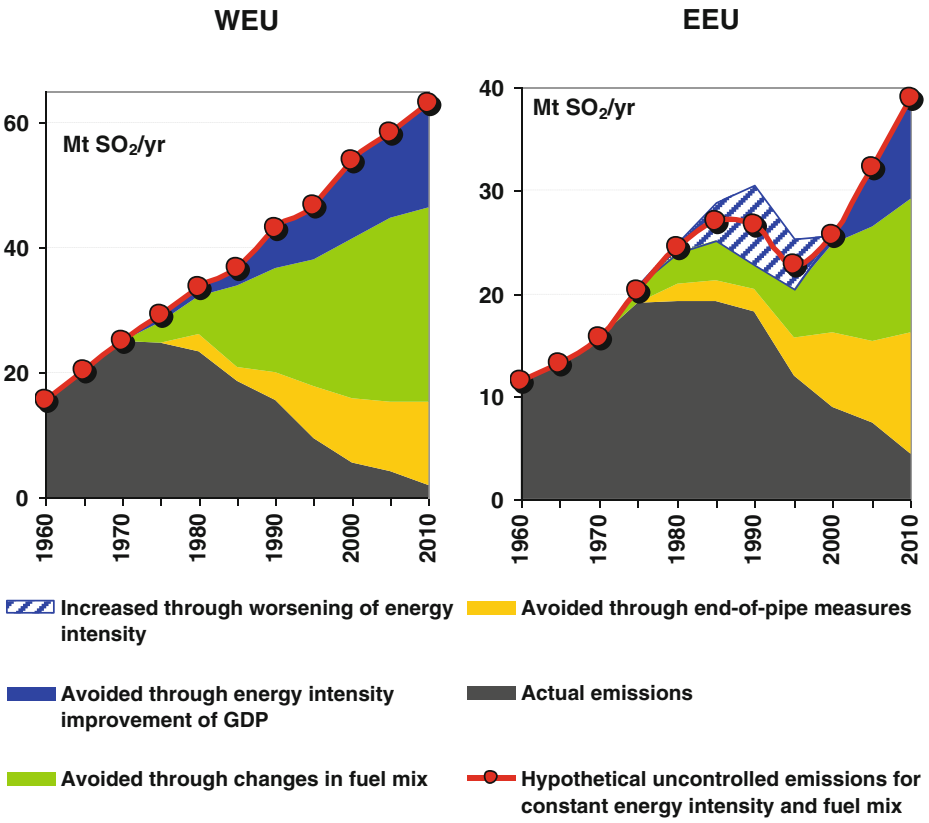

Fig. 9 Determinants of reductions in SO_2 emissions in Western Europe (WEU) and Eastern Europe (EEU), 1960–2010

improvements, coal substitution with natural gas and the adoption of pollution control legislation in most EEU countries.

It is important to note that the systematic adoption of end-of-pipe measures to reduce emissions (e.g., FGDs) did not take place before 1985. Nevertheless, modification of the characteristics of fuels used in a range of combustion processes led to changes in the average emission factor for several sectors. Some changes in fuel quality, e.g., sulphur content in coal, were autonomous, while others were enforced by legislation—for example, the sulphur content standards for transport or domestic liquid fuels (UN-ECE 1987). The evolution of the aggregated sector-specific emission factors for SO_2 in WEU and EEU is summarised in Table 2. To understand the relative impact of the areas in Fig. 9, it is necessary to examine the data at the country level, as in Section 4.4 below.

4.3.2 Nitrogen oxides

Growth in NO_x emissions differed from growth in SO_2 emissions for both regions. While SO_2 in WEU declined by some 40 % between 1970 and 1990, NO_x increased by 27 % during the same period (Fig. 10). In EEU, the corresponding increase in NO_x was over 65 %. This increase is largely a product of the growth in energy consumption, but, in contrast to SO_2, it is generated not only from stationary emission sources but also from transport. After

Table 2 Evolution of average emission factors by sector and the share of diesel in transport fuels in Western Europe (WEU) and Eastern Europe (EEU), 1960-2010. Adopted from RAINS (Amann 1990), IEA (2009a) and IEA (2009b)

	Region	Sector	1960	1970	1980	1990	2000	2010
Average emission factor for sulfur dioxide (gSO_2/MJ)	WEU	Energy	0.94	1.07	0.78	0.43	0.14	0.04
		Industry	0.55	0.63	0.40	0.28	0.10	0.03
		Domestic	0.58	0.31	0.17	0.11	0.03	0.01
		Transport	0.19	0.19	0.08	0.08	0.02	0.01
	EEU	Energy	1.73	1.47	1.18	0.74	0.56	0.25
		Industry	0.46	0.36	0.36	0.38	0.31	0.16
		Domestic	0.48	0.43	0.37	0.24	0.15	0.08
		Transport	0.55	0.24	0.23	0.16	0.16	0.05
Average emission factor for nitrogen oxides (gNO_x/MJ)	WEU	Energy	0.23	0.22	0.12	0.12	0.07	0.05
		Industry	0.16	0.13	0.13	0.17	0.13	0.04
		Domestic	0.07	0.06	0.05	0.04	0.04	0.03
		Transport	0.49	0.63	1.06	0.73	0.48	0.27
	EEU	Energy	0.30	0.27	0.19	0.17	0.12	0.08
		Industry	0.09	0.09	0.10	0.14	0.13	0.06
		Domestic	0.04	0.05	0.05	0.07	0.05	0.04
		Transport	0.43	0.67	0.98	0.92	0.88	0.55
Share of diesel fuel	WEU	Transport	23 %	29 %	32 %	37 %	44 %	55 %
	EEU	Transport	32 %	34 %	38 %	40 %	46 %	54 %

1985, control measures were phased in, gradually reducing emissions (Table 2). Structural change seems to have played only a minor role.

The analysis of changes in NO_x emissions is more difficult than for SO_2. Different factors tend to overlap and the same factors change the way they impact emissions over time. Also, the choice of reference year is very important. While structural change reduced emissions growth up to 1990, it increased emissions—or more precisely, diminished the impact of control measures—for the period after 1990. This trend was more pronounced in the EEU region (striped area).

Development in the transport sector is key to understanding the causes of NO_x emission trends. Both petrol and diesel consumption in the transport sector grew significantly over the period examined, however, the share of diesel in transportation fuels increased at a similar rate (Table 2). Between 1970 and 1990, the structural shift towards diesel was as important a factor in increasing NO_x emissions as the growth in transport, and from 1990 to 2000, when energy consumption declined, this factor significantly counteracted the reduction in emissions. While structural changes in the transport sector tend to increase emissions, structural changes for stationary sources tend to reduce emissions, as for SO_2. This also explains why the overall net effect of fuel mix change is rather small. It is also noted that initial emission regulations for automobiles within the EU were already specified by 1970 (EC 1970). Thereafter, European emission standards (Euro) for light and heavy duty vehicles were defined in a series of directives, whereas the first standards for passenger vehicles came into force in 1992, and the most recent standards (Euro5/V) have been required since 2009/2010 (EC 2007).

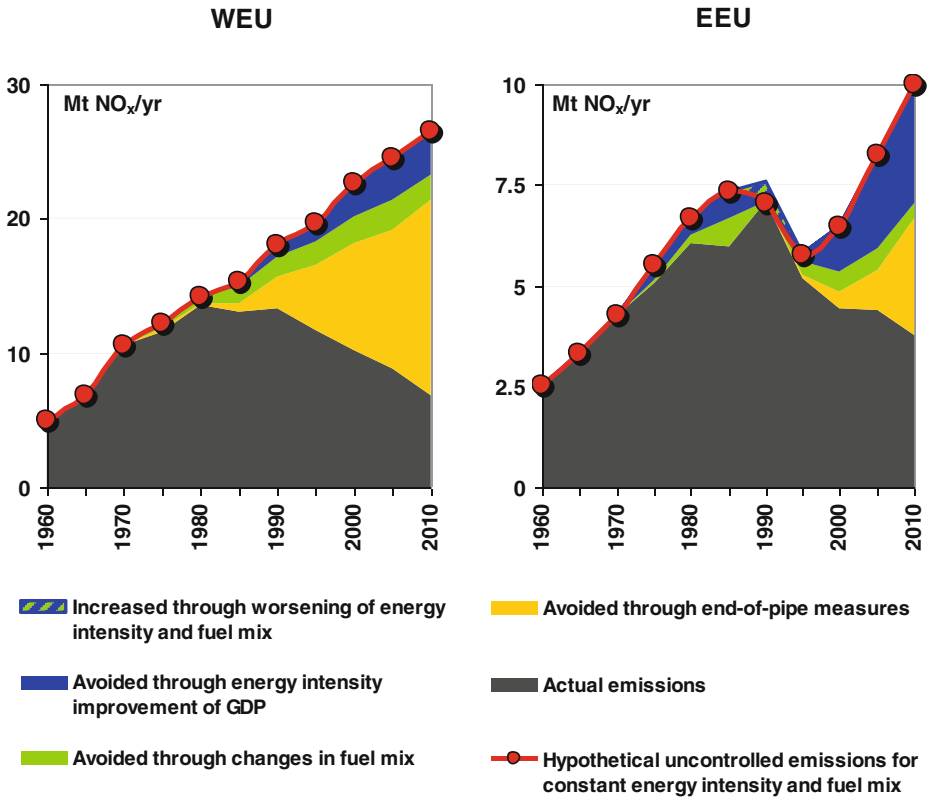

Fig. 10 Determinants of reductions in NO_x emissions in Western Europe (WEU) and Eastern Europe (EEU), 1960–2010

Another important process that plays a role in NO_x emissions is a transition across modes and categories within the transport sector. Examples include: the shift from two stroke to four stroke engines, the changing share of two-wheelers in passenger transport, the replacement of heavy duty trucks by light duty vehicles, and the ratio between fuel use in freight transport and in cars. These changes are not analyzed in detail in this study, but are reflected in aggregate in the structural emission drivers. Figure 10 also shows that control measures are the most important factor driving NO_x emission reductions— more than 75 % of effective measures through 2010 involved the transport sector. In the 1990s, pollution control measures affecting petrol-fuelled cars, e.g., catalytic converters, contributed most to reductions in WEU, but the contribution from equivalent measures for diesel-powered vehicles is expected to reach similar levels in 2010 and beyond (Amann et al. 2008; Borken-Kleefeld and Ntziachristos 2012).

4.3.3 Carbon dioxide

CO_2 emissions from fossil fuel combustion have rapidly increased in WEU, by 60 % from 1960 to 1970 (Fig. 11). The energy crisis in the 1970s followed by the oil glut resulted in temporary demand reductions in the middle of the 1980s (Salameh 2004). Changes in

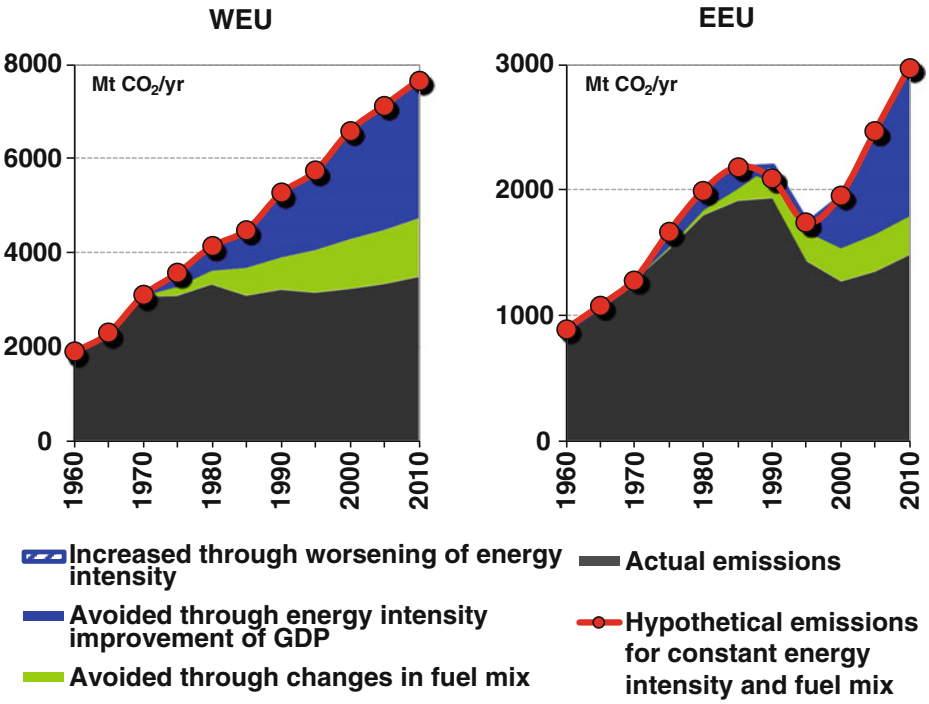

Fig. 11 Determinants of reductions in CO_2 emissions in Western Europe (WEU) and Eastern Europe (EEU), 1960–2010

economic structure, improved energy productivity, and energy-saving measures constitute the main sources of reductions in CO_2 emissions over the study period. High oil prices reinforced the introduction of alternative and less carbon-intensive fuels into energy markets (Figs. 6 and 7); through the early 1990s, fuel switching had similar impact on reductions in CO_2 emissions as the drop in energy intensity. By 2010, changes in fuel mix contributed around 30 % to overall CO_2 reductions, whereas improvements in energy intensity played a larger role.

In EEU, CO_2 emissions grew by 2.1 % per year up through 1990, in tandem with the growth of the economy (Fig. 11). Inefficient use of fossil fuels offset the CO_2-reducing effect of the growing nuclear and hydropower supply capacities experienced during this period (Fig. 7). The transition of EEU countries toward market-oriented economies resulted in the attenuated market distortion of fuel prices, and simultaneously in a rapid drop in energy use consequent to the conversion of the industrial sector. The recent economic recovery is associated with an increase in CO_2 emissions over the last decade.

4.4 Country results

Decomposition analysis for individual countries is of great value for gaining detailed insights about the performance and interplay of driving forces for pollution reductions. We present results for the United Kingdom and Poland to highlight a few of the most significant features. Additional components of emission reductions beyond those considered in Figs. 9, 10 and 11 are explicitly accounted for here. These components include growth in the power generation sector, evolution of transport activities, and the contribution of diesel fuel to the NO_x emission profile. Impacts on emissions resulting from improvements in energy

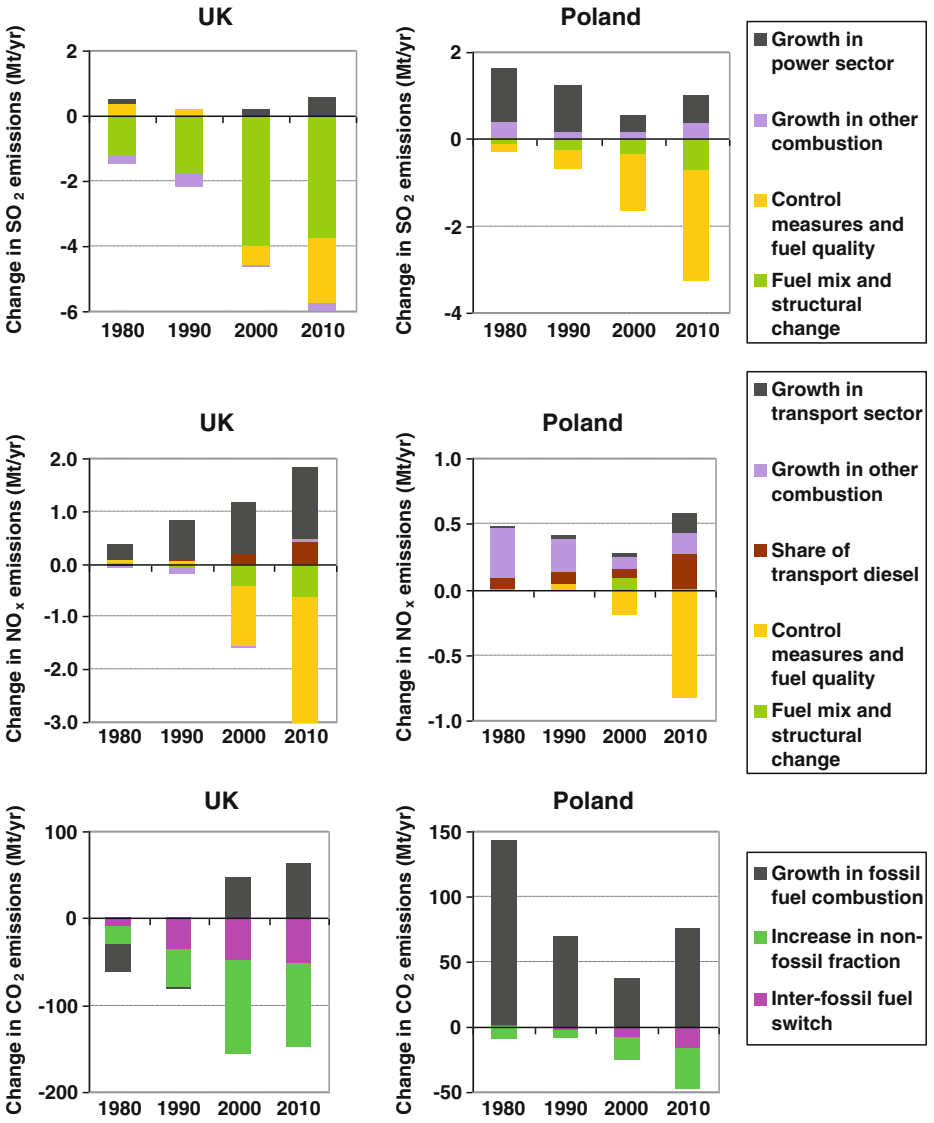

Fig. 12 Determinants of SO_2, NO_x and CO_2 emission reductions compared to 1970 in the United Kingdom and Poland

intensity and fuel mix are aggregated within one term ("Fuel mix and structural change"). Driving factors are decomposed relative to the year 1970, since their impact is obvious only after this point.

The United Kingdom reduced its emissions substantially during the 1990s through restructuring of the energy system, in particular by decreasing coal combustion in the power plant sector. A large fraction of coal power generation has been substituted by natural gas power plants, but nuclear power, too, and more recently renewable energy, figure increasingly in the fuel mix. Structural changes in the energy system thus played a dominant role in reductions of SO_2 and CO_2 emissions. End-of-pipe measures became important in SO_2

emission reductions only toward the end of the study period, as the United Kingdom started to install control equipment only after 1990 or even 1995 (UN-ECE 1995).

As was apparent at the regional level (see Section 4.3.2), the effect which overall structural change in the UK has on NO_x emissions changes with the relative importance of two opposing forces: fuel switching for stationary sources tends to reduce emissions, whereas relative growth of the transport sector increases emissions. The rising share of diesel cars in the UK nearly offsets the reductions achieved through the modified fuel mix in non-transport sectors. On the other hand, the analysis reveals a very high efficiency of control measures dedicated to NO_x abatement.

In Poland, as in most EEU countries, the tendency for emissions to grow dominated until the 1990s, whereas in later decades emissions decreased as a result of drops in energy demand and the adoption of emission control measures. In spite of growing shares of natural gas, biomass and other renewables, the Polish energy system continues to rely on coal combustion. Therefore, the effect of fuel mix changes towards SO_2 and CO_2 reductions is much lower than in the UK (Fig. 12). However, in combination with efficiency gains, fuel switching does help to moderate the growth in emissions that is the projected result of economic recovery. Add-on desulphurization technologies, gradually implemented after economic changes in the 1990s and due to EU-accession requirements in the 2000s, have been the main driver for the remarkable SO_2 reductions achieved. The decrease in average SO_2 emissions prior to the 1990s was linked with changing fuel quality and with a coal-to-lignite substitution in the power generation sector (Cofala and Bojarski 1987).

Evolution of NO_x emissions in Poland is again dominated by solid fuel combustion in power plants. Only after 2000 did growth in transport demand and a greater share of diesel vehicles outweigh the contribution from stationary sources. Similar to the UK, NO_x-controls enforced though environmental legislation have brought emissions below 1970 levels.

Individual country analyses indicate that differences among countries tend to diminish with time. While in the first half of the study period many country-specific features were evident, by 2010, the patterns have become rather similar. This may reflect the impact of international legislation regarding air pollutants, including both the Gothenburg Protocol (UN-ECE 1999) and EU legislation (EC 2001), as well as broad international climate agreements including the Kyoto Protocol (UNFCCC 1997). Continuous enforcement of environmental policies will eventually diminish the differences between countries with respect to the relative importance of structural changes compared to targeted abatement measures, as countries converge to the European average in the medium term. The overall effectiveness of control measures may vary with local circumstances. One clearly important factor is how early measures are introduced. The rate of implementation of controls may still differ slightly from country to country in the coming years, yet emissions should converge toward the European average and variability is expected to be much lower than before 2000.

5 Discussion

Our decomposition exercise proves that many emission reductions are not the result of specific control measures. Rather than resulting from targeted abatement efforts, they are shown to be the consequence of variation in energy structure, overall economic changes or technological advances.[4] These changes are autonomous of emission reduction objectives

[4] For the further discussion on the role of technological progress behind emission reductions and the effectiveness of international environmental treaties see, e.g., Barrett et al. (2006) and Dekker et al. (2012).

and are mainly a consequence of economic developments. The analysis of the observed emission reductions allows some conclusions about the substantial importance of dedicated environmental legislation and international policy efforts, such as the protocols under CLRTAP (UN-ECE 1985, 1999). Nevertheless, even countries that did not become party to the protocols and thus were not ready to support their environmental objectives have reduced emissions as a consequence of autonomous changes in the economy. Moreover, some countries that became protocol parties have reduced emissions beyond the levels required (CIAM 2007).

The analysis shows that changes in energy structure (including technological advances and other changes within sectors) are likely more important in reducing emissions for SO_2 than for NO_x. Without such changes, overall European emissions would not decrease below 1960 levels, as is now expected. For NO_x, structural change tends to act in the opposite direction, and on the whole is much less important. This difference supports the conclusion that for NO_x, there is the potential for structural change to further reduce emissions, potentially at lower cost, than is anticipated at present. It is possible, too, to imagine a dramatic shift away from the emission-intensive vehicle technology presently used for transport, similar to what has been observed in the power plant sector. Thus far, structural change and, in particular, the growth of transport, have reduced the effectiveness of measures to control NO_x. The extent of this effect explains some of the differences in overall emission reductions between countries. Also, the differences between countries with respect to the impact of structural change on SO_2 emissions were important during the 1990s, but, according to forecasts, such differences tend to diminish with time.

There is an obvious link between the adoption of the first sulphur Protocol in 1985 (UN-ECE 1985) and the timing of the introduction of controls on sulphur emissions. Among WEU countries, the United Kingdom neither joined the first sulphur Protocol nor introduced abatement measures at that time. It did, however, phase in control measures upon the adoption of the second sulphur Protocol in 1994 (UN-ECE 1994), to which it became a Party. Such an obvious link cannot be made for Central and Eastern European countries. Similarly, the adoption of the NO_x Protocol in 1988 (UN-ECE 1988) can be linked to the timing of the introduction of control measures. Finally, it is obvious that the adoption of the 1999 Gothenburg Protocol (UN-ECE 1999), which addresses not only SO_2 and NO_x, but also VOCs and ammonia, was followed by a broader application of emission control measures—in particular as it was signed by more countries than any previous Protocol (CIAM 2007).

This analysis strongly indicates that international environmental cooperation, as conducted within the framework of the CLRTAP, has had significant effects. Control measures have made a substantial contribution to SO_2 and NO_x emission reductions in Europe as a whole. For individual countries, too, the importance of control measures is growing over time, or is expected to do so. Even if particular measures and standards are not introduced in all countries on the basis of environmental or other concerns, we expect that European countries will tend to become more similar in terms of controls applied in view of European integration. This is obvious for, e.g., international vehicle regulations, but will also apply to the design of modern power plants or industrial processes.

From the perspective of the recent climate change debate and the adoption of Europe's climate and energy package (EC 2008), it is essential to examine the factors that drive changes in European greenhouse gas emissions and contribute to uncertainty in emission projections (Lesiv et al. 2013, this issue). In addition, most air pollutants also act as precursors for short-lived climate forcers, e.g., sulphur aerosols, tropospheric ozone, black carbon. Therefore, addressing uncertainties associated with

drivers of these emissions can enhance the understanding of potential near-term climate benefits (Shindell et al. 2012). For long-lived greenhouse gases such as CO_2, the methodology presented in this paper provides a quantitative basis for the investigation of uncertainties related to determinants of emission trends in both the medium- and long-term. Similarly, the decomposition analysis can provide a set of input parameters necessary for uncertainty assessment of GHG-emission inventories.

Another phenomenon recognised in studies on factors behind changes in GHG emissions is that the ongoing relocation of manufacturing industries abroad contributed to slowing down growth rates of CO_2 emissions in WEU during the past decade. Carbon emissions have in many cases leaked to countries with lower production costs, where some of the industrial activities are intended entirely for exports. As a result, national emissions of the importing country might be reduced without positive economic changes while being rather recorded and shifted elsewhere. However, global emissions do not decline in this context and the importation of goods manufactured overseas will eventually increase overall emissions (Peters and Hertwich 2008).

6 Summary and conclusions

The main objective of this study was to identify the principal factors responsible for reductions in air emissions. The work focuses on Europe, looking at 39 counties aggregated into two sub-regions (WEU and EEU), and develops long-term time series of emission data for sulphur dioxide (SO_2), nitrogen oxides (NO_x) and carbon dioxide (CO_2). In five-year intervals, it looks at emissions from 1960 through 2010. Using publicly available energy and emission databases, emission trends and drivers behind their temporal evolution are quantified and evaluated for Europe.

The results show that over this fifty-year period SO_2 and NO_x emissions rose to historical peaks, but then declined below the 1960–70 baseline by 2010. Add-on control measures started to be introduced in the late 1980s, when international policy efforts also first began to take effect. For example, the first sulphur Protocol under the CLRTAP was adopted in 1985 (UN-ECE 1985), and a NO_x Protocol followed in 1988 (UN-ECE 1988).

This study presents a methodology to isolate the main factors that influence air pollution emissions. The three pollutants examined here are strongly related to energy combustion, such that changes in energy use are key to understanding their evolution. The study distinguishes among four main determinants:

1a. Reduction of energy intensity;
1b. Improved conversion efficiency (the first two terms are aggregated for analysis);
3. Structural change as a shift of relative fuel shares; and
4. Control measures, targeted at the abatement of harmful effects of pollution.

For SO_2, structural change has been the dominant factor in emission reductions, although the reduced energy intensity of some sectors has also played a role. By the end of the study period in 2010, about 25 % of total reduction was attributed to targeted end-of-pipe abatement measures. In coming decades, the share of emission reductions due to control measures should rise as such measures penetrate the stock of existing capital and as more countries apply more advanced control measures.

For NO_x, structural change on the whole is less important. Emission-reducing structural change in the manufacturing industry and the power plant sector is outweighed by emission-

increasing structural change in the transport sector. The application of control measures is the most important factor explaining emission reductions.

We identified reductions in energy intensity and fuel-saving measures as the decisive factor for mitigation of CO_2 emissions during this timeframe. Changes in fuel mix contribute about one third of overall CO_2 abatement. In the near future, the adoption of carbon capture might play a role in carbon mitigation as a factor belonging to the group of end-of-pipe measures (Lemoine et al. 2012). In many cases, global trade of goods also results in reductions of national carbon emissions due to the relocation of energy-intensive industries to countries with less efficient production. This in turn generates carbon leakage, wherein global CO_2 emissions increase.

The relative importance of factors responsible for emission reductions differs between countries. Large differences appear between countries in WEU and EEU regions, reflecting different approaches in environmental and energy policies pursued. Over time, differences tend to diminish, which seems to be a good indication of the effectiveness of international environmental policies targeted at SO_2 and NO_x control in Europe.

One of the motivations for this study was to contribute to the understanding of the relationship between emissions and economic growth. The EKC hypothesis suggests that there is an inverted U-shaped relationship such that emissions first increase with economic growth and subsequently decrease once a certain level of wealth has been passed. Much debate remains about the reasons for such a relationship, if it exists. Two of the four factors identified in this study are clearly determined by economic parameters. Energy demand and efficiency gains (1a and 1b above), which are aggregated into one term in our analysis, are related to economic growth and tend to exhibit a Kuznets-type dependency. Technological progress, although not modelled explicitly in this study, is also driven by economic factors, but it is less clear whether and how the pollution intensities of individual sectors are related to economic growth (Dolgopolova et al. 2013, this issue). Change in the share of different fuels (2 above) is also influenced by economic development; however, in many instances, this has, rather, been determined by the evolution of energy prices and direct policy interventions. That two of the main factors responsible for emission changes follow a Kuznets curve may be sufficient for such a relationship to also be observed between emission data (at least for some countries and some pollutants) and economic growth.

There is little evidence that the control measures (3 above) that played a substantial role in reducing air pollutants over the last two decades are directly linked to economic growth. Rather than being driven by an autonomous increase in prosperity, their implementation is triggered by enforcement of deliberate mitigation policies. Formal analysis of other potential relationships, or indeed the alternative hypothesis, that emission controls are related to some environmental factor, such as, for instance, deposition in excess of critical loads, ecosystem sensitivity or the transboundary nature of pollution, remains to be undertaken.

The results of this study may allow for different perspectives on future emission scenarios and associated uncertainties, as, for example, in Jonas et al. (2013, this issue). Forecasted emission reductions are mainly driven by control measures but there is substantial opportunity for emission-reducing structural and technological change. This could imply that emission reductions are more broadly and cheaply attainable than is presently expected. One should, however, avoid over-optimism. As there seems no autonomous mechanism to ensure that EKC-like patterns observed in the past will hold in the future, there is no guarantee that determinants responsible for emission abatement will continue to play the role they have in previous decades. Because structural change, energy consumption and technology respond to many driving forces other than environmental pressures, the possibility cannot be excluded that a period of emission-reducing pressures will be followed by a period of emission increasing changes.

Acknowledgments The authors benefited from insights and discussions with J. Cofala and W. Schoepp from IIASA's Mitigation of Air Pollution & Greenhouse Gases (MAG). We thank the reviewers for valuable comments and suggestions.

References

Amann M (1990) Energy use, emissions, and abatement costs. In: Alcamo J, Shaw R, Hordijk L (eds) The RAINS model of acidification, science and strategies in Europe. IIASA and Kluwer Academic Press, Dodrecht

Amann M, Bertok I, Cofala J, Heyes C, Klimont Z, Rafaj P, Schöpp W, Wagner F (2008) National emission ceilings for 2020 based on the 2008 climate & energy package. NEC scenario analysis report #6. International Institute for Applied Systems Analysis (IIASA), Laxenburg

Andreoni J, Levinson A (2001) The simple analytics of the environmental Kuznets curve. J Public Econ 80:269–286

Ang BW, Zhang FQ (2000) A survey of index decomposition analysis in energy and environmental studies. Energy 25:1149–1176. doi:10.1016/S0360-5442(00)00039-6

Barrett S, Frankel J, Victor D (2006) Climate treaties and "breakthrough" technologies. Am Econ Rev 96:22–25. doi:10.1257/000282806777212332

Borken-Kleefeld J, Ntziachristos L (2012) The potential for further controls of emissions from mobile sources in Europe. TSAP report #4. International Institute for Applied Systems Analysis (IIASA), Laxenburg

BP (2012) Statistical review of world energy 2012. London, UK. bp.com/statisticalreview

Bruvoll A, Medin H (2003) Factors behind the environmental Kuznets curve: a decomposition of the changes in air pollution. Environ Resour Econ 24:27–48

De Bruyn SM, Van Den Bergh JCJM, Opschoor JB (1998) Economic growth and emissions: reconsidering the empirical basis of environmental Kuznets curves. Ecol Econ 25:161–175

Capros P, Mantzos L, Papandreou V, Tasios N (2008) European energy and transport trends to 2030—update 2007. European Commission Directorate-General for Energy and Transport, Brussels

CIAM (2007) Review of the Gothenburg protocol. Report of the task force on integrated assessment modelling and the centre for integrated assessment modelling. Center for Integrated Assessment Modelling, Geneva

Cofala J, Bojarski W (1987) Emissions of sulphur and nitrogen oxides resulting from the energetic utilization of fuels—the situation in Poland. Kernforschungszentrum Karlsruhe, Karlsruhe

Cole MA (2000) Air pollution and "dirty" industries: how and why does the composition of manufacturing output change with economic development? Environ Resour Econ 17:109–123

Dekker T, Vollebergh HRJ, de Vries FP, Withagen CA (2012) Inciting protocols. J Environ Econ Manag 64:45–67. doi:10.1016/j.jeem.2011.11.005

Dolgopolova I, Hu B, Leopold A, Pickl S (2013) Economic, institutional and technological uncertainties of emissions trading—a system dynamics modeling approach. Clim Chang (this issue)

EC (1970) Council directive 70/220/EEC on the approximation of the laws of the Member States on measures to be taken against air pollution by emissions from motor vehicles. Commission of the European Communities, Brussels

EC (2001) Directive 2001/81/EC of the European Parliament and of the Council of 23 October 2001 on national emission ceilings for certain atmospheric pollutants. European Parliament and Council, Luxembourg

EC (2007) Regulation No 715/2007 on type-approval of motor vehicles with respect to emissions from light passenger and commercial vehicles (Euro 5 and Euro 6) and on access to vehicle repair and maintenance information. Commission of the European Communities, Brussels

EC (2008) Communication from the Commission to the European Parliament, the Council, the European Economic and Social Committee and the Committee of the Regions. 20 20 by 2020: Europe's climate change opportunity. COM(2008) 30 final. Commission of the European Communities, Brussels

EMEP (2009) Transboundary, acidification, eutrophication and ground level ozone in Europe in 2007. Joint MSC-W & CCC & CEIP report. Norwegian Meterological Institute, Oslo

Grossman GM, Krueger AB (1995) Economic growth and the environment. Q J Econ 110:353–377

Gruver GW (1976) Optimal investment in pollution control capital in a neoclassical growth context. J Environ Econ Manag 3:165–177

Hoekstra R, van den Bergh JCJM (2003) Comparing structural and index decomposition analysis. Energy Econ 25:39–64. doi:10.1016/S0140-9883(02)00059-2

Hordijk L, Amann M (2007) How science and policy combined to combat air pollution problems. Environ Policy Law 37:336–340
IEA (2009a) Energy balances of OECD countries 2009. International Energy Agency, IEA/OECD, Paris
IEA (2009b) Energy balances of non-OECD countries 2009. International energy agency, IEA/OECD, Paris
IEA (2009c) Energy statistics of OECD countries 2009. International Energy Agency, IEA/OECD, Paris
IEA (2009d) Energy statistics of non-OECD countries 2009. International Energy Agency, IEA/OECD, Paris
IEA (2010) CO_2 Emissions from the fuel combustion, 2010th edn. International Energy Agency, IEA/OECD, Paris
Jonas M, Krey V, Wagner F, Marland G, Nahorski Z (2013) Uncertainty in in an emissions constrained world. Clim Chang (this issue)
Kaufmann RK, Davidsdottir B, Garnham S, Pauly P (1998) The determinants of atmospheric SO_2 concentrations: reconsidering the environmental Kuznets curve. Ecol Econ 25:209–220
Kaya Y, Yokobori K (1997) Environment, energy, and economy: strategies for sustainability. United Nations University Press
Kohl WL (1982) After the second oil crisis: energy policies in Europe, America, and Japan. Lexington Books
Kuznets S (1955) Economic growth and income inequality. Am Econ Rev 45:1–28
Lemoine DM, Fuss S, Szolgayova J, Obersteiner M, Kammen DM (2012) The influence of negative emission technologies and technology policies on the optimal climate mitigation portfolio. Clim Chang 113:141–162
Lesiv M, Bun A, Jonas M (2013) Analysis of change in relative uncertainty in GHG emissions from stationary sources for the EU 15. Clim Chang (this issue)
Markandya A, Golub A, Pedroso-Galinato S (2006) Empirical analysis of national income and SO_2 emissions in selected European countries. Environ Resour Econ 35:221–257
Mylona S (1996) Sulphur dioxide emissions in Europe 1880–1991 and their effect on sulphur concentrations and depositions. Tellus Ser B Chem Phys Meteorol 48:662–689
Peters GP, Hertwich EG (2008) CO_2 embodied in international trade with implications for global climate policy. Environ Sci Technol 42:1401–1407. doi:10.1021/es072023k
Rafaj P, Amann M, Cofala J, Sander R (2012) Factors determining recent changes of emissions of air pollutants in Europe. TSAP report #2. International Institute for Applied Systems Analysis (IIASA), Laxenburg
Salameh MG (2004) Oil crises, historical perspective. Encycl Energy 633–648
Schöpp W, Posch M, Mylona S, Johansson M (2003) Long-term development of acid deposition (1880–2030) in sensitive freshwater regions in Europe. Hydrol Earth Syst Sci 7:436–446
Selden TM, Song D (1994) Environmental quality and development: is there a kuznets curve for air pollution emissions? J Environ Econ Manag 27:147–162
Selden TM, Song D (1995) Neoclassical growth, the J curve for abatement, and the inverted U curve for pollution. J Environ Econ Manag 29:162–168
Shafik N (1994) Economic development and environmental quality: an econometric analysis. Oxf Econ Pap 46:757–773
Shindell D, Kuylenstierna JCI, Vignati E, Van Dingenen R, Amann M, Klimont Z, Anenberg SC, Muller N, Janssens-Maenhout G, Raes F, Schwartz J, Faluvegi G, Pozzoli L, Kupiainen K, Höglund-Isaksson L, Emberson L, Streets D, Ramanathan V, Hicks K, Oanh NTK, Milly G, Williams M, Demkine V, Fowler D (2012) Simultaneously mitigating near-term climate change and improving human health and food security. Science 335:183–189
Stern DI (2004) The rise and fall of the environmental Kuznets curve. World Dev 32:1419–1439
Stern DI (2006) Reversal of the trend in global anthropogenic sulfur emissions. Glob Environ Chang 16:207–220
Stern DI, Common MS (2001) Is there an environmental Kuznets curve for sulfur? J Environ Econ Manag 41:162–178
UN-ECE (1985) Protocol to the 1979 convention on long-range transboundary air pollution on the reduction of sulphur emissions or their transboundary fluxes by at least 30 per cent. United Nations Economic Commission for Europe, Helsinki
UN-ECE (1987) National strategies and policies for air pollution abatement. United Nations, New York
UN-ECE (1988) Protocol to the 1979 convention on long-range transboundary air pollution concerning the control of emissions of nitrogen oxides or their transboundary fluxes. United Nations Economic Commission for Europe, Sofia
UN-ECE (1994) Protocol to the 1979 convention on long-range transboundary air pollution on further reduction of sulphur emissions. United Nations Economic Commission for Europe, Oslo
UN-ECE (1995) Strategies and policies for air pollution abatement—1994. Major review under the convention on long-range transboundary air pollution. United Nations Economic Commission for Europe, Geneva

UN-ECE (1999) Protocol to the 1979 convention on long-range transboundary air pollution to abate acidification, eutrophication, and ground-level ozone. United Nations Economic Commission for Europe, Gothenburg

UNFCCC (1997) Kyoto protocol to the united nations framework convention on climate change. United Nations Framework Convention on Climate Change, Kyoto

UNFCCC (2009) 2009 GHG inventory submission from flexible GHG data queries. http://unfccc.int/di/FlexibleQueries.do

Vestreng V, Myhre G, Fagerli H, Reis S, Tarrasón L (2007) Twenty-five years of continuous sulphur dioxide emission reduction in Europe. Atmos Chem Phys 7:3663–3681. doi:10.5194/acp-7-3663-2007

Viguier L (1999) Emissions of SO_2, NO_x and CO_2 in transition economies: emission inventories and Divisia index analysis. Energy J 20:59–87

Waggoner P, Ausubel J (2002) A framework for sustainability science: a renovated IPAT identity. PNAS 99:7860–7865

World Bank (2013) Commodity price data. The World Bank Development Prospects Group, Washington

DOI 10.1007/978-3-319-15901-0_4
Reprinted from *Climatic Change* Journal, DOI 10.1007/s10584-014-1075-6

Analysis of change in relative uncertainty in GHG emissions from stationary sources for the EU 15

Myroslava Lesiv · Andriy Bun · Matthias Jonas

Received: 22 December 2012 / Accepted: 2 February 2014 / Published online: 27 February 2014
© The Author(s) 2014. This article is published with open access at Springerlink.com

Abstract Total uncertainty in greenhouse gas (GHG) emissions changes over time due to "learning" and structural changes in GHG emissions. Understanding the uncertainty in GHG emissions over time is very important to better communicate uncertainty and to improve the setting of emission targets in the future. This is a diagnostic study divided into two parts. The first part analyses the historical change in the total uncertainty of CO_2 emissions from stationary sources that the member states estimate annually in their national inventory reports. The second part presents examples of changes in total uncertainty due to structural changes in GHG emissions considering the GAINS (Greenhouse Gas and Air Pollution Interactions and Synergies) emissions scenarios that are consistent with the EU's "20-20-20" targets. The estimates of total uncertainty for the year 2020 are made under assumptions that relative uncertainties of GHG emissions by sector do not change in time, and with possible future uncertainty reductions for non-CO_2 emissions, which are characterized by high relative uncertainty. This diagnostic exercise shows that a driving factor of change in total uncertainty is increased knowledge of inventory processes in the past and prospective future. However, for individual countries and longer periods, structural changes in emissions could significantly influence the total uncertainty in relative terms.

This article is part of a Special Issue on "Third International Workshop on Uncertainty in Greenhouse Gas Inventories" edited by Jean Ometto and Rostyslav Bun.

Electronic supplementary material The online version of this article (doi:10.1007/s10584-014-1075-6) contains supplementary material, which is available to authorized users.

M. Lesiv
Systems Research Institute, Polish Academy of Sciences, Newelska 6, 01-447 Warsaw, Poland

M. Lesiv (✉)
Lviv Polytechnic National University, str. Bandera 12, PO Box 5446, Lviv 79031, Ukraine
e-mail: myroslava.lesiv@gmail.com

A. Bun
Delft University of Technology, Stevinweg 1, Postbus 5048, 2628 CN Delft, Netherlands

M. Jonas
International Institute for Applied Systems Analysis, Schlossplatz 1, 2361 Laxenburg, Austria

1 Introduction

The increase in GHG concentrations during the last decades is considered to be the main reason for global warming. The Kyoto Protocol to the United Nations Framework Convention on Climate Change (UNFCC), whose term ended in 2012, stipulated the reporting of GHG emissions at national scale. The recent goal of the UNFCC is to establish post-Kyoto emission reductions targets for the period from 2012. Meantime, the European Union (EU-27), as a Party to the UNFCC, has set ambitious targets for the year 2020: the reduction of GHG emissions by 20 % (or 30 %—see below) by 2020 compared with 1990 levels (EEA 2010b).

Overall, EU-27 GHG emissions are decreasing. According to the inventory report (EEA 2010a), the EU-27 is well on track to achieve its emission reduction target of 20 %. This overall trend is projected to continue until 2020. However, the 20 % reduction target compared to 1990 would therefore remain out of reach without the implementation of additional measures, such as the EU's energy and climate change package (EC 2008). This package underlines the objectives of limiting the rise in global average temperature to no more than 2 °C above preindustrial levels (EC 2009). So, the Member States agreed to cut GHG emissions by at least 20 % of 1990 levels (30 % if other developed countries commit to comparable cuts), which equals a 14 % reduction compared with 2005 levels; to cut energy consumption by 20 % of projected 2020 levels by improving energy efficiency; and to increase the use of renewables (wind, solar, biomass, etc.) to 20 % of total final energy consumption.

Uncertainty in GHG emissions is a crucial component of inventories. It specifies the absence of confidence in the inventory inputs as a result of casual factors, such as uncertainty of emission sources and emission factors, absence of transparency in the inventory process (IPCC 2006; API/CONCAWE/IPIECA 2009), and so on. In compliance with international obligations, countries should have guarantees that reported GHG emissions are sufficiently accurate. Up to now, GHG emissions and the corresponding uncertainties are still reported separately and are not considered in carbon emission trading (Ermolieva et al. 2010).

The application of a number of existing techniques to analyze emissions and emission changes against their uncertainty could provide useful knowledge that countries would like to have available prior to agreeing to emission targets (Jonas et al. 2004, 2010a, b; Bun et al. 2010). At the same time, countries should strive to provide more accurate results regarding GHG emissions. In order to decrease the level of uncertainty, the knowledge of inventory processes has to be expanded and the key reasons and emission sources that determine the level of uncertainty have to be identified.

Experience in assessing the uncertainty in GHG inventories and changes in uncertainty in relative terms is still insufficient (Lieberman et al. 2007; Jonas et al. 2010a, b; NRC 2010). So far, no studies have been done on the analysis of changes in uncertainties that countries reported in their national inventory reports. For example, from year to year countries report different values of relative uncertainties in total GHG emissions. What is the main reason for changes in reported uncertainties: structural changes in emissions or increased knowledge about inventory processes? How will uncertainties change in the future due to structural changes in GHG emissions under new policy treaties (e.g., the EU's 2020 targets)? Answers to these questions will help to better communicate the uncertainty and can be used to improve the setting of emission targets in the future.

Here, we conducted an analysis of the changes in uncertainty in relative terms in the past and nearby future for European countries. The input data (uncertainties by source) were derived from national inventory reports (NIR 2003–2008), and emissions scenarios were taken from the Greenhouse Gas and Air Pollution Interactions and Synergies (GAINS) model (IIASA 2010).

Our study is divided into two parts: (1) diagnostic analysis of the historical change in uncertainty, particularly the influence of structural changes in emissions; (2) a diagnostic exercise with one step forward: we calculate the total uncertainty with which we will have to cope at a specified point in time in the future using today's diagnostic capabilities. The paper presents an analysis of the historical change in uncertainty of CO_2 emissions for the EU-15 as a whole and for individual countries; and it also includes estimates of total uncertainty in GHG emissions under scenarios of changes in emissions considering the EU's "20-20-20" targets.

2 Methodological background

Parties to the UNFCCC publish their GHG inventory reports annually in consistency with standardized guidelines for national agencies developed by the Intergovernmental Panel on Climate Change (IPCC 1997, 2006). Parties are obliged to include in their reports direct or alternative estimates of uncertainty in results of GHG inventories. The quality of reported uncertainty varies significantly from country to country because countries do not use the same method for their emission and uncertainty assessments. The estimates of CO_2 emissions from fossil fuels consumption are the most accurate for comparison with other source categories (uncertainties are estimated in the range of ±5 %) (Marland et al. 2008).

The EU member states started to report their uncertainties in GHG emissions in different years. The first estimates of relative uncertainty were added to GHG inventory reports in 2000 and they did not cover all source categories and gases. In contrast, GHG emissions were calculated much earlier. The ranges of total uncertainty of GHG emissions for the EU-15 are available from the year 2003; the uncertainty of CO_2 emissions from fossil fuel combustion (stationary) has been detailed by source only since 2005.

Total uncertainty changes over time due to increased knowledge of inventorying GHGs and structural changes in emission sources (and sinks). The first estimates of changes in uncertainties in the past were provided in the Interim Report (Hamal 2010). The reported uncertainties in the national inventory reports reflect precision and do not consider accuracy. Precision expresses the degree of reproducibility of repeated emissions (random errors). Accuracy is the difference between the reported emissions estimate and the actual value (systematic errors). Hamal (2010) calculated combined relative uncertainties (for the EU-15), which consider accuracy and precision, using knowledge of emissions recalculations to estimate biases (systematic errors). The results, fitted with a trend function that follows an exponential curve with a decrease of approximately 4.24 % each year, are displayed in Fig. 1.

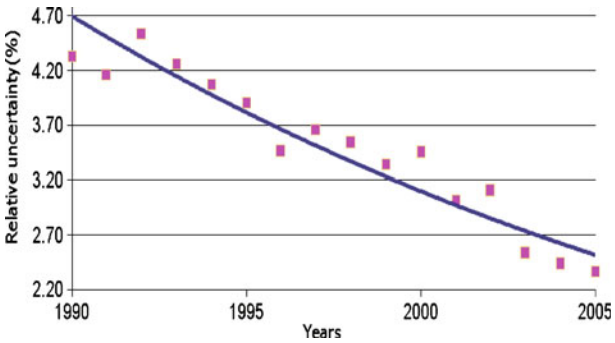

Fig. 1 Total uncertainty ranges fitted with exponential trend function (Source: Hamal 2010)

This change in uncertainty is expected to be more significant for the LULUCF (Land Use, Land-Use Change and Forestry) sector and for other GHGs that are less certain.

The decrease (Fig. 1) in the past is believed to be almost exclusively caused by "learning" and only marginally by structural changes in fossil fuel consumption. "Learning" means the process of increasing knowledge of emission factors, other parameters, and activity data and improving the inventory methods and models. However, some structural changes in emissions as the result of implementing new energy measures can cause more significant decreases or even increases in uncertainty. This happens because the uncertainty of emissions from different fuels is not the same (i.e., combustion of liquid and other fuels involves a bigger uncertainty than that of solid and gaseous fuels).

Structural changes in emissions occur all the time; for example the structure of fossil fuels consumption changes, and each fuel has a different emission factor. Replacing consumption of one fuel by another could result in an increase or decrease in the total uncertainty.

In the next two chapters, we present the methodology used to analyse historical changes in relative uncertainty and future estimates of uncertainty in GHG emissions from stationary sources. Table 1 includes a description of data sources used in the study.

2.1 Historical change in uncertainty of CO_2 emissions

We have analyzed the change in total uncertainty of CO_2 emissions by the following steps:

1. Collecting data on GHG emissions and their uncertainties by source categories (Table 1).
2. Calculation of the contribution of uncertainties in total emissions (fraction, %) at the beginning and end of the investigated period:

$$\widetilde{U}_i = \frac{x_i}{\sum_{j=1}^{n} x_j} \cdot U_i \quad \text{or} \quad \widetilde{U}_i = r_i \cdot U_i, \tag{1}$$

where $\widetilde{U}_i$ is the combined uncertainty in category i as a proportion of total emissions (%); U_i is the relative uncertainty of emissions in category i, $i=1..n$ (see Table 1) (%); x_i is the uncertain quantity (emissions) of category i (see Table 1); $r_i=x_i/\sum_{j=1}^{n} x_j$ is the fraction of source category i in total emissions.

Formula (1) follows from Approach 1 described in Chapter 3 of the IPCC Guidelines (IPCC 2006).

Table 1 Data description

Data	Source
1. Historical change in total uncertainty of CO_2 emissions	
CO_2 emissions of fossil fuels consumption by category (x_i)	National Inventory Reports (2000–2010) for the Member States (Germany, the United Kingdom, Italy, France, Spain, the Netherlands, Belgium, Greece, Austria, Portugal, Finland, Ireland, Sweden, Denmark) (UNFCCC 2010); Annual European Inventory Reports to the UNFCC (EEA 2003–2010)
Relative uncertainty by gas and category (U_i)	
2. Future change in total uncertainty	
GHG emissions in CO_2 equivalent by sectors	Annual European Inventory Reports to the UNFCC (2003-2010)
Relative uncertainty by gas and sector	

3. Analysis of the change in uncertainty due to increased knowledge: We consider that if uncertainty of elementary category (U_i) changes during the investigated period it changes due to the learning process, for example increased knowledge on uncertainty of emission factors or activity data, while the structural change (r_i) always occurs; for shorter periods it is negligible but for longer ones it could be very significant.
4. If the change in uncertainty occurs in category i due to increased knowledge, we use elements from deterministic factor analysis theory to compare the influence of the structural change in emissions and the "learning" on this change:

$$\Delta\widetilde{U}_i = \Delta\widetilde{U}_{i,r} + \Delta\widetilde{U}_{i,U}, \tag{2}$$

$$\Delta\widetilde{U}_{i,r} = \Delta\widetilde{U}_i \cdot \ln\left(\frac{r_i^1}{r_i^0}\right) \Big/ \ln\left(\frac{\widetilde{U}_i^1}{\widetilde{U}_i^0}\right), \quad \Delta\widetilde{U}_{i,U} = \Delta\widetilde{U}_i \cdot \ln\left(\frac{U_i^1}{U_i^0}\right) \Big/ \ln\left(\frac{\widetilde{U}_i^1}{\widetilde{U}_i^0}\right), \tag{3}$$

where $\Delta\widetilde{U}_{i,r}$ is the absolute change in relative uncertainty due to the structural change in emissions (%), $\Delta\widetilde{U}_{i,U}$ is the absolute change in relative uncertainty due to "learning" in source category i (%); super-indices 1 and 0 mean the end and the beginning of the investigated period, respectively.

If the change in uncertainty occurs in category i only due to the structural change in emissions, we go to the next step.

5. Analysis of change in relative uncertainty of CO_2 emissions for every source category and for the sector as whole.

A detailed example of uncertainty analysis of CO_2 emissions (stationary sources) by the steps described above is presented in Table 2, where the calculations are made for Finland, as it is one of the first countries that started to report uncertainties in GHG emissions in 2000. During the investigated period (2000–2008), knowledge of the inventory processes in some categories increased, and structural changes in fossil fuel consumption also occurred.

2.2 Future changes in uncertainty

Using today's diagnostic capabilities we are able to measure and distinguish between "learning" and structural change in the past and also in the future. We would call this "a diagnostic

Table 2 The analysis of the relative uncertainty of CO_2 emissions (stationary sources) without LULUCF for Finland (2000–2008)

Fossil fuel	Fraction of CO_2 emissions (stationary), r_i		Reported relative uncertainty, U_i, %		Uncertainty as a proportion of total CO_2 emissions (stationary),%		$\Delta\widetilde{U}_{i,U}$,%
	2000	2008	2000	2008	2000	2008	
Natural gas	0.14	0.15	1.41	1.41	0.20	0.22	0
Oil	0.43	0.45	2.83	2.83	1.22	1.28	0
Solid fuels	0.28	0.23	3.35	10.13	0.93	2.31	1.68
Other fuels	0.15	0.17	6.40	6.59	0.97	1.09	0.03
Total	1	1			1.83	2.86	
Absolute change in relative uncertainty in 2000–2008:							1.03 %

The main reason for the increase in uncertainty is "learning" processes (inventory of emissions from solid fuels combustion)

exercise with one step forward". We estimate the total uncertainty by combining uncertainties in GHG emissions from different sectors. Our main assumption is that our future knowledge of uncertainty in activity data and carbon content will be the same as today's knowledge in relative terms. So, relative uncertainty is kept constant in both activity data and carbon content during the investigated period.

To combine uncertainties, the Tier 1 approach described in Chapter 3 of the IPCC Guidelines (IPCC 2006) is used:

– Uncertainty in the results of multiplication of uncertain values is computed as:

$$U_{total} = \sqrt{U_1^2 + U_2^2 + \cdots + U_n^2}, \tag{4}$$

where U_{total} is the combined uncertainty in relative terms; U_i is relative uncertainty in value i.

– Uncertainty in the results of addition and subtraction:

$$U_{total} = \frac{\sqrt{(U_1 \cdot x_1)^2 + (U_2 \cdot x_2)^2 + \ldots + (U_n \cdot x_n)^2}}{|x_1 + x_2 + \ldots + x_n|}, \tag{5}$$

where x_i is uncertain quantity i.

While implementing Formulas (4) and (5), correlation between years is not considered, as we estimate the total uncertainty at one point in time.

The GHG inventory is principally the sum of products of emission factors, activity data, and other estimation parameters. Therefore, Approach 1 can be implemented repeatedly to estimate the uncertainty of the total inventory. We use Formula (4) to combine uncertainties in activity data and emission factor, and Formula (5) to combine uncertainties from fossil fuels consumption.

3 Results and discussion

Fossil fuel consumption is the most precise and the main key source of GHG emissions. The relative uncertainty of GHG emissions from fossil fuel burning is still considerable (up to 10 %) and influences the results of GHG inventories. The main causes of uncertainty are uncertainties in emission factors, activity data, and methods used (so far, UNFCCC methods are the most reasonable). Other sectors' emission sources, such as industrial processes, agriculture, forestry and other land uses, and waste, cause lower emissions of certain kinds. For some countries, the uncertainties in GHG emissions in these categories can be less than 25 % or more than 100 % (NRC 2010) due to the insufficient accuracy of input data and models. Sectors other than energy are not key emission sources but might be key uncertainty sources of total uncertainty of GHG inventories because of the large size of the uncertainties. Our analysis is focused mainly on the uncertainty of fossil fuel CO_2 emissions as it is the key source of GHG emissions in EU countries and the main object of international climate agreements and emission trading.

3.1 Historical change in uncertainty of CO_2 emissions

To date only a few studies have analysed the change in relative uncertainties in GHG emissions due to structural changes in emissions and "learning" (Hamal 2010; Lesiv 2012). Here, the

uncertainty analysis has been carried out for the EU-15 as a whole and for individual countries. The reported uncertainty for the EU-15 covers a short period only, which is not sufficient to carry out a proper analysis of the change in uncertainty and the factors influencing total uncertainty in relative terms. During the period 2003–2008 the emission structure did not change significantly, so the main reason for the change in uncertainty is the so-called "learning process". For such a short period it is impossible to find any tendency of the change in uncertainty.

Further research focuses on the country level because data on uncertainties of CO_2 emissions (stationary sources) are available for a longer period for individual countries. The analysis was carried out for the 15 member states.

One of the biggest GHG emitters is Germany, whose share of total emissions of the EU-15 is about 30 %. The reported uncertainty of CO_2 emissions decreased by 13 % during the period 2003–2008. During that period the structure of uncertainty estimates changed several times. The results of uncertainty analysis are shown in Table 3. The decrease in uncertainty is caused mainly by increased knowledge of the inventory processes in category "1.A.2. Manufacturing Industries and Construction".

Table 4 represents the results of analysis of the change in historical uncertainty of CO2 emissions (stationary sources) without LULUCF for Germany for the period 1990–2008 under the assumption that the relative uncertainty by category in 1990 is equal to the first estimates of uncertainty reported in 2003. During this period there were significant structural changes in fossil fuel consumption: a decrease in use of solid fuels and an increase in use of gaseous fuels. Mainly the decreasing solid fuels consumption in the category "1.A.2. Manufacturing industries and construction" reflected the decrease in total uncertainty. The ranges of total uncertainty during 1990–2008 were reduced by approximately 16 % (considering only precision).

The results of the uncertainty analysis for the EU-15 Member States are summarized in Table 5, except for Luxemburg, which first reported the uncertainty of GHG emissions in

Table 3 The analysis of relative uncertainty of CO_2 emissions (stationary sources) without LULUCF for Germany (2003–2008)

Category	Fraction of CO_2 emissions (stationary), r_i		The square of combined uncertainty as a percentage of CO_2 emissions (stationary), $\tilde{U}_i^2$ %		Analysis
	2003	2008	2003	2008	
1.A.1.a Public electricity and heat production	0.480	0.530	0.064	0.057	Change is caused by structural change in emissions and "learning"
1.A.1.b Petroleum refining	0.029	0.036	0.000	0.000	Negligible change
1.A.1.c Manufacture of solid fuels	0.031	0.022	0.000	0.000	Negligible change
1.A.2. Manufacturing industries and construction	0.192	0.158	0.020	0.002	Significant change caused by "learning" and to a lesser extent by structural change
1.A.4.a Commercial/institutional	0.073	0.067	0.003	0.003	Negligible change
1.A.4.b Residential	0.182	0.174	0.019	0.020	Negligible change
1.A.4.c Agriculture/forestry/fisheries	0.010	0.011	0.000	0.000	Negligible change
1.A.5. Others	0.003	0.002	0.000	0.000	Negligible change

Table 4 The analysis of relative uncertainty of CO_2 emissions (stationary sources) without LULUCF for Germany (2000–2008)

Category	Fraction of CO_2 emissions (stationary), r_i		The square of combined uncertainty as a part of CO_2 emissions (stationary), $\widetilde{U}_i^2$ %		Analysis
	1990	2008	1990	2008	
1.A.1.a Public electricity and heat production	0.405	0.530	0.047	0.057	Change is caused by structural change in emissions and "learning"
1.A.1.b Petroleum refining	0.023	0.036	0.000	0.000	Negligible change
1.A.1.c Manufacture of solid fuels	0.072	0.022	0.002	0.000	Negligible change
1.A.2. Manufacturing industries and construction	0.238	0.158	0.044	0.002	Significant change caused by the structural change and less by "learning"
1.A.4.a Commercial/institutional	0.075	0.067	0.003	0.003	Negligible change
1.A.4.b Residential	0.156	0.174	0.019	0.020	Negligible change
1.A.4.c Agriculture/forestry/ fisheries	0.016	0.011	0.000	0.000	Negligible change
1.A.5. Others	0.014	0.002	0.000	0.000	Negligible change

2007. Countries are sorted by emitters starting from the largest, that is, Germany, because of its larger contribution to the total emissions and uncertainty of the EU-15. The last column of Table 5, "Analysis of the influence of individual factors on the change in uncertainty" includes the "decrease" or "increase" in uncertainty and the main cause of its change.

Structural change in emissions always occurs and over longer periods it could significantly influence the total uncertainty in relative terms. The analysis of the historical change in total uncertainty of CO_2 emissions (stationary sources) shows that for individual countries the structural change in emissions may be the main factor in the uncertainty change while for the EU-15 total uncertainty varies mainly due to the increased knowledge on inventory processes ("learning"). For example, for Italy, France, the Netherlands, Belgium, Greece, and Denmark, changes in uncertainty of CO_2 emissions are caused mainly by structural changes in emissions; in contrast, for Germany, the UK, Austria, Portugal, Finland, and Sweden, they are caused mainly by "learning" (the change in estimates of emission factors and activity data).

3.2 Future change in uncertainty of total GHG emissions

Based on the above past analysis and considering the EU's ambitious targets under the Integrated Energy and Climate Change package, more structural changes in fuel consumption are expected in the future. The estimation of relative uncertainty in GHG emissions for a certain point of time in the future would show whether uncertainty in total inventory results will increase or decrease and would identify the main reason for changes in uncertainty.

Further, the results of uncertainty estimates for the year 2020 are described. As mentioned in Section 2.2, we assume that our future knowledge of uncertainty in activity data and carbon content will be the same as today's knowledge in relative terms. In other words, relative uncertainty is kept constant during the investigated period. For our calculations we took emission scenarios developed at the International Institute for Applied Systems Analysis

Table 5 The analysis of the historical change in uncertainty of CO_2 emissions without LULUCF (stationary sources) for the EU's Member States

Member State	Period of available data	Relative uncertainty at the beginning of investigated period, %	Relative uncertainty at the end of investigated period, %	Change in uncertainty, %	Analysis of the influence of individual factors on the change in uncertainty
Germany	2003–2008	3.20	2.86	–13.3	"Learning"
The United Kingdom	2000–2008	2.94	2.26	–23.0	"Learning" + structural change
Italy	2001–2008	2.60	2.62	+0.8	Structural change
France	2001–2008	1.29	1.25	–3.6	Structural change
Spain	2000–2008	2.62	2.96	+13.3	Structural change + "learning"
The Netherlands	2004–2008	2.25	2.31	+2.6	Structural change
Belgium	2004–2008	2.69	2.66	–4.8	Structural change
Greece	2002–2008	4.88	4.64	+4.9	Structural change
Austria	2003–2008	0.82	1.09	+32.5	"Learning" + structural change
Portugal	2004–2008	2.67	11.09	+315.8	"Learning" (rapid change in uncertainties by categories in 2008)
Finland	2000–2008	1.83	2.86	+56.6	"Learning" (due to the uncertainty change in "1.A.1.c. Manufacture of solid fuels")
Ireland	2001–2008	2.96	2.85	–3.79	Structural change
Sweden	2000–2008	5.11	3.66	–28.5	"Learning"
Denmark	2001–2008	2.54	1.50	–40.1	Structural change

(GAINS) because they are based on countries' emission projections and reflect the results of implementing new policies and measures and also a baseline scenario. More information on the above scenarios is available on the GAINS website (IIASA 2010).

The calculations were based on the GAINS emission scenarios for the EU-15 for the year 2020 (see Box 1).

The results of calculation of the total uncertainty are shown in Fig. 2. "C&E package + NitrDir; OPTV5" is the only scenario that results in a decrease in total uncertainty in relative terms due to the structural change, because it assumes an appreciable emission reduction in the agricultural sector, which is characterized by high uncertainties.

Assessments of total uncertainty in relative terms were also made while considering possible reductions in uncertainties of GHG emissions in fugitive emissions and the agricultural and waste sectors, which could be achieved in the future (2020). We assumed that the uncertainty of fugitive emissions will decrease to 25 %, that of GHG emissions in agriculture to 50 %, and that of GHG emissions from waste to 15 %. These assumptions were based on given possible improvements in uncertainty assessment in a few years for developed countries (NRC 2010). The results are illustrated in Fig. 3.

Figure 3 shows that reductions in uncertainties in fugitive emissions, agriculture, and waste can cause a significant decrease in total uncertainty in relative terms. Even in the case of the "worst" emission scenario, "C&E package; current legislation", which does not consider implementation of new policies legislatively, the total uncertainty decreases over time. Comparison of the results achieved (Figs. 2 and 3) shows that "learning" is a driving factor of decreases in total uncertainty in relative terms.

The conducted analysis is based on reported uncertainties in relative terms that consider only precision. The recalculations of total uncertainty considering accuracy increase uncertainty ranges and reinforce the influence of increased knowledge on inventory processes (Hamal 2010).

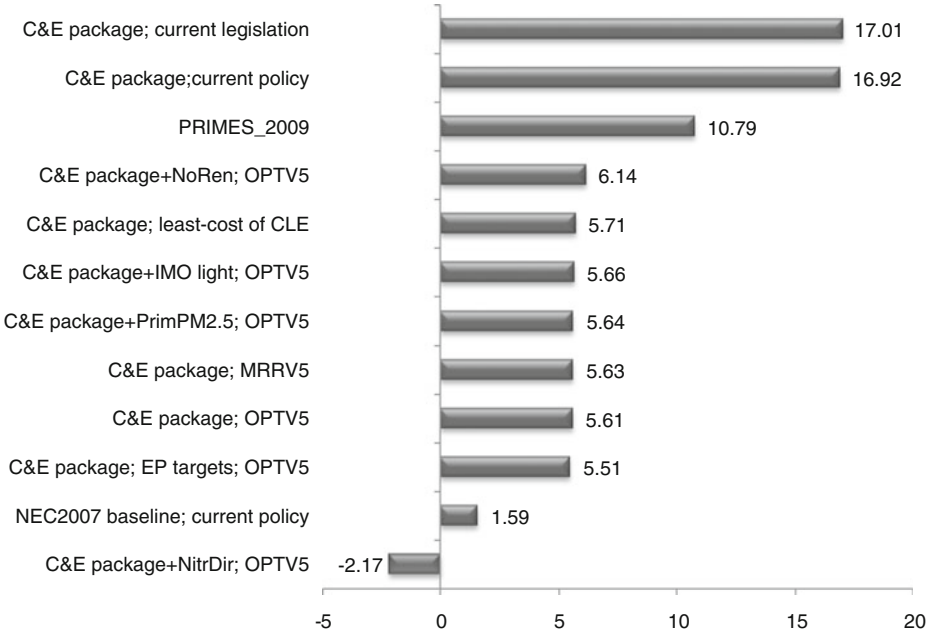

Fig. 2 Change (%) in total uncertainty of GHG emissions for EU-15 in 2020 under GAINS emissions scenarios (without LULUCF)

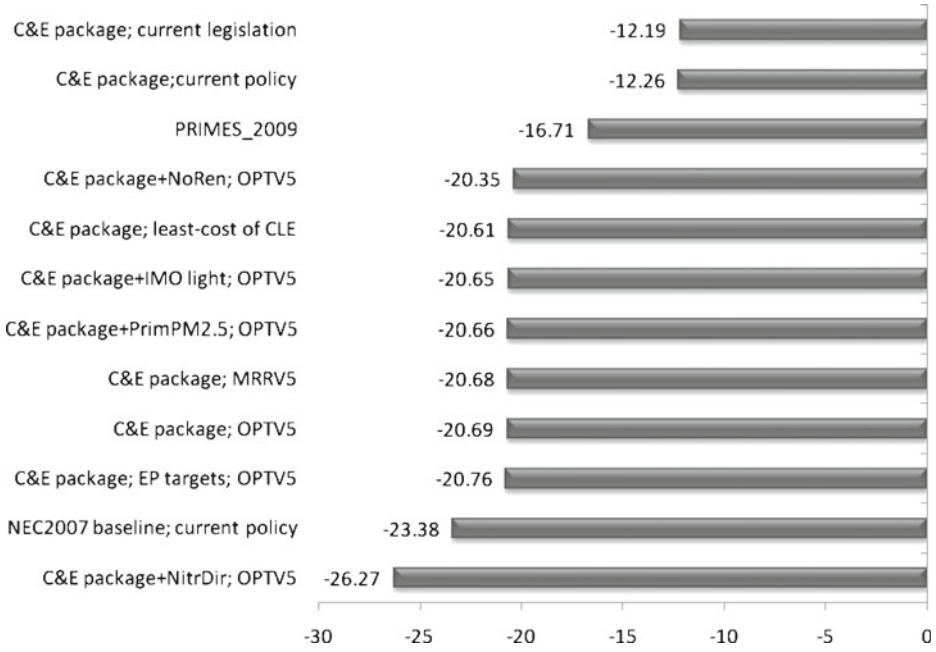

Fig. 3 Reduction (%) in total uncertainty of GHG emissions for the EU-15 in 2020 under GAINS emissions scenarios considering possible increases in knowledge in sectors with high uncertainty (without LULUCF)

The estimates of uncertainty in CO_2 emissions from stationary sources are the most certain and can be improved more because not all countries use higher tier inventory methods and emission factors or other estimation parameters and their associated uncertainties, which should be estimated from original research including country-specific data.

In terms of global carbon accounting, the sizes of changes in uncertainties are not that large. However, at country level these changes in uncertainties over time should be considered while establishing new international agreements on GHG emission targets. Also, decreased uncertainties in GHG emissions will make emissions trading between countries clearer.

Box 1. GAINS emission scenarios

C&E (Climate & Energy) package + NitrDir; OPTV5[1]—an optimized emission scenario that assumes an energy projection that is consistent with the EU's "20-20-20" targets; and an agricultural projection that explores the potential implications of a full implementation of the Nitrates Directive (EC 1991);

NEC2007 baseline; current policy—an emission scenario that employs the PRIMES baseline projection of November 2007, which illustrates a business-as-usual case without further climate measures, and an agricultural projection that reflects national perspectives on the development of the agricultural sector;

C&E package; EP targets; OPTV5—an optimized emission scenario that assumes an energy projection that is consistent with the EU's "20-20-20" targets, and an agricultural projection that reflects national perspectives on the development of the agricultural sector; it meets more stringent environmental objectives in 2020, as requested by the European Parliament;

C&E package; OPTV5—an optimized emission scenario that assumes an energy projection that is consistent with the EU's "20-20-20" targets, and an agricultural projection that reflects national perspectives on the development of the agricultural sector;

[1] OPTV5 – optimized emission scenario

C&E package; MRRV5[2] is based on the activity projections of the EU's "20-20-20" targets and estimates the potential for further emission reductions that are achievable through a full application of the most advanced technical (add-on) emission control measures that are on the market today;

C&E package + PrimPM2.5; OPTV5—an optimized emission scenario that assumes an energy projection that is consistent with the EU's "20-20-20" targets and an agricultural projection that reflects national perspectives on the development of the agricultural sector and that health impacts of particulate matter are solely caused by primary emissions of PM2.5; that is, that secondary aerosols would not cause negative health effects;

C&E package + IMO light; OPTV5—an optimized emission scenario that assumes an energy projection that is consistent with the EU's "20-20-20" targets and an agricultural projection that reflects national perspectives on the development of the agricultural sector and the new limits for emissions that were agreed at a meeting of the International Maritime Organisation (IMO) Marine Environment Protection Committee (MEPC) in April 2008;

C&E package; least-cost of CLE presents the least-cost implementation of the emission levels of the current policy case of the EU's "20-20-20" strategy;

C&E package + NoRen; OPTV5—an optimized emission scenario that assumes an energy projection that is consistent with the EU's "20-20-20" targets (the 20 % renewable target is met in this scenario within each country without international trading) and an agricultural projection that reflects national perspectives on the development of the agricultural sector;

PRIMES_2009—PRIMES baseline scenario of the year 2009;

C&E package; current policy assumes baseline for NECD plus the EU's "20-20-20" strategy;

*C&E package; current legislation2014*the "current legislation" projection for the Climate and Energy Package.

4 Conclusions

Total uncertainty in relative terms changes over time due to structural changes in GHG emissions and the increased knowledge of inventory processes or so-called "learning". Analysis of the historical change in uncertainty has been carried out for the EU-15 as well as for individual countries. The achieved results confirm that the uncertainty of CO_2 emissions of the EU-15 has changed historically mainly due to increased knowledge of GHG inventory processes. In contrast, for some individual countries (Italy, France, Netherlands, Belgium, Greece, Denmark) total uncertainty of CO_2 emissions (excluding LULUCF) changed in the past only due to structural changes in emissions. Germany, as the biggest European GHG emitter, reported a considerable decrease in uncertainty caused by "learning". The recalculations of total uncertainty considering accuracy lessen the influence of the structural change in emissions.

The calculations of total uncertainty in relative terms considering today's knowledge of inventory processes have been based on the GAINS emission scenarios until 2020. The estimates of total uncertainty that assume constant relative uncertainty during the investigated period show the increase in uncertainty for most of the emission scenarios except the scenario "C&E package + NitrDir; OPTV5", which is consistent with the EU's "20-20-20" targets and an agricultural projection that explores the potential implications of a full implementation of the Nitrates Directive. Such an increase in total uncertainty is caused by the increased proportion of renewables, which have less certain emission factors and activity data, and decreased proportion of emission categories (agriculture, waste, etc.) in energy consumption. These changes in uncertainty due to structural change in emissions are negligible, though, while the estimates of total uncertainty of GHG emissions that assume a possible decrease in uncertainty in future due to the "learning" based on the GAINS emissions scenarios show a considerable decrease in total uncertainty. Thus improving our knowledge of fugitive

[2] MRRV5—maximum emissions reductions in the RAINS model

emissions and the agricultural and waste sectors could cause significant reductions in total GHG emissions uncertainties.

This study underlines that "learning" is the main reason for the change in uncertainty in the last few decades and could be a very important factor in uncertainty reduction in the near future. Scientists and experts should put more effort into increasing knowledge of the inventory processes, especially in sectors (agriculture, waste, etc.) which are expected to be the main drivers of uncertainties in GHG emissions.

Acknowledgments This research was funded by the Marie Curie Project No. 247645, entitled: GESAPU-Geoinformation Technologies, Spatio-Temporal Approaches, and Full Carbon Account For Improving Accuracy of GHG Inventories, and the project "International PhD studies in Intelligent computing" financed with the European regional development fund, and the project of the Ministry of Education and Science of Ukraine. We thank the anonymous reviewers for their comments, which helped to improve the paper.

Open Access This article is distributed under the terms of the Creative Commons Attribution License which permits any use, distribution, and reproduction in any medium, provided the original author(s) and the source are credited.

References

API, CONCAWE, IPIECA (2009) Addressing uncertainty in oil and natural gas industry greenhouse gas inventories: technical considerations and calculation method. Pilot Version, London. Available at: http://www.api.org/ehs/climate/response/upload/Addressing_Uncertainty.pdf

Bun A, Hamal K, Jonas M, Lesiv M (2010) Verification of compliance with GHG emissions target: annex B countries. Clim Chang 103:215–225

EC (1991) Nitrates Directive. Available at: http://ec.europa.eu/environment/water/water-nitrates/index_en.html

EC (2008) Second strategic review – An EU security and solidarity action plan – Europe's current and future energy position – Demand – resources – investments. SEC (2008) 2871, Brussels, 13 November 2008. Vol. 1. Available at: http://ec.europa.eu/energy/strategies/2008/2008_11_ser2_en.htm

EC (2009) EU action against climate change – Leading global action to 2020 and beyond. Directorate-General for the Environment Information Centre (BU-9 0/11), B-1049 Brussels

EEA (2003–2010) Annual European Union greenhouse gas inventories and inventory reports. Available at: http://www.eea.europa.eu/publications/#c9=all&c14=technical_report_2002_75&c12=&c7=en&c11=5&b_start=0

EEA (2010) Annual European Union greenhouse gas inventory 1990–2008 and inventory report 2010. Available at: http://www.eea.europa.eu/publications/european-union-greenhouse-gas-inventory-2010

EEA (2010) Tracking progress towards Kyoto and 2020 targets in Europe. Denmark. Available at: http://www.eea.europa.eu/publications/progress-towards-kyoto.

Ermolieva T, Ermoliev Y, Fischer G, Jonas M, Makowski M, Wagner F (2010) Carbon emission trading and carbon taxes under uncertainties. Clim Chang 103(1):277–289

Hamal K (2010) Reporting greenhouse gas emissions: change in uncertainty and its relevance for the detection of emission changes. Interim report IR-10-003, Laxenburg, Austria: International Institute for Applied Systems Analysis. Available at: http://www.iiasa.ac.at/Publications/Documents/IR-10-003.pdf

IIASA (2010) GAINS – the greenhouse gas and air pollution interactions and synergies (GAINS)-model. Available at: http://gains.iiasa.ac.at/gains/EUR/index.login?logout=1

IPCC (2006) 2006 IPCC guidelines for national greenhouse gas inventories. In: Eggleston HS, Buendia L, Miwa K, Ngara T, Tanabe K (eds) Prepared by the National Greenhouse Gas Inventories Programme. Institute for Global Environmental Strategies, Japan

IPCC (1997) Revised 1996 IPCC guidelines for national greenhouse gas inventories, Vol. 1: Greenhouse gas inventory reporting instructions; Vol. 2: Greenhouse gas inventory workbook; Vol. 3: Greenhouse gas inventory reference manual. Intergovernmental Panel on Climate Change (IPCC) Working Group I (WG I) Technical Support Unit, IPCC/OECD/IEA, Bracknell, United Kingdom. Available at: http://www.ipcc-nggip.iges.or.jp/public/gl/invs1.htm

Jonas M, Gusti M, Jeda W, Nahorski Z, Nilsson S (2010a) Comparison of preparatory signal analysis techniques for consideration in the (post-)Kyoto policy process. Clim Chang 103:175–213

Jonas M, Marland G, Winiwarter W et al (2010b) Benefits of dealing with uncertainty in greenhouse gas inventories: introduction. Clim Chang 103(1):3–18

Jonas M, Nilsson S, Bun R, Dachuk V, Gusti M, Horabik J, Jęda W, Nahorski Z (2004) Preparatory signal detection for Annex I countries under the Kyoto protocol – a lesson for the post-Kyoto policy process. Interim report IR-04-024, International Institute for Applied Systems Analysis, Laxenburg, Austria, p 91. Available at: http://www.iiasa.ac.at/Publications/Documents/IR-04-024.pdf

Lesiv M (2012) Influence of structural changes in emissions on total uncertainty. Interim report IR-12-018, International Institute for Applied Systems Analysis, Laxenburg, Austria, p 20

Lieberman D, Jonas M, Winiwarter W et al (2007) Accounting for climate change: introduction. Water Air Soil Pollut Focus 7:421–424

Marland G, Hamal K, Jonas M (2008) How uncertain are estimates of CO2 emissions? J Ind Ecol 13:4–7

National inventory reports (2003–2008) under the UNFCCC Treaty. Available at: http://unfccc.int/national_reports/annex_i_ghg_inventories/national_inventories_submissions/items/4303.php

National Research Council (2010) Verifying greenhouse gas emissions: methods to support international climate agreements. National Academies Press, Washington. Available at: http://www.nap.edu/openbook.php?record_id=12883&page=11

UNFCCC (2010) National inventory reports (2000–2008) under the UNFCCC treaty. Available at: http://unfccc.int/national_reports/annex_i_ghg_inventories/national_inventories_submissions/items/4303.php

DOI 10.1007/978-3-319-15901-0_5
Reprinted from *Climatic Change* Journal, DOI 10.1007/s10584-013-1031-x

Compliance for uncertain inventories via probabilistic/fuzzy comparison of alternatives

Olgierd Hryniewicz · Zbigniew Nahorski · Jörg Verstraete · Joanna Horabik · Matthias Jonas

Received: 22 December 2012 / Accepted: 6 December 2013 / Published online: 15 February 2014
© The Author(s) 2014. This article is published with open access at Springerlink.com

Abstract A direct comparison among highly uncertain inventories of emissions is inadequate and may lead to paradoxes. This issue is of particular importance in the case of greenhouse gases. This paper reviews the methods for the comparison of uncertain inventories in the context of compliance checking. The problem is treated as a comparison of uncertain alternatives. It provides a categorization and ranking of the inventories which can induce compliance checking conditions. Two groups of techniques to compare uncertain estimates are considered in the paper: probabilistic and fuzzy approaches. They show certain similarities which are revealed and stressed throughout the paper. The group of methods most suitable for the compliance purpose is distinguished. They introduce new conditions for fulfilling compliance, depending on inventory uncertainty. These new conditions considerably change the present approach, where only the reported values of inventories are accounted for.

1 Introduction

A handful of solutions have been proposed to cope with the problem of emission commitment evaluation for uncertain inventories, see Jonas and Nilsson (2007). Numerous propositions have pointed to methodological incompetence in using the reported (point) values in clearing emission targets. For many environmental problems such as for greenhouse gases, only highly imprecise values of emission are available, see e.g. Jonas and Nilsson (2007); Jonas et al. (2010b); Lieberman et al. (2007); White et al. (2011). Apart from a high uncertainty level, uncertainty distributions are often asymmetric, as they reflect non-negative measurements of physical quantities. For an example, see the results in Ramirez et al. (2006) or Winiwarter and Rypdal (2001).

This article is part of a Special Issue on "Third International Workshop on Uncertainty in Greenhouse Gas Inventories" edited by Jean Ometto and Rostyslav Bun.

Electronic supplementary material The online version of this article (doi:10.1007/s10584-013-1031-x) contains supplementary material, which is available to authorized users.

O. Hryniewicz · Z. Nahorski (✉) · J. Verstraete · J. Horabik
Systems Research Institute, Polish Academy of Sciences, Newelska 6, 01-447 Warsaw, Poland
e-mail: Zbigniew.Nahorski@ibspan.waw.pl

M. Jonas
International Institute for Applied Systems Analysis, Schlossplatz 1, 2361 Laxenburg, Austria

According to the IPCC Good Practice Guidelines (IPCC 1996), a report should be "consistent, comparable and transparent". Decisions on the fulfilment of obligations should be fair for all parties, which means that it should be transparent why some inventories comply with commitments while others do not. Since greenhouse gases inventories are highly uncertain, making decisions on compliance or comparison of inventories based only on the reported values (estimated size) may contradict any conclusions inferred from considering uncertainty distributions such as uncertainty range (e.g. standard deviation) and the shape of uncertainty distribution (e.g. skewness). We argue that this knowledge should be fully utilized to make decisions on compliance and to infer a comparison of emissions.

Let us consider two uncertain emission inventories, A and B of Fig. 1a–b, which will help us to illustrate the techniques discussed. For the sake of simplicity, let us assume that both involved parties have the same emission limits, also called a target, for instance, an allocated number of emission permits. The dominant values of the uncertainty distribution densities $\mu(x)$ reflect the reported inventories of both parties, which are very close. If uncertainty is ignored, party A would be considered compliant (fulfilling the limit), while party B would not. However, confidence in the inventory value of party B is high, while that of A is low, raising the question which party is more credible? Should party A be considered compliant, while party B should not? Certainly, to compare parties with different scale of emissions, the inventories have to be normalized. For example, the value $d=(x-K)/x$, with K denoting the party's emission limit, may be a suitable normalization; then the normalized limit is equal to zero. Henceforth, the term inventory will always refer to a normalized inventory.

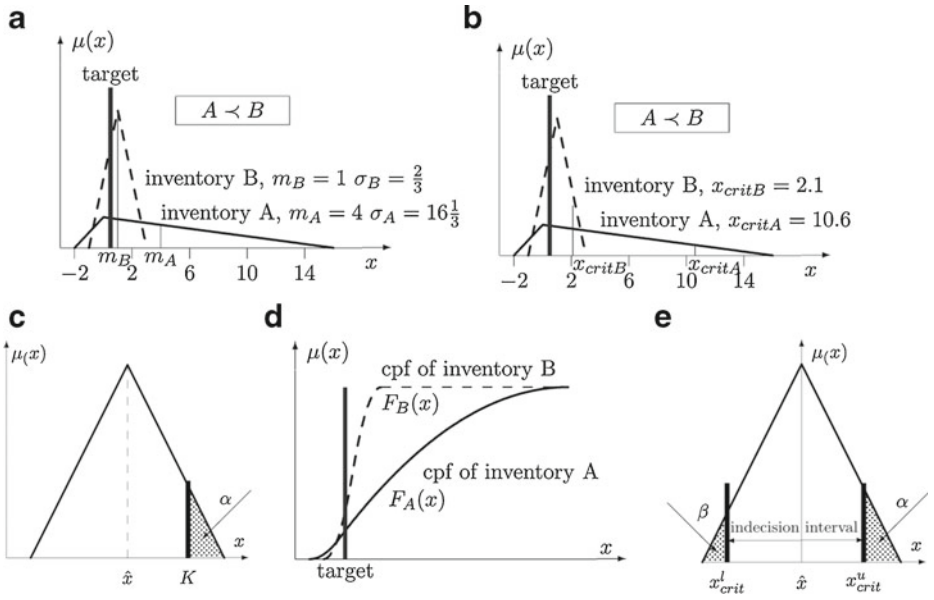

Fig. 1 Illustration for statistical approaches: **a** Comparison of means and variances; **b** Calculation of critical values; **c** Illustration of compliance in the undershooting approach; **d** Stochastic dominance criterion for comparison of inventories A and B; **e** The indecision interval

In this paper we look at the problem of fulfillment as one of the comparison and ordering of (normalized) inventories. When inventories can be ordered in a transparent way, then we can point to the threshold value, below which the inventories are compliant, and above which they are not. With the present method inventories care actually ordered according to the reported values. Those which are below the limit are considered compliant, while those above are not. As mentioned before, the ordering of uncertain inventories simply according to their reported values is dubious, since their uncertainty should also be taken into account. The idea of this paper is to review the methods for comparison of uncertain values, so that uncertain inventories can be credibly ordered. This will introduce transparency into the compliance mechanism. Henceforth, a higher ranked inventory A is considered *better in respect to* (*i.r.t.*) *the target* than inventory B, and is denoted by $B \prec A$.

Verification of emission reduction in a single country may also face the problem of uncertainty. Let us consider the case of greenhouse gases, when a reduction of emissions at the end of the commitment period is required. This is expressed as a specified rate ρ of the real emissions in the previous (basic) year. Since the real emissions are not known, only an uncertain inventory in the compliance year, x_c, can be compared with a reduced uncertain inventory in the basic year, ρx_b. From this, it has to be decided whether the former emissions are lower than the latter. In other words, these two inventories should be ranked in as convincing a manner as possible. This also motivated our search for adequate methods to compare uncertain values. But another view is also possible in this case. Consider a variable defined as $d = \frac{x_c}{x_b} - \rho$ or the so called *trend uncertainty* $d = \frac{x_b - x_c}{x_b} - (1-\rho)$. These are normalized variables, which can be used for comparison among countries with different scales of emissions, and even with different reduction rates ρ. For them, the limit for comparison equals zero. Consequently, countries can be ordered appropriately according to their values of d and accounting for uncertainty. With this ordering, compliance conditions can be formulated. Note that for the Monte Carlo simulation, which is presently the basic tool for assessment of uncertainty distributions, there is no great difference as to whether a distribution of variable d instead of variable x is to be generated.

Nevertheless, it should be stressed that ranking is only supplementary to the compliance checking rule that is adopted. It can help to justify why some inventories are considered compliant, while others are not. Ranking of inventories may facilitate avoiding paradoxical situations, when decisions on compliance or noncompliance are at variance with common sense.

Throughout the paper it is assumed that the distribution of inventory uncertainty is available. This would be the ideal case. Unfortunately, for national GHG inventories it is largely impossible to estimate distributions in the statistical sense, since inventories cannot be repeated in great numbers with different values of unsure parameters. The distributions can be, however, assessed by performing Monte Carlo calculations, which provide good insight to the distribution of national inventories. Some countries (e.g. Austria, the Netherlands) have undertaken this effort (Winiwarter and Rypdal 2001; Ramirez et al. 2006). Others report either uncertainty intervals or simply standard deviations. Although the probability-rooted methods presented in Section 2 mostly require knowledge of probability distribution, in the fuzzy-set-rooted methods, discussed in Section 3, the distribution of uncertainty may be shaped more flexibly, including interval information or, for instance, the use of expert knowledge. The assessment of uncertainty distribution and the accuracy of its estimation is a problem in itself. It requires a separate discussion, which, however, is beyond the scope of the present paper.

2 Probabilistic approaches

2.1 Introductory remarks

Although the inventories do not fully comply with randomness assumptions, treating an inventory as a random value with probabilistic distribution seems to be self-imposing.

The comparison of uncertain random values has been already considered in various fields. The problem of selection from high-risk projects has had a long history in areas such as finance, R&D projects, or IT projects (Graves and Ringuest 2009). Several methods have been proposed to compare such projects. The methods can be further divided into groups. All the methods presented below are adapted to the problem of emission inventories. Most of them require knowledge of the inventory probability distribution.

2.2 Statistical moments

Mean value and variance The most elementary technique is based on *the mean value and variance* (MV). Obviously, the smaller the mean value and variance, the better the inventory. This approach is illustrated in Fig. 1a. Although the reported value of inventory A is smaller than that of B, its mean value is greater than the mean value of B. The same is true for the standard deviations. Even this simple criterion shows that an inventory of party B should be considered better i.r.t. the target than that of party A. This is contradictory to the result based on reported values, which disregard uncertainty. According to the latter approach, the compliance mechanism would be related to a comparison of mean values, and not reported values. However, a single mean value is not enough for ranking purposes.

Semivariance Comparison of inventories using two indices, mean value and standard deviation, may lead to contradictory results. A notion of *the semivariance* (MSV) should rather be applied, following the definition

$$s_S^2 = \int_K^\infty (x-K)^2 \mu(x) dx \,,$$

where K is a chosen value and $\mu(x)$ is the distribution density function of an inventory. The smaller the value of s_S^2, the higher the inventory is ranked. In our case, K can be conveniently chosen as a given target, and this value is used in the example of Fig. 1a, as well as in the result survey of Table S1 in the supplementary material. In the considered example it holds that $s_{SA}^2 > s_{SB}^2$, thus, inventory B is better i.r.t. the target than A. According to the criterion, an inventory satisfies the target if the semivariance is smaller than a preselected value.

2.3 Critical values

Critical probability A large group of techniques use the term *critical probability* (CP), a notion first introduced in 1952 (Roy 1952). It is defined as the probability of surpassing target K

$$crp = \int_K^\infty \mu(x) dx \,.$$

A smaller value of *crp* indicates a better inventory i.r.t. the target. As seen in Fig. 1b, again, an inventory of party B is evaluated as being better. Determining compliance with a limit is based on calculation of the critical probability, which should not be greater than any prescribed value.

Risk In other related methods, as *the Baumol's risk measure* and *the value at risk* (VaR), a critical value x_{crit} is calculated for a settled probability α, so that the probability that emission value will be higher than x_{crit} is α. Without going into details, an inventory is better i.r.t. the target whenever x_{crit} is smaller. In the example from Fig. 1b, with fixed probability α=0.1, inventory B is indicated as the better one.

Undershooting A technique similar in spirit has been proposed to ensure reliable compliance. It states that only a small enough α-th part of an inventory distribution may lie above target K. This approach is called *undershooting*, see Gillenwater et al. 2007; Godal et al. 2003; Nahorski and Horabik 2010; Nahorski et al. 2003, and it is illustrated in Fig. 1c. Note, that when used for ordering inventories, the idea becomes equivalent to the CP technique.

2.4 Stochastic dominance

Stochastic dominance In *the stochastic dominance technique* inventory B is better i.r.t. the target than A if their cumulative probability functions (*cpf* s) satisfy $F_A(x) \le F_B(x)$ for all x, and the condition is strict for at least one x. It is obvious that not all inventories can be decisively compared this way, see *cpf* s of our exemplary inventories A and B depicted in Fig. 1d. Although *cpf* of party B is greater for most values of x, it is lower than *cpf* of party A for a small range of low values. This potential lack of an unequivocal answer is a serious drawback of the method. However, some modifications have been proposed to extend its usability.

Almost stochastic dominance In *the almost stochastic dominance* (ASD)[1] inventory B is better i.r.t. the target than A, if the area between both *cpf* s for $F_B(x) < F_A(x)$ is a small enough (ε times smaller, usually with $0 < \varepsilon < 0.5$) part of the whole area between *pdf* s, $\int_x |F_B(x) - F_A(x)| dx$. It can be seen by inspection of Fig. 1d that this condition is satisfied in our example of Fig. 1a–b. Thus, this technique also indicates inventory B better i.r.t. the target.

A simplified comparison of inventories would confine itself to checking the values of *cpf* s at $x=K$. This would be equivalent to a variant of critical probability approach. Thus, the analysis of fulfilment of the limit in the stochastic dominance techniques could be reduced to checking if the value of the inventory *cpf* at the limit is sufficiently high.

2.5 Two-sided comparison of inventories

The approaches discussed guarantee a proper ordering when the reported value is smaller or equal to the limit K (see supplementary material). To properly order the inventories for $K < \hat{x}$, it is useful to consider the probability

$$\beta = \int_{-\infty}^{K} \mu(x) dx.$$

[1] This is the first order ASD. For the second order ASD see Graves and Ringuest (2009).

The smaller the value of β is, the more certain the inventory is likely to be noncompliant. To make significant decisions, we would like to have a small value of α to help decide that the inventory is compliant, and a small value of β to help decide that it is noncompliant. Having fixed α and β, we can calculate the corresponding critical values x^u_{crit} and x^l_{crit}, as illustrated in Fig. 1e. Thus, there will be an indecision interval for $K \in (x^l_{crit}, x^u_{crit})$ where there is uncertainty as to whether the inventory fulfils the limit or not. This can be considered as a generalization of the undershooting method.

The question arises what can be done when the limit falls into the indecision interval. It is actually fair to say that no decision can be taken confidently. One of the answers proposed in Jonas et al. (1999) and Gusti and Jęda (2002) was to wait until the inventory subsequently crosses an indecision boundary in the consequent years. A rough method to estimate when this may take place was also designed, called *the verification time*. It is based on a linear or quadratic prognosis of future emission trajectory combined for compliance with an obligatory undershooting of the indecision boundary, so that the national emission reductions and limitations become detectable.

3 Fuzzy set approaches

3.1 Introduction

Fuzzy set and possibilistic models of uncertainty can be considered as a competitive approach to the probabilistic one, described above. In the fuzzy set theory, comparison and ranking of fuzzy (or inaccurate) values is a problem to which different solutions have been proposed. Ignoring conceptual differences, there are sufficient similarities to warrant further investigation into how the possibilistic ranking methods hold up against the other methods. In the following subsections, we will list four conceptually different groups of methods that are used to compare fuzzy numbers. Some of the methods resemble those from the probabilistic approaches; others use different paradigms. The methods illustrate the fact that various approaches can be used to tackle the comparison problem.

A short introduction to the fuzzy sets and discussion of conceptual differences between the probabilistic and fuzzy set approaches can be found in the supplementary material.

3.2 On the underlying assumptions

Most of the fuzzy comparison and ranking methods have been developed for fuzzy sets over the domain [0,1]. The main reason for this is that there are some specific advantages in developing ranking methods (e.g. integrals over the domain cannot yield a result greater than 1). For the application of the methods in the comparison and ranking of different inventories, the methods could be modified to suit a different domain. This is possible for all the methods, but may complicate the formulas somewhat. To keep the formulas simple and to remain true to the original definitions, this option was disregarded. An alternative option would be to rescale the domain of the inventories to the interval [0,1] to allow for a direct application of the methods. If the supports of the fuzzy number is finite, as we assume here, and in the original support $x \in [l,r]$, the new variable, spread in [0,1], is defined as $z=(x-l)/(r-l)$.

The ranking methods below put forward a comparison of at least two fuzzy numbers. Some authors have chosen to rank from lowest to highest; others rank from highest to lowest. The aim of this article is to present different methods and show how difficult cases can be distinguished differently. Although these are minor details that can easily be overcome this should not detract anything from the message.

Not all the techniques proposed for comparison of fuzzy sets are mentioned below. Some of those not mentioned can be found in a review paper by Bortolan and Degani (1985). A more recent technique can be found in Tran and Duckstein (2002).

3.3 An analogue to moments

Yager F1 In Yager (1981), three different ranking methods are presented. They are pure ranking methods in the sense that a number is derived for every element. This number is independent of the other elements in the set.

A weight function g is introduced to add weights to the fuzzy set A. Basically, this allows us to specify which values are more important, based on their possibility. Common weight functions are either $g(z)=1$ (reflecting that all possible values are equally important) or $g(z)=z$ (indicating that the higher the possibility of a value, the more important it is and the more it will contribute to determine the rank).

The first ranking function is defined as follows:

$$F_1(A) = \frac{\int_0^1 g(z)\mu_A(z)dz}{\int_0^1 \mu_A(z)dz}.$$

If the weight function $g(z)=z$ is used, then F_1 represents the mean value of the membership function, called usually the center of gravity of the fuzzy set. This is illustrated in Fig. 2a. Note that if the weight function $g(z)=1$ is used; no ranking conclusions can be drawn: F_1 would result in 1 for every fuzzy set.

When $g(z)=z$, this technique can be compared with the mean value technique in the probabilistic approach. The ranking function may be defined in a more general way, and one option could be to take $g(z)=[z-F_1(A)|_{g(z)=1}]^2$, as analogous to the variance. An analogue of semivariance could also be defined here, which shows the similarity of this fuzzy approach technique with the probabilistic one.

3.4 Analogues to critical values

Nahorski et al A strict analogue to a critical value technique in the probabilistic approach has been proposed in Nahorski et al. (2003); Nahorski et al. (2007); Nahorski and Horabik (2010). To get an analogue to probability, which defines the critical value, the critical area is normalized by dividing it by the area under the membership function, as in Fig. 1c.

Adamo On the other hand, Adamo (1980) proposed to consider points fulfilling $\mu_A(z)=\alpha$, $0\leq\alpha\leq1$ and choose the highest value of z as a ranking criterion. In other words, the criterion value is the rightmost value of the α-cut of the fuzzy number A. The critical value now depends on the choice of α, but in this case it has a clear fuzzy set interpretation connected with the α-cut. This idea can be compared with the one by Nahorski et al., where the critical area has a more probabilistic origin, while that of Adamo has more the flavour of a fuzzy set, see Fig. 2d. Both techniques can be related by mathematical expressions for a fixed membership function.

These techniques can be simply used for the derivation of criterions for checking the fulfilment of the limit, analogously to those which stem from similar probabilistic approaches.

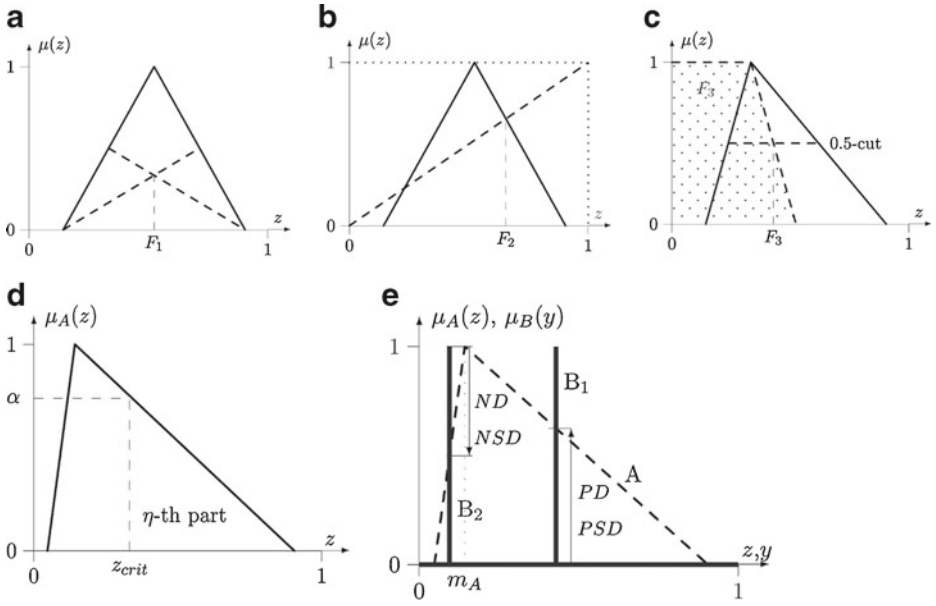

Fig. 2 Illustration for fuzzy set approaches. Ranking functions proposed by Yager: **a** F1 function; **b** F2 function; **c** F3 function; **d** Determination of the critical value z_{crit} in the Nahorski et al. (calculation of the η-th part of the distribution area) and Adamo (calculation of the α-cut) techniques; **e** Calculation of the indices for the crisp limits

Yager F2 The second ranking function introduced by Yager (1981) compares the given fuzzy set A to the linear fuzzy set B, defined by $\mu_B(z)=z$.

The second ranking function is then defined as follows:

$$F_2(A) = \max_{z \in S} \min\left(z, \mu_A(z)\right).$$

Here, S represents the support of the fuzzy set A; in our case assumed to be the interval [0,1]. Graphically, this yields an intersection point between the linear fuzzy set ($\mu_B(z)=z$) and the given fuzzy set A. This is illustrated in Fig. 2b.

This ranking function has a simple interpretation. The fuzzy set with the membership function $\mu_B(z)=z$ may be interpreted as representing a variable "high". The membership function $\min(z,\mu_A(z))$ represents a variable, which is a conjunction of A and B, i.e. the points which belong both to the variable "high" and A. In other words, it represents a distribution of the possibility that A is "high". Its maximal point satisfies these two requirements in the "best" way.

The membership function of the variable "high" may be shaped in a different way. Jain (1976) proposed a more general set of functions $\mu_B(z)=(z/z_{\max})^k, k>0$.[2] In this case, the result of a comparison of fuzzy numbers may largely depend on the choice of k, though no clear criteria exist for which value of k should be chosen.

Apart from ranking the fuzzy numbers, the critical values could be used to check on the fulfilment of obligations, analogously to the stochastic approach. The simplest approach would be to directly compare F_2 with K. However, the constructions proposed here are of a subjective character and remain difficult to interpret physically, and therefore their use may be limited.

[2] However, in this section the assumption is that $z_{\max}=1$.

Yager F3 The third ranking function defined by Yager (1981) is more complex to explain through the use of formulae, although it is simple to interpret geometrically. It is defined as

$$F_3(A) = \int_0^{\alpha_{\max}} m(A_\alpha) d\alpha \,.$$

with A_α the α-cuts of A, α_{max} is the highest occurring possibility in the fuzzy set A,[3] and m is the middle point of the α-cut.

The formula is relatively easy to grasp graphically: the index is the surface area to the left of the line that runs exactly along the middle of the fuzzy number. For triangular fuzzy numbers, this connects the top of the fuzzy number (i.e. where the possibility is one) with the middle of the support. This is represented by the shaded area in Fig. 2c.

This ranking index can be directly used for checking the satisfaction of the limit. For this we ought to remain aware that $F_3(A)$ is the mean value of the function $m(A_\alpha)$, in which α is the argument. This is because $0 \le \alpha \le 1$, so for the triangular membership functions $F_3(A) = \int_0^1 m(A_\alpha) d\alpha = m(A_{0.5})$. Thus, in this case $F_3(A)$ is equal to the middle value of the 0.5-cut of the fuzzy number A, see Fig. 2c. For other membership functions the integral will be equal to the middle value of some α-cut, possibly different from 0.5. Clearly, this index is closely related with an α-cut, where the appropriate α is determined by the shape of the membership function. It makes this approach slightly similar to the Adamo method, with the critical value determined in the middle of the α-cut instead of at the right end. This interpretation encouraged us to classify this technique within the critical values group.

Examples with a comparison of the Yager ranking methods can be found in the supplementary material.

3.5 Fuzzy dominance

3.5.1 Possibility and necessity measures

In spite of its similar name, the fuzzy dominance techniques proposed to date in the literature, differ completely in spirit from the stochastic dominance ones that are presented in subsection 2.4. It is important to remember here that we use the normalized fuzzy numbers on the domain rescaled to the interval [0,1]. The results of this subsection may be not correct if the normalization or rescaling is not conducted beforehand.

To compare fuzzy numbers using the fuzzy dominance approach, *possibility and necessity measures* can be used, as introduced by Dubois and Prade (1983), see also Hryniewicz and Nahorski (2008). A normalized fuzzy set with a membership function $\mu(z)$ induces a possibility distribution $\pi(z) = \mu(z)$ on the interval [0,1]. For simplicity, we refer to possibility distribution as $\mu(z)$. Given a possibility distribution, the possibility measure of a subset $Z \in U = [0,1]$ is defined as

$$\mathrm{Poss}(Z) = \sup_{z \in Z} \mu(z).$$

It can be interpreted as a degree of possibility that an element is located in set Z, see an interpretation in Fig. 3a. Let us draw attention to the fact that using a characteristic function $\chi_Z(z)$ of the set Z, the possibility measure can be equivalently defined as

$$\mathrm{Poss}(Z) = \sup_{z \in [0,1]} \min\{\mu(z), \chi_Z(z)\}.$$

[3] For the normalized sets, as assumed in this paper, $\alpha_{\max} = 1$.

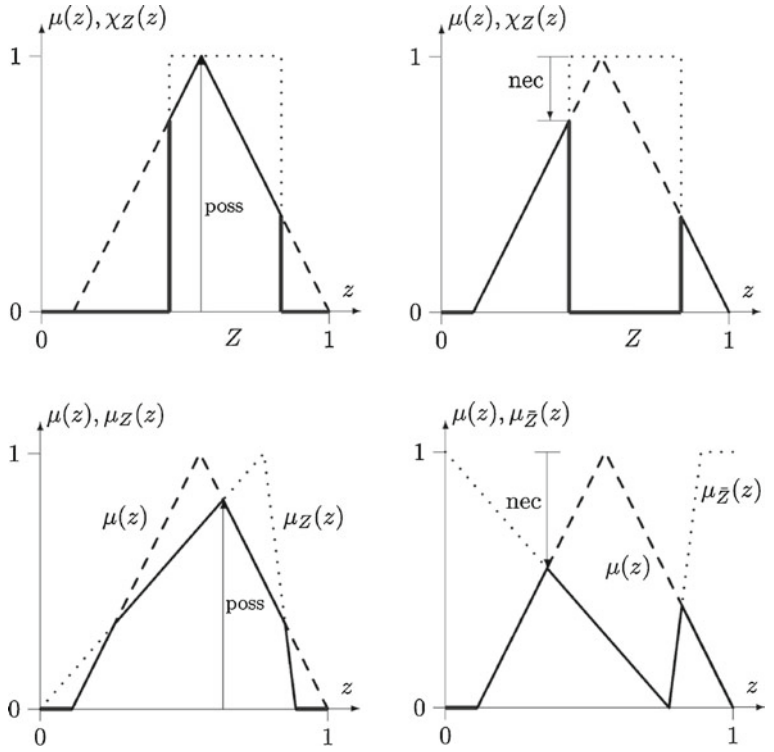

Fig. 3 Illustration for a crisp set Z: **a** possibility; **b** necessity measures; and for a fuzzy set Z: **c** possibility; **d** necessity measures

Note that when $Z=[r,1]$, then the above index can be interpreted as a measure that element x is not smaller than r, i.e. $r \leq x$.

Comparing these notions to the probabilistic ones, the possibility distribution corresponds to the probabilistic distribution, and the possibility measure Poss(Z) corresponds to the probability of the subset Z.

However, in the possibility theory an additional notion is introduced. Called the necessity measure, it is defined as

$$\mathrm{Nec}(Z) = 1 - \mathrm{Poss}\left(\overline{Z}\right),$$

where $\overline{Z}$ is the complementary set of Z in [0,1], see Fig. 3b. It can be interpreted as the degree that an element is necessarily located in set Z. Similarly as in the possibility case, an equivalent definition may be

$$\mathrm{Nec}(Z) = 1 - \sup_{z\in[0,1]} \min\left\{\mu(z), \chi_{\overline{Z}}\right\} = \inf_{z\in[0,1]} \max\{1-\mu(z), \chi_Z(z)\}.$$

It can be observed in Fig. 3a and b that a simple property holds

$$\mathrm{Nec}(Z) \leq \mathrm{Poss}(Z),$$

which may be interpreted that the measures give the lower and upper bounds on uncertainty connected with the localization of an element in set Z. The lower one, (necessity), is the degree in the range [0,1] of our conviction that the point is in set Z. The higher one, (possibility), is the degree of our supposition.

Now, taking a fuzzy set Z instead of a crisp one, the characteristic function $\chi_Z(z)$ is replaced by the membership function $\mu_Z(z)$, providing the following definitions

$$Poss(Z) = \sup_{z\in[0,1]} \min\{\mu(z), \mu_Z(z)\},$$
$$\mathrm{Nec}(Z) = 1 - \sup_{z\in[0,1]} \min\left\{\mu(z), \mu_{\bar{Z}}\right\} = \inf_{z\in[0,1]} \max\{1-\mu(z), \mu_Z(z)\}$$

see Fig. 3c and d. For further use, $\mu_{\overline{Z}(z)} = 1-\mu_Z(z)$ is introduced as the membership function of the complementary set of Z.

3.5.2 Possibility of dominance indices

Having introduced the above notions, we can pass to a definition of fuzzy dominance indices. To calculate the possibility and necessity indices, the membership functions are analyzed on a two-dimensional plane (z,y), and more specifically, either on the upper right or the bottom left half of the square $[0,1]\times[0,1]$, compare with Fig. 4a. This is analogous to consideration of two-dimensional probability density function for independent variables. To compare two fuzzy numbers, one of them, say B, is treated as a reference. Its membership function plays a role of a reference possibility distribution.

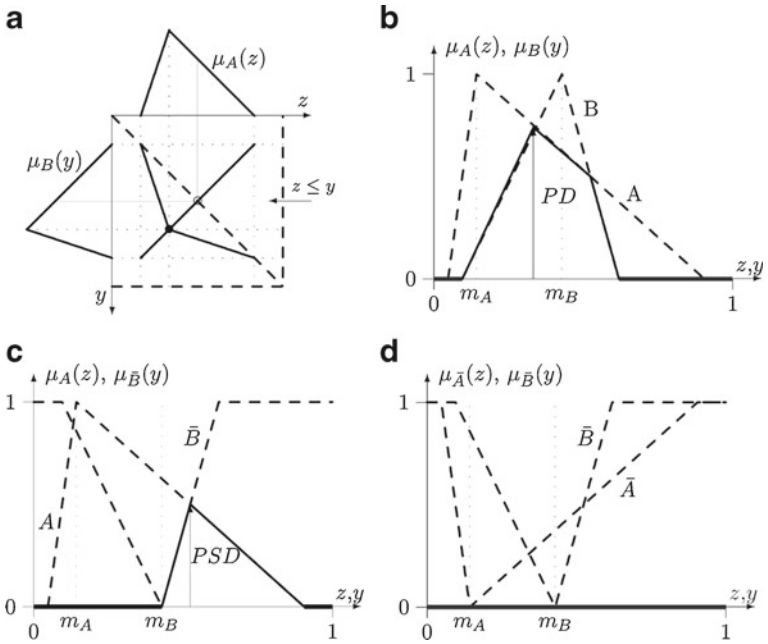

Fig. 4 Calculation of: **a** the *PD* index on the (z,y) plane; **b** the *PD* index on a line; **c** the *PSD* index; **d** the *NSD* index

Now we introduce the notion of the dominance of a fuzzy set A over B, denoted below as $A \succcurlyeq B$, and the strict dominance, denoted as $A \succ B$.

The *possibility of dominance* (*PD*) index of a fuzzy set A over a fuzzy set B is defined as

$$PD = \text{Poss}\ (A \succcurlyeq B) = \sup_{z,y;z \geq y} \min\{\mu_A(z), \mu_B(y)\}.$$

The index PD is a measure of possibility that the fuzzy numbers A is greater than B, or that the set A dominates the set B. This index was first proposed by Baas and Kwakernaak (1977). A probabilistic analogue of this index would be the probability that $A \geq B$. This index has to be analysed on the plane (z,y) in the upper right half of the square $[0,1]\times[0,1]$, see Fig. 4a, where the projection of the function $\min\{\mu_A(z), \mu_B(y)\}$ on the square is drawn with the membership functions $\mu_A(z)$ and $\mu_B(y)$ drawn on the axes. The highest value of this function (equal to 1) is located in the area $y>z$ (at the point marked with •), while the value $PD<1$ is located on the boundary of the upper half of the square, at the point marked with ○. It is now easy to notice that the value PD can be calculated as presented in Fig. 4b.

Analysing the way the value PD is calculated, with notation from Fig. 4b, it is seen that

$$\begin{aligned} &\text{Poss}\ (A \succcurlyeq B) = 1 \quad \text{if} \quad m_A \geq m_B \\ &\text{Poss}\ (A \succcurlyeq B) = 0 \quad \text{if} \quad m_A + p_{rA} \leq m_B + p_{lB} \end{aligned}$$

where p_{lB} is the left end of the support of B, and p_{lA} the right end of the support of A, see Figure S2 in the supplementary material for illustration of p_l and p_r. The possibility of dominance (*PD*) equals 0, if any point of the support of A is smaller than any point of the support of B. When the supports overlap, $PD>0$. If the core of A is greater or equal to the core of B, then $PD=1$.

The *possibility of strict dominance* (*PSD*) index for a fuzzy set A over a fuzzy set B is defined as

$$PSD = Poss\ (A \succ B) = \sup_z \inf_{y, y \geq z} \min\{\mu_A(z), 1-\mu_B(y)\},$$

where $\mu_A(z)$ and $\mu_B(y)$ are the membership functions of A and B, respectively.

Analysis of the function on the two dimensional square results in the situation depicted in Fig. 4c. Now we have

$$\begin{aligned} &Poss\ (A \succ B) = 1 \quad if \quad m_A \geq m_B + p_{rB} \\ &Poss\ (A \succ B) = 0 \quad if \quad m_A + p_{rB} \geq m_B \end{aligned}.$$

where p_{rB} is the right end of the support of B.

The possibility of strict dominance index is therefore equal to 0, when the support of A is situated to the left of the core of B. It is positive in the opposite case. It equals 1, if the support of B is situated to the left of the core of A. The membership function of A has to be shifted further to the right to achieve the same value of the index as in the possibility of dominance case.

3.5.3 Necessity of dominance indices

The *necessity of dominance* (*ND*) index of a fuzzy set A over a fuzzy set B is defined as

$$ND = \mathrm{Nec}\,(A \succcurlyeq B) = \inf_z \sup_{y,y\le z} \max\{1-\mu_A(z), \mu_B(y)\}\,.$$

As with previous analyses, calculation of this index reduces to analysis of the situation presented in Fig. 4c. It yields

$$\begin{aligned}&\mathrm{Nec}\,(A \succcurlyeq B) = 1 \text{ if } m_A - p_{lA} \ge m_B\,,\\ &\mathrm{Nec}\,(A \succcurlyeq B) = 0 \text{ if } m_A \le m_B - p_{lB}.\end{aligned}$$

Thus, the necessity of dominance index equals 0 when the core of A is to the left of the support of B. It is positive in the opposite case. It equals 1, if the support of A is situated to the right of the core of B.

The *necessity of strict dominance* (*NSD*) index of a fuzzy set A over a fuzzy set B is defined as

$$\begin{aligned}NSD = \mathrm{Nec}\,(A \succ B) = \inf_{z,y;y\le z} \max\big(1-\mu\ (z), 1-\mu_B(y)\big) =\\ = 1 - \sup_{z,y;y\le y} \min\{\mu_A(z), \mu_B(y)\} = 1 - Poss\ (B \succcurlyeq A)\,.\end{aligned}$$

This index is the opposite of the measure of possibility that set B dominates set A. It was first proposed by Watson et al. (1979). The analysis of the index reduces to analysis of the situation presented in Fig. 4d. There is

$$\begin{aligned}&\mathrm{Nec}\,(A{\succ}B) = 1 \quad if \quad m_A - p_{lA} \ge m_B + p_{rB}\\ &\mathrm{Nec}\,(A{\succ}B) = 0 \quad if \quad m_A \le m_B.\end{aligned}$$

An example, with a comparison of the above methods, can be found in the supplementary material.

3.5.4 Checking fulfilment of a limit

Next, the question is asked as to whether the techniques described can be used for limit verification. To this end, the limit can be interpreted as a point value, which is a fuzzy variable with a membership function

$$\mu_B(z) = \begin{cases} 1 & if \quad z = \tilde{L} \\ 0 & if \quad z \ne \tilde{L} \end{cases},$$

where $\tilde{L}$ is the rescaled value of the limit L. In this situation *PD*=*PSD* and *ND*=*NSD*, so the analysis can be confined only to the necessity N and possibility P indices.

In Fig. 2e two cases are depicted: the limit B_1 higher than m_A, and the limit B_2 smaller than m_A. In the former case $P>0$ and $N=0$. In the latter $P=1$ and $N>0$. It becomes apparent that the necessity index is equivalent to the Adamo method with $N=1-\alpha$. The possibility index gives information on the degree of a failure to achieve the limit (recall that here the limit is achieved when A is greater than B), which could be used for determining noncompliant inventories.

Thus, we can formulate the following rules. The inventory is considered compliant if the necessity index is high enough. The inventory is considered noncompliant if the possibility index is small enough. This leads to the situation, which is fully analogous to the indecision interval in the probabilistic approach, as presented in Fig. 1e. Fixing the minimal necessity N and maximal possibility P indices brings us to the notion of an indecision interval, where the necessity index is too small and the possibility index is too high.

The application of the Dubois and Prade method provides useful information with respect to the compliance evaluation. Nevertheless, analysis of membership functions in three dimensions is rather cumbersome. Simple interpretations on the plane, as in Fig. 4, can help in the analysis. Necessity indices give practically the same information as in the methods of Adamo and Nahorski et al. The possibility indices can be useful for quantifying noncompliance.

4 Conclusions

The paper presents the methods for the comparison of uncertain emission inventories, and discusses their usefulness for evaluation of emission reduction limits. The review shows a variety of approaches and techniques. It clearly demonstrates that the comparison of the reported inventories with no account of uncertainty distributions leads to paradoxes, and it is not well scientifically grounded. Some of the approaches, like the undershooting method, have been proposed earlier (Godal et al. 2003; Nahorski et al. 2003; Jonas et al. 2010a), and adapted for emission trading, see additionally Nahorski et al. (2007); Nahorski and Horabik (2010, 2011). Any use of the techniques outlined in the paper takes uncertainty into account, see Table 1, and thus inevitably necessitates changes to the presently used rules of compliance checking. To date, the verification mechanisms depend only on reported inventories. They give a decisive answer, which may, however, be difficult to support when uncertainty of the inventories is considered, as shown in Fig. 1. In terms of probability or other measures, like possibility, only weaker statements on compliance can be formulated; for example, the probability of not fulfilling the limit. This means that either conservative decisions have to be taken or indecision situations may occur. However, these lack any controversy and are thus transparent, since the inventories can be compared and ordered. Ignoring uncertainty is more hazardous for asymmetric distributions, which may occur in many national inventories. It is also of great importance for comparisons of emission uncertainty distributions representing sectors of different activities, such as energy and agriculture.

Within the fuzzy approach, some problems arise with the representation of the incomplete information on the inventories uncertainty in the form of membership functions. However, the membership functions can be constructed and interpreted as approximations to the inventory uncertainty, formulated on the basis of the best available knowledge. The present state of the development in this area allows only weak statements on comparison to be formulated, providing only some indices of possibility or necessity for instance. For decision making, one can set critical values on these indices, however, it may be more difficult than for the stochastic case due to smaller intuition on the indices interpretation.

In spite of basic conceptual differences between the probabilistic and fuzzy approaches, many techniques are surprisingly similar. Among them, the critical values and fuzzy dominance methods provide similar techniques for checking compliance, with small technical differences in terminology and decision parameters. This paper has not been intended to elaborate legislation propositions for compliance rules, due in part to restrictions on its length. Examples of analytical conditions for checking compliance can be found in the literature mentioned.

Table 1 Comparison of methods discussed in the paper

Group of methods	Required information	Characteristics and usefulness of the methods
Based on distribution moments	Means and variances	The methods use simple information but their application is rather inconvenient. Two indicators can contradict each other. For asymmetric distributions, mean values are different from the reported (dominant) values. Application of semivariance requires information on the uncertainty distribution.
Based on critical values	Probability or possibility mass of the inventory uncertainty above a specific value	This group of methods seems to be particularly convenient for the compliance problem; some variants of these methods have been already proposed independently in several papers. The methods need more advanced information on the uncertainty distribution, which requires more sophisticated methods for its acquisition. Moreover, a good understanding of the applied inference techniques is required for decision making, as the values used in the compliance rules differ from the reported inventories. This may be questioned on the ground of deterministic common-sense arguments.
Based on dominance	Full distribution of inventory uncertainty	Although the same notion of dominance is used in both stochastic and fuzzy approaches, the methods are very different. The stochastic methods are not always decisive and rather difficult for practical applications. The fuzzy methods use little known notions of possibility and necessity indices, and require understanding of the sophisticated underlying theory. The geometrical calculation of the indices proposed in the present paper may make the method easier to grasp. As shown, comparison of an inventory against an exact (crisp) limit allows for its reduction to a variant of methods from the critical values group.

Possible approximations of the uncertainty distributions in the fuzzy approach give rise to the question of the impact of approximations on the final compliance condition. This issue is also valid in the stochastic approach, since the required probability characteristics are not easy to be gathered by simple statistical treatment to get accurate estimates. It may be argued that this second-order uncertainty impacts the results to a lesser extent than the first-order uncertainty of the inventory itself. It seems that this question can be solved using the idea underlying the methods described in the present paper: the worse the data are, the lower the reported inventory should be to achieve a sufficient credibility. Thorough investigation of this problem is left for further studies.

Acknowledgments O. Hryniewicz, Z. Nahorski and J. Verstraete gratefully acknowledge financial support from the Polish State Scientific Research Committee within the grant N N519316735 as well as from statutory fund of the Systems Research Institute. J. Horabik was financially supported by the Foundation for Polish Science under International PhD Projects in Intelligent Computing, which is financed by The European Union within the Innovative Economy Operational Programme 2007–2013 and European Regional Development Fund. The authors thank the anonymous reviewers for the comments, which helped us to improve the paper.

Open Access This article is distributed under the terms of the Creative Commons Attribution License which permits any use, distribution, and reproduction in any medium, provided the original author(s) and the source are credited.

References

Adamo JM (1980) Fuzzy decision trees. Fuzzy Sets Syst 4:207–219

Baas SM, Kwakernaak H (1977) Rating and ranking of multiple-aspect alternatives using fuzzy sets. Automatica 13:47–58

Bortolan G, Degani R (1985) A review of some methods for ranking fuzzy subsets. Fuzzy Sets Syst 15:1–19

Dubois D, Prade H (1983) Ranking fuzzy numbers in the setting of possibility theory. Inf Sci 30:183–224

Gillenwater M, Sussman F, Cohen J (2007) Practical policy applications of uncertainty analysis for national greenhouse gas inventories. Water, Air & Soil Pollution: Focus 7(4–5):451–474

Godal O, Ermolev Y, Klaassen G, Obersteiner M (2003) Carbon trading with imperfectly observable emissions. Environ Resour Econ 25:151–169

Gusti M., Jęda W. (2002) Carbon management: new dimension of future carbon research. IR-02-006. IIASA, Austria. http://www.iiasa.ac.at/Publications/Documents/IR-02-006.pdf

Graves SB, Ringuest JL (2009) Probabilistic dominance criteria for comparing uncertain alternatives: A tutorial. Omega 37:346–257

Hryniewicz O., Nahorski Z. (2008) Verification of Kyoto Protocol - a fuzzy approach. In: L. Magdalena, M. Ojeda-Aciego, J. L. Verdegay (Eds.) Proc. IPMU'08. Torremolinos, Spain, 729–734. http://www.gimac.uma.es/ipmu08/proceedings/papers/096-HryniewiczNahorski.pdf

IPCC (1996) Revised 1996 IPCC Guidelines for national Greenhouse Gas Inventories. Vol. 1. Reporting Instructions. IPCC. Available at: http://www.ipcc-nggip.iges.or.jp/public/gl/invs4.html

Jain R (1976) Decision-making in the presence of fuzzy variables. IEEE Trans Systems Man Cybernet 6:698–703

Jonas M, Nilsson S, Obersteiner M, Gluck M, Ermoliev YM (1999) Verification times underlying the Kyoto protocol: Global benchmark calculations. IR-99-062. IIASA, Austria. http://www.iiasa.ac.at/Publications/Documents/IR-99-062.pdf

Jonas M, Nilsson S (2007) Prior to economic treatment of emissions and their uncertainties under the Kyoto Protocol: Scientific uncertainties that must be kept in mind. Water, Air, and Soil Pollution: Focus 7:495–511

Jonas M, Gusti M, Jęda W, Nahorski Z, Nilsson S (2010a) Comparison of preparatory signal analysis techniques for consideration in the (post-)Kyoto policy process. Clim Chang 103(1–2):175–213

Jonas M, Marland G, Winiwarter W, White T, Nahorski Z, Bun R, Nilsson S (2010b) Benefits of dealing with uncertainty in greenhouse gas inventories: introduction. Clim Chang 103(1–2):3–18

Lieberman D, Jonas M, Winiwarter W, Nahorski Z, Nilsson S (eds) (2007) Accounting for climate change: Uncertainty in greenhouse gas inventories—verification, compliance, and trading. Springer, Dordrecht

Nahorski Z, Horabik J (2010) Compliance and emission trading: rules for asymmetric emission uncertainty estimates. Clim Chang 103(1–2):303–325

Nahorski Z, Horabik J (2011) A market for pollution emission permits with low accuracy of emission estimates. In: Kaleta M, Traczyk T (eds) Modeling multi-commodity trade: Information exchange methods. Springer, Verlag, pp 151–165

Nahorski Z, Horabik J, Jonas M (2007) Compliance and emission trading under the Kyoto Protocol: Rules for uncertain inventories. Water, Air & Soil Pollution: Focus 7(4–5):539–558

Nahorski Z, Jęda W, Jonas M (2003) Coping with uncertainty in verification of the Kyoto obligations. In: Studziński J., Drelichowski L., Hryniewicz O. (Eds.) Zastosowania informatyki i analizy systemowej w zarządzaniu. SRI PASm, 305–317.

Ramirez RA, de Keizer C, van der Sluijs JP (2006) Monte Carlo analysis of uncertainties in the Netherlands greenhouse gas emission inventory for 1990–2004. Copernicus Institute for Sustainable Development and Innovation, Utrecht, the Netherlands. Available at: http://www.chem.uu.nl/nws/www/publica/publicaties2006/E2006-58.pdf

Roy AD (1952) Safety first and the holding of assets. Econometrica 20:431–449

Tran L, Duckstein L (2002) Comparison of fuzzy numbers using a fuzzy distance measure. Fuzzy Sets Syst 130:331–341

Watson SR, Weiss JJ, Donell ML (1979) Fuzzy decision analysis. IEEE Trans Systems Man Cybernet 9:1–9

White T, Jonas M, Nahorski Z, Nilsson S (eds) (2011) Greenhouse gas inventories. Dealing with uncertainty. Springer, Dordrecht

Winiwarter W, Rypdal K (2001) Assessing the uncertainty associated with national greenhouse gas emission inventories: A case study for Austria. Atmos Environ 35:5425–5440

Yager RR (1981) A procedure for ordering fuzzy subsets of the unit interval. Inform Sci 24:143–161

DOI 10.1007/978-3-319-15901-0_6
Reprinted from *Climatic Change* Journal, DOI 10.1007/s10584-014-1063-x

The improvement of greenhouse gas inventory as a tool for reduction emission uncertainties for operations with oil in the Russian Federation

Nina E. Uvarova · Vladimir V. Kuzovkin · Sergey G. Paramonov · Michael L. Gytarsky

Received: 10 January 2013 / Accepted: 5 January 2014 / Published online: 20 February 2014
© Springer Science+Business Media Dordrecht 2014

Abstract The high quality inventory is an important step to greenhouse gas emission mitigation. The inventory quality is estimated by means of the uncertainty analysis. The level of uncertainty depends upon the reliability of activity data and the parameters used. An attempt has been made to improve the accuracy of the estimates through a shift from production-based method (IPCC Tier 1) (IPCC 2000) to enhanced combination of production-based and mass balance methods (IPCC Tier 2) (IPCC 2006) in the estimation of emissions from operations with oil that are key in the national greenhouse gas inventory of the Russian Federation. The IPCC Tier 2 (IPCC 2006) was adapted for the national conditions. The greenhouse gas emissions were calculated for 1990 to 2009 with the use of both methods. The quantitative uncertainty assessment of the calculations was performed, and the outcomes were compared. The comparison showed that the estimates made with the use of higher tier method resulted in higher accuracy and lower uncertainties (26 % respectively compared to previously derived 54 %).

1 Introduction

According to the IPCC Fourth Assessment Report, the increased concentration of human-induced greenhouse gases in the atmosphere caused dramatic temperature raise and the global climate change (IPCC 2007). China, USA, European Union (the 27 countries altogether), Russian Federation and India are the main contributors to the global greenhouse gas (GHG) emissions (excluding LULUCF), which in 2005 correspondingly provided for 19.1 %, 18.3 %, 13.3 %, 5.2 % and 4.9 % of the emission profile (CAIT 2.0 Climate data explorer 2013). With the entry into force of the Kyoto Protocol, the international community of 37 developed countries is committed to undertake joined efforts to reduce anthropogenic emissions to the atmosphere of the greenhouse gases. The efficiency of the implementation of the commitments under the Kyoto Protocol is judged through the national inventory reports, which are annually

This article is part of a Special Issue on "Third International Workshop on Uncertainty in Greenhouse Gas Inventories" edited by Jean Ometto and Rostyslav Bun.

N. E. Uvarova (✉) · V. V. Kuzovkin · S. G. Paramonov · M. L. Gytarsky
Institute of Global Climate and Ecology, str. Glebovskaya, 20-B, Moscow 107258, Russian Federation
e-mail: n.uvarova@inbox.ru

submitted and subject to subsequent reviews by the designated groups of international experts. As a Party to the United Nations Framework Convention on Climate Change (UNFCCC) and its Kyoto Protocol, since 2006 the Russian Federation regularly prepares and submits its national greenhouse gas inventories (NIR 2006, 2009). The greenhouse gases released from the exploration, production, preliminary treatment, transport and storage of oil are addressed as fugitive emissions and included in the annual emission estimates (IPCC 2000, 2006). According to the National Inventory Report of the Russian Federation the contribution of fugitive emissions from oil and gas industry to the national totals is shown on Fig. 1 (NIR 2009).

From 1990 to 2009, the fugitive GHG emissions from oil and gas industry made up almost 17 % of the national emissions. It should be noted that the scale of emissions has no inclination to decrease, being stipulated by intensive the oil production (Fig. 1). The national statistical data indicates that from 1990 to 2009, annual oil production in the Russian Federation fluctuated between 0.3 and 0.5 Gt (Rosstat 2007, 2010). Given the significant amount of oil production, the GHG emissions from the operations with oil in the country make an important contribution to the global emissions.

As indicated in the National Inventory Report of the Russian Federation, the operations with oil (fugitive emissions) are key because of their contribution to the entire emission profile and according to the trend assessment (NIR 2009). The accuracy of the inventory is assessed with the use of uncertainty analysis, which is especially important for key categories providing for greatest contribution to the national emission totals. The improved estimates for the key categories clarify their input to the national emission profile and promote for subsequent prioritization of the reduction efforts.

As follows from the several studies, about 110 billion cubic meters of associated petroleum gas (APG) are annually flared at oil production facilities worldwide, while 60 % of which are provided by 8 oil producing countries (The World Bank 2004; Solovyanov et al. 2008). The Russian Federation is responsible for about 11 % of global APG flaring. Consequently the first phase of improving fugitive emission quality concentrated on the emission estimates from oil

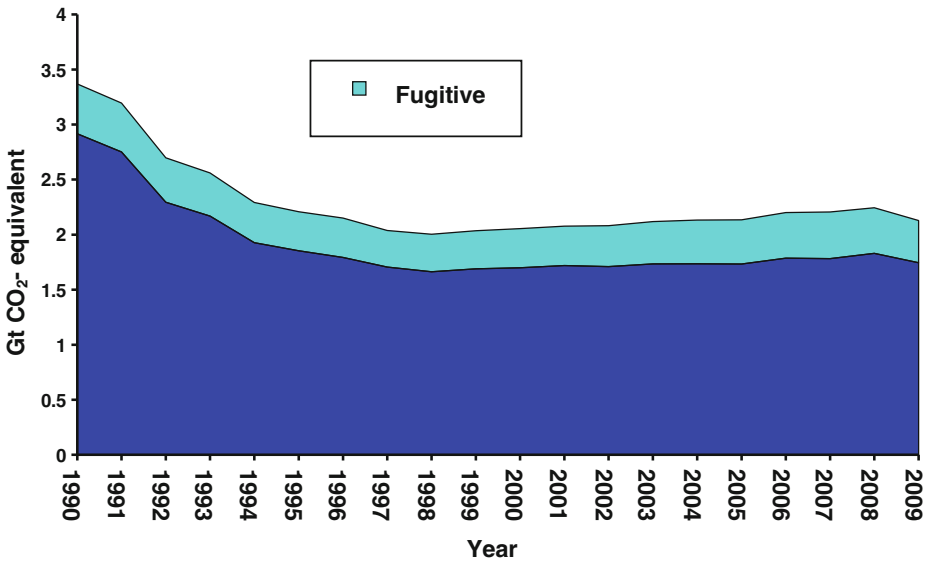

Fig. 1 Contribution of fugitive emission to the total GHG emission profile of the Russian Federation

production. The aim of our work was to improve the greenhouse gas emission calculations for operations with oil and to use the uncertainty analysis to evaluate the accuracy of the estimates performed. The authors of the paper are the members of the national greenhouse gas inventory team of the Russian Federation with the responsibility for oil and gas sector. This paper represents the outcomes of the on-going work on the improvement of the national greenhouse gas inventory of the Russian Federation.

2 The improvement of the greenhouse gas calculations for the operations with oil

In the national inventory of the Russian Federation, the greenhouse gas emissions from the operations with oil are currently calculated with the use of production-based method, which corresponds to the IPCC Tier 1 approach (IPCC 2000). In general, the estimates in accordance with the production-based method perform a product of the activity data and the emission factor that represents the portion of the substance concerned, which is released to the atmosphere as the greenhouse gas. The activity data are taken from the national statistics, whereas the emission factors are mainly the IPCC defaults. Thus, the CO_2, CH_4 and N_2O emissions from the exploration, production (fugitives), venting and APG flaring and transport in the oil sector are calculated with the use of the Eqs. 1 and 2 which are based on IPCC Tier 1 approach (IPCC 2000):

$$E_{CO2,CH4,N2O} = N \cdot EF_{CO2,CH4,N2O}, \quad (1)$$

$$E_{CO_2CH_4,N_2O} = \frac{AD}{\rho} \cdot EF_{CO_2,CH_4,N_2O}, \quad (2)$$

where $E_{CO2,\ CH4,\ N2O}$—the greenhouse gas emission estimate from oil operation in question, Gg; N — the total amount of drilled/producing wells, units; AD—the activity data on total oil produced otherwise transported, refined and stored, 10^3 t; ρ—the average weighted oil density, t • m^{-3} $EF_{CO2,\ CH4,\ N2O}$—the GHG emission factors for well maintenance, Gg • $well^{-1}$ $EF_{CO2,\ CH4,\ N2O}$—the emission factor(s) for production, transport, venting and flaring operations, Gg • m^{-3} • 10^{-3}.

The total amount of drilled wells (N) is estimated as the sum of exploration and operation wells. The amount of exploration, producing and idle well stock is obtained from the national statistical data. The Eq. 2 contains oil density to harmonize national activity data of oil sector. The weighted average density of oil produced in the Russian Federation is 857.8 kg • m^{-3} under T=20 °C (Grigoryev and Popov 2002). Figure 2 represents the activity data on the operations with oil in the Russian Federation taken from the yearly national statistical reports (Rosstat 2007, 2010).

As follows from Fig. 2, oil production and transport were lower by 5.5 % and 4.7 % correspondingly, compared to 1990 levels. Oil refining was by 20.1 % lower in 2009 compared to 1990. The decreases are associated with oil production fall due to economic reasons in the mid-90s.

The amount of the APG produced, which was subsequently either utilized and further processed or flared, is also provided in the national statistical reports (Rosstat 2007, 2010). They are shown on Fig. 3.

As follows from the Fig. 3, in 2009 production of the APG and its flaring subsequently increased above the 1990 levels by 46.8 % and 19.8 % correspondingly. However, it should be noted that the flaring is about 21 % of the total APG production (the average value from 1990 to 2009). The latter indicates that the major part of the produced APG is utilized rather than

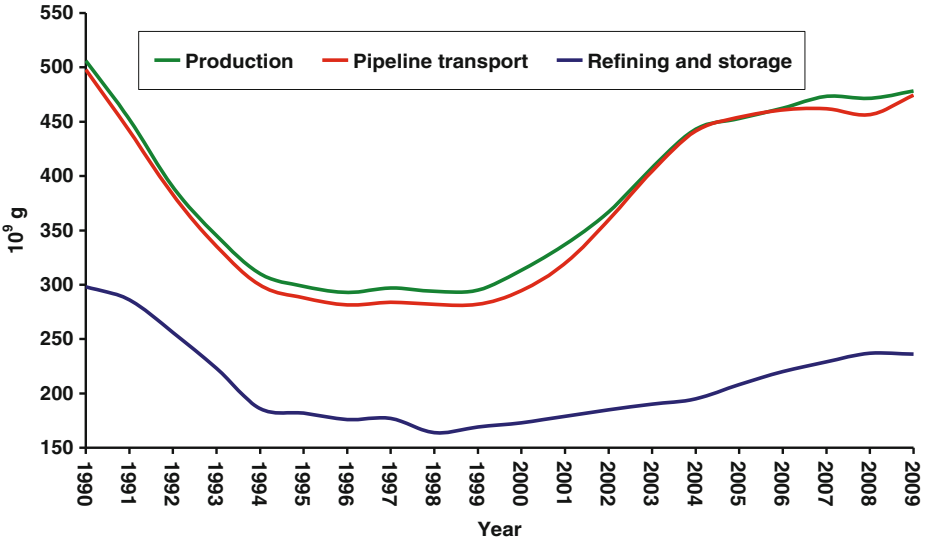

Fig. 2 The activity data on the operations with oil in the Russian Federation

flared. Nevertheless, the amounts of APG flaring are still rather substantial, which indicates of significant potential for greenhouse gas emission reduction for this emission category.

The emission factors for calculation the greenhouse gas emissions from oil operations are provided in Good Practice Guidance and Uncertainty Management in National Greenhouse Gas Inventories (hereinafter IPCC Good Practice Guidance) (IPCC 2000). Despite exploration, APG flaring and oil transport, the emission factors commonly used are the average values from the range recommended by the IPCC guidelines (IPCC 2000). The N_2O emission factor for APG flaring, $2.3 \cdot 10^{-5}$ Gg $\cdot 10^{-6}$ m^{-3}, is also given by the IPCC (IPCC 2000).

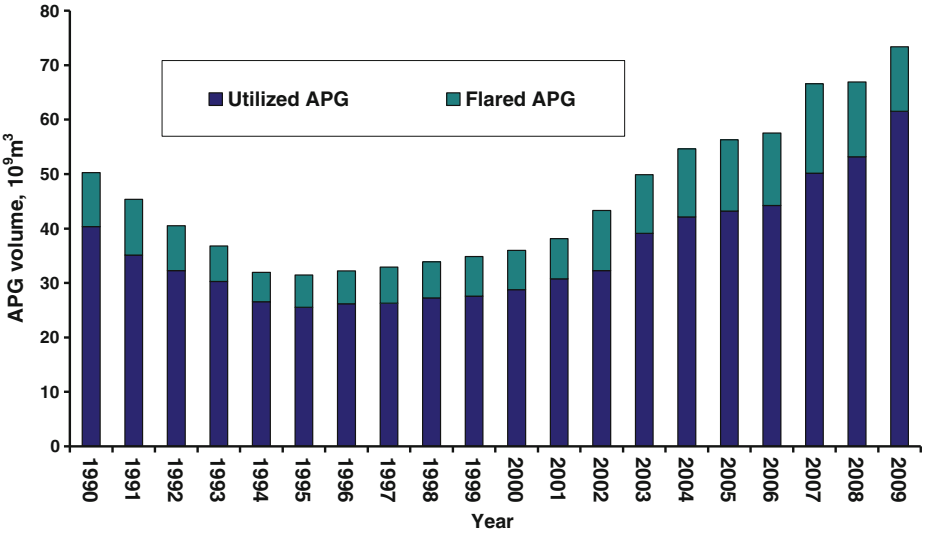

Fig. 3 The treatment of the APG in the Russian Federation

With the aim at improving the accuracy of the estimates, a shift from production-based method (IPCC Tier 1) to the enhanced combination of production-based and mass balance methods (IPCC Tier 2) was made for the same source categories, namely exploration, production (fugitives), venting and APG flaring, transport. Mass balance method was employed for the major contributors to the emission profile—oil production, venting and APG flaring. The IPCC Tier 2 method implies the following equations (IPCC 2006):

$$E_{venting} = GOR \cdot Q_{oil} \cdot (1-CE) \cdot \left(1-X_{flared}\right) \cdot M_{gas} \cdot y_{gas} \cdot 42.3 \cdot 10^{-6}, \quad (3)$$

$$E_{CH_4\,flaring} = GOR \cdot Q_{oil} \cdot (1-CE) \cdot X_{flared} \cdot (1-FE) \cdot M_{CH_4} \cdot y_{CH_4} \cdot 42.3 \cdot 10^{-6}, \quad (4)$$

$$E_{CO_2\,flaring} = GOR \cdot Q_{\mathrm{oil}} \cdot (1-CE) \cdot X_{\mathrm{flared}} \cdot M_{CO_2} \cdot \left[y_{CO_2} + \left(Nc_{CH_4} \cdot y_{CH_4} + Nc_{NMVOC} \cdot y_{\mathrm{NMVOC}} \cdot (1-X_{soot})\right] \cdot 42.3 \cdot 10^{-6}, \quad (5)$$

$$E_{N_2O\ flaring} = GOR \cdot Q_{oil} \cdot (1-CE) \cdot X_{flared} \cdot EF_{N_2O}, \quad (6)$$

where $E_{venting}$—the direct amount (Gg y^{-1}) of the GHG emitted due to venting at oil production facilities; $E_{CO2,\ CH4,\ N2Oflaring}$—the direct amount (Gg y^{-1}) of the greenhouse gas emitted due to flaring at oil production facilities; GOR is the average gas to oil ratio ($m^3\ m^{-3}$) referenced at 15 °C and 101.325 kPa; Q_{oil}—the total annual oil production ($10^3\ m^3\ y^{-1}$); M_{gas}—the molecular weight of the gas of the interest; N_{Ci}—the number of moles of carbon per mole of compound *i*; y_i—mol or volume fraction of the APG that is composed of substance *i*; CE—the gas conservation efficiency factor; X_{flared}—the fraction of the waste gas that is flared rather than vented; FE—flaring destruction efficiency; X_{soot}—fraction of the non-CO_2 carbon in the input waste gas stream that is converted to soot or particulate matter during flaring; EF_{N2O}—the emission factor for N_2O from flaring (Gg $10^{-3}\ m^{-3}$ of APG flared); $42.3 \cdot 10^{-6}$—the number of kmol per m^3 referenced at 101.325 kPa and 15 °C (i.e.$42.3 \cdot 10^{-6}$ kmol m^{-3}) times a unit conversion factor of 10^{-3} Gg Mg^{-1}, which brings the results of each applicable equation to units of Gg y^{-1}.

The Eqs. (3)–(5) correspond to the mass balance method, whereas the Eq. (6) is the production-based method. The production-based method is also applied for N_2O emission estimates due to the complexity of its formation in the APG flaring (Hayhurst and Lawrence 1992). The Eqs. (3)–(6) merge specific oil operations inscribed in step-by-step Tier 1 calculation approach. This combination adequately represents activities in the oil sector of the Russian Federation. The Tier 2 was applied to estimate emissions from sources with the main contribution to the entire emission profile. The parameters in the Eqs. (3)–(6) were recalculated to comply with specific conditions of the Russian Federation. The invariable value of $42.3 \cdot 10^{-6}$ kmol m^{-3}, which is the number of kmol per m^3 (i.e. $42.3 \cdot 10^{-6}$) times a unit conversion factor of 10^{-3} Gg Mg^{-1} (the inverse of the Molar volume, i.e. Vm^{-1}), was recalculated to standard conditions of the country (101.325 kPa and 20 °C) with the use of molar volume and the Mendeleev-Clapeyron ideal gas equation. The recalculated invariable is $41.6 \cdot 10^{-6}$ kmol m^{-3}. To accommodate the national data on the APG operations, the parameter $GOR \cdot Q_{OIL}$ in the Eqs. (3) to (6) was replaced with $\frac{Q_{APG\_USED}}{CE}$, which is of the same meaning. The validity of the parameter was cross-checked by inverse calculation

of the gas factor (IPCC 2006). The fraction of the waste gas that is flared rather than vented (X_{flared}) was estimated based on the data for operations with APG as:

$$X_{FLARED} = \frac{Q_{FLARED}}{\frac{Q_{APG\_USED}}{CE} \bullet (1-CE)}$$

The fraction of non-CO_2 carbon in the input waste gas stream converted to soot or particulate matter during flaring (X_{soot}) was assumed 0, i.e. an assumption was made that all non-CO_2 carbon in the input waste gas stream releases to the atmosphere without any soot formation. It is a conservative approach enabling to avoid underestimation of greenhouse gas emission.

The flaring destruction efficiency (FE) is based on underburning coefficient, which was experimentally derived by Scientific Research Institute for Atmospheric Air Protection for different types of flaring facilities. Underburning coefficient is equal about 0.0006 for non-soot flaring facilities, whence it follows that flaring destruction efficiency is estimated to be equal about 0.9994 (NII Atmosphera 1997).

The number of moles of carbon per mole of NMVOC (Nc_{NMWOC}) and mol or volume fraction of the APG that is composed of substance *i* (y_i) are directly dependent from APG composition. The calculations were performed based on the chemical composition of the West-Siberian oils in a view that it is the largest oil producing region in Russia being up to 66 % of the national oil production (Andreykina 2005). As provided by IPCC Guidelines, the number of moles of carbon per mole of NMVOC for natural gas and crude oil vapors vary from 2.1–2.7 to 4.6 respectively (IPCC 2006). So that country-specific value derived is within the recommended scope.

All country-specific parameters used in Tier 2 method are summarized in the Table 1.

The greenhouse gas emissions from operations with oil were calculated for the time series from 1990 to 2009 with the use of Tier 1 (Eqs. (1) to (2)) and Tier 2 (Eqs. (1) to (6)). All the emission factors used were taken from IPCC Good Practice as the middle-value of the recommended scope (IPCC 2000). The results of the estimates were further recalculated into CO_2 equivalent on the basis of the global warming potentials (Houghton et al. 1996). Figure 4

Table 1 The country-specific parameters for the estimation the greenhouse gas emissions from operations with oil in the Russian Federation

Parameter in the Eqs. (3)–(6)	Replaced with country-specific parameter	Justification of the replacement
$GOR \bullet Q_{oil}$	$\frac{Q_{APG\_USED}}{CE}$	Provided in the national statistics
$42.3 \bullet 10^{-6}$	$41.6 \bullet 10^{-6}$	Oil density is reported at the temperature 20 °C and pressure 101,325 kPa
y_{gas}	$y_{CH4}=0.583$ $yco_2=0.009$ $y_{NMVOC}=0.373$	Derived from the national data on composition of the APG
Nc_{NMVOC}	2.9	
X_{flared}	$X_{FLARED} = \frac{Q_{FLARED}}{\frac{Q_{APG\_USED}}{CE} \bullet (1-CE)}$	Recalculated based on the national statistics on the APG operations
FE	0.9994	Based on underburning coefficient derived by Scientific Research Institute for Atmospheric Air Protection for non-soot flaring facilities

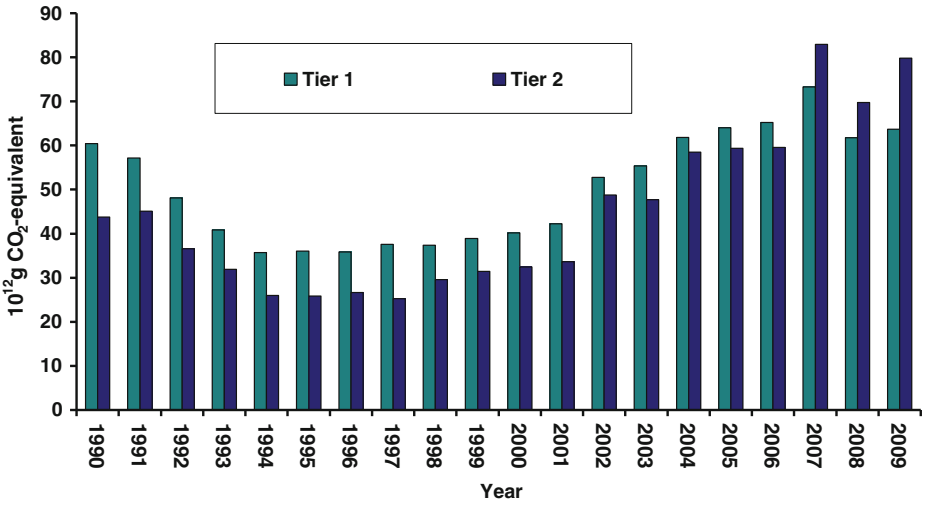

Fig. 4 The estimates of the greenhouse gas emissions from operations with oil performed with the use of Tier 1 and Tier 2 methods

shows the estimates of the greenhouse gas emissions from operations with oil performed with the use of Tier 1 and Tier 2 methods.

The calculations performed with the use of Tier 1 show that oil production operations make the highest contribution to the emission profile—99.7 % (fugitives and venting operations due to oil production provide about 57.7 % followed by the flaring operations—42.1 %). The main component of the emissions from oil production operations is methane (71.6 %). Exploration and transport together are responsible for less than 0.5 % of the total greenhouse gas emissions from the sector. Consequently, the oil production operations are the priority emission categories for oil sector in the Russian Federation. Similar results were obtained, when Tier 2 was used: the oil production operations contributed to 99.7 %, which, however, consist of 11.3 % fugitives and venting operations and 88.3 % for APG flaring. The APG flaring comprises for about 98.9 % of the carbon dioxide due to significant volume of APG flared. The exploration and transport taken together provided for less than 0.5 % to the emissions.

In general for the for Tier 1 estimates, the equivalent greenhouse gas emissions varied from 36 to 73 Tg CO_2-equivalent with an average value of 50 Tg CO_2-equivalent (from 1990 to 2009). For the same period, the equivalent greenhouse gas emissions derived with the use of the Tier 2 method varied from 25 to 83 Tg CO_2-equivalent with an average of 45 Tg CO_2-equivalent. The comparison of the estimates shows that the calculations with the use of the enhanced combination of production-based and mass balance methods (IPCC Tier 2) are of the same order of magnitude with those derived from the production-based method (IPCC Tier 1). Evidently, the difference is because of the higher accuracy in the Tier 2 estimates performed with the use of the country-specific parameters and more precise equation method.

3 Uncertainty analysis of the greenhouse gas emission estimates for the operations with oil

The reliable national inventory is a core element for the efficient emission mitigation. The level of uncertainty mainly depends upon the reliability of activity data and parameters in use. The

Table 2 The errors of parameters for uncertainty assessment of the greenhouse gas emission calculations with the use of the Tier 1 and Tier 2 method

Parameter	Uncertainty, %	Source
Gas composition	±2.5	Ministerstvo… (1991)
Activity data	±5.0	Rosstat (2010)
X_{soot}	±25.0	IPCC (2000)
EF	±100.0	IPCC (2000)

quality of the estimates obtained with the use of Tier 1 and Tier 2 methods was judged by the uncertainty analysis undertaken in line with the IPCC provisions.

To assess uncertainty level of both estimates Monte-Carlo analysis was applied, which corresponds IPCC Tier 2 uncertainty assessment. In accordance to IPCC Good Practice Guidance, Monte-Carlo analysis included the following steps (IPCC 2000; Barry 1996):

- Step 1 - Source category uncertainties were specified which included uncertainties of the emission factors, activity data and parameters, the probability distribution functions, and cross correlation between source categories. The uncertainty analysis for the Tier 2 calculation implied the assessment of the larger number of parameters. Gas compositions are usually estimated accurately with errors being within ±2.5 % for the individual components (Ministerstvo… 1991). Hence, the ±2.5 % value was used for the methane, carbon dioxide, non-methane volatile organic compounds and the estimation of the number of moles of carbon per mole of NMVOC in the relevant equations for each source category. The flared fraction of non-CO_2 carbon in the input waste gas stream converted to soot or particulate matter (Xsoot) and emission factors were chosen in accordance with the IPCC guidelines. Their errors were ±25 % and ±100 % respectively (IPCC 2000, 2006). Summary of the parameters applied in the uncertainty assessment for the Tier 1 and Tier 2 calculations is provided in Table 2.

  It was supposed that distribution function for all parameters in the emission estimates was normal (Gaussian). The uncertainty analysis was performed under the 95 % confidence interval.
- Step 2 - The emission inventory calculation, the probability density functions and the correlation values were set up in the Monte Carlo software package.
- Step 3 - For each input data item, emission factor or activity data, a number was randomly selected from the probability density function of that variable.
- Step 4 - The iterations number determination depends on the following equation (Hahn and Shapiro 1967; Sobol 1973):

$$\delta = \frac{t_\beta \bullet \sigma}{\sqrt{m}}, \tag{7}$$

where δ—measurement error; m—the iterations number; σ—measurement dispersion; t_β—Laplace coefficient, which is equal 1.96 for the 95 % confidence interval.

Table 3 The results of the uncertainty analysis performed for the Tier 1 and Tier 2 method estimates

Method of greenhouse gas emission estimation	Total average emission, Tg CO_2-equivalent	Uncertainty, %
Tier 1 method	50	54
Combination of Tier 1 and Tier 2 methods	45	26

As follows from the Eq. (7) 10^6 iterations were determined to obtain the three-place accuracy of the calculations. Due to uncertainty analysis 10^6 iterations were performed for each source category for the time series from 1990 to 2009.

- Step 5 - Upon completing 10^6 iterations the outcomes were sorted by ascending taking into account 95 % confidence interval, i.e. 2.5 - and 97.5-percentile were considered. All the negative values derived were considered as logically impossible and 0-meaning was assigned to each negative value.

The results derived for the time series from 1990 to 2009, are summarized in Table 3.

The results of the uncertainty assessment showed that the estimates performed by means of the combination Tier 1 and Tier 2 methods associated with lower values of uncertainty compared with the Tier 1 estimates. Representing the same levels of the total emissions for both of the estimates, the uncertainties are equal about 54 % and 26 % for the Tier 1 and the combination of Tier 1 and Tier 2 respectively (Table 3).

4 Conclusion

The uncertainties of the greenhouse gas emissions were calculated with the use of default production-based (Tier 1) and enhanced combination of production based and mass-balance (Tier 2) approaches in accordance with the IPCC Tier 2 (IPCC 2000, 2006). The uncertainty value for 1990 and 2009 correspondingly was 26 %, when the Tier 2 estimation method was used. It is lower than the 54 % uncertainty obtained, for the (Tier 1) method. Thus, the improvement in the accuracy in the national greenhouse gas inventory results in the reduction of the emission uncertainty. The lower values of uncertainty indicate of the higher quality of the greenhouse gas estimates. Furthermore, the IPCC Tier 2 method allows not only obtaining highly accurate assessments, but also streamlining calculation procedures, improving transparency and adequacy of the estimates and their conformity to typical operations with oil in the Russian Federation.

The use of default emission factors for Tier 1 emission estimates from oil production operations decreases the accuracy estimates and hence leads to considerable value of uncertainty. The further reduction of the greenhouse gas emission uncertainty for operations with oil can be achieved by the enhancement of the APG utilization and the improvement of the accuracy of the parameters included in the calculations and national emission factors derivation.

Acknowledgments The authors acknowledge the financial support provided by the Russian Foundation for Basic Research, which enabled their participation in the 3rd International Workshop on Uncertainty in Greenhouse Gas Inventories, where the outcomes of this work were presented. Furthermore, we would like to thank Prof. Rostislav Bun and Dr. Khrystyna Hamal from the Lviv Polytechnic National University for their efforts in hosting the Workshop and providing friendly and cooperative atmosphere for interesting discussions and valuable comments, which allowed us to improve our manuscript while preparing it for the publication.

References

Andreykina LV (2005) Sostav, svoystva i pererabotka poputnih gazov neftyanih mestorozhdeniy zapadnoy Sibiri (Composition, properties and processing of casing-head gases of oil deposits of Western Siberia). Dissertation, NIIReaktiv

Barry TM (1996) Recommendations on the testing and use of pseudo-random number generators used in Monte Carlo analysis for risk assessment. Risk Assess 16(1):93–105

CAIT 2.0 Climate data explorer (2013) World Resource Institute, Washington. http://cait2.wri.org/wri/Country%20GHG%20Emissions?indicator=Total%20GHG%20Emissions%20Excluding%20LUCF&indicator=Total%20GHG%20Emissions%20Including%20LUCF&year=2010&sortIdx=&sortDir=&chartType=# Cited 2 Now 2011

Grigoryev M, Popov V (2002) Proveryayte "probu" ne othodya ot skvazhin. Neftegazovaya vertical (Check the Sample at the Well. Oil and Gas Vertical) J 12:36–39

Hahn GJ, Shapiro SS (1967) Statistical models in engineering, wiley classics library. Wiley, New York

Hayhurst AN, Lawrence AD (1992) Emissions of nitrous oxide from combustion sources. Prog Energy Combust Sci IS:529–552

Houghton JT, Meira Filho LG, Callander BA, Harris N, Kattenberg A, Maskell K (eds.) (1996) Climate Change 1995. The Science of Climate Change, Contribution of Working Group I to the Second Assessment Report of the Intergovernmental Panel on Climate Change. Cambridge University Press, Cambridge

IPCC (2000) Good practice guidance and uncertainty management in national greenhouse gas inventories. IPCC National Greenhouse Gas Inventories Programme. IGES/OECD/IEA, 2000

IPCC (2006) In: Eggleston HS, Buendia L, Miwa K, Ngara T, Tanabe K (eds) 2006 IPCC Guidelines for National Greenhouse Gas Inventories, Prepared by the National Greenhouse Gas Inventories Programme. IGES, Japan

IPCC (2007) Climate Change 2007—The Physical Science Basis Contribution of Working Group I to the Fourth Assessment Report of the IPCC. Geneva, 104 pp

Ministerstvo neftyanoy i gazovoy promyshlennosti SSSR (1991) Edinaya sistema ucheta poputnogo gaza i soputstvuyuschih produktov gaza ot skvazhin k potrebitelyam (Ministry of Oil and Gas Industry USSR. Unified Accounting System for Associated Gas and Associated Gas Products from Well to Consumers)

NII Atmosphera (1997) Metodika rascheta vybrosov vrednih veschestv v atmosferu pri szhiganii poputnogo neftyanogo gaza na fakelnih ustanovkah (Scientific Research Institute for Atmospheric Air Protection under Ministry of Natural Resources. Method of calculating the emission of harmful substances into the atmosphere from burning of associated gas in flares). NII Atmosphera, St. Petersburg

NIR (2006) Nacionalniy doklad o kadastre antropogennyh vybrosov iz istochnikov i absorbcii pogltitelyami parnikovih gazov ne reguliruemyh Monrealskim protokolom (The National Report on the Inventory of Emissions by Sources and Removals by Sinks of the Greenhouse Gases of the Russian Federation). Federalnaya sluzhba po gidrometeorologii i monitoringu okruzhayuschey sredy, FGBU IGKE Rosgidrometa i RAN, Moskva http://unfccc.int/national_reports/annex_i_ghg_inventories/national_inventories_submissions/items/3734.php Cited 20 Apr. 2013

NIR (2009) Nacionalniy doklad o kadastre antropogennyh vybrosov iz istochnikov i absorbcii pogltitelyami parnikovih gazov ne reguliruemyh Monrealskim protokolom (The National Report on the Inventory of Emissions by Sources and Removals by Sinks of the Greenhouse Gases of the Russian Federation). Federalnaya sluzhba po gidrometeorologii i monitoringu okruzhayuschey sredy, FGBU IGKE Rosgidrometa i RAN, Moskva. http://unfccc.int/national_reports/annex_i_ghg_inventories/national_inventories_submissions/items/4771.php Cited 2 Nov. 2011

Rosstat (2007) Rossiyskiy statisticheskiy ezhegodnik (Russian Statistical Yearbook). Rosstat, Moskva

Rosstat (2010) Rossiyskiy statisticheskiy ezhegodnik (Russian Statistical Yearbook). Rosstat, Moskva

Sobol IM (1973) Chislennye metody Monte-Karlo (Monte Carlo Numerical Methods). Nauka, Moskva

Solovyanov AA, Andreeva NN, Kryukov VA, Lyats KG (2008) Strategiya ispolzovaniya poputnogo neftyanogo gaza v Rossiyskoy Federacii (Strategy of using associated petroleum gases in Russian Federation). Quorum, Moskva

The World Bank (2004) Flared gas utilization strategy. Opportunities for small-scale uses of gas. The International Bank for Reconstruction and Development

DOI 10.1007/978-3-319-15901-0_7
Reprinted from *Climatic Change* Journal, DOI 10.1007/s10584-014-1058-7

Amazon forest biomass density maps: tackling the uncertainty in carbon emission estimates

Jean Pierre Ometto · Ana Paula Aguiar · Talita Assis · Luciana Soler · Pedro Valle · Graciela Tejada · David M. Lapola · Patrick Meir

Received: 8 January 2013 / Accepted: 5 January 2014 / Published online: 11 February 2014
© Springer Science+Business Media Dordrecht 2014

Abstract As land use change (LUC), including deforestation, is a patchy process, estimating the impact of LUC on carbon emissions requires spatially accurate underlying data on biomass distribution and change. The methods currently adopted to estimate the spatial variation of above- and below-ground biomass in tropical forests, in particular the Brazilian Amazon, are usually based on remote sensing analyses coupled with field datasets, which tend to be relatively scarce and often limited in their spatial distribution. There are notable differences among the resulting biomass maps found in the literature. These differences subsequently result in relatively high uncertainties in the carbon emissions calculated from land use change, and have a larger impact when biomass maps are coded into biomass classes referring to specific ranges of biomass values. In this paper we analyze the differences among recently-published biomass maps of the Amazon region, including the official information used by the Brazilian government for its communication to the United Nation Framework on Climate Change Convention of the United Nations. The estimated average pre-deforestation biomass in

This article is part of a Special Issue on "Third International Workshop on Uncertainty in Greenhouse Gas Inventories" edited by Jean Ometto and Rostyslav Bun.

J. P. Ometto (✉) · A. P. Aguiar · T. Assis · G. Tejada
Earth System Science Center (CCST), National Institute for Space Research (INPE), Av dos Astronautas 1758, 12227-010 São José dos Campos, SP, Brazil
e-mail: jean.ometto@inpe.br

L. Soler
Centro Nacional de Monitoramento e Alertas de Desastres Naturais (CEMADEN), Rod. Presidente Dutra, Km 40, 12630-000 Cachoeira Paulista, SP, Brazil

P. Valle
GeoPixel, Rua Euclides Miragaia, 433, São José dos Campos 12245-902 SP, Brazil

D. M. Lapola
Earth System Science Lab (LabTerra), Department of Ecology, Universidade Estadual Paulista (UNESP), Av. 24A, 1515, 13506-900 Rio Claro, SP, Brazil

P. Meir
Research School of Biology, Australian National University, Canberra, ACT 0200, Australia

P. Meir
School of Geosciences, University of Edinburgh, Edinburgh EH89XP, UK

the four maps, for the areas of the Amazon region that had been deforested during the 1990–2009 period, varied from 205±32 Mg ha^{-1} during 1990–1999, to 216±31 Mg ha^{-1} during 2000–2009. The biomass values of the deforested areas in 2011 were between 7 and 24 % higher than for the average deforested areas during 1990–1999, suggesting that although there was variation in the mean value, deforestation was tending to occur in increasingly carbon-dense areas, with consequences for carbon emissions. To summarize, our key findings were: (i) the current maps of Amazonian biomass show substantial variation in both total biomass and its spatial distribution; (ii) carbon emissions estimates from deforestation are highly dependent on the spatial distribution of biomass as determined by any single biomass map, and on the deforestation process itself; (iii) future deforestation in the Brazilian Amazon is likely to affect forests with higher biomass than those deforested in the past, resulting in smaller reductions in carbon dioxide emissions than expected purely from the recent reductions in deforestation rates; and (iv) the current official estimate of carbon emissions from Amazonian deforestation is probably overestimated, because the recent loss of higher-biomass forests has not been taken into account.

1 Introduction

The increasing rate of global carbon dioxide (CO_2) emissions to the atmosphere and, additionally, the increasing atmospheric CO_2 concentration has no parallel in the preceding hundred to millions years of Earth's history (IPCC 2013). From 1958 to 2004 the mean global CO_2 emissions increased at approximately 1.3 % per year, whilst from 2004 to 2010 this rate rose to approximately 3 % per year (Global Carbon Project (GCP) www.globalcarbonproject.org). Most of this increase is associated with fossil fuel burning. According to the Global Carbon Project CO_2 budget, the estimated uncertainty of fossil fuel CO_2 emissions at the global scale is 6–10 % for the 2009–2010 analysis. The Fourth Assessment Report of the Intergovernmental Panel for Climate Change (IPCC 2007) states that tropical deforestation accounts for 10–20 % of anthropogenic CO_2 emissions, with the uncertainty on this range being mostly due to estimates of pre-deforestation biomass, and spatial heterogeneity in biomass. Biomass burning-driven greenhouse gas emissions follow a different trajectory to those from fossil fuel combustion. Recent reductions in deforestation rates in tropical regions (e.g. in Brazil, Indonesia) mean that the fractional contribution of the land use CO_2 source to total anthropogenic emissions to the atmosphere has decreased in recent years (Le Quéré et al. 2009).

In spite of technological advances in mapping land use change and biomass, the most recent emissions estimates for tropical forests contain even more variance than those from previous decades (Houghton 2010), because of the large estimated spatial variability in biomass. Given the widely-acknowledged importance of tropical forests for climate, carbon storage and sequestration, biodiversity and for ecosystem services, improved biomass estimates remain an important scientific and social priority (Nobre et al. 1991; Hoffmann et al. 2003; Malhi 2010).

Tropical forests, classified as humid forests by the Global Land Cover Classification (2000), cover about 13.4 million km^2 within the global tropical belt. In tropical America humid broadleaf forest covers about 47 % of the region, mostly in South America, particularly the Amazon region. In Brazil, the Amazon basin covers more than 5 million km^2, of which ~80 % are still intact forest (Davidson et al. 2012; Ometto et al. 2011). Tropical forests are highly diverse ecosystems, hosting a large fraction of the current known terrestrial biodiversity. The Amazon forest alone is thought to house 25 % of the terrestrial global plant species (Lambin et al. 2001; Strassburg et al. 2010). Tropical forests also regulate climate by influencing the hydrological cycle at multiple scales, via differences in surface roughness,

albedo and through the control of transpiration (e.g., Spracklen et al. 2012; Werth and Avissar 2002). Spatial variation in vegetation composition and biomass is partly determined by the prevailing climate, but is also influenced by soil fertility and physical structure (Quesada et al. 2011). Together with constraints to seed dispersal, these factors strongly influence the distributions in vegetation type and associated biomass observed in natural vegetation, and whose patchy nature presents a challenge to mapping efforts.

Vegetation type varies from sparse open savanna to dense broadleaf evergreen forest, with species composition, forest structure and ecological dynamics varying greatly throughout the region (http://www.ibge.gov.br; Hoffmann et al. 2004; Malhi et al. 2004). Estimates of the total carbon stock in Amazonia range widely, from 70 to 120 PgC (Malhi et al. 2009; Potter et al. 2009; Saatchi et al. 2007) and this variation partly reflects uncertainty in the biomass content and areal extent of different vegetation types. More than 10 years ago (Houghton et al. 2001) observed that estimates of biomass for the Amazon forests in Brazil varied more than two-fold, with disagreement in the distribution of maximum and minimum biomass content in the seven estimates analyzed. Surprisingly, the most recent updates have not substantially changed this observation, noting wide variance in the estimated spatial distribution of biomass classes as well as total biomass (Malhi et al. 2009; Saatchi et al. 2007, 2011; Fearnside 1997; Malhi et al. 2006; Saatchi et al. 2007; Nogueira et al. 2008a; Saatchi et al. 2011; Baccini et al. 2012). Although there is uncertainty in emissions resulting from the deforestation process itself, uncertainty in the underlying original biomass remains the largest contributor to uncertainty in deforestation emissions (Aguiar et al. 2012).

In this paper we explore the available biomass classification maps for the Brazilian Amazon, estimating the range in current estimates in the literature and then comparing with the Brazilian Government-based map used for reporting carbon emissions to the United Nations Framework Convention on Climate Change. Also we examine the influence of the use of different biomass maps on uncertainty in carbon emission calculations due to land cover change in recent years, and in future scenarios (unpublished data, Ana Paula Aguiar, Ima Vieria, Peter Toledo and Jena Pierre Ometto, Earth System Science Centre, National Institute for Space Research Internal Report), using the IPCC Tier 1 methodology (www.ipcc-nggip.iges.or.jp/public/2006gl/vol4.html).

Within the scope of the 3rd International Meeting on Uncertainty in Greenhouse Gas Inventories, (held in Lviv, Ukraine from 22 to 24 September 2010), our analysis aims improve the validation of land use and land use change (LULUC) emission models for the Brazilian Amazon region. The issues discussed here have important implications for national greenhouse gas emissions inventories, future emissions scenarios, forest management and the possible implementation of REDD + initiatives, among others (REDD: 'Reducing Emissions from Deforestation and Forest Degradation in Developing Countries').

2 Methods

2.1 Biomass data sources

The biomass maps used for this analysis were derived from recent publications in the scientific literature and from the map used by the Brazilian Ministry of Science and Technology (MCT 2010) for reporting the national greenhouse gas emissions estimates to the United Nations Framework Convention on Climate Change (The National GHG Communication). The sources and the structure of the data used in this analysis are described below and presented in Fig. 1.

- (Baccini et al. 2012), hereafter BB12. Pan-Tropics above-ground biomass map based on satellite observation using LiDAR data (spatial resolution of 70 m) and multispectral

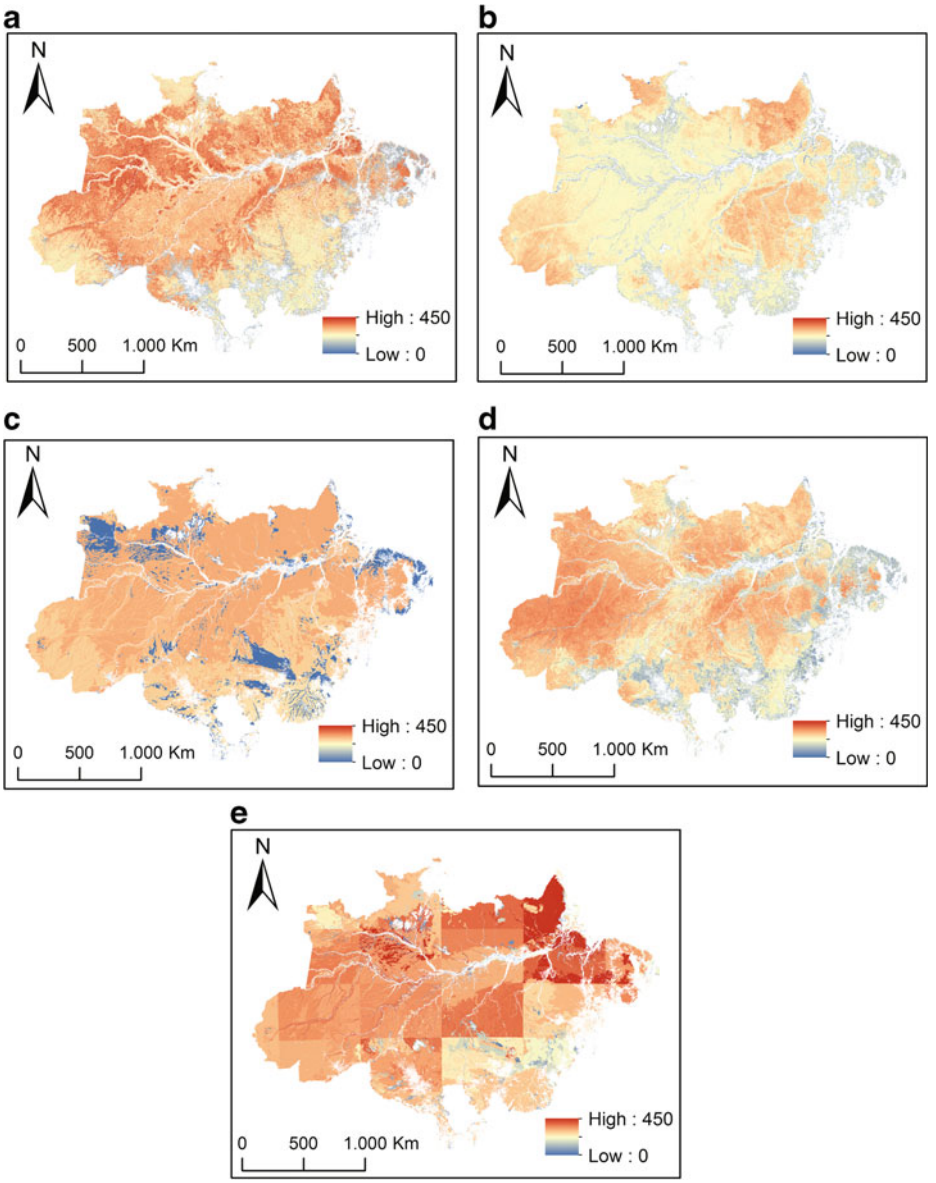

Fig. 1 Biomass original data with PRODES deforestation mask. Data, starting from the upper left panel, are from: **a** BS07 (Saatchi et al. 2007); **b** BS11 (Saatchi et al. 2011); **c** BN08 (Nogueira et al. 2008a, b); **d** BB12 (Baccini et al. 2012); **e** BM10 (MCT 2010)

surface reflectance imagery (at 500 m spatial resolution). The authors also collected field data in the global tropics from 2008 to 2010 at sample points co-located with the LiDAR 'footprints'. LiDAR data were obtained from the Geoscience Laser Altimeter System (GLAS) database. Surface reflectance data were obtained from the Moderate Resolution Imaging Spectro radiometer (MODIS). Digital elevation data were acquired as part of NASA's Shuttle Radar Topography Mission (SRTM) database.

- (Saatchi et al. 2011), hereafter BS11, produced a global map of AGLB and BGLB (Above- and Below-Ground Biomass) analyzing both ground and remotely sensed data for the following types of vegetation: (i) old growth tropical forest; (ii) woodland savanna; (iii) dry forest; (iv) and regrowth forests. BS11 uses radar remote sensing data derived from the Geoscience Laser Altimeter System (GLAS) LiDAR. The analysis was performed across the global tropics at 1 km spatial resolution. Ground observations and error propagation were used to assess the uncertainty involved in translating remotely sensed data into AGLB estimates. This error is reported to be, on average, >30 %. The BGLB is derived as a proportion of AGLB (Saatchi et al. 2011).
- (Nogueira et al. 2008a, b) hereafter BN08, propose an AGLB for the Amazon region following (Fearnside 1997; Fearnside and Laurance 2004), with a wood density re-analysis and new allometric equations produced for relatively fertile soils in the southern Amazon. The BN08 map for the whole region was based on data from the RADAM-BRASIL (http://www.cprm.gov.br/publique/cgi/cgilua.exe/sys/start.htm?UserActiveTemplate=cprm_layout_EN&tpl=home), but it also incorporated corrections for wood density and wood volume, and incorporated expansion factors used to include the bole volume of small trees, and the biomass of large tree crowns. The variation in AGLB is smaller than in Saatchi et al. (2007), but overall, the values are considerably higher (see increase in red color in Fig. 3c). This map shows a strong data saturation, as some classes had null values. The authors report BGLB spatially as percentage of AGLB, with a mean value for the region as 25.8 % of the AGLB.
- (Saatchi et al. 2007), hereafter BS07, used remote sensing, environmental variables and ground measurements to estimate AGLB in the Amazon basin. The method used a decision tree to spatially distribute seven distinct biomass classes for primary vegetation. BGLB was estimated as 21 % of the AGLB (according to published data at the time). The authors reported 80 % accuracy in relation to their ground-truth data, which is similar in relative terms if compared to the uncertainty of 30 % found in BS11,taking into account the different types of remote sensing data used to create these two maps. A regression based on satellite data was used to estimate biomass of herbaceous savannas and secondary forest.
- MCT (2010), hereafter BM10, produced biomass estimates based on 2702 plots inventoried by the RADAMBRASIL project, which extensively mapped the Amazon region from 1971 to 1986 in a 1:1000.000 scale. The RADAM project was designed to inventory areas from 0.5 to 1.0 ha, randomly distributed across the region, with all trees over 38 cm of DBH measured (diameter at breast height, 1.3 m). Biomass for trees smaller than 38 cm diameter 1.3 m was estimated according to a distribution histogram produced from subsamples made as part of the RADAM project. Allometric equations used to estimate AGLB and below-ground living biomass (BGLB) from DBH were based on Higuchi et al. (1998). MCT (2010) reports Below Ground Biomass (BGB) as 28 % of AGB.

For the two more recent remote sensing maps (BS11 and BB12), produced at global scale using similar input data (as described above), there are some key differences: (i) for the allometric equations, BB11 used tree height, diameter and wood density, but BB12 did not use wood density; and (ii) the authors used a different interpolation method. An equivalent analysis proposed in our work, but with fewer biomass maps and with different biomass classes, can be found at: (www.geos.ed.ac.uk/~emitchar/carbonmapcomparison/Index.html)

2.2 Data preparation

In order to perform an appropriate comparison among different biomass maps and datasets the BS07, BM10, BS11 and BB12 were resampled according to BN08, the biomass map with the

Table 1 Biomass data source and processing

BS07	Saatchi et al. (2007)	Remote sensing and field plots. MODIS images from 2001 to 2004. Spatial scale: resolution 1×1 km2; extent: Amazon Basin.	Original biomass raster data is classified into 11 classes, representing a range of biomass intervals. The middle value of each interval was taken as the pixel value. The procedure to fill the cells is the following. Each cell initially receives the average of the pixels inside that cell, excluding pixels below 100 Mgha−1 (classes 1–4). Then the correction to eliminate the influence of previously deforested areas on the biomass was applied.
BN08	Nogueira et al. (2008a, b)	Field plots and allometric equations for forest. Spatial scale: resolution 1×1 km2; extent: Brazilian Amazon Basin.	Each cell initially receives the average of the pixels inside that cell, excluding pixels below 100 Mgha−1 (which are few for this map). If a cell has no valid biomass values, a simple correction attributes the average values of neighborhood cells (using a Moore neighborhood), or an overall average (in case the neighbors cells are also empty).
BM10	MCT (2010)	Field plots, vegetation and soil maps, and allometric equations for different types of vegetation Spatial scale: resolution 1×1 km2; extent: Brazilian Amazon Basin.	Same process as B2.
BS11	Saatchi et al. (2011)	Combines all biomass measurements that were made after 1995 and before 2005. ICES at GLAS Lidar data from 2003 to 2004. MODIS from 2001 to 2003. Spatial scaleresolution 1×1 km2; extent: global coverage.	Each cell initially receives the average of the pixels inside that cell, excluding pixels below 100 Mgha−1. Then we apply the correction to eliminate the influence of previously deforested areas on the biomass.
BB12	Baccini et al. (2012)	Combination of remote sensing and field data for period 2008/2010. Spatial scale: resolution 500×500 m ; extent: Pan-Tropics	Same process as B4.

coarsest resolution classes (Table 1). Then all maps were masked to only show their common mapped areas and to remove the areas already deforested according to land use data from the PRODES project (INPE 2011); Fig. 1 illustrates the resulting pre-processed maps.

2.3 Data analysis

In order to compare the core differences in the magnitude and spatial distribution of carbon in live biomass we adopted four alternative and complementary approaches:

a) Visual comparison of classified maps: we used the 11 biomass classes used by BS07 to classify BN08, BM10, BS11 and BB12 (Fig. 2). Then, difference maps were calculated in relation to BS11 (BS11-BS07; BS11-BN08; BS11-BM10;

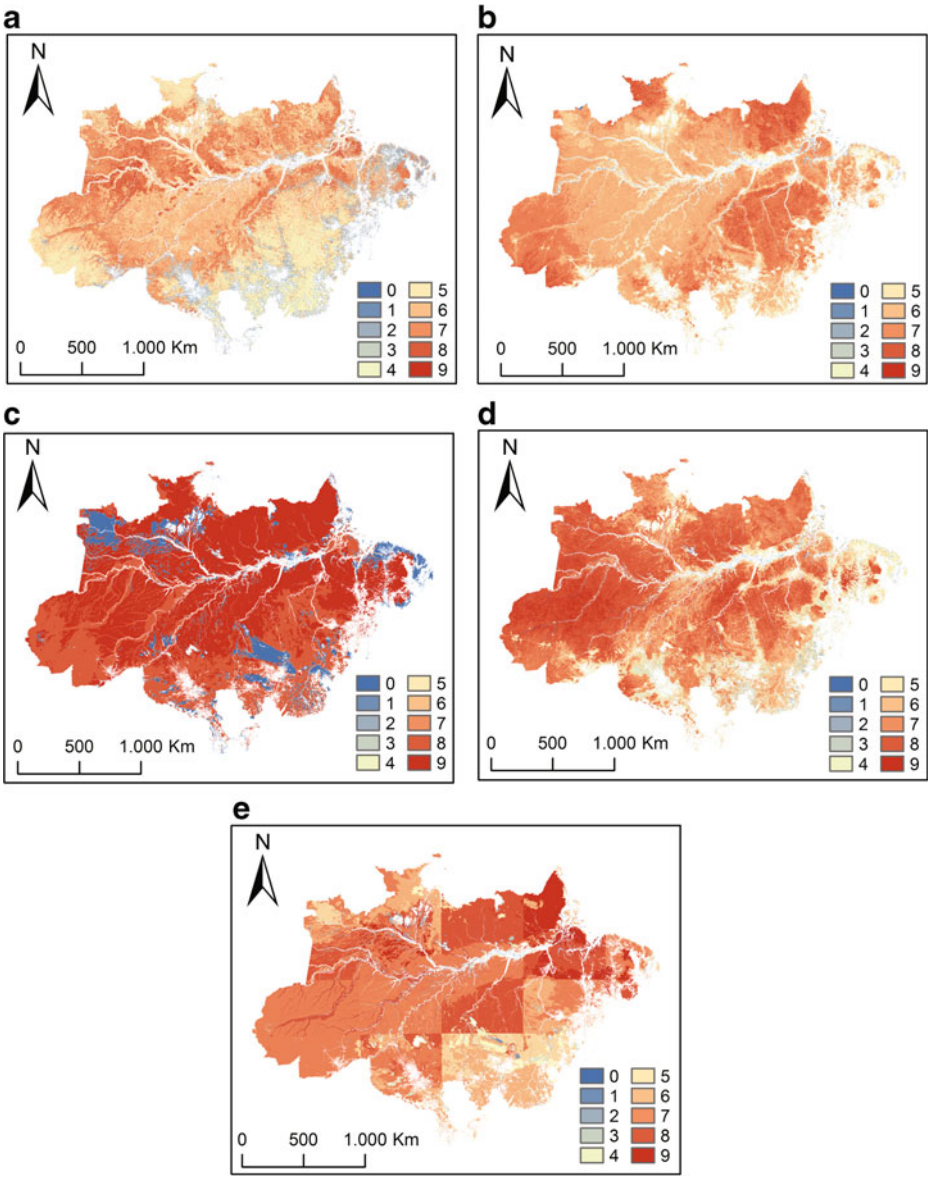

Fig. 2 Amazon region biomass estimates classified as in BS07. *Warmer colors* are representing higher biomass classes. **a** BS07 (Saatchi et al. 2007); **b** BS11 (Saatchi et al. 2011); **c** BN08 (Nogueira et al. 2008a, b); **d** BB12 (Baccini et al. 2012); **e** BM10 (MCT 2010)

BS11-BS12). We chose BS11 as a reference because it has a global coverage and 1 km^2 resolution. By using a simple difference between raster-based datasets we obtained difference maps that attempt to capture where, and by how much, the different biomass maps differ.

b) Quantitative analysis (region-based): a regional-scale analysis was performed in order to analyze broader differences among the maps, their average values and standard deviations

Table 2 Average above ground biomass (AGB), in Mg.ha^{-1}, considering values above 100 Mg.ha^{-1}, and "pre-deforestation" values, per states

	(a) Average AGB (above 100 Mgha) considering all cells						(b) Average AGB ("pre-deforestation") considering all cells						% change (b-a)				
	BS07	BN08	BM10	BS11	BB12	Mean (a)	BS07	BN08	BM10	BS11	BB12	Mean (b)	BS07	BN08	BM10	BS11	BB12
Brazilian Amazon	232	287	329	219	246	263	231	281	326	223	269	266	0 %	−2 %	−1 %	2 %	9 %
Acre	194	287	311	262	252	261	194	287	311	274	274	268	0 %	0 %	0 %	5 %	9 %
Amazonas	263	299	335	221	289	281	263	299	335	222	297	283	0 %	0 %	0 %	0 %	3 %
Rondônia	220	272	312	202	190	239	220	272	312	221	246	254	0 %	0 %	0 %	9 %	29 %
Roraima	219	287	312	224	228	254	219	282	312	228	243	257	0 %	−2 %	0 %	2 %	7 %
Mato Grosso	181	245	281	189	180	215	182	239	287	189	221	224	1 %	−2 %	2 %	0 %	23 %
Pará	230	296	345	240	234	269	230	295	343	249	270	277	0 %	0 %	−1 %	4 %	15 %
Amapá	254	296	386	258	243	287	254	295	385	258	253	289	0 %	0 %	0 %	0 %	4 %
Tocantins	214	233	269	132	127	195	214	231	290	130	219	217	0 %	−1 %	8 %	−2 %	72 %
Maranhão	244	286	336	160	153	236	242	266	328	181	231	250	−1 %	−7 %	−2 %	13 %	51 %
	(c) Average AGB (above 100 Mgha) weighted by total deforested area in each cell in 2010						(d) Average AGB ("pre-deforestation") weighted by total deforested area in each cell in 2010						% change (d-c)				
	BS07	BN08	BM10	BS11	BB12	Mean (c)	BS07	BN08	BM10	BS11	BB12	Mean (d)	BS07	BN08	BM10	BS11	BB12
Brazilian Amazon	207	277	316	188	160	230	207	275	314	210	241	249	0 %	−1 %	−1 %	12 %	51 %
Acre	250	297	324	206	225	260	250	297	324	218	278	273	0 %	0 %	0 %	6 %	24 %
Amazonas	213	294	316	205	184	242	213	294	316	256	267	269	0 %	0 %	0 %	25 %	45 %
Rondônia	208	274	319	185	145	226	208	274	319	225	243	254	0 %	0 %	0 %	22 %	68 %
Roraima	217	298	308	193	184	240	217	298	308	217	242	256	0 %	0 %	0 %	12 %	32 %
Mato Grosso	167	250	279	178	154	206	168	248	282	186	213	219	1 %	−1 %	1 %	4 %	38 %
Pará	219	292	337	201	162	242	219	291	334	234	259	267	0 %	0 %	−1 %	16 %	60 %
Amapá	249	283	377	217	195	164	249	283	377	228	230	273	0 %	0 %	0 %	5 %	18 %
Tocantins	208	273	269	138	122	202	206	269	274	128	216	219	−1 %	−1 %	2 %	−7 %	77 %
Maranhão	237	289	333	165	137	232	237	278	329	196	238	256	0 %	−4 %	−1 %	19 %	74 %

Reprinted from the journal

for the whole area, grouped by Federal State (Table 2) and river basins (Fig. 3). Estimates of uncertainty for each map are reported in the "Biomass data sources" section.

c) Biomass in the deforested areas: as a final comparison, we show the results of the average biomass values considering the newly deforested areas from 2002 to 2012, using PRODES data, and from 2012 to 2010, using a spatially-explicit deforestation scenario (unpublished data: Ana Paula Aguiar, Ima Vieria, Peter Toledo, Jean Pierre Ometto, Earth System Science Centre, National Institute for Space Research Internal Report), in which the Brazilian voluntary commitment to reduce deforestation in the Amazon region by 80 % until 2020 is assumed (United Nations Framework Convention on Climate Change, Copenhagen, Denmark, 2009). In order to do this, we used a procedure developed by Aguiar et al. (2012) to estimate the original vegetation prior to the deforestation process. This correction is critical for the maps based on remote sensing (mainly BS11 and BB12) that are influenced by the deforestation and secondary vegetation dynamics that occurred prior to the image acquisition dates. For carbon emissions calculation purposes, we implemented the following procedure for processing biomass maps: for any deforested cell (above 10 % of cell area), the prior biomass is the average of the non-deforested (below 10 %) neighbor cells, assuming a 10×10 km neighborhood.

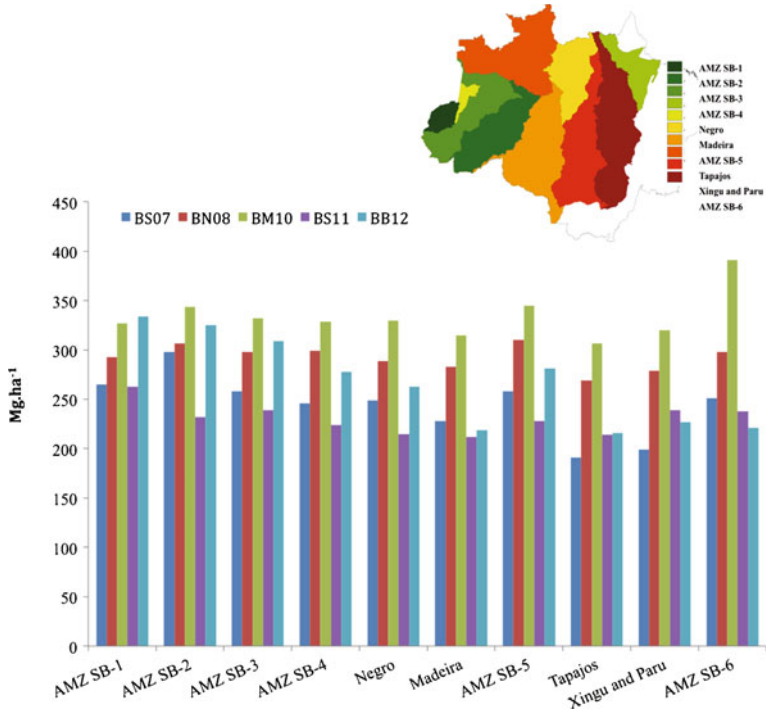

Fig. 3 Estimated pre-deforestation biomass distributed in eco-regions. The legend refers to the following rivers sub-basins: AMZ SB1 (Amazon river basin from Brazilian border to Javari river); AMZ SB2 (Amazon river basin from Javari to Auati-Parana rivers); AMZ BS3 (Amazon river basin from Auati-Parana river to Coari); AMZ BS4 (Amazon river basin from Coari to Purus river); Negro river basin; Madeira river basin; AMZ BS5 (Amazon river basin from Madeira to Trombetas rivers); Tapajós river basin; Xingú and Parú river basin; AMZ BS6 (Amazon river basin from Xingu river to the Atlantic ocean)

3 Results

The histograms in Fig. 4 demonstrate the differences in the biomass class and values occurrence in each of the five maps. Large differences among the maps in terms of what is considered the mean biomass and the statistical distribution of that biomass are shown in Table 2.

BM10 and BN08 show biomass density ranges of 150–250 and 250–350 Mg ha^{-1} respectively, although their spatial distributions of biomass density classes are similar. Overall the BN08 and BB12 maps suggest larger biomass density values throughout the region in comparison to BS11, although the biomass class distributions differ, with BN08 similar to BS07 and BB12 similar to BS11. Perhaps most notably, major differences between the maps can be observed in the spatial distribution of total biomass, as Figs. 2, 3, and 5 illustrate. Differences in biomass at the scale of eco-regions are shown in Fig. 5. Figure 6 presents time-traces of mean biomass, per map, estimated to be associated with deforestation during the

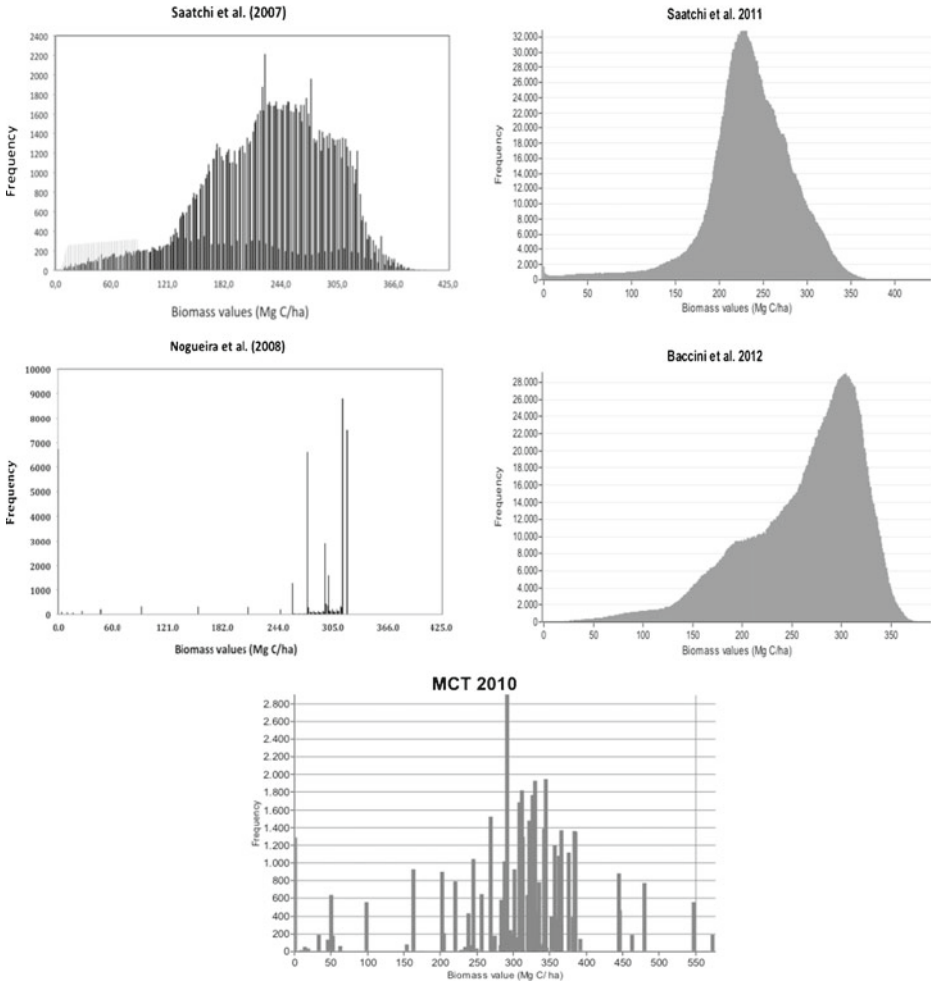

Fig. 4 Histograms of biomass distribution for the BS07, BS11, BN08, BB12 and BM10: biomass classes and frequency

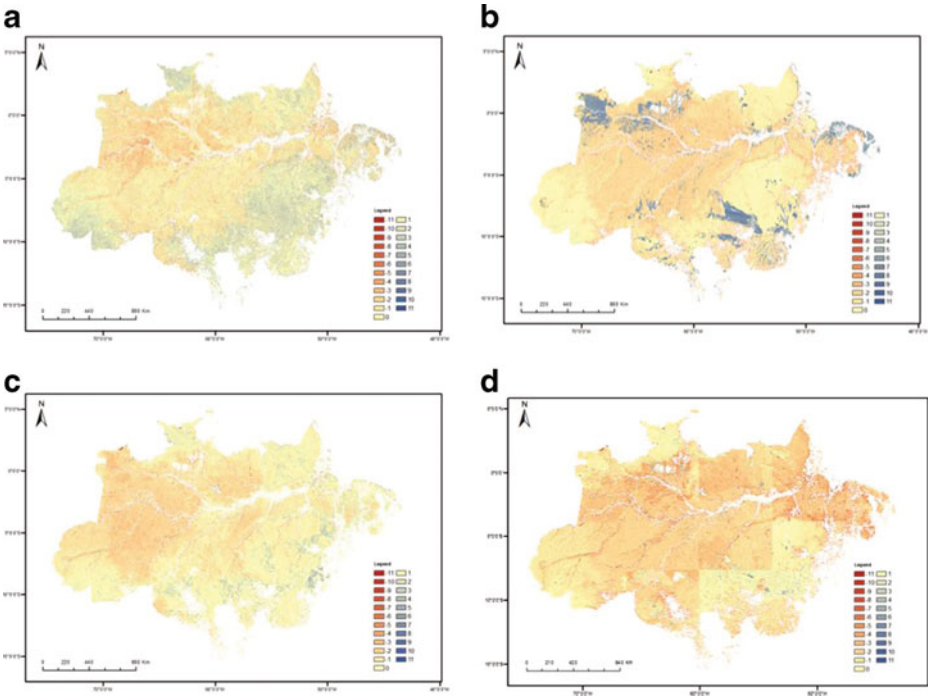

Fig. 5 Class differences in relation to BS11: (BS11-BS07; BS11-BN08; BS11-BM10; BS11-BS12)

period 2002 to 2020; the substantial inter-map differences of up to 50 % underline how large inter-map variability is, and its potential impact on emissions estimates. The location of new deforestation frontiers coupled with intra-regional variation in biomass density will influence

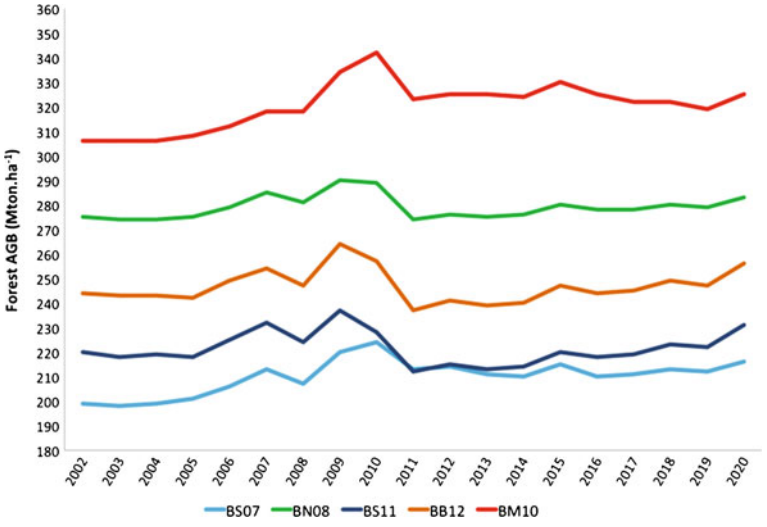

Fig. 6 Average mean forest biomass per map in the deforested areas from 2002 to 2012 and in areas of potential deforestation evolution from 2013 to 2020

estimates of any future emissions represented in this figure, including those affected by REDD + or similar activities.

Overall, the results show some similarities in biomass for non-deforested regions of the State of Amazonas, but important differences in biomass among other regions, in particular in the east and far north of the Amazon region, and at the Brazilian borders with Colombia and Venezuela (Fig. 5). Despite the larger number of sample plots used to estimate biomass in BS11, most were located in old growth forests, with only a small portion of them in secondary forest and swamp areas, implying that estimates for these latter vegetation types may be less well constrained. In BS07, the sample plots were better distributed among old growth forests, secondary forests of different ages and areas of savanna. These differences in underlying ground data might be responsible for the divergence between the two maps provided by Saatchi and co-authors. More generally, the observed variance in recent biomass estimates likely reflect: (i) differences in sample plot measurements adopted to calibrate each model; (ii) differences in the remote sensing data product combinations used; and (iii) the exclusion for some analyses of GLASS images from very steep terrain (>20 % slope) to avoid large tree height error estimates, to , with the latter potentially leading to an underestimation of above-ground biomass, where very structured and old-growth forests can occur (Araújo et al. 2002).

Finally, the methodology used by BM10, based on the RADAM data (1:1,000,000), resulted in large differences in biomass with respect to the other maps, and large changes in biomass between adjacent surveyed areas and regions (corresponding to different RADAM data sheets) within BM10. This made, spatial comparisons with BM10 less informative, although the large apparent disparities in biomass calculated for the BM10 map were not propagated into CO_2 emissions as the deforestation front in the analysis had not advanced to these areas (INPE 2012). However, as future deforestation approaches the northwestern edge of the region, a large shift in calculated emissions rates is likely using BM10.

4 Discussion

In general, our analysis indicates substantial differences in the estimates of biomass density by region, and provides details on where and by how much the maps differ. In this section, we discuss the potential reasons for such differences and the alternatives for reducing such uncertainties.

4.1 Methods underlying the maps

Houghton et al. (2001) made a number of recommendations for reducing uncertainty in the estimation of biomass across Amazonia. In the intervening period, there has been improvement in some but not all of these areas. Major differences in biomass estimates are frequently related to inconsistencies in field measurements: weak allometric relationships for some vegetation types such as secondary forest, savanna and/or degraded forest areas; incomplete or insufficient field parameters used to construct or calibrate the relevant allometric equation (e.g. due to under sampling of certain plant groups, or biogeographic areas; Feldpausch et al. 2011a, b); the size of the sampling plot (Anderson et al. 2010); and the strategies used to extrapolate the data. The maps that use remote sensing data to extrapolate biomass from a core ground-based dataset may also be influenced by unaccounted-for variation in soil characteristics and the preceding history of forest disturbance and deforestation (BS07, 11 and BB12), a source of variability that may potentially lead to larger errors when aggregated at larger pixel scales. On the other hand, maps based solely on field inventory depend on interpolation techniques and may suffer from lack of detail in the quantification of spatial heterogeneity (Aguiar et al. 2012).

The stratification of biomass into different classes is fundamental for the extrapolation of data derived from field and remote sensing based measurements. Therefore, the scale of sampling is also relevant, for example whether data collection was for traditional forest inventory or specifically for biomass assessment. The development and use of a widely and densely distributed network of permanent sample plots designed for biomass estimation would substantially improve point and interpolated biomass estimates, and further would advance the refinement of allometric regression equations used to estimate biomass from simpler measurements (e.g. Feldpausch et al. 2011a, b). With this in mind, Brazil is currently developing an extensive forest plot network in a 20×20 km grid in some parts of the country, with finer-scale grids in vegetation transition areas and highly heterogeneous landscapes (http://ifn.florestal.gov.br/); this will become a very important data base in the near future.

4.2 Changes in biomass due to growth/decline/degradation

The biomass maps used in the current analysis do not consider changes over time. However annual changes in forest growth and biomass accumulation have been reported to be in the range of 0.5 to 1.0 t C/ha/y (Vieira et al. 2005). Ultimately variation in old-growth forest dynamics, rates of regrowth in secondary forests and rates of forest degradation must be adequately quantified to fully inform carbon stock and emissions analyses over time. For example, even in undisturbed old-growth forest, there is evidence for differences in the mortality, growth and recruitment processes determining forest dynamics (Phillips et al. 2004). These differences are evident in the spatial variation in biomass and above-ground carbon residence times from east to west across the Amazon basin (Malhi et al. 2006; BN08, BS07 and BM10), and over time in repeatedly measured forest plots across the region (Phillips et al. 2004). The reported increasing dynamism in Amazonian forests may also result in changes in functional composition and in increased vulnerability to drought, potentially leading to reductions over time in standing biomass (Phillips et al. 2002; Potter et al. 2011), and this may also be accompanied further by alterations to the residence time in different decomposing carbon pools, especially under contrasting climate regimes of, for example, drought or flood.

In addition to changes over time in old growth forest carbon stocks, the dynamics of degraded primary forest, or of previously-cleared secondary forest represent further important contributions to overall uncertainty in land-use related carbon emissions. The former (degradation of primary forest) has often been considered a relatively small component, although recent remote sensing assessments of primary forest degradation through selective logging and fire estimated substantial annual changes in the affected areas: 15,987 km^2 in 2007; 27,417 km^2 in 2008; and 13,301 km^2 in 2009 (INPE 2011). Thus, even in the absence of deforestation, degradation alone can alter biomass over substantial areas of natural forest, with downstream effects on carbon stock dynamics, for example following increased vulnerability to climate extremes. The need to understand the secondary forest recovery cycle following disturbance has been recognized for some time, even though quantification studies covering the full cycle from clearance through regrowth to re-clearance still remain sparce. Recently, Brazil's National Institute for Space Research (INPE) developed a method to classify land use in deforested areas previously mapped by the project PRODES, thus identifying not only classes of land use, but also mapping regrowth of secondary vegetation (TerraClass-INPE). According to this monitoring and classification system the amount of secondary forest in the Brazilian Amazon up 2010 was 21 % of the mapped clear-cut deforestation (close to 740,000 km^2). The regrowth rate for secondary vegetation, and consequent rate of carbon accumulation, depends partly on the previous history of the abandoned land. (Feldpausch et al.

2005) reported post-pasture biomass accumulation for two secondary forests in Central Amazonia of 120 to 135 Mg/ha after 14 years of abandonment and found that biomass accumulation rates were similar to those obtained from lightly-used pastures in eastern and central Amazônia. More generally, Houghton (2010) and Ramankutty et al. (2007) have suggested that Amazon forests recover 70 % of their original biomass in the first 25 years following clear-cutting, and the remaining 30 % over the following 50 years. These and similar data serve as a starting point to inform dynamic modelling of forest recovery post-disturbance, but much more empirical data are needed to improve the spatial resolution and ecological interpretation of forest regrowth across the Basin.

5 Conclusions

The biomass density maps analyzed in this study use different approaches to estimate and interpolate ground-based and remotely-sensed data sources, and produced markedly different distributions of estimated biomass density classes. Reducing uncertainty in estimating biomass in the Amazon region is centrally important for estimating carbon emissions from land cover change and deforestation, as well as for underpinning the development of policy mechanisms aimed at reducing total land-use related emissions, such as the UN-REDD + framework. Land use planning in the Brazilian Amazon has the potential to achieve substantial emissions reductions over the coming decade, especially in the context of the national commitment from Brazil to reduce deforestation by 80 %. To make the most of this opportunity, improved biomass estimation should be considered a high priority. Our results underline the need for higher resolution biomass maps based on a combination of remote sensing data and an intensified field network of permanent forest plots. Whilst an improved ground-truth database is essential, improvements in post-processing of remotely sensed data (e.g. to account for variation in soil and topography) are also necessary, as are advances in the estimation of the effects of previously-ignored forest degradation processes, and the dynamic modelling of forest regrowth trajectories. The goal of better management of greenhouse gas emissions from deforestation in the Brazilian Amazon offers great opportunities for the development of mechanisms and programs focusing on changing deforestation patterns in the region. Brazil potentially has a globally important role to play in forest-related carbon dioxide emissions reductions, and the national commitment to an 80 % reduction in the deforestation rate in the Amazon region may alone lead to substantial reductions in emissions from land use in tropical forests.

Acknowledgments We thank Thelma Krug, Ubirajara Freitas, Euler Melo Nogueira, Philip Martin Fearnside, Sassan Saatchi and Alessandro Baccini for providing the biomass spatial data for the production of maps. We are grateful to J. Reid (JWR Associates) for revising the English. We acknowledge financial support and the Planetary Skin Institute (PSI) for initial discussions and for financial support. JPO gratefully acknowledges the *Fundação de Amparo a Pesquisa do Estado de São Paulo* (FAPESP) through the project n. 2009/52468-0. PM gratefully acknowledges ARC support through FT110100457 and NERC support through NE/J011002/1.

References

Aguiar APD, Ometto JP et al (2012) Modeling the spatial and temporal heterogeneity of deforestation-driven carbon emissions: the INPE-EM framework applied to the Brazilian Amazon. Glob Chang Biol. doi:10.1111/j.1365-2486.2012.02782.x

Anderson LO, Malhi Y, Aragao LEOC, Ladle R, Arai E, Barbier N, Phillips O (2010) Remote sensing detection of droughts in Amazonian forest canopies. New Phytol 187(3):733–750

Araújo AC et al. (2002) Comparative measurements of carbon dioxide fluxes from two nearby towers in a central Amazonian rainforest: the Manaus LBA site, J Geophys Res 107(D20):58–51 - 58–20.
Baccini A et al (2012) Estimated carbon dioxide emissions from tropical deforestation improved by carbon-density maps. Nat Clim Chang 2(3):182–185
Davidson EA et al (2012) The Amazon basin in transition. Nature 481(7381):321–328
Fearnside PM (1997) Wood density for estimating forest biomass in Brazilian Amazonia. For Ecol Manag 90(1):59–87
Fearnside PM, Laurance WF (2004) Tropical deforestation and greenhouse-gas emissions. Ecol Appl 14(4):982–986
Feldpausch TR, Riha SJ, Fernandes ECM, Wandelli EV (2005) Development of forest structure and leaf area in secondary forests regenerating on abandoned pastures in Central Amazonia. Earth Interact 9(6):1–22
Feldpausch TR et al (2011a) Height-diameter allometry of tropical forest trees. Biogeosciences 8(5):1081–1106
Feldpausch TR et al (2011b) Height-diameter allometry of tropical forest trees. Biogeosciences 8:1081–1106
Higuchi N, Santos J, Ribeiro RJ, Minette L, Biot Y (1998) Biomassa da parte aerea da vegetacão da Oloresta tropical úmida de terra-firme da Amazonia brasileira. Acta Amazôn 28:153–166
Hoffmann WA, Schroeder W, Jackson RB (2003) Regional feedbacks among fire, climate, and tropical deforestation. J Geophys Res Atmos 108:4721
Hoffmann WA, Orthen B, Franco AC (2004) Constraints to seedling success of savanna and forest trees across the savanna-forest boundary. Oecologia 140(2):252–260
Houghton RA (2010) How well do we know the flux of CO(2) from land-use change? Tellus Ser B Chem Phys Meteorol 62(5):337–351
Houghton RA, Lawrence KT, Hackler JL, Brown S (2001) The spatial distribution of forest biomass in the Brazilian Amazon: a comparison of estimates. Glob Chang Biol 7(7):731–746
INPE (2011) PRODES-Amazon deforestation database. Available online at: www.obt.inpe.br/prodes
INPE (2012) Amazon deforestation database, edited, Sao Jose dos Campos, SP, Brazil
IPCC (2007) Climate change 2007: the physical science basis. Rep., Intergovernmental Panel on Climate Change. Cambridge, UK
IPCC (2013) Summary for policymakers. In: Stocker TF, Qin D, Plattner G-K, Tignor M, Allen SK, Boschung J, Nauels A, Xia Y, Bex V, Midgley PM (eds) Climate change 2013: the physical science basis. Contribution of working group I to the fifth assessment report of the intergovernmental panel on climate change. Cambridge University Press, Cambridge, United Kingdom and New York, NY, USA
Lambin EF et al (2001) The causes of land-use and land-cover change: moving beyond the myths. Glob Environ Chang 11(4):261–269
Le Quéré C et al (2009) Trends in the sources and sinks of carbon dioxide. Nat Geosci 2(12):831–836
Malhi Y (2010) The carbon balance of tropical forest regions, 1990–2005. Curr Opin Sustain 2(4):237–244
Malhi Y et al (2004) The above-ground coarse wood productivity of 104 Neotropical forest plots. Glob Chang Biol 10:563–591
Malhi Y et al (2006) The regional variation of aboveground live biomass in old-growth Amazonian forests. Glob Chang Biol 12(7):1107–1138
Malhi Y, Aragao LEOC, Galbraith D, Huntingford C, Fisher R, Zelazowski P, Sitch S, McSweeney C, Meir P (2009) Exploring the likelihood and mechanism of a climate-change-induced dieback of the Amazon rainforest. Proc Natl Acad Sci U S A 106(49):20610–20615
MCT (Ministry of Science and Technology) (2010) Second National Communication of Brazil to the United Nations Framework Convention on Climate Change. Brasília 2 v. : il. col., map.; 30 cm. + 1 CD-ROM (4 3/4 in.)
Nobre CA, Sellers PJ, Shukla J (1991) Amazonian deforestation and regional climate change. J Clim 4:957–988
Nogueira EM, Fearnside PM, Nelson BW (2008a) Normalization of wood density in biomass estimates of Amazon forests. For Ecol Manag 256(5):990–996
Nogueira EM, Fearnside PM, Nelson BW, Barbosa RI, Keizer EWH (2008b) Estimates of forest biomass in the Brazilian Amazon: new allometric equations and adjustments to biomass from wood-volume inventories. For Ecol Manag 256(11):1853–1867
Ometto J, Aguiar A, Martinelli L (2011) Amazon deforestation in Brazil: effects, drivers and challenges. Carbon Manag 2(5):575–585
Phillips OL et al (2002) Increasing dominance of large lianas in Amazonian forests. Nature 48:770–774
Phillips OL et al (2004) Pattern and process in Amazon tree turnover, 1976–2001. Phil Trans R Soc Lond B 359: 381–407. doi:10.1098/rstb.2003.1438
Potter C, Klooster S, Genovese V (2009) Carbon emissions from deforestation in the Brazilian Amazon Region. Biogeosciences 6(11):2369–2381
Potter C, Klooster S, Hiatt C, Genovese V, Castilla-Rubio JC (2011) Changes in the carbon cycle of Amazon ecosystems during the 2010 drought. Environ Res Lett 6(3):034024
Quesada CA, Lloyd J, Anderson LO, Fyllas NM, Schwarz M, Czimczik CI (2011) Soils of amazonia with particular reference to the RAINFOR sites. Biogeosciences 8:1415–1440

Ramankutty N, Gibbs HK, Achard F, Defriess R, Foley JA, Houghton RA (2007) Challenges to estimating carbon emissions from tropical deforestation. Glob Chang Biol 13(1):51–66

Saatchi SS, Houghton RA, Dos Santos Alval RC, Soares ÁJV, Yu Y (2007) Distribution of aboveground live biomass in the Amazon basin. Glob Chang Biol 13(4):816–837

Saatchi SS et al (2011) Benchmark map of forest carbon stocks in tropical regions across three continents. Proc Natl Acad Sci U S A 108(24):9899–9904

Spracklen DV, Arnold SR, Taylor CM (2012) Observations of increased tropical rainfall preceded by air passage over forests. Nature 489(7415):282–285

Strassburg BBN et al (2010) Global congruence of carbon storage and biodiversity in terrestrial ecosystems. Conserv Lett 3(2):98–105

Vieira S, Trumbore S, Camargo PB, Selhorst D, Chambers JQ, Higuchi N, Martinelli LA (2005) Slow growth rates of Amazonian trees: consequences for carbon cycling. Proc Natl Acad Sci U S A 102(51):18502–18507

Werth D, Avissar R (2002) The local and global effects of Amazon deforestation. J Geophys Res 107:8087. doi: 10.1029/2001JD000717

DOI 10.1007/978-3-319-15901-0_8
Reprinted from *Climatic Change* Journal, DOI 10.1007/s10584-013-1040-9

Regional spatial inventories (cadastres) of GHG emissions in the Energy sector: Accounting for uncertainty

Khrystyna Boychuk · Rostyslav Bun

Received: 2 January 2013 / Accepted: 19 December 2013 / Published online: 1 February 2014
© Springer Science+Business Media Dordrecht 2014

Abstract An improvement of methods for the inventory of greenhouse gas (GHG) emissions is necessary to ensure effective control of commitments to emission reduction. The national inventory reports play an important role, but do not reflect specifics of regional processes of GHG emission and absorption for large-area countries. In this article, a GIS approach for the spatial inventory of GHG emissions in the energy sector, based on IPCC guidelines, official statistics on fuel consumption, and digital maps of the region under investigation, is presented. We include mathematical background for the spatial emission inventory of point, line and area sources, caused by fossil-fuel use for power and heat production, the residential sector, industrial and agricultural sectors, and transport. Methods for the spatial estimation of emissions from stationary and mobile sources, taking into account the specifics of fuel used and technological processes, are described. Using the developed GIS technology, the territorial distribution of GHG emissions, at the level of elementary grid cells 2 km×2 km for the territory of Western Ukraine, is obtained. Results of the spatial analysis are presented in the form of a geo-referenced database of emissions, and visualized as layers of digital maps. Uncertainty of inventory results is calculated using the Monte Carlo approach, and the sensitivity analysis results are described. The results achieved demonstrated that the relative uncertainties of emission estimates, for CO_2 and for total emissions (in CO_2 equivalent), depend largely on uncertainty in the statistical data and on uncertainty in fuels' calorific values. The uncertainty of total emissions stays almost constant with the change of uncertainty of N_2O emission coefficients, and correlates strongly with an improvement in knowledge about CH_4 emission processes. The presented approach provides an opportunity to create a spatial cadastre of emissions, and to use this additional knowledge for the analysis and reduction of uncertainty. It enables us to identify territories with the highest emissions, and estimate an influence of uncertainty of the large emission sources on the

This article is part of a Special Issue on "Third International Workshop on Uncertainty in Greenhouse Gas Inventories" edited by Jean Ometto and Rostyslav Bun.

Electronic supplementary material The online version of this article (doi:10.1007/s10584-013-1040-9) contains supplementary material, which is available to authorized users.

K. Boychuk · R. Bun (✉)
Lviv Polytechnic National University, Bandery str., 12, Lviv 79013, Ukraine
e-mail: rbun@org.lviv.net

R. Bun
Academy of Business, Cieplaka str., 1c, Dąbrowa Górnicza 42300, Poland

uncertainty of total emissions. Ascribing emissions to the places where they actually occur helps to improve the inventory process and to reduce the overall uncertainty.

1 Introduction

Uncertainty estimation is an integral part of a multifaceted process of greenhouse gas (GHG) inventory. A high quality of uncertainty estimates for a GHG inventory is crucial for the implementation of mechanisms under the Kyoto Protocol (such as Emissions Trading, the Clean Development Mechanism and Joint Implementation), as well as for establishing new treaties of environmental protection (Jonas et al. 2014). The importance of this problem is increasing because scientists have outlined a target so that the average global temperature should not increase by more than 2°C from its pre-industrial level. Therefore, the uncertainty of the GHG inventory is an important part of the general problem of uncertainty underlying climate change (Yohe and Oppenheimer 2011).

International agreements regarding the reduction of GHG emissions operate with estimates of emission and absorption on a country scale, and therefore uncertainty estimates of total emissions at country level are of great interest (Winiwarter 2007). However, these uncertainties are not constant, and change constantly (Lesiv et al. 2014). The main two factors of uncertainty changes in relative terms are 'knowledge increase' and structural changes in GHG emissions. Therefore, increasing knowledge on uncertainty and on reasons for its change is very important for reducing uncertainties in GHG inventories, and setting realistic emissions targets (Lesiv 2011).

Moreover, for governmental bodies it is desirable to possess an effective tool, enabling the analysis of the separate constituents of complex processes of GHG emissions and absorptions, both at regional (Feliciano et al. 2013), as well as at spatial levels (Hamal 2009; Mendoza et al. 2013). Such a tool would give the possibility of obtaining integrated information on the actual spatial distribution of GHG sources and sinks, and thus of finding optimum ways of solving a number of economic or environment protection problems (Bucki 2010; Bun et al. 2010). Spatial analysis of GHG emissions provides very important information about actual location of anthropogenic sources of emissions at the regional level. Corresponding regions, or large-scale point emission sources with the greatest influence on overall emissions, can be identified, and investments decreasing the uncertainty in input data should increase mainly in these sources. Therefore, referring emissions to the places where they actually occur provides the opportunity to greatly improve the inventory process, and reduce the uncertainty of the overall inventory. This provides very useful opportunities for analysing the separate constituents of inventory results' uncertainty (Uvarova et al. 2014), using specialised techniques for uncertainty estimations (Joerss 2014) or spatial resolution improvement (Horabik and Nahorski 2014; 2010), and helps to find the most efficient ways for reducing uncertainty (Jonas et al. 2010; Nahorski et al. 2007).

This article discusses the bottom-up inventory of GHG emissions in the energy sector. The approaches to achieving geo-referenced cadastres of emissions are described, and methods of uncertainty reduction are presented. The main idea of the approach is to carry out a spatial cadastre of emissions, and to use the additional information on spatial distribution of emissions for uncertainty abatement.

2 GHG spatial inventory

In principle, the approach and methods for the spatial analysis of greenhouse gas emissions presented in this article can be applied to any region. As an example, techniques to analyse and

create spatial emission inventories for the region of Western Ukraine are used in this article. The study area is described in the supplementary material in (see Online Resource 1).

The results of the spatial inventory of GHG emissions contain the emission data for a certain time period, and additional information on geographical coordinates. For climatic models, and for the analysis of the territorial distribution of total emissions, it is desirable to operate with emission estimates at the level of elementary plots of equal, possibly small, areas. The size of a grid cell depends on the purpose of the inventory and on the total size of the territory under investigation. For example, dividing the territory into 30 km×30 km cells is reasonable for a large country, but such cells wouldn't properly reflect the emission distribution in the case of an inventory for a single city or administrative region.

The spatial inventory of GHG emission consists of the following steps: (i) carrying out an inventory for each grid cell, and for each category of activity using the 'bottom-up' approach; and (ii) summing up the inventory results for all activity subsectors. The GHG emissions of a certain economic activity in a single grid cell are, in turn, a sum of emissions from all the emission sources, which are fully or partially located within borders of this grid cell. In order to build a spatial cadastre of a particular gas emission, one calculates the specific emissions (emission per unit area) of this gas on each grid cell. Such specific emission values are calculated using the parameters and data which define the emission process for selected activity, also taking into account the geographical location of the emission sources; that is, for each category of anthropogenic activity characterised by relevant emission coefficients, the specific emission of GHG can be presented as a function of activity intensity in a certain territory (geographical coordinates) and time period.

2.1 Point, line and area emission sources

According to the internationally approved methodology of GHG emission inventory, the energy sector, or any other sector, consists of a number of subsectors, which in turn may be divided further into separate emission source groups (IPCC 2006). Within a separate grid cell, the dissimilar emission sources are located: large and small in size; mobile and stationary etc. (see Fig. 1).

To carry out a spatial analysis, it is reasonable to categorise all emission sources into three groups: line, area, and large-scale point sources. Approaches to modelling GHG emissions differ significantly among these.

Large emission sources with significant emissions and relatively small area are treated as large-scale point sources. For example, power stations, large industrial installations, as well as refineries, belong to this group. In the case of an inventory carried out for administrative regions, units or a country as a whole, these emission sources are introduced as large-scale point sources.

Large-scale point sources need to be localised precisely in the territory. Their corresponding emissions need to be positioned directly to the point in space, using geographical coordinates. The approach requires the following information to be available for each plant: activity data (e.g. amount of fuel used in technological process; amount of industrial production sold etc.), and additional parameters influencing emission coefficients (e.g. age and productivity of equipment on a plant; chemical characteristics of fuel used; detailed information on technological processes; efficiency of emission control equipment etc.).

The line emission sources include the sources which are represented in the form of lines. Roads, railways, oil and gas pipelines are treated as line emission sources. These emission sources are divided into sections, using the grid cells that overlap the road or pipeline network.

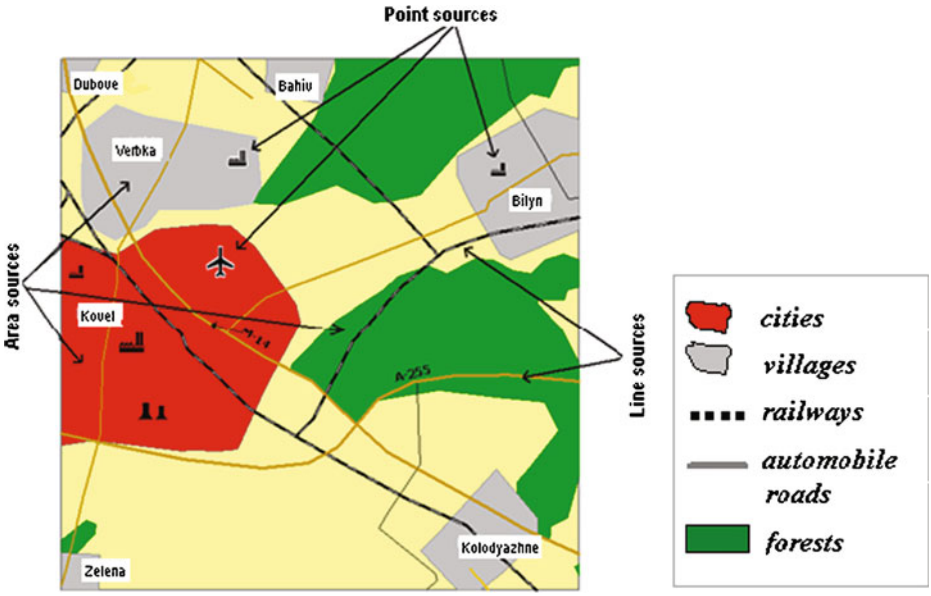

Fig. 1 Example of classification of GHG emission sources in separate grid cells, divided into three types of sources: large-scale point sources, line and area sources

Furthermore, for each fragment of line, the corresponding emissions are calculated taking into account a number of parameters. These parameters include: road category; daily or annual traffic capacity; distance from settlements for road segments; presence of railway stations or other objects for railways etc.

The area sources encompass the sources where emissions occur from a surface occupying a certain area. Agricultural fields, forests, oceans, seas etc. are examples of area emission/absorption sources. It is reasonable to also include in this group the territories where a large number of small point or line emission sources are concentrated. For instance, in this paper, the area sources also encompass the urban road network, because of the high density of roads and streets. Other examples include households, territories where agricultural and building work is conducted, small enterprises and plants, small boiler plants, as well as territories where coal, oil or gas are extracted etc.

The spatial approach for GHG inventory takes into account a number of specific features, such as: economic activity for rather small territories; methods and technologies of fossil-fuel combustion in different economic sectors; technological specificity of extraction and refinement of primary fuels; availability and efficiency of cleaning installations etc. Therefore, in comparison to a 'traditional' GHG inventory, based on aggregated emission data for the whole country, the spatially referenced inventory may have a significant impact on the accuracy of the total emission estimates (Bun et al. 2010).

2.2 Main objects of geo-referenced inventory

The presented approach requires the possibility to operate with administrative units and separate sources of emissions, such as geographical objects, which have their own set of properties, including geographical characteristics.

Let us define a set of geographic objects and some special operations, which will be used in this paper:

$\widetilde{O} = \{O_1, O_2, .., O_n\}$	is a set of all administrative regions (such as a province)
$\widetilde{R} = \{R_1, R_2, \ldots\}$	is a set of all small administrative regions (such as a district)
$\widetilde{N} = \{N_1, N_2, \ldots\}$	is a set of geographical objects, such as cities of direct regional subordination
$\widetilde{S} = \{S_1, S_2, \ldots\} = \left\{\widetilde{S}^{Urb}, \widetilde{S}^{Rur}\right\}$	is a set of settlements of all types
$\widetilde{S}^{Urb} = \left\{S_1^{Urb}, S_2^{Urb}, \ldots\right\}$	is a set of cities and towns
$\widetilde{S}^{Rur} = \left\{S_1^{Rur}, S_2^{Rur}, \ldots\right\}$	is a set of villages
$\widetilde{D} = \{D_1, D_2, \ldots\}$	is a set of geographical features, such as roads
$\Delta = \{\delta_1, \delta_2, \ldots\}$	is a set of geographical objects, such as elementary square areas dividing territory into cells — for example 2 km × 2 km — but are also limited by the regional border.

For the GHG spatial inventory, we should also identify some ratios over the geographical features. They will not be used further in the set-theoretic sense, but for a definition of territorial belonging and mutual placement of such objects.

For geographical objects A and B, let's define the following operations:

1) $A \widehat{\in} B$ – geographically, object A is located entirely within object B;
2) $A \widehat{\cap} B = C$ – object C is the common territory of objects A and B; and $C \neq O$, if the objects A and B have at least one common point on the boundary;
3) $A \widehat{\cup} B = C$ – object C is the territory that is formed by combining the territories of geographical objects A and B;
4) $A \widehat{-} B = C$ – object C is a territory that was formed after cutting-off the object B territory from the object A territory.

The following properties of geographic objects are also used: *area*(A) is the area of the object A; *len*(A) is the length of linear object A; *wid*(A) is the width of object A; and *dist*(A,B) is the distance between objects A and B.

2.3 Spatial inventory of GHG emissions from stationary sources

Emissions from stationary sources in the energy sector contain emissions from processes of heat and power production, oil refineries, heating of residential buildings and industry, as well as fugitive emissions from oil, gas and coal extraction processes (IPCC 2006). A common feature for all these sources is that emissions should be located directly in the place where they occur.

In the sectors of heat and power production, as well as in oil refinery processes, all the emission sources should be classified into two types: large-scale point sources; or small territorially dispersed sources (Hamal 2009). For each selected large point source, information has to be collected on fuel consumption, technology of fuel treatment, implemented emission control systems, age of equipment, chemical characteristics of fuel used etc. Based on this, GHG emissions are estimated and geocoded to the elementary cell, using the address of a plant (power stations, big boiler plants, refineries etc.). The total amounts of fuel, combusted in small dispersed sources (small power stations, boiler plants), are ascribed to settlement areas (area emission sources), where these sources are located, proportionally to consumers' presence or heat production.

The mathematical model of the G-th gas emission (carbon dioxide, methane, nitrous oxide etc.) for category 'Power and Heat Production' at the δ-th elementary cell is defined as the amount of emissions from corresponding point and area sources:

$$E^{G}_{En}(\delta) = \sum_{i=1}^{I_\delta}\sum_{f=1}^{F}\left[M_{i,f}{*}EF^{G}_{i,tech}(f)\right] + \\ + \sum_{s\in\left\{\widetilde{S}^{E}\bigcap\delta\right\}} \frac{\sum_{f=1}^{F}\left(M^{En}_{R,f}-\sum_{i=1}^{I_\delta}M_{i,f}\right){*}Q(s){*}EF^{G}_{En}(f)}{\sum_{k\in\left\{\widetilde{S}^{E}\bigcap R\right\}}Q(k)}; R=\left\{R\in\tilde{R}\wedge\delta\in R\right\},$$

where R is the administrative region/district, where the δ-th elementary cell is located; I_δ is the number of point emission sources in the elementary cell belonging to the category 'Power and Heat Production'; F is the number of fossil fuel types; $M_{i,f}$ and $M^{En}_{R,f}$ are consumption of the f-th type of fuel, respectively by the i-th point source, and at the region in total; $\widetilde{S}^{E}\in\widetilde{S}^{Urb}$ is a set of urban settlements, where big power or heat plants are located; $Q(x)$ is the number of residents in the geographical object x; $EF^{G}_{i,tech}(f)$ and $EF^{G}_{En}(f)$ are the emission factors of the G-th gas from combustion of the f-th type fuel, respectively, on the i-th power plant, taking into account technological process specifics, and the average rate for all small heat and power plants; and index En reflects belonging to the sector 'Power and Heat Production'.

As an example, the total specific emissions of carbon dioxide from burning coal, natural gas and other fossil fuels for electricity and heat production, in the Lviv region of Ukraine, are presented in a form of 3D thematic map in Fig. 2 (21.8 ths.km^2 area, 20 administrative districts). For better visual representation, the highest column, corresponding to the Dobrotvirska power station has been cut out from the map. Its emission is so high that makes it impossible to display differences in emissions from other sources.

In the residential sector, households constitute small and territorially dispersed emission sources. In the models for this sector, the sources are represented by territories of settlements, and are classified as area sources. For most cities, accurate statistics on fuel usage in the residential sector are available, and the data can be directly related to the city territory. The remaining fuel is distributed among settlements, based on fuel type, settlement type, population density, parameters of average fuel usage for certain types of settlement in rural and urban territories etc.

Mathematical models and spatial inventory results for residential and other sectors are available as supplementary material (see Online Resource 1).

2.4 Spatial inventory of GHG emission from mobile sources

Emissions from all types of transport refer to GHG emissions from mobile sources. During fuel combustion in transport, the direct-acting GHG emissions occur; that is carbon dioxide, methane, nitrous oxide etc.

In the sector of road transportation, automobiles are the source of emissions. Since the investigation of emissions from each vehicle is not feasible in practice, it is reasonable to treat

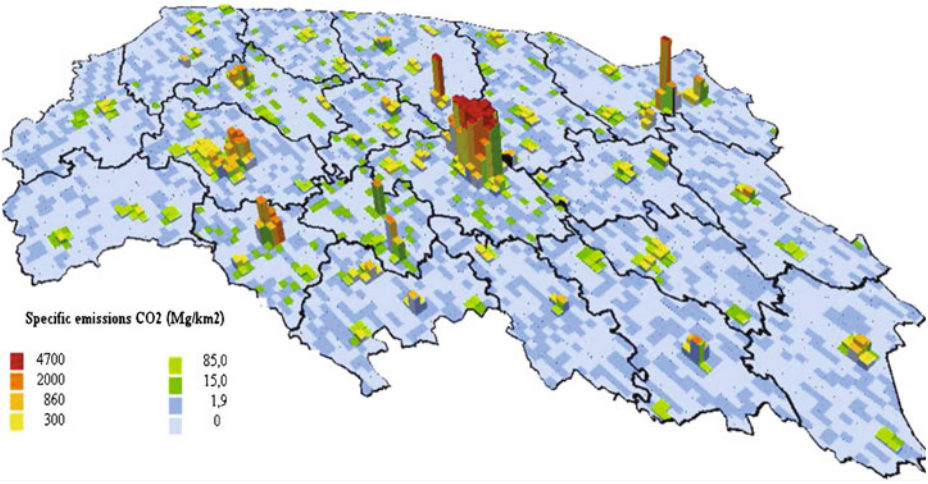

Fig. 2 Total specific emissions of carbon dioxide from burning all types fossil fuels in sector 'Power and Heat Production', at the level of elementary cells 2 km×2 km, Lviv region, 2008

roads and highways as GHG emission sources. According to the classification presented in Section 2.1, roads and highways belong to line emission sources. However, the urban road network is treated as an area source because of very high density, and only main urban roads are treated separately as line sources.

Statistical information on fossil-fuel usage in the road transport sector is available for the level of administrative units and cities from the yearbooks of fuel statistics (TSLR 2009). Other parameters, which will be used in the present model are available from statistical publications containing transport statistics, and from summarising yearbooks. In Ukraine, the input data for the GHG inventory are available either at the level of administrative regions and cities, or at the level of the province as a whole, depending on the administrative province.

In general, the level of GHG emissions in a certain grid cell depends on the amount of fuel consumed by transport within the cell borders. That is, prior to the spatial GHG emission inventory from the road transport, it is necessary to disaggregate the amount of fossil fuel used by transport to concrete emission sources, and to multiply the fuel quantity with the corresponding emission factors, in order to obtain emission estimates for a certain GHG. All the fuel used within an urban road network in a region is disaggregated directly to the territories of cities and suburban areas around cities. Therefore, the suburban territories of three levels are built around administrative borders of each city: $Z^0(i)$ is a territory of the i-th city; the first suburban territory $Z^1(i)$ (the first buffer zone) has a width of half the radius of the city area; the second zone $Z^2(i)$ has one radius; and the third zone $Z^3(i)$ has a radius of one and a half parts of the city radius. Then $\widetilde{Z} = \left\{Z^1(i), i \in \widetilde{S}^Z\right\} \cup \left\{Z^2(i), i \in \widetilde{S}^Z\right\} \cup \left\{Z^3(i), i \in \widetilde{S}^Z\right\}$ is a set of analysed buffer zones around the cities, with more intensive automobile traffic. Here, $Z^n(i)$ is the n-th level zone for the i-th city, and $\widetilde{S}^Z \subset \widetilde{S}$ is a set of cities, the buffer zones for which have been built.

For big cities, the corresponding fuel consumption in the transport sector is gathered, and the data is located directly in the territory of the city and surrounding suburban areas. For small cities, the disaggregation of fuel used in transport is made proportional to population density.

The rest of fuel used in the transport sector in a region is divided among the automobile roads of a region (including main roads within settlements), according to the developed algorithms. The algorithms take into account the length and width of each road segment, its capacity and current state. In accordance with the above approach, the part of fuel (60 %), which was bought in a region, is used (burnt) within settlements borders, for the needs of internal transport. Moreover, it is assumed that, for cities, this part of fuel is divided additionally on automobile roads in suburban territories, located within a certain distance from the administrative borders of the settlement (zones Z^0, Z^1, Z^2, Z^3 in proportion 40 %, 10 %, 6 %, 4 %, accordingly). The rest of the fuel (40 %) is assumed to be used outside the settlements, and is appointed to the road segments according to the road maps. The values of these coefficients are based on specific statistical data of automobile traffic (TSLR 2009), and on expert opinion.

Emissions for each source type (area and line sources) are calculated using the bottom-up approach. The quantity of a certain fuel type (diesel, gasoline etc.) is multiplied by the corresponding emission factor. Using the above assumptions, the emissions of carbon dioxide per year in the city S (or in a suburban zone built around it for $S \in \widetilde{S}^Z$), which belong to the administrative district R, are modelled with the formula:

$$E_{Tr}^{CO_2}[Z^n(S)] = \sum_{b=1}^{B} \sum_{t=1}^{T} \sum_{f=1}^{F} \left[\frac{M_b^O(f,t) \cdot P^R(f,t,b)}{P^O(f,t,b)} \cdot EF_{Tr}^{CO_2}(f) \right] \cdot \frac{Q(S)}{\sum_{s \in \widetilde{S}^R} Q(s)} C_n;$$

$$n = \overline{0,3}; \quad O = \left\{ O \in \widetilde{O} \wedge S \widehat{\in} O \right\}; \quad R = \left\{ R \in \widetilde{R} \wedge S \widehat{\in} R \right\}; \quad \widetilde{S}^R = \left\{ \widetilde{S} \widehat{\cap} R \right\},$$

where $E_{Tr}^{CO_2}[Z^n(S)]$ is the emission of carbon dioxide in the settlement S (if n=0) or in one of the conventionally constructed buffer zones around S (n=1,2,3); $M_b(f,t)$ is the amount of the f-th type fuel used for vehicles of the t-th type, owned by b; $P(f,t,b)$ is the indicator used for the disaggregation of the total regional (like province) fuel consumption of the f-th type for the t-th type of vehicle, owned by b, at the level of administrative regions/district (such as mileage of cars using gasoline; diesel fuel sales through service stations; distribution of the number of cars in administrative units; the number of gas filling stations etc.); $Q(s)$ is the number of habitants in settlement s; $EF_{Tr}^{CO_2}(f)$ is the emission factor for carbon dioxide, which depends on the type of fuel burnt; C_n is the coefficient, which reflects the proportion of fuel sold in the city for transport activity, in the n-th zone of this city; O and R are, respectively, provinces and regions/districts, where the city is located; B is the number of vehicle ownership types; F is the number of fossil fuel types (gasoline, diesel, etc.); T is the number of vehicle types (motor cars, buses, etc.); index Tr indicates that the corresponding parameters belong to the road transport sector.

For cities of province/regional subordination, the relevant statistical data about the consumption of fuel for transport activity are reflected separately in statistical reports. Hence for the needs of the spatial inventory, they can be ascribed directly to the territory of city and its suburban zones, in accordance with accepted ratios. For n-th suburban zone Z^n of the city N with regional subordination, the carbon dioxide emissions can be calculated by the formula:

$$E_{Tr}^{CO_2}[Z^n(N)] = \sum_{b \in B} \sum_{t \in T} \sum_{f \in F} \left[M_b^N(f,t) \cdot EF_{Tr}^{CO_2}(f) \right] \cdot C_n, n = \overline{0,3}$$

where $M_b^N(F,T)$ is an amount of the f-th type fuel used in the N-th city of regional subordination, for transport activity of the t-th type vehicles, owned by b.

For any section of the road d, the coefficient $C_{total}(d)$ is determined, which describes the status and parameters of this road section, and has the following form:

$$len(d)\ C\ [k(d), wid(d)]\ Cond(d),$$

where $len(d)$ is the total length of the road d, $C[k(d),wid(d)]$ is the coefficient of the road d capacity, that depends on the road width $wid(d)$ and category (or type) $k(d)$; $Cond(d)$ is the coefficient of a road current state (road is used, $Cond(d)=1$; at the stage of repair or construction, or is unusable for any other reasons, $Cond(d)=0$).

For the purpose of emission analysis, the road network is divided into sections within the borders of administrative districts and suburban zones $\widetilde{S}^z$, located around the cities. The set of zones that includes a corresponding section of the road, can be marked as $\widetilde{Z}_d = \left\{ z \in \widetilde{Z} d \in Z \right\}$. It should be noted that the zones of zero order — i.e. territories of the cites — do not belong to this set.

Modelling of carbon dioxide emissions on the road section $D \in \widetilde{D}$ located within the region R is performed with the formula:

$$E_{Tr}^{CO_2}(D) = \sum_{b=1}^{B} \sum_{t=1}^{T} \sum_{f=1}^{F} \left[\frac{M_b^O(f,t) \cdot P^R(f,t,b)}{P^O(f,t,b)} \cdot EF^{CO_2}(f) \right] \cdot \frac{C_{total}(D)}{\sum_{d \in \widetilde{D}^R} C_{total}(d)} +$$

$$+ \sum_{z \in \widetilde{Z}_D} \frac{E^{CO_2}(z) \cdot C_{total}(D)}{\sum_{i \widehat{\in} z} C_{total}(i)}; \quad O = \left\{ O \in \widetilde{O} \wedge D \widehat{\in} O \right\}; \ R = \left\{ R \in \widetilde{R} \wedge D \ \widehat{\in} \ R \right\}; \ \widetilde{D}^R = \widetilde{D} \cap R,$$

where $E_{Tr}^{CO_2}(D)$ are the carbon dioxide emissions on the road D section; $M_b(f,t)$ is the amount of the f-th type fuel, used by the t-th type vehicles, owned by b; $P(f,t,b)$ is the indicator used for the disaggregation of the total regional (like province) consumption of fuel of the f-th type for the t-th type vehicle, owned by b, at the level of administrative regions/district; $C_{total}(D)$ is the parameter of a road D, that determines its capacity; $EF_{Tr}^{CO_2}(f)$ is the emission factor for carbon dioxide, that depends on the type of fuel burnt; O and R are provinces/regions and districts, respectively, in which a corresponding segment of the road D is located.

At the level of the elementary plot (i.e. grid cells level), all the emission sources of the transport sector are analysed (the territories of settlements and roads), which are partially or completely located within the corresponding grid cell. Therefore, the total emissions for the line and area sources can be found:

$$E_{Tr}^{CO_2}(\delta) = \frac{1}{2} \left[\sum_{s \in \widetilde{S}} \frac{E_{Tr}^{CO_2}(s) \cdot area\left(s \widehat{\cap} \delta\right)}{area(s)} + \sum_{d \in \widetilde{D}} \frac{E_{Tr}^{CO_2}(d) \cdot len\left(d \widehat{\cap} \delta\right)}{len(d)} \right],$$

where $E^{CO_2}(x)$ is the carbon dioxide emission, caused by a corresponding geographical object x; $area(x)$ is the object x area; $len(x)$ is the length of a linear object x; and δ is the elementary plot (grid cell).

Spatial inventory of gases other than the carbon dioxide, as well as emissions from off-road and railway transport, is described in the supplementary material (see Online Resource 1). As an example of spatial analysis results, the specific emissions of CO_2 from gasoline combustion by road vehicles of firms (not private cars) for the western regions of Ukraine, are presented in a form of 3D thematic map, in Fig. 3.

Based on the approaches presented in (Hamal 2008), the geo-information system is developed for a practical implementation of algorithms for the geo-spatial inventory of GHG emissions, automatic creation of digital maps, visual analysis of obtained results, and

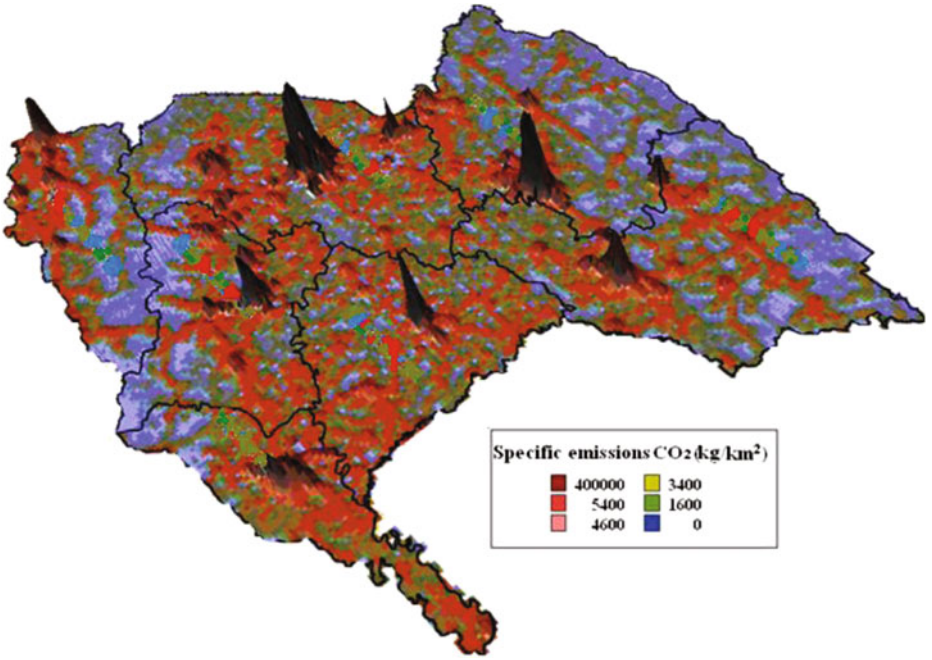

Fig. 3 Specific emissions of CO_2 from gasoline combustion by road vehicles of firms in Western Ukraine regions (kg/km^2, 2 km×2 km grid cells, 2009)

for uncertainty analysis. This geo-information system is described in the supplementary material (see Online Resource 1). The results may be visualised as digital maps with various thematic layers (see Fig. 4 as an example).

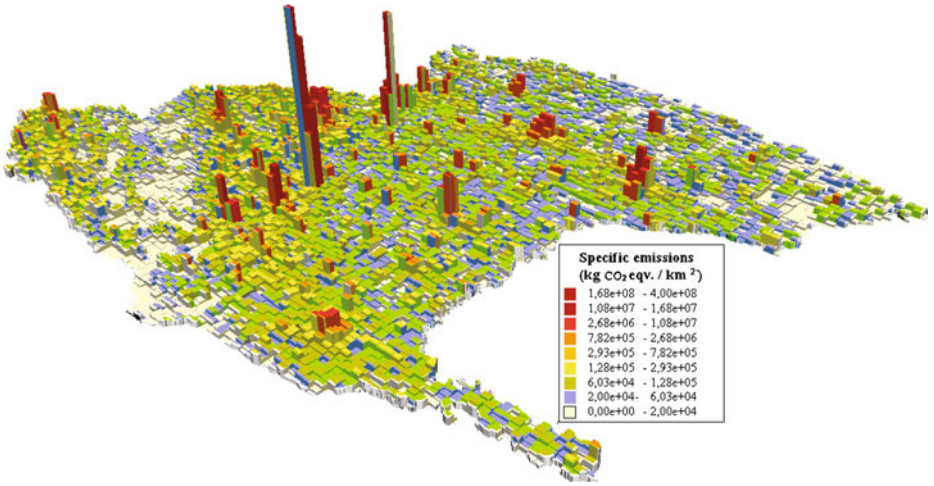

Fig. 4 Prism map of specific direct-acting GHG emissions, summarised by all subsectors of the energy sector for Western Ukraine regions (2009, 4 km×4 km; CO^2-eqv., kg/km^2; owing to incompatibly high emission rates at Burshtyn and Dobrotvir power plants the scale of power 0.4 is used for visualisation)

3 Uncertainty evaluation and sensitivity analysis

Uncertainty of GHG emissions represents a lack of knowledge about the true value of emissions for a certain area. Uncertainties resulting from the assessment of GHG emissions depend largely on the method used, the quality of input data, uncertainties from expert judgements etc. (IPCC 2006).

Increasing knowledge about the investigated process can help to decrease uncertainties (Marland et al. 2009). Therefore, compared to a traditional inventory on the scale of the whole country, spatially referenced emissions have additional parameters: geographical coordinates. This provides new possibilities of analysis and uncertainty reduction. The introduction of new independent information about GHG emission processes, for separate emission sources or groups of sources, leads to a decrease in uncertainty of the total results (Winiwarter 2007).

The verification of spatial emissions disaggregation is described in supplementary material (see Online Resource 1), but uncertainty evaluation and sensitivity analysis is presented below.

Total uncertainty of emission modelling depends on uncertainties of all the input parameters. These uncertainties may be combined into a total uncertainty estimate of inventory results using the statistical tools specified in (IPCC 2006). For such an analysis it is important to have independent uncertainty ranges for emission coefficients, statistical data and other parameters of inventory process (Bun 2009).

In calculations, 'national' uncertainty ranges were used mainly for statistical data, emission coefficients and net calorific values. When the 'national' data were missing, the default IPCC uncertainty ranges were implemented. In the first step, the spatial results of emissions in each category, at the scale of 2 km×2 km, were summarised to a subregional level. Then the uncertainty ranges were estimated for all subsectors and greenhouse gases at the subregional level, using the Monte Carlo procedure. In the next step, these results were used as input data for uncertainty range estimates for the main subsectors in the Western Ukraine, also using the Monte Carlo method. Table 1 contains modelling results of emissions and uncertainty ranges by GHGs, and by economic sectors for Western Ukraine, in 2008.

Table 1 Uncertainty estimates of GHG emissions by economic subsectors (Western Ukraine, 2008)

Sector	Emissions Uncertainty	CO_2	CH_4	N_2O	Total emissions, CO_2 eqv.
Heat & power production, refinery	E (Gg)	20027,0	0,287	0,286	20122,1
	U(%)	−8.99..+9.45	−31,7.+0.46,74	−68,37..+160.3	−9,02..+9,48
Industry	E (Gg)	1731,5	0,067	0,011	1736,2
	U(%)	−6,61..+6.85	−42,33.+0.66,34	−58,97..+123.3	−6,62..+6,85
Road transport	E (Gg)	5191,5	1,867	0,332	5332,8
	U(%)	−5,65..+5.71	−38,33.+0.61,64	−42,97..+69.3	−5,72..+5,81
Railway and off-road transport	E (Gr)	730,5	0,123	0,315	830,5
	U(%)	−12,35..+12.36	−34,72..+51,64	−58,87..+112.9	−14,53..+17,91
Residential	E (Gg)	8135,1	2,281	0,039	8195,0
	U(%)	−11,44..+11.92	−48,92..+81,64	−62,87..+128.9	−11,47..+11,94
Oil, gas, coal extraction	E (Gg)	34,02	43,431	0,0012	946,43
	U(%)	−78,94..+81.72	−45,82..+48,54	−92,87..+328.9	−44,47..+46,94

Uncertainty ranges of total GHG emissions from the energy sector in the territory of Western Ukraine are as follows:

- for CO_2: – 5.76 %..+6.02 %;
- for CH_4: – 41.45 %..+44.28 %;
- for N_2O: – 36,93 %..+60.12 %;
- for total emissions taking into account Global Warming Potential factor: −5.74 %..+ 5.97 %.

The highest uncertainty of total emissions is noted for the processes of coal, gas and oil extraction, for transport (with the exception of road transport), and for the residential sector (Table 1). Relatively high uncertainties refer to emissions in the sector of heat and power production, mainly as a result of the domination of solid fuel.

Furthermore, the sensitivity of uncertainty in total emissions to the change of uncertainties in input parameters is investigated. The considered input parameters include: statistical data on economic activity; calorific values; and emission coefficients. Fig. 5 shows the results of analysis and sensitivity graphics of uncertainties of emission estimates for the improvement of accuracy of input parameters as a percentage *P*.

The results show that the relative uncertainty in emission estimates for both CO_2 and total emissions in CO_2 equivalent depends largely on uncertainty in the statistical data, and on uncertainty for calorific values of fuel. Uncertainty for total emissions stays almost the same with the change of uncertainty in N_2O emission coefficients, and it is hardly correlated with an

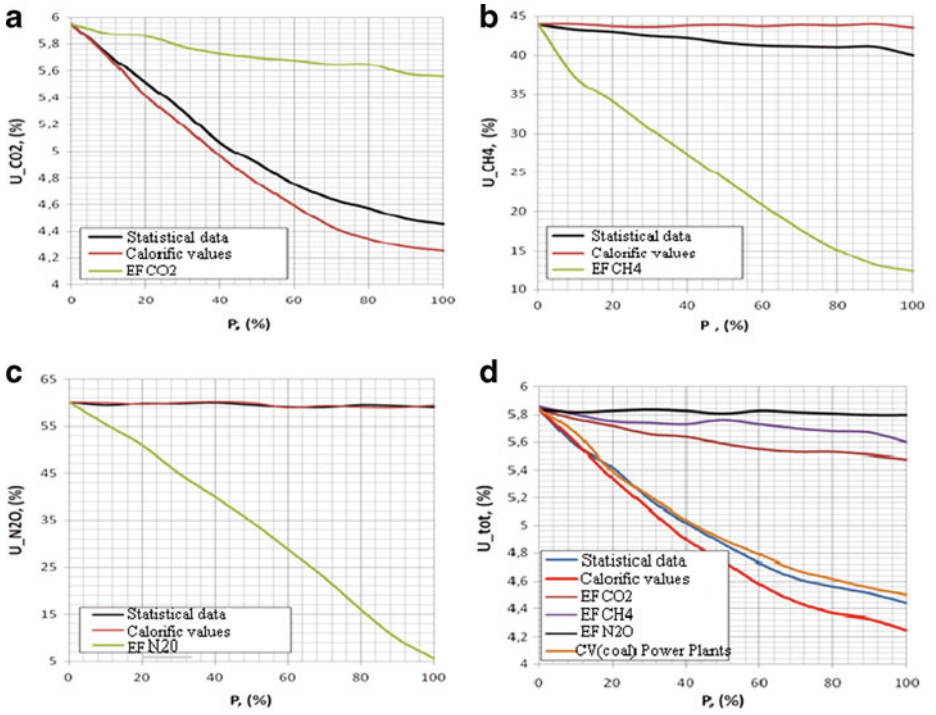

Fig. 5 Dependence of total uncertainty of emission estimates on the changes of uncertainty (on *P* %) of input parameters of inventory (Monte Carlo approach): **a** CO_2; **b** CH_4; **c** N_2O; **d** total emissions

improvement in knowledge about CH_4 emission processes. For example, with the reduction by half of uncertainty in CH_4 emission coefficients, the uncertainty of total inventory results stays almost unchanged. On the other hand, the uncertainty in overall CH_4 emissions changes from 44 % to 24 %. A similar situation is revealed in the case of the reduction by half of uncertainty in N_2O emission coefficients. The overall uncertainty of inventory results for all the direct-acting GHGs doesn't change, but there is a considerable reduction of N_2O emission uncertainty, from 60 % to 35 % (the upper bounds of 95 % confidence intervals).

To summarise, despite large uncertainties in CH_4 and N_2O emission coefficients, the improvement in their accuracy has no significant impact on the uncertainty reduction of total emissions in CO_2 equivalent. The most efficient way of reducing uncertainty is by improving the accuracy of statistical data on fuel statistics and calorific values.

In the energy sector, a reduction by half of uncertainty in the statistical data leads to a reduction of uncertainty in total emissions from 5.84 % to 4.87 %. An equivalent reduction of calorific value uncertainty leads to a reduction of overall uncertainty, to 4.75 %. Moreover, improvement only in the accuracy of physical and chemical characteristics of coal used in the power plants of Western Ukraine has a significant impact on a reduction of uncertainty in the overall GHG emission cadastre.

4 Conclusions

The spatial analysis of GHG emissions provides important information about the actual location of the main anthropogenic emissions at the regional level. This approach provides an opportunity to carry out a spatial cadastre of emissions, and to use this additional knowledge for the analysis and reduction of uncertainty. Therefore, it enables us to analyse separate constituents of the complex processes of GHG emission and absorption, and also to obtain integrated information on the spatial distribution of the GHG sources. It also provides very useful opportunities for analyzing the distinct components of inventory uncertainty, using specialised techniques for uncertainty estimations, or the improvement of spatial resolution. Hence, in general, it helps to find the most efficient ways for uncertainty reduction.

A spatial integration of the geo-referenced inventory results for all the elementary plots (grid cells) yields a generalised result of the traditional inventory. The approach enables the identification of territories with the highest emissions, and estimates the influence of uncertainty from the large emission sources on the uncertainty of total emissions. Investments for the decrease of uncertainty in input data should be placed mainly in these sources. Therefore, ascribing emissions to the places where they actually occur helps to improve the inventory process and to reduce the overall uncertainty.

The results achieved for the western region of Ukraine demonstrated that the relative uncertainty of emission estimates for CO_2 and for total emissions (in CO_2 equivalent) depends largely on uncertainty in the statistical data, and on uncertainty in fuels' calorific values. The uncertainty of total emissions stays almost constant with the change of uncertainty of N_2O emission coefficients, and is hardly correlated with an improvement in knowledge about CH_4 emissions processes. Despite great uncertainties regarding CH_4 and N_2O emission coefficients, the improvement in their accuracy has no significant impact on the uncertainty reduction of total emissions in CO_2 equivalent. The most efficient way of reducing uncertainty is the improvement in the accuracy of data on fuel statistics and calorific values.

In conclusion, the geo-information technology of GHG spatial inventory at the regional level seems to be an effective tool to support decision-making regarding the considered problems of environmental protection.

Acknowledgments The study was conducted within the 7FP Marie Curie Actions IRSES project No. 247645, and was partially supported by Ministry of Education and Science of Ukraine.

References

Bucki R (2010) Modelling synthetic environment control. Artificial Intelligence 4:315–321

Bun A (2009) Methods and tools for analysis of greenhouse gas emission processes in consideration of input data uncertainty. Dissertation, Lviv Polytechnic National University

Bun R, Hamal KH, Gusti M, Bun A (2010) Spatial GHG inventory on regional level: Accounting for uncertainty. Climatic Change 103:227–244

Feliciano D, Slee B, Hunter C, Smith P (2013) Estimating the contribution of rural land uses to greenhouse gas emissions: A case study of North East Scotland. Environmental Science & Policy 25:36–49

Hamal K (2008) Carbon dioxide emissions inventory with GIS. Artificial Intelligence 3:55–62

Hamal Kh (2009) Geoinformation technology for spatial analysis of greenhouse gas emissions in Energy sector. Dissertation, Lviv Polytechnic National University

Horabik J, Nahorski Z (2010) A statistical model for spatial inventory data: a case study of N_2O emissions in municipalities of southern Norway. Climatic Change 103:263–276

Horabik J, Nahorski Z (2014) Improving resolution of spatial inventory with a statistical inference approach. This issue.

IPCC (2006) IPCC Guidelines for National Greenhouse Gas Inventories, Prepared by the National Greenhouse Gas Inventories Programme, Eggleston HS, Buendia L, Miwa K, Ngara T, Tanabe K (eds).

Joerss W (2014) Determination of the uncertainties of the German emission inventories for particulate matter and aerosol precursors using Monte-Carlo analysis. This issue.

Jonas M, White T, Marland G, Lieberman D, Nahorski Z, Nilsson S (2010) Dealing with uncertainty in GHG inventories: How to go about it? Lecture Notes in Economics and Mathematical Systems 633:229–245

Jonas M, Krey V, Wagner F, Marland G, Nahorski Z (2014) Uncertainty in an emissions constrained world. This issue.

Lesiv M (2011) Mathematical modeling and spatial analysis of greenhouse gas emissions in regions bordering Ukraine. Dissertation, Lviv Polytechnic National University

Lesiv M, Bun A, Jonas M (2014) Analysis of change in total uncertainty in GHG emissions for the EU-15 countries. This issue.

Marland G, Hamal K, Jonas M (2009) How uncertain are estimates of CO_2 emissions? Journal of Industrial Ecology 13:4–7

Mendoza D, Gurney K, Geethakumar S, Chandrasekaran V, Zhou Y, Razlivanov I (2013) Implications of uncertainty on regional CO_2 mitigation policies for the U.S. onroad sector based on a high-resolution emissions estimate. Energy Policy 55:386–395

Nahorski Z, Horabik J, Jonas M (2007) Compliance and emissions trading under the Kyoto protocol: Rules for uncertain inventories. Water, Air, and Soil Pollution: Focus 7(4–5):539–558

TSLR (2009) Transport Statistics of Lviv Region: Statistical Yearbook. Main Statistical Agency of Lviv Region, Lviv

Uvarova N, Paramonov S, Gytarsky M (2014) The improvement of greenhouse gas inventory as a tool for reduction emission uncertainties for operations with oil in the Russian Federation. This issue.

Winiwarter W (2007) National greenhouse gas inventories: understanding uncertainties versus potential for improving reliability. Water Air Soil Pollution: Focus 7:443–450

Yohe G, Oppenheimer M (2011) Evaluation, characterization, and communication of uncertainty by the intergovernmental panel on climate change – an introductory essay. Climatic Change 108:629–639

DOI 10.1007/978-3-319-15901-0_9
Reprinted from *Climatic Change* Journal, DOI 10.1007/s10584-013-1029-4

Improving resolution of a spatial air pollution inventory with a statistical inference approach

Joanna Horabik · Zbigniew Nahorski

Received: 2 January 2013 / Accepted: 1 December 2013 / Published online: 28 January 2014
© The Author(s) 2014. This article is published with open access at Springerlink.com

Abstract This paper presents a novel approach to allocation of spatially correlated data, such as emission inventories, to finer spatial scales, conditional on covariate information observable in a fine grid. Spatial dependence is modelled with the conditional autoregressive structure introduced into a linear model as a random effect. The maximum likelihood approach to inference is employed, and the optimal predictors are developed to assess missing values in a fine grid. An example of ammonia emission inventory is used to illustrate the potential usefulness of the proposed technique. The results indicate that inclusion of a spatial dependence structure can compensate for less adequate covariate information. For the considered ammonia inventory, the fourfold allocation benefited greatly from incorporation of the spatial component, while for the ninefold allocation this advantage was limited, but still evident. In addition, the proposed method allows correction of the prediction bias encountered for the upper range emissions in the linear regression models.

1 Introduction

The development of high-resolution emission inventories is essential for designing suitable abatement measures. Spatial distributions of emissions can serve as an input for atmospheric dispersion models, which in turn may produce concentration maps of pollutants contributing to the adverse health effects, like ammonia emissions. For other air pollutants, such as greenhouse gasses (GHG), spatial patterns become helpful in improving identification of distributed emission sources.

Numerous issues underlying preparation of spatially resolved GHG inventory were discussed e.g. in Boychuk and Bun (this issue), Bun et al. 2010 or Thiruchittampalam et al. 2010. In general, the task crucially depends on availability of spatially distributed activity data. For instance, at present in Poland the activity data relevant to GHG emissions can be obtained at a level of country regions (voivodships). Information of higher spatial resolution can be often obtained only for some proxy data related to GHG emissions, such as land use and linear emission sources. Recently, also nighttime lights observed by a satellite have been used for

This article is part of a Special Issue on "Third International Workshop on Uncertainty in Greenhouse Gas Inventories" edited by Jean Ometto and Rostyslav Bun.

J. Horabik (✉) · Z. Nahorski
Polish Academy of Sciences, Systems Research Institute, ul. Newelska 6, 01-447 Warsaw, Poland
e-mail: Joanna.Horabik@ibspan.waw.pl

more accurate estimation of spatial distribution of CO_2 emissions (Ghosh et al. 2010; Oda and Maksyutov 2011).

Typically, the regression models have been applied for spatial allocation of emission data (Dragosits et al. 1998; Oda and Maksyutov 2011). However, emissions in general tend to be spatially correlated, which provides opportunity for potential improvements. This idea motivated us to develop a more advanced approach for accurate disaggregation of air pollution data.

Making inference on variables at points or grid cells different from those of the data is referred to as the change of support problem (Gelfand 2010). Several approaches have been proposed to address this issue. The geostatistical solution for realignment from point to a real data is provided by block kriging (Gotway and Young 2002). Areal weighting offers a straightforward approach if the data are observed at a real units, and the inference is sought at a new level of spatial aggregation. Some improved approaches with better covariate modeling were also proposed e.g. in Mugglin and Carlin 1998 and Mugglin et al. 2000.

In this study we propose to apply methods of spatial statistics to produce higher resolution emission inventory data, taking advantage of more detailed land use information. The approach resembles to some extent the method of Chow and Lin (1971), originally proposed for disaggregation of time series based on related, higher frequency series. Here, a similar methodology is employed to disaggregate spatially correlated data.

Regarding an assumption on residual covariance, we apply the structure suitable for areal data, i.e. the conditional autoregressive (CAR) model. Although the CAR specification is typically used in epidemiology (Banerjee et al. 2004), it was also successfully applied for modelling air pollution over space (Kaiser et al. 2002; McMillan et al. 2010). Compare also Horabik and Nahorski (2010) for another application of the CAR structure to model spatial inventory of GHG emissions. The maximum likelihood approach to inference is employed, and the optimal predictors are developed to assess missing concentrations in a fine grid.

The application part of the study concerns an ammonia (NH_3) emission inventory in a region of Poland. Ammonia is emitted mainly by agricultural sources such as livestock production and fertilized fields. Its high concentrations can lead to acidification of soils, forest decline, and eutrophication of waterways. Ammonia emissions are also recognized for their importance in contributing to fine particulate matter; hence its spatial distribution is of great importance. However, agricultural emission sources cannot be measured directly, and spatial emission patterns need to be assessed otherwise. This issue was addressed, among others, by Dragosits et al. 1998, where agricultural and land cover data were used to disaggregate the national NH_3 emission totals across Great Britain. We demonstrate that the straightforward approaches based on linear dependences might be improved by introducing a spatial random effect.

Nevertheless, the proposed approach is of wider applicability, and can be used in numerous situations where higher resolution of spatial data is needed. In the context of the greenhouse gasses, the method might be particularly adequate to improve resolution of these activity data which tend to be spatially correlated. The plausible sectors include agriculture, transportation and forestry. Improved resolution may in turn contribute to reduction in uncertainties underlying GHG inventories.

2 Disaggregation framework

This section presents the statistical approach to the issue of spatial disaggregation. We have available data on a spatially distributed variable (inventory of emissions) integrated in a coarse grid. The aim is to estimate the distribution of this variable in a fine grid, conditional on some

explanatory variables observable in this grid. It is assumed that the variable of interest is spatially correlated. Its residual covariance structure is set and the conditional autoregressive model is applied. An additional important assumption of the method is that the covariance structure of the variable in a coarse grid is the same as that in a fine grid.

Below we specify the model and provide details on its estimation in the coarse grid as well as on prediction in the fine grid.

2.1 Model

Fine grid We begin with the model specification in a fine grid. Let Y_i denote a random variable associated with a missing value of interest y_i defined at each cell i for $i=1,...,n$ of a fine grid (n denotes the overall number of cells in a fine grid). Assume that each random variable Y_i follows the Gaussian distribution with the mean μ_i and variance σ_Y^2

$$Y_i|\mu_i \sim Gau\left(\mu_i, \sigma_Y^2\right). \tag{1}$$

Given the values μ_i and σ_Y^2, the random variables Y_i are assumed independent, thus the joint distribution of $\boldsymbol{Y}=(Y_1,..., Y_n)^{\mathrm{T}}$ conditional on the mean process $\boldsymbol{\mu}=(\mu_1,\ldots,\mu_n)^T$ is the Gaussian

$$\boldsymbol{Y}|\boldsymbol{\mu} \sim Gau_n\left(\boldsymbol{\mu}, \sigma_Y^2\boldsymbol{I}_n\right), \tag{2}$$

where $\boldsymbol{I}_n$ is the $n\times n$ identity matrix; the superscript $^{\mathrm{T}}$ stands for the transpose.

The mean $\boldsymbol{\mu}$ represents the true process underlying emissions, and the (missing) observations are related to this process through a measurement error with the variance σ_Y^2. The model for the mean process is formulated as a sum of the regression component with available covariates, and a spatially varying random effect. For this, the conditional autoregressive model is used. The CAR model is given through the specification of the full conditional distribution functions of μ_i for $i=1,...,n$ (Cressie 1993; Banerjee et al. 2004)

$$\mu_i|\boldsymbol{\mu}_{-i} \sim Gau\left(\boldsymbol{x}_i^T\boldsymbol{\beta} + \rho \sum_{\substack{j=1 \\ j\neq i}}^{n} \frac{w_{ij}}{w_{i+}}\left(\mu_j - \boldsymbol{x}_j^T\boldsymbol{\beta}\right), \frac{\tau^2}{w_{i+}}\right), \tag{3}$$

where $\boldsymbol{\mu}_{-i}$ denotes all elements in $\boldsymbol{\mu}$ but μ_i, w_{ij} are the adjacency weights ($w_{ij}=1$ if j is a neighbour of i and 0 otherwise, also $w_{ii}=0$); $w_{i+}=\sum_j w_{ij}$ is the number of neighbours of an area i; $\boldsymbol{x}_i$ is a vector containing 1 as its first element (for the intercept β_0) and k explanatory covariates of an area i as the next elements; $\boldsymbol{\beta}=(\beta_{\boldsymbol{0}},\beta_1, \ldots,\beta_k)^T$ is a vector of regression coefficients. For calculation of the adjacency weights we use the Queen Method, i.e. two cells are considered neighbours if they share a side or a vertex. The CAR structure follows an assumption of similar random effects in adjacent cells; this is reflected in the second summand of the conditional expected value of μ_i, which is proportional to the average values of remainders $\mu_j-\boldsymbol{x}_j^T\boldsymbol{\beta}$ for neighbouring sites (i.e. when $w_{ij}=1$). This proportion is calibrated with the parameter ρ. Thus ρ reflects the strength of spatial association. The variance of the full conditional distribution of μ_i is inversely proportional to the number of neighbours w_{i+}, and τ^2 is a variance parameter.

Given (3), the joint probability distribution of the process $\boldsymbol{\mu}$ is as follows, see e.g. Banerjee et al. (2004)

$$\boldsymbol{\mu} \sim Gau_n\left(\boldsymbol{X\beta}, \tau^2(\boldsymbol{D}-\rho\boldsymbol{W})^{-1}\right), \tag{4}$$

where $\boldsymbol{X}$ is the matrix whose rows are the vectors $\boldsymbol{x}_i^T$

$$\boldsymbol{X} = \begin{bmatrix} 1 & x_{11} & \cdots & x_{1k} \\ \vdots & \vdots & \ddots & \vdots \\ 1 & x_{n1} & \cdots & x_{nk} \end{bmatrix};$$

$\boldsymbol{D}$ is an $n\times n$ diagonal matrix with w_{i+} on the diagonal; and $\boldsymbol{W}$ is an $n\times n$ matrix with adjacency weights w_{ij}. Equivalently we can write (4) as

$$\boldsymbol{\mu} = \boldsymbol{X\beta} + \boldsymbol{\varepsilon}, \quad \boldsymbol{\varepsilon} \sim Gau_n(\boldsymbol{0}, \Omega), \tag{5}$$

where $\Omega=\tau^2(\boldsymbol{D}-\rho\boldsymbol{W})^{-1}$.

Coarse grid The model for a coarse grid (aggregated) observed data is obtained by multiplication of (5) with the $N\times n$ *aggregation matrix* $\boldsymbol{C}$ consisting of 0's and 1's, indicating which cells have to be aggregated together

$$\boldsymbol{C\mu} = \boldsymbol{CX\beta} + \boldsymbol{C\varepsilon} \quad \boldsymbol{C\varepsilon} \sim Gau_N\left(\boldsymbol{0}, \boldsymbol{C\Omega C}^T\right) \tag{6}$$

where N is the number of observations in a coarse grid. Now, suppose that the random variable $\boldsymbol{\lambda}=\boldsymbol{C\mu}$ is the mean process for random variables $\boldsymbol{Z}=(Z_1,\ldots,Z_N)^T$ associated with observations $\boldsymbol{z}=(z_1,\ldots,z_N)^T$ of the aggregated model

$$\boldsymbol{Z}|\boldsymbol{\lambda} \sim Gau_N\left(\boldsymbol{\lambda}, \sigma_Z^2\boldsymbol{I}_N\right). \tag{7}$$

Thus, random variables Z_i, $i=1,\ldots,N$ are conditionally independent

$$Z_i|\lambda_i \sim Gau\left(\lambda_i, \sigma_Z^2\right) \tag{8}$$

where λ_i is the i-th element of the vector $\boldsymbol{\lambda}$.

2.2 Estimation and prediction

Having available observations of Z_i in the coarse grid, we can estimate parameters $\boldsymbol{\beta}, \sigma_Z^2, \tau^2$ and ρ with the maximum likelihood (ML) method. First, from (6) and (7) the joint unconditional distribution of $\boldsymbol{Z}$ is derived

$$\boldsymbol{Z} \sim Gau_N\left(\boldsymbol{CX}\beta, \boldsymbol{M} + \boldsymbol{C\Omega C}^T\right), \tag{9}$$

where $\boldsymbol{M}=\sigma_Z^2\boldsymbol{I}_N$, $\boldsymbol{I}_N$ is the $N\times N$ identity matrix; see e.g. Lindley and Smith (1972). Next, the log likelihood function associated with (9) is formulated

$$L\left(\boldsymbol{\beta}, \sigma_Z^2, \tau^2, \rho\right) = -\frac{1}{2}\log\left|\boldsymbol{M} + \boldsymbol{C\Omega C}^T\right| - \frac{N}{2}\log(2\pi) - \frac{1}{2}(\boldsymbol{z}-\boldsymbol{CX\beta})^T\left(\boldsymbol{M} + \boldsymbol{C\Omega C}^T\right)^{-1}(\boldsymbol{z}-\boldsymbol{CX\beta}),$$

where $|\cdot|$ denotes the determinant. With fixed σ_Z^2, τ^2 and ρ, the above log likelihood is maximised for

$$\boldsymbol{\beta}\left(\sigma_Z^2,\tau^2,\rho\right)=\left[(\boldsymbol{CX})^T\left(\boldsymbol{M}+\boldsymbol{C}\Omega\boldsymbol{C}^T\right)^{-1}\boldsymbol{CX}\right]^{-1}(\boldsymbol{CX})^T\left(\boldsymbol{M}+\boldsymbol{C}\Omega\boldsymbol{C}^T\right)^{-1}\boldsymbol{z},$$

which substituted back into the function $L(\boldsymbol{\beta},\sigma_Z^2,\tau^2,\rho)$ provides the profile log likelihood

$$\begin{aligned}L\left(\sigma_Z^2,\tau^2,\rho\right)=&-\frac{1}{2}\log|\boldsymbol{M}+\boldsymbol{C}\Omega\boldsymbol{C}^T|-\frac{N}{2}\log(2\pi)\\&-\frac{1}{2}\left[\boldsymbol{z}-\boldsymbol{CX}\left[(\boldsymbol{CX})^T\left(\boldsymbol{M}+\boldsymbol{C}\Omega\boldsymbol{C}^T\right)^{-1}\boldsymbol{CX}\right]^{-1}(\boldsymbol{CX})^T\left(\boldsymbol{M}+\boldsymbol{C}\Omega\boldsymbol{C}^T\right)^{-1}\boldsymbol{z}\right]^T\\&\times\left(\boldsymbol{M}+\boldsymbol{C}\Omega\boldsymbol{C}^T\right)^{-1}\times\left[\boldsymbol{z}-\boldsymbol{CX}\left[(\boldsymbol{CX})^T\left(\boldsymbol{M}+\boldsymbol{C}\Omega\boldsymbol{C}^T\right)^{-1}\boldsymbol{CX}\right]^{-1}(\boldsymbol{CX})^T\left(\boldsymbol{M}+\boldsymbol{C}\Omega\boldsymbol{C}^T\right)^{-1}\boldsymbol{z}\right].\end{aligned}$$

Further maximisation of $L(\sigma_Z^2,\tau^2,\rho)$ is performed numerically, including checks on ρ to ensure that the matrix $\boldsymbol{D}-\rho\boldsymbol{W}$ is non-singular, see Banerjee et al. (2004).

To obtain the standard errors of the estimated parameters, one needs to derive the Fisher information matrix. The asymptotic variance-covariance matrix of the ML estimators is obtained by inverting the expectation of the negative of the second derivatives (the Hessian) of the log likelihood function, and the expectation is evaluated at the ML estimates. In other words, the expected Fisher information matrix is used to obtain the standard errors of parameters. Calculation of the Hessian with respect to the regression coefficients is relatively straightforward, but it becomes more burdensome for the covariance parameters. A detailed derivation of the explicit formulas for the expected Fisher information matrix will be provided elsewhere; here we report the standard errors of the parameter estimators obtained in the case study.

To estimate the required values in a fine grid, the following prediction procedure is applied. Note that our primary interest is the underlying emission inventory process $\boldsymbol{\mu}$. The predictors optimal in the minimum mean squared error sense are given by $E(\boldsymbol{\mu}|\boldsymbol{z})$. The joint distribution of $(\boldsymbol{\mu},\boldsymbol{Z})$ is given by

$$\begin{bmatrix}\boldsymbol{\mu}\\\boldsymbol{Z}\end{bmatrix}\sim Gau_{N+n}\left(\begin{bmatrix}\boldsymbol{X\beta}\\\boldsymbol{CX\beta}\end{bmatrix},\begin{bmatrix}\Omega & \Omega\ \boldsymbol{C}^T\\\boldsymbol{C}\Omega & \boldsymbol{M}+\boldsymbol{C}\Omega\boldsymbol{C}^T\end{bmatrix}\right).\tag{10}$$

The distribution (10) allows for full inference, yielding both the predictor $\widehat{\boldsymbol{\mu}}=\widehat{E}(\boldsymbol{\mu}|\boldsymbol{z})$ and its error $\widehat{\sigma}_\mu^2=\widehat{Var}(\boldsymbol{\mu}|\boldsymbol{z})$

$$\widehat{\boldsymbol{\mu}}=\boldsymbol{X}\widehat{\boldsymbol{\beta}}+\widehat{\Omega}\boldsymbol{C}^T\left(\widehat{\boldsymbol{M}}+\boldsymbol{C}\widehat{\Omega}\boldsymbol{C}^T\right)^{-1}\left[\boldsymbol{z}-\boldsymbol{CX}\widehat{\boldsymbol{\beta}}\right]\tag{11}$$

$$\widehat{\sigma}_\mu^2=\widehat{\Omega}-\widehat{\Omega}\boldsymbol{C}^T\left(\widehat{\boldsymbol{M}}+\boldsymbol{C}\widehat{\Omega}\boldsymbol{C}^T\right)^{-1}\boldsymbol{C}\widehat{\Omega},\tag{12}$$

where $\widehat{\cdot}$ denotes the estimated values.

3 Case study

3.1 Data

The proposed procedure is illustrated using a real dataset of gridded inventory of NH_3 (ammonia) emissions from fertilization (in tonnes per year) reported in the northern region of Poland (the Pomorskie voivodship). The inventory grid cells are of a regular size 5 km×

5 km, and the whole of cadastral survey compiles $n = 800$ cells, denoted $\boldsymbol{y}=(y_1,\ldots,y_n)^T$, see Fig. 1. For explanatory information we use the CORINE Land Cover Map for this region, available at the European Environment (2010). Specifically, for each grid cell we calculate the area of these land use classes, which are related to ammonia emissions. The following CORINE classes were considered (the CORINE class numbers are given in brackets):

Non-irrigated arable land (211), denoted $\boldsymbol{x}_1=(x_{1,1},\ldots,x_{n,1})^T$;
Fruit tree and berry plantations (222), denoted $\boldsymbol{x}_2=(x_{1,2},\ldots,x_{n,2})^T$;
Pastures (231), denoted $\boldsymbol{x}_3=(x_{1,3},\ldots,x_{n,3})^T$;
Complex cultivation patterns (242), denoted $\boldsymbol{x}_4=(x_{1,4},\ldots,x_{n,4})^T$;
Principally agriculture, with natural vegetation (243), denoted $\boldsymbol{x}_5=(x_{1,5},\ldots,x_{n,5})^T$.

Performance of the proposed disaggregation framework depends on a few factors. Perhaps the most crucial ones are the following two: (i) explanatory power of covariates available in the fine grid, and (ii) an extent of disaggregation, which is connected with preservation of the spatial correlation. The impact of both these features will be evaluated in our case study.

Regarding the first factor, we will examine models with all the above land use classes (set 1), and compare the results with models including only two of them: non-irrigated arable land and complex cultivation patterns (set 2). This subset of land use classes was chosen on the basis of its explanatory power. When limiting the number of explanatory variables, these two covariates provided the best results. Secondly, we compare linear regression with independent (iid) errors versus spatially correlated errors modelled by the CAR process. We consider the following models:

Model CAR1: - CAR errors, set 1 of covariates;
Model LM1: - iid errors, set 1 of covariates;
Model CAR2: - CAR errors, set 2 of covariates;
Model LM2: - iid errors, set 2 of covariates.

This setting of four models is intended to enable the analysis of extent to which a limited number of explanatory information can be compensated by spatial modelling.

Regarding the second factor, we test the disaggregation from 10×10 km to 15×15 km (coarse) grids into a 5 km×5 km (fine) grid. To examine performance of the disaggregation procedure, first the original fine grid emissions are aggregated into respective coarse grid cells. Next, the proposed model is fitted and ammonia emissions are predicted for a 5 km×5 km (fine) grid. Finally, the obtained results are checked with the original inventory emissions of a 5 km×5 km (fine) grid. Thus, our simulation study tests the cases of a fourfold and ninefold

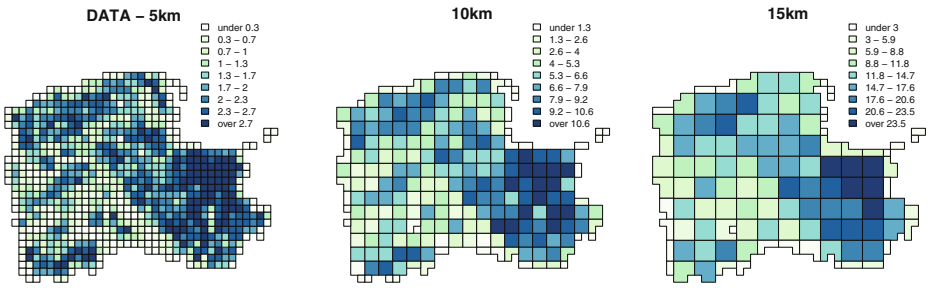

Fig. 1 Ammonia emissions: inventory data in 5 km grid, and aggregated values in 10 km and 15 km grids

disaggregation. The aggregated values of the two coarse grids as well as the actual inventory data in the fine grid are shown in Fig. 1.

3.2 Results of disaggregation from the 10 km grid

This subsection presents the model testing results for disaggregation from the 10 km grid. Table 1 (the upper part) displays the maximum likelihood estimates (denoted by Est.) and standard errors (denoted by Std.Err.) of the parameter estimators for each model. Note that in the models with set 1 of covariates (CAR1, LM1) the regression coefficient β_0 was dropped as it was statistically insignificant. In the table, we can observe that the ML estimates of the regression coefficients are similar for all the models. From the ratio of regression coefficients and its respective standard errors (i.e. the *t*-test statistic), we can roughly conclude that all the considered land use classes are statistically significant; in fact, in each case respective *p*-values proved to be less than 0.05 (not shown). Next, let us turn our attention to the error part of the models. Significantly lower values of σ_Z^2 estimates under both the CAR models, as compared with their linear regression counterparts, indicate that greater variability is explained by the models with spatially correlated errors than by the corresponding models with independent errors. As expected, among the spatially correlated models, both variance parameters σ_Z^2 and τ^2 are higher for CAR2 than for CAR1 model with five land use classes as explanatory variables. Furthermore, the parameter ρ reflects strength of the spatial correlation. Note that $\rho=0$ corresponds to a model with independent errors, see also Banerjee et al. (2004) for more details. A value of parameter ρ is higher for CAR2 model, which illustrates that in the models of limited explanatory power, the importance of spatial correlation becomes more pronounced.

The results of the four models are also summarized using the Akaike criterion (AIC). The idea of AIC is to favour a model with a good fit and to penalize it for a number of parameters; models with smaller AIC are preferred to models with larger AIC. Table 2 (the upper part) displays AIC for each model, and additionally it reports the negative log likelihood (-L). Naturally, the models with set 1 of covariates provide much better results than the models with another set. Among these respective sets, the models with the spatial structure considerably improve results obtained with the models of independent errors. Note, that this improvement is higher for the models with set 2 of covariates (797.6–742.8=54.8) than for the models with set 1 of covariates (685.1–640.7=44.4).

The values of ammonia emissions predicted in a 5 km×5 km grid (y_i^*) are featured in Fig. 2. Differences between the four models are negligible, although a visual comparison with the original emissions in Fig. 1 (the left-hand-side plot) suggests that the both models based on set 1 of covariates (CAR1, LM1) provide slightly better results. Since the mapped emission values are classified into just 9 bins, therefore some features might not be easily distinguishable on the maps in Fig. 2. To remedy this, Fig. 3 presents the model residuals ($d_i=y_i-y_i^*$). Now the difference in prediction results among the models is evident—the best results are obtained for CAR1 model and the worst for LM2 model.

At this point it must be stressed that the values predicted in a fine grid (y_i^*) are calculated with the formula (11) based on the aggregated values of 10 km grid; the calculations are made as if the true emissions were unknown. On the other hand, recall that these true emissions in the fine grid (y_i) are available; see the left-hand-side map in Fig. 1. From now on, our analysis is based on a comparison between the prediction results obtained with the proposed technique and the original fine grid ammonia emissions (observations).

Figure 4 presents, for each model, a scatterplot of predicted values y_i^* versus observations y_i. The straight line has slope 1, thus if the predicted values are close to the original data, points

Table 1 Maximum likelihood estimates

	CAR1		LM1		CAR2		LM2	
	Est.	Std.Err.	Est.	Std.Err.	Est.	Std.Err.	Est.	Std.Err.
10 km grid								
β_0	–	–	–	–	0.386	9.29e-02	0.452	5.45e-02
β_1	1.13e-07	3.26e-09	1.09e-07	2.46e-09	1.06e-07	5.03e-09	9.58e-08	4.43e-09
β_2	2.56e-07	1.94e-07	4.48e-07	1.97e-07	–	–	–	–
β_3	9.77e-08	1.19e-08	1.08e-07	1.08e-08	–	–	–	–
β_4	1.18e-07	2.13e-08	1.21e-07	1.76e-08	1.27e-07	2.72e-08	1.60e-07	2.22e-08
β_5	1.27e-07	1.32e-08	1.35e-07	1.11e-08	–	–	–	–
σ_Z^2	0.334	0.073	1.165	0.109	0.522	0.111	1.95	0.184
τ^2	0.536	0.082	–	–	0.807	0.124	–	–
ρ	0.948	9.98e-04	–	–	0.972	9.98e-04	–	–
15 km grid								
β_0	–	–	–	–	0.424	1.04e-01	0.476	6.82e-02
β_1	1.12e-07	3.95e-09	1.09e-07	3.42e-09	1.00e-07	7.01e-09	9.35e-08	5.79e-09
β_2	–	–	–	–	–	–	–	–
β_3	1.07e-07	1.84e-08	1.16e-07	1.55e-08	–	–	–	–
β_4	1.24e-07	2.77e-08	1.29e-07	2.34e-08	1.56e-07	3.65e-08	1.75e-07	2.79e-08
β_5	1.27e-07	1.65e-08	1.33e-07	1.49e-08	–	–	–	–
σ_Z^2	2.339	0.424	3.50	0.474	2.681	0.548	5.55	0.753
τ^2	0.214	0.088	–	–	0.414	0.088	–	–
ρ	0.966	4.91e-04	–	–	0.982	5.55e-05	–	–

are close to the straight line. This setting, once again, illustrates much better explanatory power of models based on all the land use classes (set 1 of covariates). It also illustrates the importance of the spatial structure component. In the case of models CAR2 and LM2, the introduction of spatial dependence has evidently improved the accuracy of prediction. Whereas in the case of models CAR1 and LM1, the applied spatial structure considerably limited a number of highly overestimated predictions (points below the straight line).

Table 2 Model comparison and analysis of residuals ($d_i=y_i-y_i^*$)

Model	-*L*	AIC	MSE	min(d_i)	max(d_i)	*r*
10 km grid						
CAR1	312.3	640.7	0.064	−1.717	1.104	0.961
LM1	336.5	685.1	0.186	−2.544	0.268	0.882
CAR2	365.4	742.8	0.158	−1.917	1.362	0.901
LM2	394.8	797.6	0.291	−2.498	1.765	0.808
15 km grid						
CAR1	220.6	455.3	0.136	−2.428	0.646	0.915
LM1	222.9	455.9	0.189	−2.600	0.516	0.880
CAR2	240.4	492.8	0.190	−2.132	1.446	0.880
LM2	248.1	504.4	0.295	−2.511	1.746	0.807

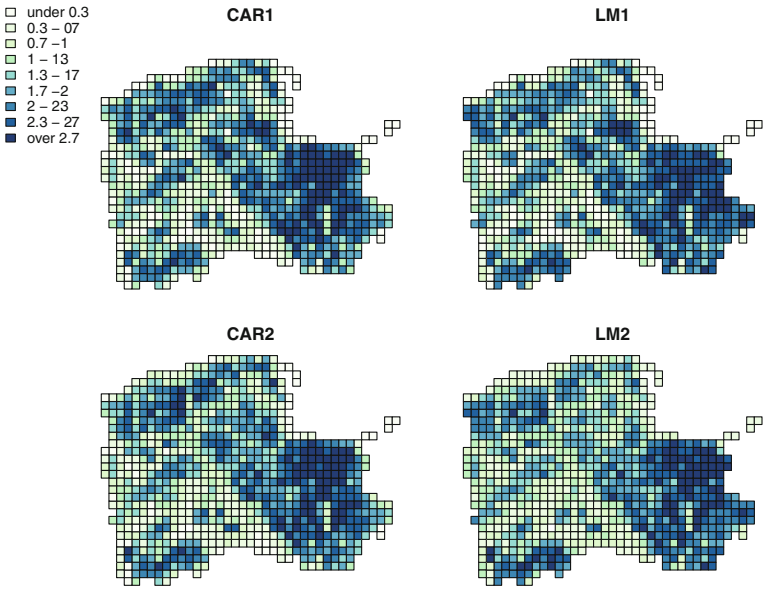

Fig. 2 Ammonia emissions predicted in a fine grid—disaggregation from 10 km grid

Furthermore, we note that for a prevailing number of cases in the high emission range (emissions over 1.5 tonnes) the linear regression LM1 provides biased (underestimated) predictions, while CAR1 model allows overcoming this deficiency. This is due to the fact that the analysed emissions are spatially correlated, that is, cells located nearby tend to have

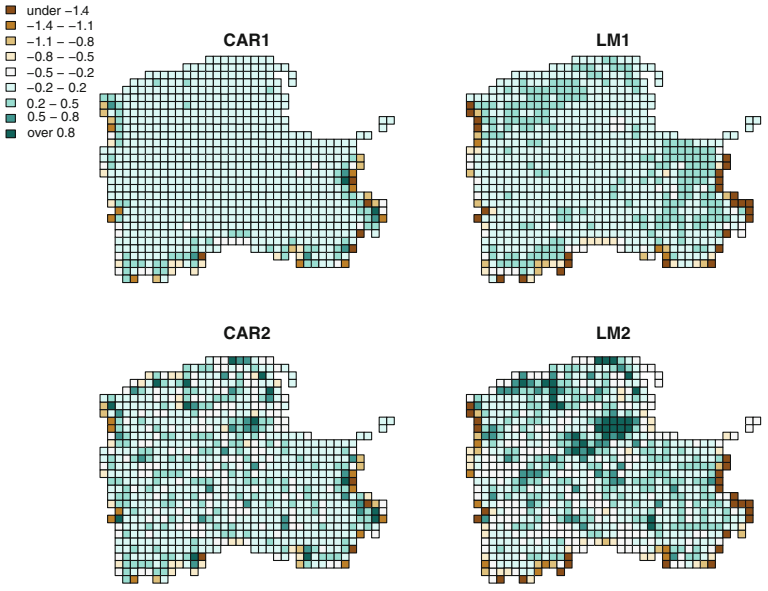

Fig. 3 Residuals from predicted values—disaggregation from 10 km grid

similar values. In particular, the majority of high emission values are located in the eastern part of the voivodeship as well as in the north-west stripe along the coastline (compare Fig. 1). The covariates applied in the linear regression LM1 explain emission variability only to some extent, and the point is that the unexplained variability remains spatially correlated. This can be noticed on the map in Fig. 3 for LM1 model, where clusters of residual values (0.2–0.5) in the mentioned areas indicate underestimated predictions. The autocorrelation term in the model CAR1 allows for this feature. In Fig. 4 it can be seen as a slope of a dotted line, which is visibly higher than 1 for LM1 model, while for CAR1 it lines up with the one of slope 1.

The residuals d_i are further analysed in Table 2 (the upper part). Namely, the mean squared error (MSE) is calculated

$$MSE = \frac{1}{n}\sum_i \left(y_i - y_i^*\right)^2,$$

and it should be as low as possible. The mean squared error reflects how well a model predicts data. In Table 2 we report also the minimum and maximum values of d_i, and the sample correlation cofficient r between the predicted y_i^* and observed y_i values. In terms of both the mean squared error and the coefficient r, the best model is CAR1 and the poorest one is LM2, following the previous assessments. Interestingly, the remaining two models changed their ranks compared with the AIC criterion. That is, CAR2 model has lower MSE=0.158 and higher coefficient r=0.901 than the linear model based on set 1 of covariates (LM1 model with MSE=0.186 and r=0.882). This proves that the model with a limited number of covariates but having a spatial component (CAR2) can provide better disaggregation results than the model based solely on linear regression, even though its covariate information is richer (LM1). Note that the analysis based on residuals is more robust than the AIC rating, which basically tests a model fit to the aggregated data.

Following the formula (12), we also calculate the prediction error. Since in the present case study the correct values of predicted emissions are known, we are in a position to compare the

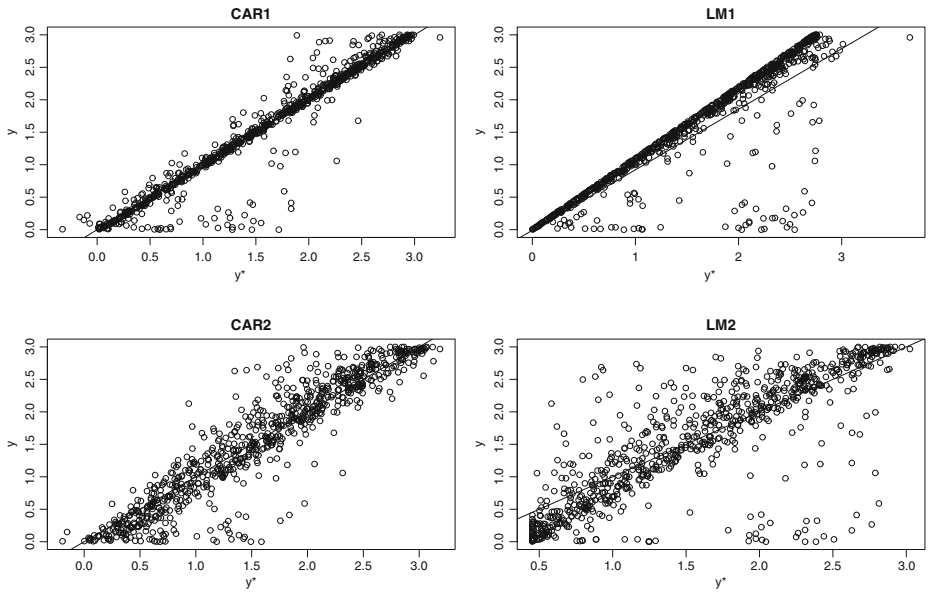

Fig. 4 Predicted (y^*) versus observed (y) values—disaggregation from 10 km grid

prediction error with the actual residuals (more precisely, with its absolute values). In Fig. 5 these values are presented for CAR2 model. It is noticeable that the prediction error is significantly underestimated, and moreover, it does not reflect the diversification of the actual residuals properly. Note that in the both maps the highest errors are reported on the border of the domain; this fact is known in spatial modelling as the edge effect.

3.3 Results of disaggregation from the 15 km grid

Next, we present the results of disaggregation from the 15 km grid. The conducted analysis is similar to the one of the 10 km grid and, where appropriate, both settings are compared.

The lower part of Table 1 contains the maximum likelihood estimates for the 15 km grid data. In the models with set 1 of covariates, the regression coefficient β_0 was again dropped. Moreover, in all the models at this level of aggregation the land use class "Fruit tree and berry plantations" (β_2) was statistically insignificant, and thus it was also dropped. The remaining land use classes were informative, with respective p-values lower than 0.05.

As regards the error part, all the comments reported for 10 km disaggregation remain valid also here, although their degree is significantly lower. Both CAR models provide lower values of σ_Z^2 than their linear regression counterparts. However, the reduction of unexplained variability between the models, for instance, LM1 and CAR1 is only 1.5 (3.5/2.339), while it was over 3 (1.165/0.334) for respective models of 10 km disaggregation. This suggests that the spatial correlation strength of the 15 km grid model is smaller than the 10 km grid one. Thus, here the CAR models are less competitive than the LM models, as compared to the former grid.

The values of AIC criterion and of the negative log likelihood (-L) are reported in the lower part of Table 2. Similarly as for the disaggregation from a 10 km grid, also in this case the models based on set 1 of covariates provide better results. The CAR structure improves obtained linear regression results of both respective covariate sets. Note, however, that in the setting of 15 km disaggregation, the impact of the spatial component is not that substantial anymore as it was previously. Again, a bigger improvement is noted for the models with a limited number of covariates (504.4–492.8=11.6 in terms of the AIC criterion), and the gain from incorporation of the spatial component is only marginal for the models with set 1 of covariates (455.9–455.3=0.6).

For the four considered models, the maps of ammonia emissions disaggregated from the 15 km grid and predicted in the fine grid provided visually similar results (not shown). The residual maps proved to be more informative, see Fig. 6. While for the 10 km disaggregation

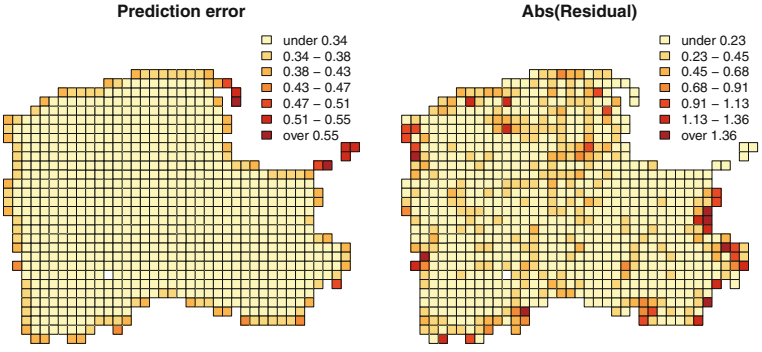

Fig. 5 Prediction error and absolute values of residuals for CAR2 model. Note that the maps are drawn in different scales

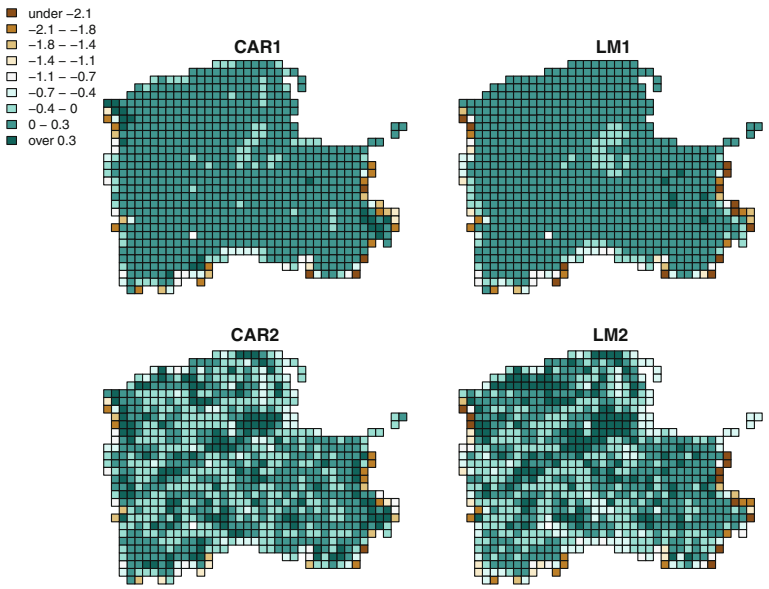

Fig. 6 Residuals from predicted values—disaggregation from 15 km grid

the residual maps clearly indicated discrepancies among the models, here it is not easily visible. The models based on set 1 of covariates (CAR1, LM1) provide smaller residuals. However, the differences between the spatial models and their linear regression counterparts seem to be negligible.

Again, Table 2 (the lower part) provides further analysis of residuals. The mean squared error MSE and the correlation coefficient r yield a consistent ranking of the models. Obviously the best model is CAR1 with r=0.915 and MSE=0.136, while the poorest one is LM2 with r= 0.807 and MSE=0.295. When it comes to the remaining two models, LM1 slightly outperforms CAR2 (in terms of the mean squared error). Note that this order is reversed when compared with the results of the 10 km grid disaggregation (the upper part of the table). Therefore, when disaggregating from the 10 km grid, the spatial structure is more informative than some of the covariates, but this is not true anymore when disaggregating from the 15 km grid. From this we conclude that in this particular case study, the proposed framework offers an efficient tool for a quadruple and nine-times disaggregation, but it may become less adequate for higher order allocations.

The actual interplay among the four models is illustrated on the scatterplots in Fig. 7. In general, the 15 km disaggregation preserves the features reported previously—the performance of respective models is analogous as for the 10 km disaggregation. It means that for the models based on set 2 of covariates, the spatial correlation significantly improves prediction quality. Also for the other two models, the introduction of spatial structure is still beneficial as it allows correction of the prediction bias and a slight reduction in the number of overestimates. We highlight the difference between the models CAR2 and LM1 that yield almost the same MSE and coefficient r, but provide completely distinct plots, see Fig. 7. The residuals of CAR2 model are more dispersed owing to a limited set of explanatory covariates. On the other hand, improved covariate modelling of LM1 leads to the residuals gathered close to the diagonal, but a lack of spatial averaging results in larger amount of overestimated values. Altogether, the assessment of residuals for both models becomes the same.

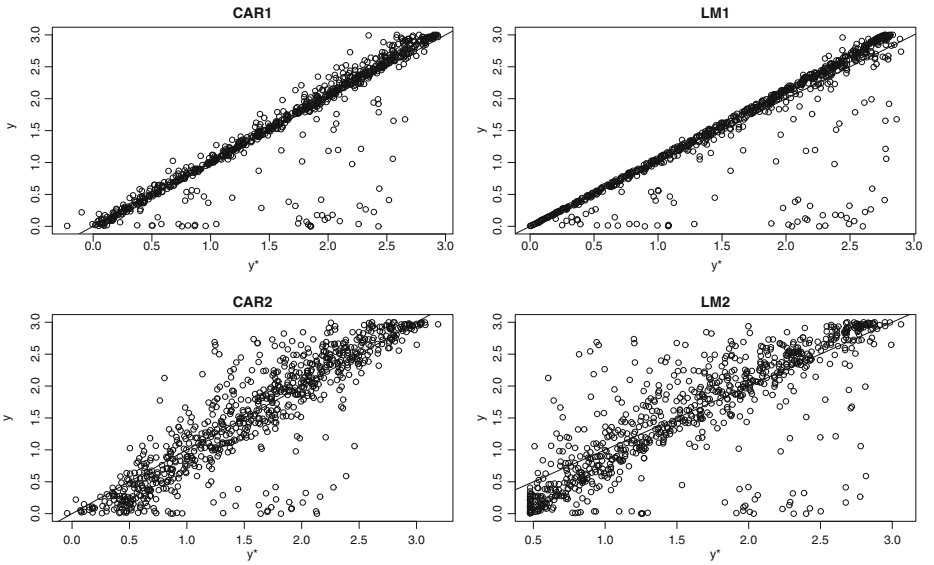

Fig. 7 Predicted (y^*) versus observed (y) values—disaggregation from 15 km grid

4 Discussion and conclusions

The major objective of this study was to demonstrate how a variable of interest (here, emissions) available in a coarse grid plus information on covariates available in a finer grid can be combined together to provide the variable of interest in a finer grid, and therefore to improve its spatial resolution. We proposed a relevant disaggregation model and illustrated the approach using a real dataset of ammonia emission inventory. The idea is conceptually similar to the method of Chow and Lin (1971), originally designed for time series data; see also Polasek et al. (2010). It was applied to the spatially correlated data, and spatial dependence was modelled with the conditional autoregressive structure introduced into a linear model as a random effect.

The model allows for this part of a spatial variation which has not been explained by available covariates. Thus, if the covariate information does not correctly reflect a spatial distribution of a variable of interest, there is potential for improving the approach with a relevant model of a spatial correlation. The underlying assumption of the method is that the covariance structures of the variable in a coarse grid and in a fine grid are the same. In the present study of ammonia emissions examined in 5 km, 10 km, and 15 km grids, this assumption proved to be reasonable.

Performance of the proposed framework was evaluated with respect to the following two factors: explanatory power of covariates available in a fine grid, and the extent of disaggregation. The results indicate that inclusion of a spatial dependence structure can compensate for less adequate covariate information. For the considered ammonia inventory, the fourfold allocation benefited greatly from the incorporation of the spatial component, while for the ninefold allocation this advantage was limited, but still evident. In addition, the proposed method allowed to correct the prediction bias encountered for upper range emissions in the linear regression models.

We note that in this case study we used the original data in a fine grid to assess the quality of resulting predictions. For the purpose of potential applications, we developed also a relevant measure of prediction error (the formula 12). Although not entirely faultless, it is the first attempt to quantify the prediction error in situations, where original emissions in a fine grid are not known.

Other approaches, such as a geostatistical model, might be potentially used in the case of spatial allocation. Application of the geostatistical approach brings us to the concept of block kriging (Gelfand 2010). However, it should be stressed that geostatistics is more appropriate for point referenced data, while our proposition is dedicated to the case of emission inventories which involve a real data. Thus, the choice between these two options should be considered on a case by case basis.

Another possibility to deal with the issue of spatial disaggregation could be to use some expert knowledge and logical inference; compare Verstraete (this issue) for a fuzzy inference system to the map overlay problem.

The described method opens the way to uncertainty reduction of spatially explicit emission inventories, hence the future work will also include testing the proposed disaggregation framework for inventories of greenhouse gasses.

Acknowledgments The study was conducted within the 7FP Marie Curie Actions IRSES project No. 247645. J. Horabik acknowledges support from the Polish Ministry of Science and Higher Education within the funds for statutory works of young scientists. This contribution is also supported by the Foundation for Polish Science under International PhD Projects in Intelligent Computing; project financed from The European Union within the Innovative Economy Operational Programme 2007–2013 and European Regional Development Fund. Z. Nahorski was financially supported by the statutory funds of the Systems Research Institute of Polish Academy of Sciences.

The authors gratefully acknowledge the provision of data for the case study from Ekometria – Biuro Studiów i Pomiarów Proekologicznych in Gdańsk, Poland.

Open Access This article is distributed under the terms of the Creative Commons Attribution License which permits any use, distribution, and reproduction in any medium, provided the original author(s) and the source are credited.

References

Banerjee S, Carlin BP, Gelfand AE (2004) Hierarchical modeling and analysis for spatial data. Chapman & Hall/CRC, Boca Raton

Boychuk K, Bun R (this issue) Regional spatial cadastres of GHG emissions in energy sector: accounting for uncertainty

Bun R, Hamal K, Gusti M, Bun A (2010) Spatial GHG inventory at the regional level: accounting for uncertainty. Clim Chang 103(1–2):227–244

Chow GC, Lin A (1971) Best linear unbiased interpolation, distribution, and extrapolation of time series by related series. Rev Econ Stat 53(4):372–375

Cressie NAC (1993) Statistics for spatial data. John Wiley & Sons, New York

Dragosits U, Sutton MA, Place CJ, Bayley AA (1998) Modelling the spatial distribution of agricultural ammonia emissions in the UK. Environ Pollut 102(S1):195–203

European Environment Agency (2010) Corine land cover 2000. http://www.eea.europa.eu/data-and-maps/data. Cited August 2010

Gelfand AE (2010) Misaligned spatial data: the change of support problem. In: Gelfand AE, Diggle PJ, Fuentes M, Guttorp P (eds) Handbook of spatial statistics. Chapman & Hall/CRC, Boca Raton

Ghosh T, Elvidge CD, Sutton PC et al (2010) Creating a global grid of distributed fossil fuel CO_2 emissions from nighttime satellite imagery. Energies 3:1895–1913

Gotway CA, Young LJ (2002) Combining incompatible spatial data. J Am Stat Assoc 97:632–648

Horabik J, Nahorski Z (2010) A statistical model for spatial inventory data: a case study of N_2O emissions in municipalities of southern Norway. Clim Chang 103(1–2):263–276

Kaiser MS, Daniels MJ, Furakawa K, Dixon P (2002) Analysis of particulate matter air pollution using Markov random field models of spatial dependence. Environmetrics 13:615–628

Lindley DV, Smith AFM (1972) Bayes estimates for the linear model. J Roy Stat Soc B 34:1–41

McMillan AS, Holland DM, Morara M, Fend J (2010) Combining numerical model output and particulate data using Bayesian space-time modeling. Environmetrics 21:48–65

Mugglin AS, Carlin BP (1998) Hierarchical modeling in geographical information systems: population interpolation over incompatible zones. J Agric Biol Environ Stat 3:111–130

Mugglin AS, Carlin BP, Gelfand AE (2000) Fully model-based approaches for spatially misaligned data. J Am Stat Assoc 95:877–887

Oda T, Maksyutov S (2011) A very high-resolution (1 km×1km) global fossil fuel CO_2 emission inventory derived using a point source database and satellite observations of nighttime lights. Atmos Chem Phys 11: 543–556

Polasek W, Llano C, Sellner R (2010) Bayesian methods for completing data in spatial models. Rev Econ Anal 2: 194–214

Thiruchittampalam B, Theloke J, Uzbasich M et al. (2010) Analysis and comparison of uncertainty assessment methodologies for high resolution Greenhouse Gas emission models. In: Proceedings of the 3rd International Workshop on Uncertainty in Greenhouse Gas Inventories, Lviv Polytechnic National University, Ukraine, 22–24 Sept 2010

Verstraete J (this issue) Solving the map overlay problem with a fuzzy approach

DOI 10.1007/978-3-319-15901-0_10
Reprinted from *Climatic Change* Journal, DOI 10.1007/s10584-014-1053-z

Solving the map overlay problem with a fuzzy approach

Jörg Verstraete

Received: 9 January 2013 / Accepted: 5 January 2014 / Published online: 8 February 2014
© The Author(s) 2014. This article is published with open access at Springerlink.com

Abstract The map overlay problem occurs when mismatched gridded data need to be combined, the problem consists of determining which portion of grid cells in one grid relates to the partly overlapping cells of the target grid. This problem contains inherent uncertainty, but it is an important and necessary first step in analysing and combining data; any improvement in achieving a more accurate relation between the grids will positively impact the subsequent analysis and conclusions. Here, a novel approach using techniques from fuzzy control and artificial intelligence is presented to provide a new methodology. The method uses a fuzzy inference system to decide how data represented in one grid can be distributed over another grid using any additionally available knowledge, thus mimicking the higher reasoning that we as humans would use to consider the problem.

1 Introduction

In order to compare different countries, the FCCC requires a single national value per country for e.g. CO2 emissions that stem from fossil-fuel burning. The authors in Boychuk and Bun (2014); Jonas and Nilsson (2007) explain that for countries with good emission statistics, the national fossil-fuel CO2 emissions are believed to exhibit a relative uncertainty of about ±5 % (95 % CI), but that a sub-national approach can differ considerably (i.e., the ±5 % for the 95 % CI does not hold any more). This is due to uncertainty at various levels, both uncertainty inherently present in the data, but also uncertainty introduced by processing and pre-processing the data. The International Workshop Series on Uncertainty in GHG Emission Inventories focuses on both the presence and on techniques on understanding, modelling and decreasing these uncertainties (Bun et al. 2007, 2010; Jonas et al. 2010). The sub-national data are usually obtained through the analysis of data coming from various sources, processed and combined into a national value, but the way the data are processed has a big impact on the introduced uncertainty and, consequently, on the results. To eliminate any inter-country uncertainty, a uniform and well-tested methodology should be used when building on sub-

This article is part of a Special Issue on "Third International Workshop on Uncertainty in Greenhouse Gas Inventories" edited by Jean Ometto and Rostyslav Bun.

Electronic supplementary material The online version of this article (doi:10.1007/s10584-014-1053-z) contains supplementary material, which is available to authorized users.

J. Verstraete (✉)
Systems Research Institute, Polish Academy of Sciences, ul. Newelska 6, 01-447 Warszawa, Poland
e-mail: jorg.verstraete@ibspan.waw.pl

national emission approaches. However, even when using the same methodology, the uncertainty introduced by the processing of data is dependent on the source formats of the data, and how it behaves under subsequent processing. The solution to this is found by either obtaining data in a more similar way, to make all data compatible. But with most infrastructures in place, changes to this are unlikely to happen. The alternative is to pre-process the data so that the data exhibit a similar behaviour under the subsequent processing. The data are often represented in a gridded format, yet often different grids (e.g. CO_2 emissions and land use) are incompatible. By transforming them to compatible, matching grids, the processing should yield more consistent results.

This article presents a novel approach to pre-process data, to transform the data (e.g. emission data) so that it is better suited to be combined with other data (e.g. land use) while at the same time ensuring that the uncertainty and errors introduced by this transformation are kept to a minimum. As such, this methodology is at a very low level in the processing chain, but any decrease in uncertainty at such a low level should provide far more reliable results at the end of the processing and thus allow for more accurate analysis and comparison.

Commonly, data relating to different topics come from different sources: land use data can be provided by one source, emission data may come from another source, population data is again obtained elsewhere. Usually, the data are provided in a gridded format (Rigaux et al. 2002; Shekhar and Chawla 2003), which means that the map (or the region of interest) is overlayed with a grid dividing the map in different cells. In the case of a rectangular grid, each grid cell will be a rectangle or a square. With each cell, there is an association with a numerical value; which is deemed to be representative for the cell. The cell is however the smallest item for which there is data: the value associated with the cell can be the accumulation of data of 100 different points in the cell, can stem from one single point in the cell, can stem from several line sources, etc. There is no difference in appearance between these cells and no way of knowing this once the data is presented in the grid format. This is illustrated on Fig. 1a. There are, however, several problems with the data, particularly when the data need to be combined. As the data are obtained from different sources, the format in which they are provided can differ: the grids may not line up properly, the size of the grid cells may be different, or the grids might be rotated when compared to one another, etc.; as illustrated on Fig. 1b–e. This makes it difficult to relate data that is on different grids to one other and thus introduces uncertainty or errors. Additionally, not all data is complete, and cells of the grid may be without data.

This article does not contain any specific data analysis, nor are there any conclusions that directly relate to climate change, but it does introduce a novel solution method to transform a grid in order to match it to a different grid, a process that is used in many climate related studies. The proposed methodology makes use of data analysis, geometric matching and mathematical connections to solve format mismatches, it does not consider the higher concepts that relate to the meaning of the data (e.g. using ontologies to match differently labelled data, as in (Duckham and Worboys 2005)). The proposed methodology is still in a very early stage of development. As such, the examples shown are quite simple, but the prototype implementation and experiments on artificial datasets show promising results. The methodology is expected to be able to cope with any uncertainties and missing information, but the main focus for the time being is on developing the basic workings of the method. In Section 2, the map overlay problem along with current solution methods will be described. Reasoning about the problem and the possible use of any additional knowledge is also covered here. Section 3 considers how the intuitive approach can be simulated using techniques from artificial intelligence; it briefly introduces the necessary concepts (fuzzy set theory, fuzzy inference system) that will be used further along with giving a description of the new methodology. In

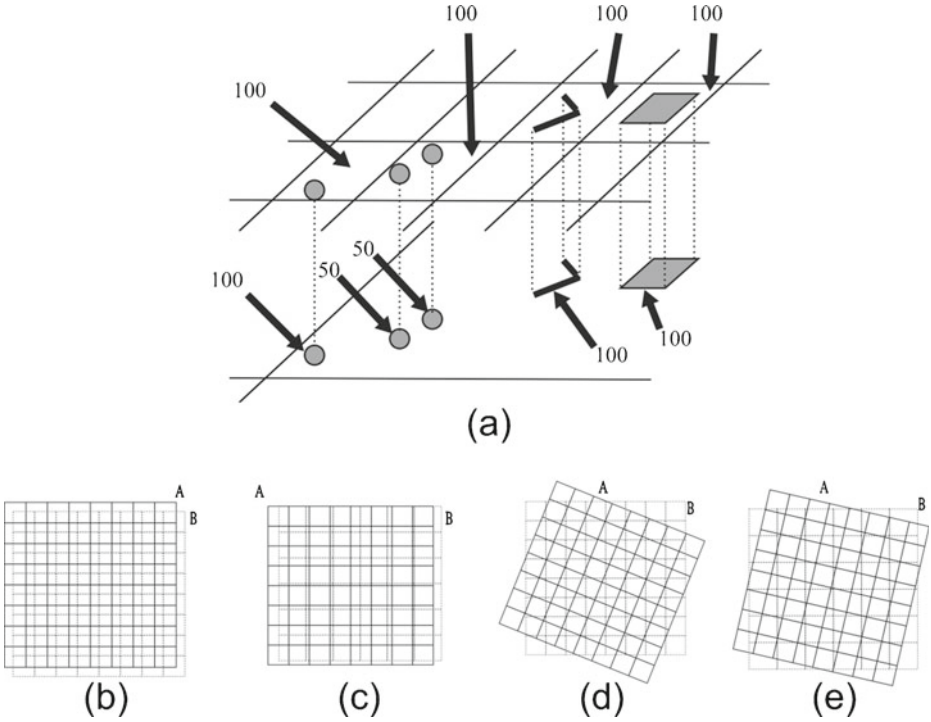

Fig. 1 Different data distributions within a grid cell that result in the same value for the grid cell are shown in (**a**). The examples are: a single point source of value 100, two point sources of value 50, a line source of value 100 and an area source of value 100. Each of these are such that they are in one grid cell, which then has the value 100. When viewing the grid cell, it is not known what the underlying distribution is. Different incompatible grids are shown in **b**–**e**: a relative shift (**b**), a different grid size (**c**), a different orientation (**d**) and a combination (**e**)

Section 4, the methodology is applied to some examples and suggestions for future research are listed. Section 5 summarizes the article and contains conclusions.

2 The map overlay problem

2.1 Problem description

Spatially correlated numerical data are often represented by means of a data grid. This grid basically divides the map (or the region of interest) into a number of cells. For most grids, these cells are equal in size and shape (regular grid) and most commonly take the form of rectangles or squares. Each cell is considered to be atomic in the sense that it is not divided into smaller parts, and contains aggregated information for the area covered by the cell. With each cell, a numeric value is associated that is deemed representative for the cell. If we consider the example of the presence of a greenhouse gas, then the value associated with the cell indicates the amount of this particular gas in that particular cell. In reality, this amount may be evenly spread over the entire cell or it may be concentrated in a very small part of the cell; but as the cells are the smallest object considered, there is no way to confirm whether it is one or the other. This is illustrated in Fig. 1a.

Commonly, data from different sources need to be combined to draw conclusions: for instance, relating the measured concentrations of a particular gas in the atmosphere to the land use would

require data from both concentrations and land use. While both data can be represented as gridded data, the grids used often don't match: not only can there be a difference in cell sizes and shapes, but one grid can also be rotated when compared to another grid, translated, or a combination of these. This is a common problem with many data in literature, called the *map overlay problem*; the data are then said to be *incompatible*; some examples are shown on Fig. 1b–e.

To make these different datasets compatible, it is necessary to transform one of the grids to match the layout of the other grid: it needs to have the same number of grid cells, oriented in the same way, so that there is a 1:1 mapping of each cell in one grid to a cell in this other grid. The map overlay problem concerns the finding of such a mapping: it considers an input grid which contains data and a target grid that provides the new grid structure on which the input grid needs to be mapped. As mentioned before, nothing is known at a scale smaller than the cells; which makes the mapping of one grid to another extremely challenging. Consider the simple example on Fig. 2a.

Remapping the values of the grid cells of the input grid A to the output grid B is done by determining the values of x_i^j in these formulas:

$$\begin{aligned} f(B_1) &= x_1^1 f(A_1) \\ f(B_2) &= x_2^1 f(A_1) \\ f(B_3) &= x_3^1 f(A_1) + x_3^2 f(A_2) \\ &= \left(1 - x_1^1 - x_2^1\right) f(A_1) + \left(1 - x_4^2 - x_5^2\right) f(A_2) \\ f(B_4) &= x_4^2 f(A_2) \\ f(B_5) &= x_5^2 f(A_2) \\ &\cdots \end{aligned}$$

Where in x_i^j, the index i refers to the cell number in the output grid, and j refers to the cell number in the input grid. This can be generalized as:

$$f(B_i) = \sum_j x_i^j f\left(A_j\right) = \sum_{j \mid A_j \bigcap B_i \neq \varnothing} x_i^j f\left(A_j\right)$$

with constraints that

$$\forall j, \sum_i x_i^j = 1$$

While this looks straight forward, the problem is in finding the values of x_i^j. In more complicated examples, it is obvious that more than two grid cells can make a contribution to the value of a new grid cell. From the example on Fig. 2a, it can also be seen that there is no single solution: there are different possible values for B_1 and B_2, providing their sum is constant.

The key to resampling the original grid to the new grid, is the ability to determine the true distribution of the data; thus going into further detail than that which the grid cells offer. Most current solution methods either assume a distribution of the data or aim to estimate the distribution of the data, and resample it in order to match the new grid. The output grid is specified by the user; the initial map overlay problem concerns transforming the input grid to this grid. The proposed method uses an additional grid, also specified by the user, to help transform the input grid, but the grid specification (cell size, orientation) does not have to match either the input or the output and does not change the output format. The additional grid should contain data that has a known and established correlation to the input data. The grid on which the data is provided does not have to match either input or output grids; however, the finer the grid, the better the results for transforming the input grid.

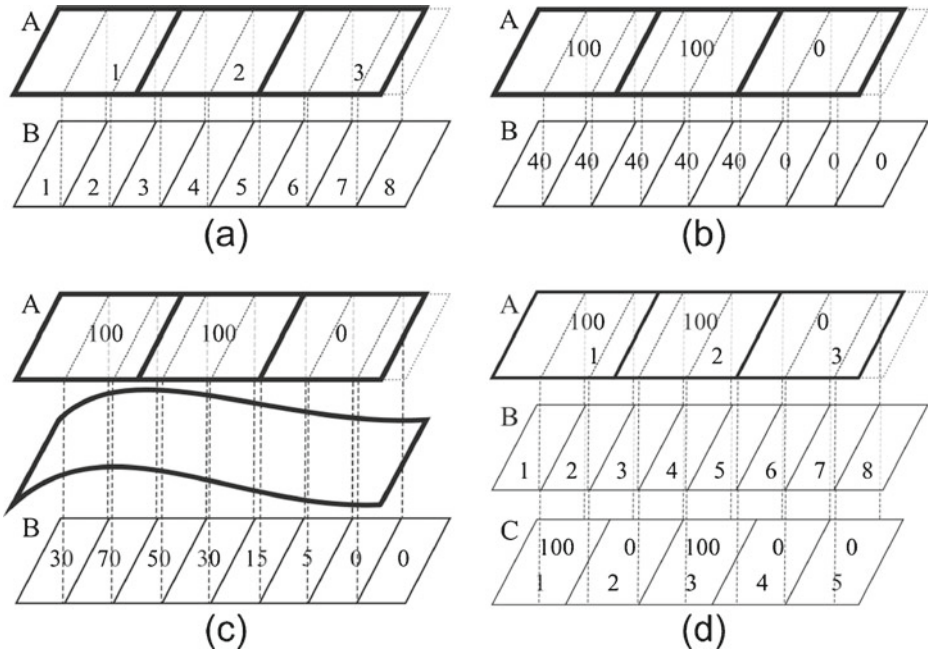

Fig. 2 Examples to explain the problem: **a** Problem illustration: remapping grid *A* onto grid *B*, **b** Areal weighting: the value of each output cell is determined by the amount of overlap, **c** Areal smoothing: the value of each output cell is determined resampling a smooth surface that is *fitted* over the input data, **d** Intelligent reasoning using additional data: grid *C* supplies information on the distribution, which can be used to determine values in the output grid

2.2 Current solution methods

Transforming one grid to another grid is comparable to determining what the first grid would be if it were represented by using the same grid cells as in the second grid. In literature, a number of solution methods exist. The grid cells as shown in Fig. 2a will be used to explain the most common method; for a more detailed overview we refer to (Gotway and Young 2002). In the example used, the input grid *A* contains three cells, the output grid *B* contains eight cells.

2.2.1 Areal weighting

The simplest and most commonly used method is areal weighting. It uses the portion of overlap of the grid cell to determine what portion of its associated numerical value will be considered in the new grid. This approach is considered to be relatively easy and straightforward. The result of areal weighting is illustrated on Fig. 2b. It will clear that the values of x_i^j are determined by the surface area *S*:

$$
\begin{aligned}
&f(B_1) = S(B_1)f(A_1)\\
&f(B_2) = S(B_2)f(A_1)\\
&f(B_3) = S(B_3 \cap A_1)f(A_1) + S(B_3 \cap A_2)f(A_2)\\
&f(B_4) = S(B_4)f(A_2)\\
&\cdots
\end{aligned}
$$

Basically, in this approach, it is assumed that the data in the cell are evenly distributed throughout the cell and that all cells are considered to be completely independent of one

another. Resampling can be done over any grid without any difficulty. In some situations, the assumption combined with the simplicity may indeed be justification for its employment. The spread of a gas in the atmosphere in the absence of extreme sources is an example where use of the method is legitimate. However, when the associated numeric data is the result of a small number of extreme sources in the grid cell (e.g. a factory), then this approach may lead to either an over- or an underestimate in the new grid cell, depending on whether or not the factory is in the overlapping area.

2.2.2 Spatial smoothing

Spatial smoothing is a more complicated approach than areal weighting. Rather than assume that the data is evenly spread out over a cell, the distribution of the data within a cell is dependent on the neighbouring cells.

This is achieved by considering the grid in three dimensions, with the third dimension representing the associated data. In spatial smoothing methods, a smooth three-dimensional surface is fitted over the grid, as illustrated in Fig. 2c, after which the smooth surfaced is sampled using the target grid. Consequently, this method does not assume that the data modelled by the grid is evenly distributed over each cell, but rather assumes a smooth distribution over the region of interest: if the value of a cell is high, one expects higher values closer to it in the surrounding cells. In many situations, this method is more accurate than the previous method, but is still unable to cope with data that in reality is concentrated in a small area of the cell. This is, for instance, the case when modelling air pollution when a single factory is responsible for the value that will be associated with the grid cell in which it is contained (a point source): the presence of a point source in one cell does not imply sources close to it in neighbouring cells (in some urban planning schemes, it might even be the opposite, to avoid the placing of too many point sources in close proximity to one another).

2.2.3 Regression methods

In regression methods, the relation between both grids is examined, and patterns of overlap are established. Different methods exists, based on the way the patterns are established. (Flowerdew and Green 1994) determine zones, which are then used to establish the relation. This is then combined with an assumption of the distribution of the data (e.g. Poisson) in order to determine the values for the incompatible zones. Several underlying theoretical models can be used, but all the regression methods require key assumptions that normally are not part of the data and cannot be verified using the data. These assumptions mainly concern the distribution of the data, e.g. if the data is distributed in a Poisson or binomial distribution.

2.3 Using additional knowledge

2.3.1 Data fusion

The problem under consideration resembles to some extent the problem described in (Duckham and Worboys 2005). Both the problem and solution are, however, completely different: the authors in (Duckham and Worboys 2005) combine different datasets that relate to the same area of interest in order to create a new dataset that has the combined information of both source data sets. This combined information can be richer or have a higher accuracy. Their approach, however, is not intended for numerical data, but for labelled information. The different datasets can use a different schema (set of labels) to describe regions in the region of

interest (the example uses land coverage and land use terms). As the labels are not always fully compatible, the authors propose a method of linking both schemas with a common ontology, and obtaining geometric intersections if the labelled regions do not match. The authors in (Fritz and See 2005) tackle the data fusion problem using a different approach. An expert supplies input regarding the assigned labels in different datasets; this knowledge is then modelled and matched using a fuzzy agreement. This allows the labels in different sets to be compared and combined correctly.

While both these approach are also using multiple datasets, the type of data processed and the goal of the processing is quite different from that which is presented in this article. In the aforementioned data fusion approaches, the goal is the combine annotations and labels added in different datasets by different people. This is not numerical information, but e.g. true land use information. The datasets are also not represented by grids but by vectorial maps.

2.3.2 Intuitive approach to grid remapping

The methods mentioned in Section 2.2 work on gridded data and transform the grid without any possibility to use additional data that might be available. Some key assumptions regarding data distribution are implied within the methods. While at first it seems that the only knowledge available is the input grid, it is very likely that there is additional knowledge available. Consider, for instance, an input grid that represents CO_2 concentrations on a course grid. From other research, the correlation between CO_2 levels and traffic is known. This means that we can use this known correlation to improve the CO_2 data set we have by using traffic information that is also available for the same region. Of course, the correlation between the input and additional datasets should be known beforehand, as this is a key assumption of the method. When this correlation is known, this information can be used to transform the grid that represents CO_2 emissions to a grid with a different cell size or with a different orientation.

The method that is presented allows for additional data to be taken into account when resampling the data to a new grid. Suppose additional data, which relates to the data in the input grid, is available in a grid containing five cells as shown on Fig. 2d.

Based on the values in the additional grid C, it is possible to guide the distribution of the values modelled on grid A to the new grid B. A low value in a cell of grid C suggests that the values in the overlapping cells of the output grid should also be lower.

By adopting a strict approach in the interpretation of this additional grid, it is possible to intuitively derive a simple distribution: proportional values for $f(B_1)$, $f(B_2)$, $f(B_4)$, $f(B_5)$. This interpretation means that the cells in the output grid B should have a value that is proportional to both the input grid A and the auxiliary grid C. In many situations, however, this cannot be achieved, as data in the grids can be slightly contradictory, a consequence of the fact that grids are approximations of the real situation. It is often not possible to derive a distribution when interpreting the related data grid with too strict an approach; but it is possible to derive a distribution that is still consistent with the input grid, and to some extent follows the related grid C. The related grid is thus only used to help determine the original, unknown distribution. Obviously, the grid used to help in transforming the data should contain a well established known relation to the input data. If the relationship between input grid and auxiliary grid are under investigation, any usage of the auxiliary grid in transforming the input grid may distort conclusions on the relationship between both grids.

To come to an intuitive solution consider cell B_3. To derive the $f(B_3)$, it is necessary to look at the grids A and C in the area around B_3. The cells that are of interest are A_1 and A_2. Both have the same value, so they will not provide much information. On the other hand, the cell C_2 that overlaps B_3 has a very low value ($f(C_2)=0$), whereas its neighbouring cells have high

values ($f(C_1)=f(C_3)=100$). As the data in grid C are known to be related to the data in A, we can conclude that the data of grid A for this region should be spread more towards the neighbouring cells of B_3, so the value $f(B_3)$ should be low.

Consider B_4. Again, the values of the overlapping cells in A are the same, so this will not influence the result. But the overlapping cell of grid C, C_3 has a high value. The neighbouring cells of C_3 have a low value. This basically implies that the distribution of A over the cells in B should also be lower in the proximity of cell C_3.

Finally, consider B_5. Here, the values of the overlapping cells in A are different: $f(A_2)=100$, $f(A_3)=0$. The distribution of the data in grid C tell us that in B_5, the value should be lower: no contribution from A_3, and C_3 has a much higher value than C_4.

The use of additional information, in this example a single grid, can doubtless contribute to securing a distribution that is still consistent with the input grid, but at the same time it takes into account the added available knowledge. From the examples though, it can be seen that it is not always possible to find a unique solution, implying there is still some uncertainty on the accuracy of the newly obtained grid.

The above example only uses a proportional or inverse proportional relationship between cells. This relationship is, however, only considered at a local scale, meaning that high and low for both input grid and additional grid are defined for the location under consideration, independent of the definition of other locations. As such, the connection between the input grid and the additional grid is not quantitatively verified, but only relative values are considered, which makes the approach not dependent on linearity or non-linearity. By considering different rules, it is even possible to model different connections, e.g. : *if a value is high or a value is low, then the output value should be high*. The ultimate goal is to allow multiple additional data layers, and make allowance for different possible combinations (e.g. a high value in one and a low value in another can yield a result that might well be the same as a low value in one and a high value in the other). On the other hand, consideration of the more quantitative connection between the layers can also provide better results. Both of these aspects are an area of future research.

3 Using intelligent techniques

3.1 Introduction to fuzzy sets and fuzzy inference

3.1.1 Fuzzy sets

Fuzzy set theory was introduced by Zadeh in (Zadeh 1965) as an extension of classical set theory. In a classical set theory, an object either belongs or does not belong to a set. In fuzzy set theory, the objects are assigned a membership grade in the range [0,1] to express the relation of the object to the set. These membership grades can have different interpretations (Dubois and Prade 1999): a veristic interpretation means that all the objects belong to some extent to the set, with the membership grade indicating the extent; whereas a possibilistic interpretation means that doubt is expressed as to which elements belong; now the membership grade is expressing the possibility that an element belongs to the set. Lastly, it is also possible for the membership grades to represent degrees of truth. In (Dubois and Prade 1999) it was shown that all other interpretations can be traced back to one of these three. The formal definition of a fuzzy set $\widetilde{A}$ in a universe U is given below

$$\widetilde{A} = \left\{ \left(x, \mu_{\widetilde{A}}(x) \middle| x \in U \right) \right\}$$

Its membership function $\mu\widetilde{A}(x)$ is

$$\mu_{\widetilde{A}} : U \rightarrow [0,1], \quad x \mapsto \mu_{\widetilde{A}}(x)$$

Various operations on fuzzy sets are possible: intersection and union are defined by means of functions that work on the membership grades, called respectively t-norms and t-co-norms. Any function that satisfies the specific criteria is a t-norm, respectively t-conorm and can be used to calculate intersection or union (Klir and Yuan 1995; Zimmerman 1999). Commonly used t-norms and t-conorms are the Zadeh-min-max norms, which use the minimum as the intersection and the maximum as the union (other examples are limited sum and product, Lukasiewicz norm, …).

Fuzzy sets can be defined over any domain, but of particular interest here are fuzzy sets over the numerical domain, called fuzzy numbers: the membership function represents uncertainty about a numerical value. The fuzzy set must be convex and normalized (some authors also claim the support must be bounded, but this property is not strictly necessary) (Klir and Yuan 1995). Using Zadeh's extension principle (Zadeh 1965), it is possible to define mathematical operators on such fuzzy numbers (addition, multiplication, etc.). Fuzzy sets can also be used to represent linguistic terms, such as "high" and "low"; this allows one to determine which numbers are considered high in a given context. Linguistic modifiers also exist and are usually a function that alters the membership function for the term it is associated with, allowing for an interpretation of the words like "very" and "somewhat".

Finally, it is necessary to make a distinction between an inclusive and an exclusive interpretation: are values that match "very high" still considered to be "high"? In the real world, people could say about a person: "he is not tall, but he is very tall", which is an exclusive interpretation: "very tall" does not imply "tall". The main difficulty when using fuzzy sets is the definition of the membership functions: why are the fuzzy sets and membership grades chosen as they are, and on what information is this choice based?

3.1.2 Fuzzy inference system

A fuzzy inference system is a system that uses a rulebase and fuzzy set theory to arrive at solutions for given (numerical) problems (Mendel 2001; Klir and Yuan 1995). The rulebase consists of fuzzy premises and conclusions; it is comprised a set of rules that are of the form

$$\text{if } \underbrace{x \text{ is } A}_{\text{premise}}, \text{ then } \underbrace{y \text{ is } B}_{\text{conclusion}}$$

Here "x is A" is the premise and "y is B" is the conclusion; x and y are values, with x the input value and y the output value. Both are commonly represented by fuzzy sets, even though x is usually a crisp value (crisp means not fuzzy). In the rule, A and B are labels, such as "high" or "low", also represented by fuzzy sets as described above.

The "is" in the premise of the rules is a fuzzy match: this will return a value indicating how well the value x matches with label A. As all the rules are evaluated and the values are fuzzy, it is typical that more than one rule can match: a value x can be classified as "high" to some extent and at the same time as "low" to a much lesser extent. All the rules that match will play a part in determining the outcome, but of course the lower the extent to which a rule matches, the less important its contribution will be. It is possible to combine premises using logical operators (and, or, xor) to yield more complex rules. As multiple rules match, y should be assigned multiple values by different rules: all these values are aggregated using a fuzzy

aggregator to yield one single fuzzy value. For each rule, the extent to which the premise matches impacts the value that is assigned to y.

The "is" in the conclusion is a basic assignment and will assign y with a fuzzy set that matches the label B. It is important to note that x and y can be from totally different domains, a classic example from fuzzy control is "if temperature is high, then the cooling fan speed is high".

While the output of the inference system is a fuzzy set, in practise the output will be used to make a decision and as such it needs to be a crisp value. To derive a crisp value (defuzzification), different operators exist. The centroid calculation is the most commonly used; it is defined as the centre of the area under the membership function.

3.2 Defining the inference system

The parameters for the inference system used are derived from generated sample cases, for which an optimal solution is known. The relations between the parameters that are found and the optimal solution are then reflected in the rules. Due to the more technical nature of this explanation, and the strict page limitation, a detailed explanation of the procedure is available as supplementary material in (Online Resource 1).

4 Experiments

4.1 Description of the results

In this section, results of the methodology applied on the example in Fig. 2d for several inputs will be shown and discussed. The input grid A has three grid cells, the output grid B contains eight grid cells, but does not exactly overlap with A and the auxiliary grid C has five grid cells and overlaps fully with grid A. It is obvious that the grids are not aligned properly.

Table 1 holds the data for the input grid, the auxiliary grid; and the computed output grid. The first three cases have a distribution of the input data such that $f(A_1)=f(A_2)=100$ and $f(A_3)=0$; the last three cases have the input distribution such that $f(A_1)=f(A_3)=100$ and $f(A_2)=0$. In each of the cases, a different distribution of the auxiliary grid was considered, as shown in Table 1. Figure 3 offers a graphic view of each of the cases. For each case, the grid cells are shown; the surface area of the circles is representative of the values associated with the grid cells. Consequently, the sum of the areas of the circles in grid B equals the sum of the areas in

Table 1 Overview of the cases used in the simulations

	Input grid A			Auxiliary grid C					Output grid B							
Case 1	100	100	0	100	100	100	0	0	25	50	52	27	46	0	0	0
Case 2	100	100	0	100	100	0	0	0	25	50	57	23	46	0	0	0
Case 3	100	100	0	100	0	0	100	0	29	50	44	23	54	0	0	0
Case 4	100	0	100	100	0	0	0	100	29	50	21	0	0	26	37	37
Case 5	100	0	100	100	100	0	0	100	25	50	25	0	0	26	37	37
Case 6	100	0	100	0	100	0	0	100	21	50	29	0	0	26	37	37

The grid layout is illustrated on Fig. 2d, these results are graphically illustrated in Fig. 3

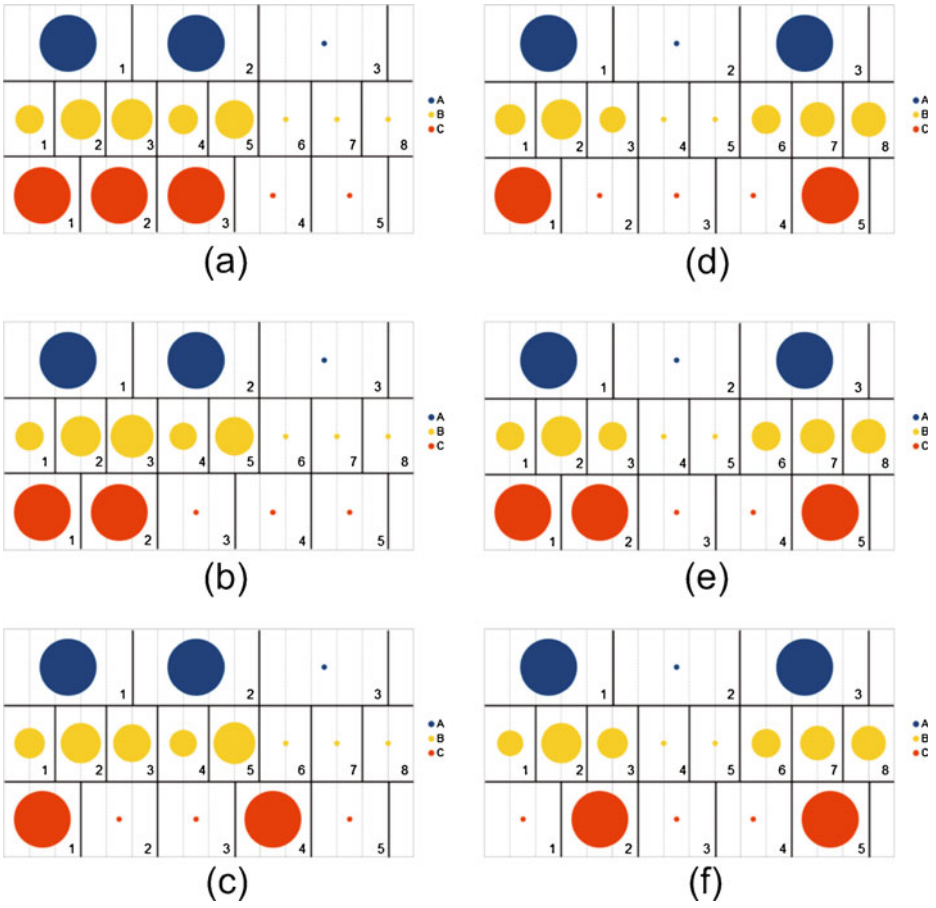

Fig. 3 Illustrations for the different cases from Table 1: *A* is the input grid, *B* is the output grid and *C* the auxiliary grid. The grid cells are drawn above each other for ease of visibility, but should cover each other as shown on Fig. 2d. The size of the circles reflects the relative value of the associated cell (a *small circle* is shown for 0 values, for purposes of illustration)

grid *A*. There is no quantitative relation assumed between the auxiliary grid *B* and the grid *A*, it is just assumed that high values in *B* are an indication for high values in *A*.

The behaviour of the methodology in different cases is clearly illustrated in Fig. 3.

Consider output cell B_2. From (Online Resource 1), the considered cells that play a part are: A_1 (proportionally), C_1 and C_2 (proportionally), A_2 (inverse proportionally). In all six cases, the value assigned to B_2 is the same. The reason is that, while the values of the involved cells differ (C_2 changes value), the locally computed definition for the fuzzy sets that defines low and high for the auxiliary grid is also changes. This is done in such a way, that the differing input is cancelled out. In the system, there is no difference between a value of, for example, 100 when low is defined as 0 and high is defined as 100, and a value of, for example, 200 when low is defined as 0 and high is defined as 200.

Cell B_3 shows a much bigger variation. The cells involved in determining the output value are A_1 and A_2 (proportionally), C_2 (proportionally), C_1 and C_3 (inverse proportionally). In case

1, the proportional and inverse proportional data is almost cancelled out, resulting in a value close to 50. In case 2, the value for C_3 is much smaller than in case 1, which results in a larger value of 57 for B_3. In case 3, the value of C_2 is decreased, and, as it is has a proportional relation to B_3, the value for B_3 is again decreased. It is smaller than in case 1, as the higher value of C_3 results in a higher value in B_5, which therefore compensates. The difference in cases 4 to 6 are explained by the change in the proportional and inverse proportional data from the auxiliary grid: in case 4 there is more inverse proportional than proportional (the value of C_1 is greater than the value of C_2), in case 5 they are equal, and in case 6 the proportional value is greater than the inverse proportional.

Cell B_4 is influenced by A_2 (proportional), C_3 (proportional), C_2 and C_4 (inverse proportional). The first case has a greater value than cases 2 and 3, as C_3 has a much higher value. The second and third cases result in the same value, as the change in the auxiliary grid also changes the definition for high, causing the change in values to be nullified. The value of 0 in the last three cases is due to the overlapping input field having 0 as an associated value.

Cell B_5 is determined by A_2 (proportional), C_3 and C_4 (proportional), A_3 (inverse proportional) and C_2. The first two cases are the same, as the definitions for high for the auxiliary grid is also changed. Case 3 shows a higher value, as there is a greater proportional contribution from C_4.

The cells B_6, B_7 and B_8 can be considered together. They all are 0 in the first three cases, as the overlapping input field has a value of 0. In cases 4, 5 and 6, the latter two have higher values, which is the expected behaviour due to the values of C_4 and C_5.

4.2 Observations of the methodology

From the cases in Fig. 3, it can be seen that the goal of using an auxiliary grid to guide the new distribution yields some interesting results. In general, the methodology does not yield contradictory effects: the output grid fully complies with the input grid. Compared to the traditional approaches (e.g. areal weighting, which would provide the same result for the first three cases), and the same result for the last three cases, it is clear that the additional data has an effect on the result.

The distribution in the output grid to some extent follows the auxiliary grid, but there are some exceptions. In the last three cases, the results appear to be consistent and as expected: larger values where the auxiliary grid overlaps, smaller values elsewhere. In the first two cases, the larger value of cell B_5 stands out. This is mainly explained by the fact that B_5 fully overlaps with A_2, and by the fact that the values of cells considered in the auxiliary grid cancel each other out, or the definition of high for the auxiliary values changes to yield this effect. Similarly, the value of B_3 in case 3 stands out as counter intuitive, but with a value of 44 it is still considerably smaller than in cases 1 (52) and 2 (57), which is consistent with the desired result. A similar observation can be made for cell B_6 in the last three cases: its value is perhaps higher than would be desired based on the auxiliary grid, but still the values for the cells that overlap with the cells of the auxiliary grid that have higher values also have higher values than B_6.

The results appear to achieve the desired goals, but still further testing and development of the methodology is required.

4.3 Future developments

The approach presented is a new concept and the first prototype implementation of a methodology that shows promising results, and as such justifies further research. The

prototype allows us to experiment in order to see how the system behaves and derive reasons for its behaviour. The outcome of the fuzzy inference system is dependent on a large number of parameters.

Firstly, there are the parameters that concern the geometrical aspects of the problems, the definition of the cells that are considered to have an influence on a given output cell. This not only concerns choosing which cells will take part in determining the value for the output cell, but also determining the behaviour (proportional or inverse proportional) and adding weights to the cells to decrease their influence (e.g. if the distance becomes too great to be relevant). In the current implementation, no quantitative relationship between auxiliary and input grid is assumed, meaning that the quantitative relation between input grid and additional grid is only considered for the vicinity of a cell. A quantitative relation on a bigger scale can, however, be used to derive how big the impact of the auxiliary cell should be, and as such should provide better results. This is, however, not a trivial step, as too tight a relationship may cause overly narrow constraints and consequently prevent the system from reaching a satisfactory solution when data is contradictory or missing.

Secondly, there are the parameters that define the rule base: this is not only the number of rules, but also the definition of the rules themselves and the weights assigned to the rules. At present, the number of rules is derived from all the possible combinations of the values of the cells that play a part. It is, however, possible to limit the rules and, for instance, consider a fixed number of rules that are determined automatically by means of training data. The full impact of this is quite difficult to estimate for the time being, however. Each of the rules can also be assigned a weight, and at present, lower weights are assigned to contradicting rules. In the examples in this article, this yielded little impact, as the data used in the input was not really contradictory. This parameter may become more important when confronting the system with real world data or missing data.

Lastly, there are the parameters that relate to the fuzzy sets used and their definitions. This includes the definitions of the fuzzy sets that represent high and low; the definitions of minimal and maximal values that are used in these fuzzy sets and the number of sets that are considered for both input and output. Also, the definitions of minimum and maximum of the domain (explained in (Online Resource 1)) can be improved: the current definitions may impose to big limitations upon possible input sets.

5 Conclusion

In this article, a completely novel approach to the map overlay problem was presented. The described methodology is in a very early stage, but already shows interesting results. Rather than assuming a distribution of the data, knowledge from external data that are known to relate to the input data are used to find a more optimal distribution of the data after transformation to a new grid. The methodology uses concepts from fuzzy set theory and algorithms from artificial intelligence in order to mimic reasoning about the input data. A prototype implementation is under construction and can already process artificially generated data. The results show that in simple cases, the methodology achieves the pre-set goal, but additional testing and fine tuning is necessary in order to find the best possible solution for a given input. The current prototype already makes allowance for the processing of larger datasets. The next step is to generate artificial but large scale data, in order to fine tune the workings of the methodology using a fully controlled environment and to assess the performance; both in accuracy and processing speed. Experiments on real world data are expected to follow, in order to fully study the potential and outcome of the proposed methodology.

Acknowledgments The study was conducted within the 7FP Marie Curie Actions IRSES project No. 247645, acronym GESAPU.

Open Access This article is distributed under the terms of the Creative Commons Attribution License which permits any use, distribution, and reproduction in any medium, provided the original author(s) and the source are credited.

References

Boychuk K, Bun R (2014) Regional spatial inventories (cadasres) of ghg emissions in the energy sector: accounting for uncertainty. Clim Chang. doi:10.1007/s10584-013-1040-9

Bun R, Gusti M, Kujii L, Tokar O, Tsybrivskyy Y, Bun A (2007) Spatial ghg inventory: analysis of uncertainty sources. A case study for ukraine. Water Air Soil Pollut Focus 7(4–5):483–494

Bun R, Hamal K, Gusti M, Bun A (2010) Spatial ghg inventory on regional level: accounting for uncertainty. Clim Chang 103:227–244

Dubois D, Prade H (1999) The three semantics of fuzzy sets. Fuzzy Sets Syst 90:141–150

Duckham M, Worboys M (2005) An algebraic approach to automated information fusion. Int J Geogr Inf Syst 19(5):537–558

Flowerdew R, Green M (1994) Areal interpolation and types of data. In: Fotheringham S, Rogerson P (eds) Spatial analysis and GIS. Taylor & Francis, London, pp 141–152

Fritz S, See L (2005) Comparison of land cover maps using fuzzy agreement. Int J Geogr Inf Sci 19:787–807

Gotway CA, Young LJ (2002) Combining incompatible spatial data. J Am Stat Assoc 97(458):632–648

Jonas M, Nilsson S (2007) Prior to economic treatment of emissions and their uncertainties under the kyoto protocol: scientific uncertainties that must be kept in mind. Water Air Soil Pollut Focus 7(4–5):495–511

Jonas M, Marland G, Winiwarter W, White T, Nahorski Z, Bun R, Nilsson S (2010) Benefits of dealing with uncertainty in greenhouse gas inventories: introduction. Clim Chang 103:3–18

Klir GJ, Yuan B (1995) Fuzzy sets and fuzzy logic: theory and applications. Prentice Hall, New Jersey

Mendel JM (2001) Uncertain rule-based fuzzy logic systems, introduction and new directions. Prentice Hall, Upper-Saddle River

Rigaux P, Scholl M, Voisard A (2002) Spatial databases with applications to GIS. Morgan Kaufman Publishers, San Francisco

Shekhar S, Chawla S (2003) Spatial databases: a tour. Pearson Educations, London

Zadeh LA (1965) Fuzzy sets. Inf Control 8:338–353

Zimmerman HJ (1999) Practical applications of fuzzy technologies. Kluwer Academic Publishers, Dordrecht

DOI 10.1007/978-3-319-15901-0_11
Reprinted from *Climatic Change* Journal, DOI 10.1007/s10584-013-1028-5

Determination of the uncertainties of the German emission inventories for particulate matter and aerosol precursors using Monte-Carlo analysis

Wolfram Joerss

Received: 14 January 2013 / Accepted: 1 December 2013 / Published online: 20 December 2013
© Springer Science+Business Media Dordrecht 2013

Abstract This paper presents the application of a Monte-Carlo simulation for assessing the uncertainties of German 2005 emissions of particulate matter (PM_{10} & $PM_{2.5}$) and aerosol precursors (SO_2, NO_x, NH_3 and NMVOC) carried out in the PAREST (PArticle REduction STrategies) research project. For the uncertainty analysis the German Federal Environment Agency's emission inventory was amended and integrated with a model on the disaggregation of energy balance data. A series of algorithms was developed in order to make efficient and pragmatic use of available literature and expert judgement data for uncertainties of emission model input data. The inventories for PM_{10} (95 %-confidence interval: −16 %/+ 23 %), $PM_{2.5}$ (−15 %/+19 %) and NO_x (−10 %/+23 %) appear most uncertain, while the inventories for SO_2 (−9 %/+9 %), NMVOC (−10 %/+12 %) and NH_3 (−13 %/+13 %) show a higher accuracy. The source categories adding the most relevant contributions to overall uncertainty vary across the pollutants and comprise agriculture, mobile machinery in agriculture and forestry, construction sites, small businesses/carpentries, cigarette smoke and fireworks, road traffic, solvent use and stationary combustion. The PAREST results on relative uncertainties have been quoted in the German Informative Inventory Reports since 2012. A comparison shows that the PAREST results for Germany are within the range of (for NH_3: close below) other European countries' results on air pollutant inventory uncertainties as reported in the 2013 Informative Inventory Reports.

1 Introduction

The assessment of the uncertainties of air pollutant and greenhouse gas emission inventories is important both for the management of inventory improvement and for the choice of mitigation measures. It is good practice according to the respective international reporting guidelines (EMEP/EEA 2009; IPCC 2001; Eggleston et al. 2006). In these guidelines, two basic

This article is part of a Special Issue on "Third International Workshop on Uncertainty in Greenhouse Gas Inventories" edited by Jean Ometto and Rostyslav Bun.

W. Joerss (✉)
Energy & Climate, Oeko-Institut e.V., Schicklerstr. 5-7, 10179 Berlin, Germany
e-mail: w.joerss@oeko.de

approaches for key category analysis are proposed: Approach1/Tier1 is based on error propagation while Approach2/Tier2, makes use of Monte Carlo analysis.

The importance of statistical dependence in input data (which is better captured by Monte Carlo analysis) for the overall inventory uncertainty was explored e.g. by Winiwarter and Muik (2010) for the example of the Austrian national greenhouse gas inventory. Monte-Carlo analysis so far has rarely been used for air pollutant emission inventories (e.g. Passant 2002; van Gijlswijk et al. 2004; SYKE 2005). For greenhouse gas emission inventories, however, a wider range of Monte Carlo based uncertainty studies is available. An overview is contained e.g. in Fauser et al. 2011.

In the PAREST research project, (PArticle REduction STrategies, cf. Builtjes et al. 2010), funded by the German Federal Environment Agency (UBA), emission scenarios until 2020 were constructed for particulate matter (PM_{10} und $PM_{2.5}$) as well as aerosol precursors SO_2, NO_x, NH_3 and NMVOC, both for Germany and Europe. Reduction measures were assessed and finally air quality in Germany was modelled. In this framework, also the uncertainties of the nationally aggregated German 2005 emission estimates for all covered pollutants were assessed.

The objective of the exercise was on one hand to assess the accuracy of the emission estimates and to identify those source categories which add most to the inventories' total uncertainties, which is the topic of this paper, as well. On the other hand, the results on uncertainties were used within the PAREST project to construct sensitivity runs for air quality modelling (cf. results in Stern 2010).

In the operationalisation of uncertainties we concentrate on the aspect of accuracy in contrast to completeness (for a discussion of different aspects of uncertainty in emission inventories cf. Aardenne 2002). For the uncertainty analysis, a Monte-Carlo analysis was deemed to be preferable to a "simple" calculation of error propagation, as the uncertainties met for the input data to the considered inventories are often rather high (up to an order of magnitude) and correlated.

The results of the exercise presented here have been quoted in the German Informative Inventory Reports beginning with the 2012 report (cf. UBA 2012 and UBA 2013).

2 The emission model

The emission inventories used and enhanced in PAREST build upon the German Federal Environment Agency's emission data base ZSE (Central System Emissions, copy of 08 June 2007), including a wide range of sectoral emission estimation models which are used to feed the database with activity rates (AR), emission factors (EF), emissions (EM) and/or other relevant variables for the calculation of emissions, e.g. split factors (SF). For the inventories relevant for PAREST, the ZSE data base features approx. 900 time series of activity rates and approx. 450 to 700 time series of emission factors for each of the pollutants respectively.

Notably, energy related data for stationary use are processed in the separate model BEU ("Balance of Emission Causes", described in Joerss and Kamburow 2006), which is used to disaggregate the official German energy balance into more than 400 segments of fuel use in order to meet a highly differentiated set of emission factor structure distinguishing a variety of fuels, economic sectors, combustion technologies, installation sizes and applicable environmental legislation. Other sophisticated external models are used to generate ZSE input data e.g. for traffic and mobile machinery, agriculture and solvent use. The full data set is characterised in Joerss et al. 2010.

3 Operationalising uncertainties

The mathematical operations in the assessed deterministic emission model (consisting mainly of the ZSE and BEU models/data bases) can be roughly reduced to three types of equations:

$$AR_i * EF_{i,x} = EM_{i,x}, \tag{1}$$

where AR_i is the activity rate for source category i, $EFi_{,x}$ is the emission factor for pollutant x in source category i, $EM_{i,x}$ is the emission of pollutant x from source category i,

$$EM_{i,x} + EM_{j,x} = EM_x, \tag{2}$$

where $EM_{i,x}$ is the emission of pollutant x from source category i, $EM_{i,x}$ is the emission of pollutant x from source category j, EM_x is the total emission of pollutant x from source categories i and j, and

$$AR_m = AR_P * f \text{ in conjunction with } AR_n = AR_P * (1-f), \tag{3}$$

where AR_m is the activity rate for source category m, AR_n is the activity rate for source category n, AR_P is the primary activity rate (sum of source categories m and n), f is the split factor.

Thus, in the uncertainty assessment of the emission model, we need to attribute an uncertainty to all input variables, .i e. in the example of Eqs. (1) to (3) above to the variables AR_i, $EF_{i,x}$, AR_P and f (the factor f is subject to uncertainty as well!). Based on that, we can compute uncertainties of the model results, in the example above that is for EM_x, AR_m and AR_n, and as well for $EM_{i,x}$ and $EM_{j,x}$.

In line with the 2006 IPCC guidelines (Eggleston et al. 2006), we use a relative uncertainty, expressed in percent of the mean (or reference) value which are used in the deterministic model: Mathematically/stochastically, these uncertainties are defined through the 95 % confidence interval of an assumed probability distribution. In the interpretation of the application to an emission inventory, however, we switch from a statistical concept of probability to a Bayesian concept which defines probability as the subjective degree of belief (cf. Morgan and Henrion 1990). With this presumption, we interpret expert judgement and literature sources on uncertainties of input data as explained below.

For the aggregation of uncertainties in an emission model/inventory along Eqs (1) to (3) above, the 2006 IPCC guidelines offer two basic approaches, i.e. error propagation rules and Monte-Carlo simulation. Error propagation is easier to perform. However, it does not produce reliable results for comparably high uncertainties: Eggleston et al. (2006) set a variation coefficient of 0.3 as a limit which corresponds to ±58 % for a normal distribution. Furthermore it is restricted to symmetric probability density functions and cannot account for correlations. As all the restrictions are not met in our application, a Monte-Carlo simulation approach was chosen.

In a Monte-Carlo simulation, each input variable of the emission model is represented by a full probability density function, defined by a shape (e.g. normal, lognormal etc.) a mean (the reference of the deterministic model) and 2.5 % and/or 97.5 % percentiles (as the borders of the 95 % confidence interval). The Monte-Carlo analysis simulates a large number of random experiments. In each run, for every input variable a random value is taken which then feeds the calculation of the model results. For the whole set of model runs (we generally used 10,000 runs, using @Risk 5.5 software package) the predefined probability distribution for each input variable is maintained. Consequently, the model outputs, i.e. usually aggregated emissions or any intermediate calculation step, are distribution functions as well and can be characterised e.g. by mean value and the 95 % confidence interval.

For the characterisation of the input variable we have used a set of mathematically well-defined distributions, i.e. normal, triangle, uniform, lognormal and inverse lognormal (Fig. 1):

While normal, triangle and uniform distributions have symmetric probability density functions, the lognormal distributions are asymmetric and feature different percentage values for the upper and lower border of the confidence interval. These upper and lower values cannot be chosen freely, though: A lognormal distribution is characterised by the parameters μ and σ, and each specific lognormal distribution is well defined through its mean value plus only one percentile (cf. Müller 1991):

$$E(X) = e^{\mu + \frac{\sigma^2}{2}} \tag{4}$$

where *E(Xn* is the mean of the lognormal distribution, μ and σ are location parameters of the lognormal distribution and

$$x_{(p)} = e^{\mu + u_{(p)} \cdot \sigma}, \tag{5}$$

where $x(p)$ is p-quantile of the lognormal distribution, $u(p)$ is the p-quantile of the standardised normal distribution (for p=2.5 %, $u(p)$ equals −1.96; for p=97.5 %, $u(p)$ equals 1.96), μ and σ are location parameters of the lognormal distribution.

With a known (or pre-defined) mean value (i.e. the reference value of the deterministic model) and a guess for just one of the borders of the 95 % confidence interval, the other border can be computed. Furthermore, it can be deducted from Eqs. (4) to (5) that for a lognormal distribution the 97.5 % quantile's maximum deviation from the mean is approx. 583 %. Accordingly, the minimum 2.5 % quantile is at approx. −99.7 %

This has important implications for the use of expert judgement or literature for feeding the model with uncertainties of input variables, as a quote of e.g. "mean value X, +200 %/−70 %, lognormal" does not meet both Eqs. (4) and (5) and thus cannot be translated into the Monte Carlo analysis without further processing. In parallel, an expert estimation like "factor 10" (i.e. +900 %) cannot directly be used as a 97.5 % quantile of a lognormal distribution.

In order to pragmatically make use of existing data sources for uncertainties, we developed an algorithm to generate a mathematically well-defined lognormal distribution:

1. The distribution type "lognormal" and the mean (reference) value are kept unchanged.
2. The expert guess of the lower deviation is interpreted as a 2.5 % quantile. A fitting 97.5 % quantile is calculated through Eqs. (4) and (5)
3. We compare the thus calculated value with the original expert guess for the upper deviation and take the arithmetic mean (as a maximum, however the above mentioned 583 % limit) as the 97.5 % quantile for the Monte-Carlo simulation.
4. The 2.5 % quantile of the distribution used for the simulation can again be calculated using Eqs. (4) and (5).

This algorithm was chosen in order to maintain the mean (reference) value for emission calculation unchanged, which was a prerequisite in the PAREST context. In a project

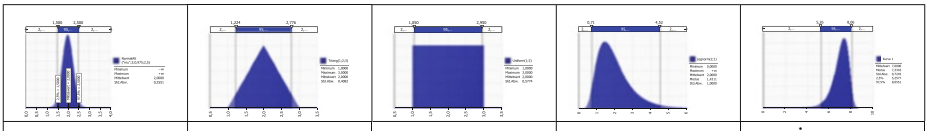

Fig. 1 Distribution types used for input variables

framework which allows for a change or improvement of a "best guess" reference, other choices might deem appropriate.

As mentioned above, correlations between input variables have to be regarded in the uncertainty assessment. To account for that, the emission model was cleared from all redundancies to make sure that each piece of information on the physical world which is used in several parts of the model is transferred into a probability function exactly once during each model run. This applies both to correlation within a given pollutant inventory as well as across pollutants, if e.g. the same activity rates are used for emission calculation of several pollutants. Additionally, $PM_{2.5}$ emissions and emission factors are calculated using (uncertain) split factors based on PM_{10} emissions/emission factors.

4 Data sources and choice of distributions types for input parameters

In order to carry out a Monte-Carlo simulation it was then necessary to determine the shapes and quantiles of the probability functions that replace the deterministic input variables. This means in particular the respective types of distribution and 2.5 %/97.5 % quantiles (the means were fixed anyway through the deterministic model). The sources for these parameters were taken over from primary and secondary literature or estimated through expert judgement and varied with the source categories, pollutants and type of values (i.e. emission factors (EF), emissions (EM), activity rates (AR) or split factors (SF). For a full and detailed documentation of all data sources for uncertainty parameters, assumptions made and sectoral allocations we refer the reader to Joerss and Handke 2010. Table 1 gives a rough overview, though:

Comparable effort was put into split factors, concerning whose uncertainties hardly any literature source was available. In our emission model, split factors (determining one entity to represent x% (x in the range of 0 %–100 %) of logically larger entity already calculated in the model) are in particular important on one hand for the disaggregation of energy balance activity data (technology splits, fuel splits, full load hours etc. in the BEU model) and on the other hand for the calculation of $PM_{2.5}$ emissions based on PM_{10} emissions. While split factors bearing the values of straight 100 % or 0 % in the deterministic model were kept unchanged as constant factors in the probabilistic model (otherwise, the mean of the probability distribution could not have met the reference value), for all "real" split factors with the value x with $0\ \% < x < 100\ \%$ algorithms were defined for the conversion into a probability function: First, the distribution type was defined (lognormal if close to 0 % or 100 %, normal if rather medium. Second, the 2.5 %/97.5 % quantiles were defined depending on both the chosen distribution and on relative position of the reference/mean value. The details of the algorithms uses are documented in Joerss and Handke 2010 (p.30f).

Generally, for the implementation of Monte-Carlo analysis to the emission model, logical correlations within the respective sets of EF, AR and SF were considered, based on a thorough understanding of the modelled emission sources. For example, the German emission model separates fuel use in cogeneration plants into fuel use for power generation and fuel use for heat generation. Both amounts of fuel are multiplied with the same emission factors for emissions calculation. In the Monte Carlo calculation, a single emission factor (per pollutant) was used in order to make sure that high and low variations of the emission factors of these cogeneration plants would not outweigh each other.

A detailed description of the analysis performed and a full documentation of assumptions made is given in Joerss and Handke 2010.

Table 1 Data sources for uncertainty parameters

Source category	Data source		
	Research project reports commissioned by the German Federal Environment Agency (UBA) targeted on emissions, emission factors and/or uncertainties	EMEP/EEA air pollutant emission inventory guidebook—2009	Own estimates
Stationary combustion	Energy balance (AR), Distribution parameters for energy balance (partly) EF SO_2, NO_x, NMVOC, PM_{10}	EF NH_3	distribution parameters for energy balance
Road traffic	AR, EF NO_x, NMVOC & SO_2	EF NH3 & PM_{10} (exhaust); EF PM_{10} road/break/tyre wear	EF PM_{10} resuspension
Other surface traffic	AR, EF NO_x & PM_{10}	EF NMVOC, SO_2 & NH_3	
Agriculture	AR, EF NH_3, NO_x, & NMVOC	EF PM_{10}	
Solvent use	EM		
Handling of bulk materials	AR & EF (UBA expert judgement)		
Other source categories	partly	partly	partly
References	Dämmgen 2008; Dämmgen et al. 2009; Degel and Joerss 2009; Harthan et al. 2007; Handke et al. 2004; Joerss and Handke 2010; Joerss 2010; Kludt 2009; Knörr et al. 2009; Rentz et al. 2002; Schaap et al. 2009; Struschka et al. 2003; Struschka et al. 2008; Theloke 2005		

Reprinted from the journal

5 Results for germany

The aggregated results of the uncertainty assessment are summarised in Table 2:

A more specific view on the sectoral contributions to the overall uncertainties shows Fig. 2 below, using an adapted version of the SNAP emission reporting format.

Looking at the aggregated results (Table 2 above), the inventories for PM_{10} (95 %-confidence interval: −16 %/+23 %), $PM_{2.5}$ (−15 %/+19 %) and NO_x (−10 %/+23 %) appear most uncertain, while the inventories for SO_2 (−9 %/+9 %), NMVOC (−10 %/+12 %) and NH_3 (−13 %/+13 %) show a higher accuracy.

The uncertainty of PM_{10} emissions is spread over a wide range of source categories the most important being (in decreasing order) construction sites, small businesses/carpentries and resuspension of road dust by road traffic. For $PM_{2.5}$, a wide spread is observed as well. Top contributions are calculated for small businesses/carpentries, Fireworks & cigarette smoke, mobile machinery in agriculture & construction and resuspension of road dust. SO_2 emission uncertainties are mostly allocated to fuel combustion (coal-fired power plants & light fuel oil boilers), with further relevant contributions by industrial processes and refineries. NO_x emission uncertainties, however, are dominated by the emission of fertilizer application in agriculture. Other relevant contributions to overall uncertainties are calculated for road transport and mobile machinery. NH_3 uncertainties are strongly dominated by agricultural emissions (−13 %/+14 % corresponding to −77/+79 Gg). These uncertainties split into CRF/NFR 4B emissions from manure management (−14 %/+14 % corresponding to −65/+66 Gg) and CRF/NFR 4D emissions from soils (−44 %/+43 % corresponding to −42/+42 Gg). The two major sources for NMVOC emission uncertainties are solvent use and agriculture (manure management). Furthermore, wood combustion and road traffic (petrol engines).

Looking across the analysed pollutants (Fig. 2 above), the source categories adding the most relevant contributions to overall uncertainty vary across the pollutants and comprise

- agriculture (NO_x from fertiliser application, NMVOC from manure management, NH_3 from animal husbandry and cultivation of land, PM_{10} from pig fattening),
- mobile machinery in agriculture and forestry (PM_{10}, $PM_{2.5}$ and NO_x),
- construction sites (PM_{10}),
- small businesses/carpentries (PM_{10} and $PM_{2.5}$),
- cigarette smoke and fireworks ($PM_{2.5}$),

Table 2 Aggregated uncertainties in the German emission inventory 2005

Uncertainties in the German emission inventory 2005

PAREST reference scenario, emission calculation according to inland principle

Pollutant	2005 emission level	95 %-confidence interval	
	[Gg]	2.5 %-quantile	97.5 %-quantile
PM_{10}	262	−16 %	23 %
$PM_{2.5}$	136	−15 %	19 %
SO_2	562	−9 %	9 %
NO_x	1 544	−10 %	23 %
NH_3	607	−13 %	13 %
NMVOC	1 438	−10 %	12 %

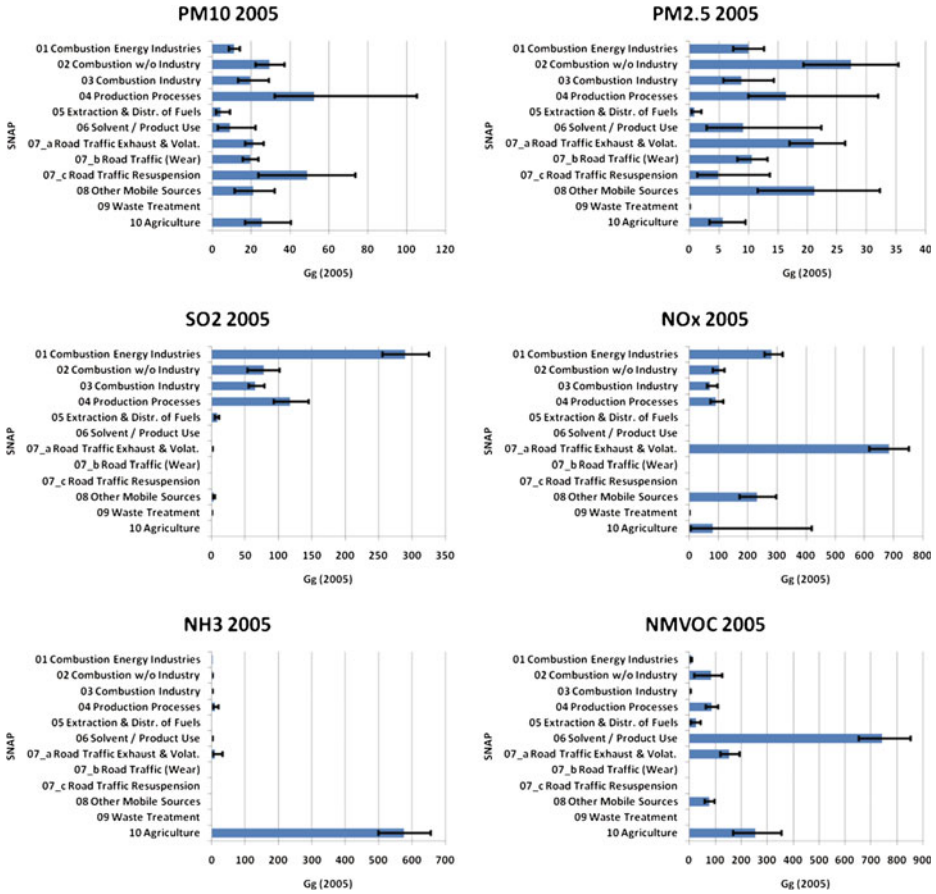

Fig. 2 German 2005 Emissions and Uncertainties (SNAP format)

- road traffic (PM_{10} and $PM_{2.5}$ from resuspension of road dust, NO_x from heavy duty vehicles and passenger cars, NMVOC and NH_3 from petrol engines),
- solvent use (NMVOC) and
- stationary combustion (SO_2 from coal-fired power plants and oil-fired domestic furnaces, PM_{10} and NMVOC from wood firing).

No other comprehensive estimation of recent German emissions of particulate matter is available which might be used to compare the outcomes for $PM_{2.5}$ and PM_{10}. The same situation holds for NMVOC.

For SO_2, NO_X and NH_3, Suutari et al. (2001) have complied uncertainties of emission inventories for 1990 and 2010 projections for individual countries in Europe based on IIASA's RAINS model. In that study, German 1990 SO_2 emissions were assessed with an uncertainty of ±6 % for the Old German Länder (former West Germany) and ±16 % for the New German Länder (former GDR). 1990 NO_X uncertainties are estimated as ±15 % for New Länder and ±11 % for Old Länder and 1990 NH_3 uncertainties are estimated as ±16 % for New Länder and ±11 % for Old Länder. An aggregation of those figures to the level of Germany as a whole using error propagation

results in 5 280 Gg SO_2 ±13 %, 2 662 Gg NO_X ±9 % and 757 Gg NH_3 ± 9 %. However, given the very high difference in emission levels between 1990 (Suutari et al. 2001) and 2005 (this paper) the uncertainty percentages can hardly be compared.

6 Comparison with other countries

Next to Suutari et al. (2001), few estimates of single national emission inventories of aerosol precursors were made in the past decade, e.g. Rypdal (2002), van Gijlswijk et al. (2004) or the annual series of Dutch "environmental balances", the latest including uncertainty data being PBL (2009). However in recent Informative Inventory Reports to the UNECE Convention on Long-range Transboundary Air Pollution a growing number of parties reports on quantified uncertainty assessments:

Figure 3 below shows an overview of relative uncertainties as reported in 2013 Informative Inventory Reports to the UNECE Convention on Long-range Transboundary Air Pollution as documented in CEIP 2013 (Norwegian data not included as they are methodologically not comparable).

For NH_3, the German PAREST results (±13 %) show the lowest uncertainties of all countries contained in Fig. 3, however, in the same range as the Netherlands (±17 %) and

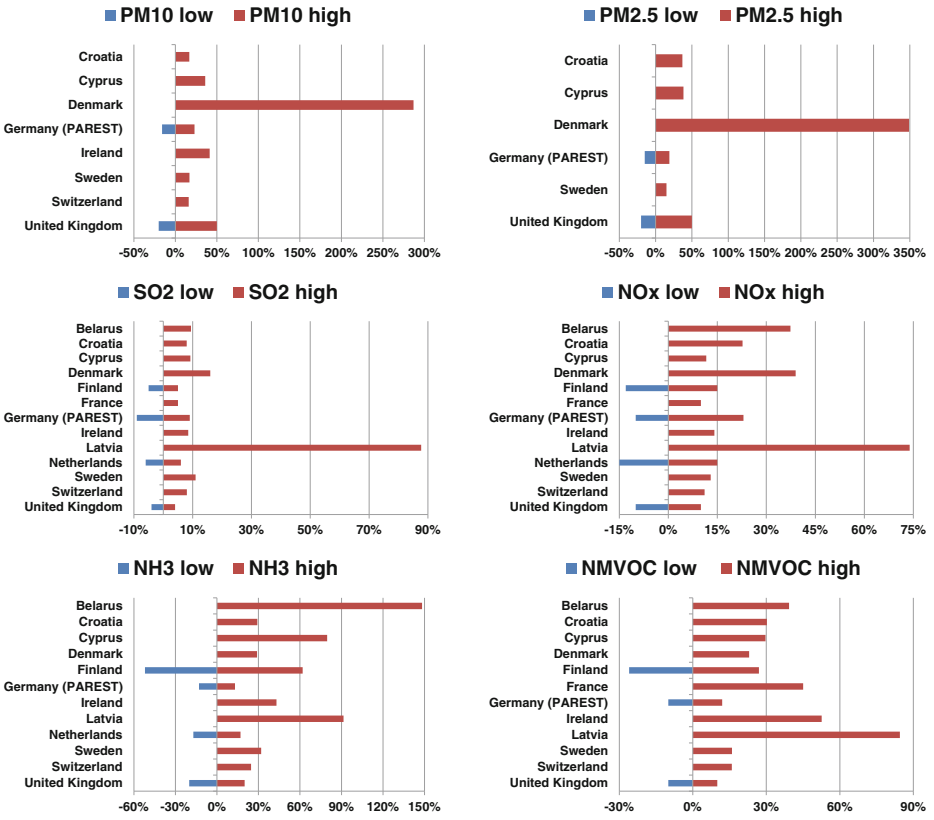

Fig. 3 Comparison of relative uncertainties as reported in 2013 Informative Inventory Reports (collected in CEIP 2013)

the United Kingdom (±20 %). For all other pollutants, the German results on relative uncertainties as developed in the PAREST project are within the range of other countries' uncertainty data.

Next to the German data, the uncertainty results for Finland, the Netherlands and the United Kingdom were calculated using a Monte Carlo approach. All other countries' data are based on Tier1 error propagation methodologies. Underlying studies considerably differ in reference years, aggregation levels of assessed sectoral emissions and methodologies applied. However, an in-depth analysis of differences of the relative uncertainties is beyond the scope of this paper.

7 Conclusions and look ahead

Within the PAREST project, the German Federal Environment Agency's (UBA's) 2005 emission inventories for particulate matter (PM_{10} & $PM_{2.5}$) and aerosol precursors (SO_2, NO_x, NH_3, NMVOC) was amended and for the first time successfully fed into a Monte-Carlo analysis for uncertainty assessment. Progress was made in particular by fully integrating into the uncertainty analysis the UBA's "BEU" model for processing energy balance data into the inventory. Overall uncertainties of the covered pollutants were determined, and rough sectoral analyses were made. The uncertainty results calculated for Germany are in the range of other recent uncertainty assessment of European countries.

Looking ahead, however, there appear a couple of issues worthwhile to be treated in future work:

- A full key source analysis according to IPCC standards for each of single pollutant inventories.
- A cross-pollutant key source analysis taking into account ambient air PM generation potentials which can be deducted from the air quality modelling performed in PAREST.
- A further validation of the developed probabilistic emission inventory model by performing sensitivity runs on parameter settings and reviewing of key parameters.
- An application of the methodological advance in particular of energy related uncertainties on the German greenhouse gas inventories.

References

Aardenne JA (2002) Uncertainties in emission inventories. Thesis Wageningen University, ISBN 90-5808-641-0

Builtjes P, Theloke J, Stern R, Joerss W (2010) PAREST-final report to the German federal environment agency (UBA), FKZ 206 43 200/01 "Strategien zur Verminderung der Feinstaubbelastung", UBA-TEXTE Nr. 9/2012, Dessau-Roßlau: Umweltbundesamt, ISSN 1862–4804

CEIP 2013: EMEP Centre on Emission Inventories and Projections: CLRTAP Inventory Submissions 2013; available in the internet: http://www.ceip.at/status-of-reporting/2013-submissions/; accessed 8 August 2013

Dämmgen U (2008) Expert Judgement on uncertainties of German agricultural emissions, 01. 04.2008.

Dämmgen U, Haenel HD, Rösemann C, Conrad J, Lüttich M, Döhler H, Eurich-Menden B, Laubach P, Müller-Lindenlauf M, Osterburg B (2009) Calculations of emissions from German agriculture—national emission inventory report (NIR) 2009 for 2007. Johann Heinrich von Thünen-Institut Bundesforschungsinstitut für Ländliche Räume, Wald und Fischerei (vTI) Braunschweig, 2009. ISSN 0376–0723, ISBN 978-3-86576-049-4.

Degel, M Joerss W (2009) Aufbereitung von Daten der Emissionserklärungen gemäß 11. BImSchV aus dem Jahre 2004 für die Verwendung bei der UNFCCC-und UNECE-Berichterstattung—Teilbericht Stationäre Verbrennungsmotoren. UBA-TEXTE Nr. 45/2009, Dessau-Roßlau: Umweltbundesamt, ISSN 1862–4804

Eggleston HS, Buendia L, Miwa K et al. (ed.) (2006) IPCC guidelines for national greenhouse gas inventories. Prepared by the national greenhouse gas inventories programme. Japan. http://www.ipcc-nggip.iges.or.jp/public/2006gl/index.html

EMEP/EEA air pollutant emission inventory guidebook—2009; EEA Technical report No 6/2009, Copenhagen, 2009; ISBN 978-92-9213-034-3; DOI 10.2800/23924; http://www.eea.europa.eu/publications/emep-eea-emission-inventory-guidebook-2009

Fauser P, Sørensen P, Nielsen M, Winther M, Plejdrup M, Hoffmann L, Gyldenkærne S, Hjorth Mikkelsen M, Albrektsen R, Lyck E, Thomsen M, Hjelgaard K, Nielsen O (2011) Monte Carlo (Tier 2) uncertainty analysis of Danish Greenhouse gas emission inventory. Greenhouse Gas Measurement and Management 1(3–4):145–160

Handke V, Joerss W, Pfitzner R, Brinkschneider F, Schollenberger H (2004) Das Qualitäts-System-Emissionsinventare-Handbuch. Report to the German Federal Environment Agency (UBA) FKZ 202 42 266; Berlin: IZT

Harthan R, Graichen J, Graichen V, Repenning R, Ziesing HJ, Wittke F (2007) Dokumentation der Datenqualität von Aktivitätsdaten für die Berichte über Emissionen aus stationären Feuerungen im Rahmen des Nationalen Inventarberichtes und des Monitoring Mechanismus nach RL EG 99/296; Report to the German Federal Environment Agency (UBA) FKZ 204 41, Berlin, 2007

IPCC (2001) Good practice guidance and uncertainty management in national greenhouse gas inventories. IPCC National Greenhouse Gas Inventories, Technical Support Unit

Joerss W, Kamburow C (2006) Bilanzierung und Modellierung emissionsrelevanter Daten zum Energieverbrauch in stationären Quellen. WerkstattBericht Nr. 78. Berlin: IZT—Institut für Zukunftsstudien und Technologiebewertung

Joerss W (2010) Emissionen aus Offener Verbrennung in Deutschland. Report to the German Federal Environment Agency (UBA), in the framework of the PAREST project FKZ 206 43 200/01 „Strategien zur Verminderung der Feinstaubbelastung, UBA-TEXTE Nr. 42/2013, Dessau-Roßlau: Umweltbundesamt, ISSN 1862–4804

Joerss W, Handke V (2010), Unsicherheiten der PAREST-Referenz-Emissionsdatenbasis; Report to the German Federal Environment Agency (UBA), in the framework of the PAREST project FKZ 206 43 200/01 "Strategien zur Verminderung der Feinstaubbelastung", UBA-TEXTE Nr. 45/2013, Dessau-Roßlau: Umweltbundesamt, ISSN 1862–4804

Joerss W, Kugler U, Theloke J (2010) Emissionen im PAREST-Referenzszenario 2005 – 2020; Report to the German Federal Environment Agency (UBA), in the framework of the PAREST project FKZ 206 43 200/01 "Strategien zur Verminderung der Feinstaubbelastung", UBA-TEXTE Nr. 46/2013, Dessau-Roßlau: Umweltbundesamt, ISSN 1862–4804

Kludt R (2009) Expert Judgement on uncertainties of activity rates and emission factors for particulate matter emissions from handling of bulk materials. Berlin 26(8):2009

Knörr W, Heldstab J, Kasser F, Keller M (2009) Ermittlung der Unsicherheiten der mit den Modellen TREMOD und TREMOD-MM berechneten Luftschadstoffemissionen des landgebundenen Verkehrs in Deutschland. INFRAS AG Zürich, Schweiz. ifeu-Institut für Energie- und Umweltforschung. Heidelberg. Commissioned by the German Federal Environment Agency (UBA). FKZ 360 16 023. Heidelberg/Zürich/Bern, 20. Juli 2009

Morgan MG, Henrion M (1990) Uncertainty. A guide to dealing with uncertainty in quantitative risk and policy analysis. Cambridge University Press, Cambridge. ISBN 0-521-42744-4

Müller PH (1991) Lexikon der Stochastik. Akademie Verlag, Berlin, 5. Auflage

Passant NR (2002): Estimation of Uncertainties in the National Atmospheric Emissions Inventory; AEA Technology; Report No. AEAT/ENV/R/1039 issue 1

PBL 2009: N.J.P. Hoogervorst and A. Hoen (project management), H.S.M.A. Diederen, F.J. Dietz, A.H. Hanemaaijer, R.B.A. Koelemeijer, K. Kovar, S. Kruitwagen, P. Lagas, C.J. Peek, G.A. Rood, M. Verdonk, H.J. Westhoek, W.J. Willems (2009): Milieubalans 2009; PBL-report 500081015; ISBN: 978-90-6960-231-8

Rentz O, Karl U, Peter H (2002) Ermittlung und Evaluierung von Emissionsfaktoren für Feuerungsanlagen in Deutschland für die Jahre 1995, 2000 und 2010. UBA-report 299 43 142.

Rypdal K (2002) Uncertainties in the Norwegian emission inventories of acidifying pollutants and volatile organic compounds. In: Environmental Science & Policy, Jg. 5, H. 3, S. 233–246.

Schaap M, Manders AMM, Hendriks ECJ, Cnossen JM, Segers AJS, van der Gon Denier HAC, Jozwicka M, Sauter F, Velders G, Mathijssen J, Builtjes PJH (2009) Regional modelling of particulate matter for the Netherlands. Technical report BOP, research carried out for Ministry of Housing, Spatial Planning and the Environment (VROM), Bilthoven, Netherlands

Stern R (2010) Analyse der Unsicherheiten/Bandbreiten in der im PAREST-Projekt verwendeten Kausalkette Emission-Transmission-Immission; Report to the German Federal Environment Agency

(UBA), in the framework of the PAREST project FKZ 206 43 200/01 “Strategien zur Verminderung der Feinstaubbelastung”, UBA-TEXTE Nr. 66/2013, Dessau-Roßlau: Umweltbundesamt, ISSN 1862–4804

Struschka M, Zuberbühler U, Dreiseidler A, Dreizler D, Baumbach G, Hartmann H, Schmid V, Link H (2003) Ermittlung und Evaluierung der Feinstaubemissionen aus Kleinfeuerungsanlagen im Bereich der Haushalte und Kleinverbraucher sowie Ableitung von geeigneten Maßnahmen zur Emissionsminderung, Report to the German Federal Environment Agency (UBA); UBA-TEXTE 41/03, ISSN 1862–4804.

Struschka M, Kilgus D, Springmann M, Baumbach G (2008) Effiziente Bereitstellung aktueller Emissionsdaten für die Luftreinhaltung; Universität Stuttgart, Institut für Verfahrenstechnik und Dampfkesselwesen (IVD) UBA-FB 205 42 322. UBA-FB 001217; UBA Texte 44/08. Dessau-Roßlau, November 2008. ISSN 1862–4804.

Suutari R, Amann M, Cofala J, Klimont Z, Schöpp W (2001) From economic activities to critical load Exceedances in Europe – An uncertainty analysis of two scenarios of the RAINS integrated assessment model. IIASA. Laxenburg. (IIASA Interim Report, IR-01-020)

SYKE 2005: Air Emission Team of the Finnish Environment Institute (SYKE): Kristina Saarinen, Santtu Mattila, Johanna Mikkola, Jouko Petäjä and Sirpa Silander (2005): Air Pollutant Emissions in Finland 1990–2003 – National Inventory Report to the Secretariat of the UNECE Convention on Long-Range Transboundary Air Pollution; 13th May 2005

Theloke, J (2005).: NMVOC-Emissionen aus der Lösemittelanwendung und Möglichkeiten zu ihrer Minderung. Fortschritt-Berichte VDI Reihe 15 Nr. 252. Düsseldorf: VDI-Verlag 2005

UBA 2012: Umweltbundesamt (Publ.): German Informative Inventory Report; submitted to the UNECE Convention on Long-range Transboundary Air Pollution on 15 March 2012; available in the internet: http://iir-de-2012.wikidot.com/; accessed 8 August 2013

UBA 2013: Umweltbundesamt (Publ.): German Informative Inventory Report; submitted to the UNECE Convention on Long-range Transboundary Air Pollution on 18 March 2013; available in the internet: http://iir-de.wikidot.com/; accessed 8 August 2013

van Gijlswijk R, Coenen P, Pulles T, van der Sluijs J (2004) Uncertainty assessment of NOx, SO2 and NH3 emissions in the Netherlands. (TNO-Report, R 2004/100).

Winiwarter W, Muik B (2010) Statistical dependence in input data of national greenhouse gas inventories: Effects on the overall inventory uncertainty. Clim Chang 103:19–36

DOI 10.1007/978-3-319-15901-0_12
Reprinted from *Climatic Change* Journal, DOI 10.1007/s10584-014-1057-8

Pricing of uncertain certified emission reductions in a Chinese coal mine methane project with an extended Rubinstein-Ståhl model

Xiangyang Xu · Joanna Horabik · Zbigniew Nahorski

Received: 2 January 2013 / Accepted: 5 January 2014 / Published online: 1 March 2014
© The Author(s) 2014. This article is published with open access at Springerlink.com

Abstract The development of coal mine methane (CMM) projects is subject to various kinds of risk, one of these being their highly variable methane content. In this study, a new methodology is proposed to reflect the impact of this uncertainty on a negotiated Certified Emission Reduction (CER) price, which is based on the available information. To simulate a process of price negotiation the Rubinstein-Ståhl bargaining game is utilized, where a buyer's discount factor is unknown. It is assumed that a buyer's willingness to accomplish price negotiations depends on the CER uncertainty. The bargaining model has been extended by introducing dependence of its three parameters on the probability of a failure to fulfil the contracted CER amount. To quantify this probability, we develop a conditional distribution given information on the point estimate of methane amount for the project under consideration, and on the distribution of available estimates from coal mines having similar characteristics. The proposed approach is applied to a particular CMM capture and utilization project in Anhui province, China. The results indicate that the uncertainty influence is significant, particularly when the credibility of a seller increases, i.e. the probability of a failure to fulfil the project decreases. The analysis can be of use to both negotiating parties at an early stage of a comprehensive CMM project planning.

1 Introduction

The Clean Development Mechanism (CDM) has been introduced as one of the three flexible mitigation mechanisms in the Kyoto Protocol. The CDM allows developed countries listed in Annex 1 of the UN Framework Convention on Climate Change (UNFCCC) to invest in

This article is part of a Special Issue on "Third International Workshop on Uncertainty in Greenhouse Gas Inventories" edited by Jean Ometto and Rostyslav Bun.

Electronic supplementary material The online version of this article (doi:10.1007/s10584-014-1057-8) contains supplementary material, which is available to authorized users.

X. Xu
China University of Mining and Technology (Beijing), D11 Xueyuan Road, Haidian District, Beijing 100083, China

J. Horabik (✉) · Z. Nahorski
Systems Research Institute, Polish Academy of Sciences, Newelska 6, 01447 Warsaw, Poland
e-mail: Joanna.Horabik@ibspan.waw.pl

greenhouse gas (GHG) emission reduction projects in non-Annex 1 developing countries. It enables Annex 1 countries to offset this part of their emissions reduction commitments, and the host developing countries gain in return from the technology and financing necessary for GHG prevention.

The CDM market is dominated by China. By the 1st of March 2011, over 1,200 Chinese CDM projects had been registered, accounting for 43.25 % of the total number globally. The estimated annual Certified Emission Reductions (CERs) from these projects account for 62.63 % of the total CERs from all remaining CDM projects (UNFCCC 2011).

Among the above-mentioned Chinese CDM projects, there are 42 coal bed methane (CBM) and coal mine methane (CMM) projects. In CBM, methane is drawn to the surface, and the exploitation process is similar to that of natural gas. In CMM, methane is extracted during underground coal mining operations. The introduction of advanced technologies enables it to be used as a fuel, see e.g. Utaki (2010), which may be approved as a GHG Certified Emission Reduction. Otherwise, the methane discharged from coal seams is usually emitted into the atmosphere. The reported annual CERs from the mentioned Chinese methane CDM projects amount to over 16 million tCO_2eq, as of the 1st March 2011 (UNFCCC 2011). Recovery and usage of CMM resources is enthusiastically promoted by the Chinese government for CDM projects.

The methane global warming potential (GWP) is 21[1] times higher than that of carbon dioxide (IPCC 2007). Effective methods to restrict methane emissions from a variety of sources are investigated in e.g. Brown et al. (2010); Magalhães et al. (2010); Oh et al. (2010). CMM projects provide one more opportunity to reduce methane emissions.

Compared with other CDM mechanisms, the number of registered CMM projects is relatively low. Among others, one of the recognized reasons for this is the fact that the methane content of CMM differs substantially among projects; this may even be the case for one particular project. The quantification of the CER amount from a CMM project is based upon estimates of carbon emissions from coal resources. Numerous factors underlie these estimations. Firstly, the geological conditions of a coal mine: the methane content in coal resources, methane quality and stability, which is of great importance for the final-users, as well as coal methane reserves. The coal methane reserve factor includes the thickness of a coal seam, the depth of the deposit, permeability (Zhang et al. 2004) as well as the reserve pressure (Shimada et al. 2005). Secondly, the technology employed in mining coal methane resources matters (Zhang et al. 2005; Xu 2007a). An estimation of the amount of CER is conducted as a result of expert knowledge of the geological conditions and technology available. However, this is a challenging task. For the vast majority of inaccurate estimations, CER amounts tend to be overestimated.

In this paper, we analyse the influence of an uncertainty of CER amount on its price. Specifically, we focus on the uncertainty that is related to an imprecise knowledge of the methane content in a coal bed. Thus far, this kind of uncertainty has not been formally taken into account in price negotiations, nor in the Kyoto Protocol compliance condition of buyers. It is, however, reasonable to assume that an uncertain amount of CER has an influence on the buyer's decision. While an inclusion of this uncertainty in the buyer's compliance can be solved by adaptation of the methodology proposed in Nahorski et al. (2007), and by that shortly to be presented in Nahorski et al. (2014), the influence of uncertainty on the price negotiation process has not been previously analysed.

[1] According to the IPCC 2nd assessment report, relevant for emissions reporting under Kyoto Protocol. The 4th assessment report (IPCC 2007) gives a GWP of 25 and is likely to be taken on board in future.

To start a CDM project, a buyer and a seller have to sign the Emission Reduction Purchase Agreement (ERPA), which is the contract underlying the trading of CERs. For this, a unit price of CERs is of great importance. In Chinese CDM projects, the CER price usually has to be bargained at the initial point of negotiations. In this study, to simulate a price negotiation process, we utilize the two-player Rubinstein-Ståhl bargaining game of alternating offers.

The Rubinstein-Ståhl game has been applied to model practical bargaining settings, such as labor negotiation (Vannetelbosch 1997) or conflict resolution in the conjunctive use of surface and groundwater resources (Kerachian et al. 2010). It provides a suitable tool to model CER pricing, since impatient bargaining plays an important role in this kind of negotiations. Buyers, being usually international or governmental agencies, are not willing to put much effort into negotiating a single project. Typically, if after one or two rounds the parties cannot reach an agreement, the buyer gives up since they has many other opportunities for investment. For instance, Hovi (2001) considered the Rubinstein-Ståhl bargaining scheme while modelling the issue of international bargaining and enforcement, and for this the CDM was used as an example.

The main idea of our proposition is that for highly uncertain CERs, buyers tend to offer lower unit prices. Starting from this assumption, we propose to reflect this uncertainty in the parameters of the incomplete information case of the Rubinstein-Ståhl bargaining game (Rubinstein 1985), hereafter called the *extended Rubinstein-Ståhl bargaining game*. The functional dependence of the parameters upon the uncertainty is proposed. To quantify the uncertainty of the amount of CER, two technical indices of methane content are used independently. Each of them provides information on a point estimate of the amount of methane and on the distribution of its uncertainty. These two types of information are combined by means of the probability theory. The results of the bargaining process are compared for the two methane content indices, for the modified bargaining parameters, and with respect to the introduced probability parameter α of being unable to fulfil the contracted amount of CER.

The methodology is exemplified by a particular CMM capture and utilization project in Anhui province, China. Nevertheless, the proposed approach is general in nature, and it can be applied for modelling the influence of the uncertainty of other estimated variables, subject to relevant modifications.

2 Methodology

The proposed approach for the pricing of uncertain CERs with the Rubinstein-Ståhl includes several stages. We propose to express the uncertainty underlying the estimation of the amount of CER as a conditional distribution given information on a point estimate of the amount of methane in the project under consideration and on a distribution of available estimates from similar coal mines. Furthermore, the layout of the bargaining game is extended by introducing the uncertainty in two parameters: (i) discount factor reflecting buyer's patience and (ii) the probability that the buyer is weak. The following sections describe the main components of the methodology.

2.1 The Rubinstein-Ståhl bargaining model

The Rubinstein- Ståhl game simulates a negotiation process where two players: a buyer and a seller, denoted with the superscripts ^{B} and ^{S}, respectively, bargain to share a surplus of size k. Starting at an initial period $t=0$, each player makes a proposal in turn as to how to divide the surplus, and the other player may agree to the offer or reject it. The acceptance of the offer terminates the bargaining process. On the other hand, a rejection means that the players enter

the next negotiation period $t+1$, in which the roles of the two players are reversed and the side who had rejected the first offer makes a counter offer, as illustrated in Fig. 1.

Both players discount the future at a constant rate. The discount factors $\delta^i, i=B,S$ reflect the players' impatience—the closer they approach 1, the greater the players' patience.

Rubinstein (1982) used the concept of the subgame perfect equilibrium strategy to solve the negotiating problem for an infinite horizon in the case of complete information. Complete information means that the preference relations of both players are common knowledge. For the fixed discounting factors Rubinstein (1982) showed that a unique pair of bargaining strategies exist, specifying the best response to each player's offer at every point in time. In the equilibrium, the surplus k is divided between the player making the initial offer, I, and the one following, F, as $\frac{1-\delta^F}{1-\delta^I\delta^F}$ and $\frac{\delta^I\left(1-\delta^F\right)}{1-\delta^I\delta^F}$, respectively.

Unlike the original exposition of the Rubinstein (1982) game, with the commonly known discount factors of both players, in this paper we consider a somewhat more realistic version of the scheme with incomplete information. Assume that both players know the seller's discount factor δ^S, but the buyer's discount factor δ^B remains undisclosed. A buyer can be one of two types: *weak* (i.e. impatient), with a lower discount factor δ_l or *strong* (i.e. patient), with a higher discount factor δ_h, and it holds $0<\delta_l<\delta_h<1$. To simplify the notation we drop the superscript ^{B} denoting the buyer's discount factor, both above and in the following. A seller needs to assess the probability p that the buyer is weak. It may be concluded from the buyer's behavior; although a buyer may try to pretend that they are stronger than they actually are.

Bargaining with one-sided uncertainty has been studied by Rubinstein (1985) and re-examined by Bikhchandani (1992), see also Srivastava (2001) for an experimental testing. Rubinstein (1985) showed that a unique bargaining sequential equilibrium exists and takes the form of the following theorem. For a game starting with the seller's offer:

(i) If p is high enough so that $y^p>\delta^S V_h$, then a seller offers x^p. The weak buyer accepts this offer, while the strong buyer rejects it and offers $y^p \le x^p$, which is accepted. Both x^p and y^p denote the seller's share.

(ii) If p is low enough so that $y^p<\delta^S V_h$, then a seller offers V_h and both the weak and strong buyer accepts it.

Here,

$$V_h = \frac{1-\delta_h}{1-\delta^S\delta_h},$$
$$x^p = \frac{(1-\delta_l)\left(1-\left(\delta^S\right)^2(1-p)\right)}{1-\left(\delta^S\right)^2+\delta^S\left(\delta^S-\delta_l\right)p} \tag{1}$$

and

$$y^p = \frac{\delta^S(1-\delta_l)p}{1-\left(\delta^S\right)^2+\delta^S\left(\delta^S-\delta_l\right)p}. \tag{2}$$

The theorem states that the equilibrium is reached not later than the second period. The value V_h is equal to the seller's share in the complete-information-game equilibrium where the seller starts bargaining and the buyer is a strong one. Thus, for low p, the weak buyer is better off than in the complete-information case. For high p, both x^p and y^p increase in p. This is intuitive, because the more likely the buyer is weak, the more favourable the situation is for the seller.

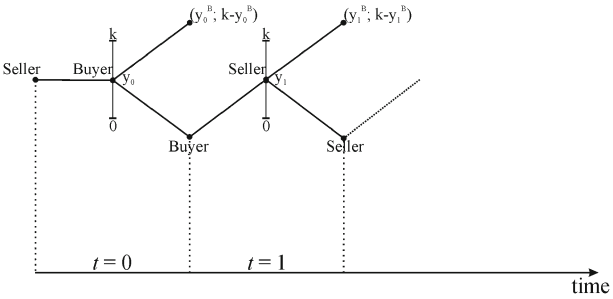

Fig. 1 Scheme of bargaining game with alternating offers

For the convenience of calculation, we can determine the boundary point p^* as that at which $y^p=\delta^S V_h$

$$p^* = \frac{\delta^S + 1}{\delta^S + \frac{1-\delta_l}{1-\delta_h}}. \tag{3}$$

If $p>p^*$ case (i) holds.

2.2 Modelling uncertainty of the methane content distribution

Various kinds of risk influence the CER price negotiations. For the methane CDM projects these include: selection of a project site, supply and demand constraints on the electricity market in neighboring regions, potential difficulties with CER approval, validation, registration, monitoring or certification.

Among other risks, the uncertainty of estimating the amount of CER is of special importance for the methane related CDM projects. Usually only a point estimate of the methane amount is provided, denoted as $\widehat{x}$. However, this amount is uncertain and the real value may differ. The uncertainty will be expressed by a conditional probability distribution $f(x|I)$, where I stands for our *prior* knowledge. In this study, it is assumed that a priori we know the probability distribution function $g(x)$ of the uncertain amount of CER with its variance σ^2, and the estimate $\widehat{x}$. The lognormal distribution is adopted, in accordance with the statistical inference described in Subsection 3.3, i.e.

$$g(x) = \frac{1}{\sqrt{2\pi}\sigma x}\exp\left[-\frac{(\ln x-\mu)^2}{2\sigma^2}\right], \quad x>0. \tag{4}$$

Its mean is $E(X)=\exp\left(\frac{1}{2}\sigma^2+\mu\right)$, median $m=\exp(\mu)$, and the variance is $Var(X)=\exp(\sigma^2+2\mu)(\exp\sigma^2-1)$. We use this distribution to infer on the uncertainty of the observation $\widehat{x}$. In the situation under consideration, the value $\widehat{x}$ actually adds information to our knowledge of the *prior* distribution $g(x)$. We make the assumption about the parameter μ, that it belongs to a given set M, i.e. $\mu\in M$. Now, using the law of total probability we have

$$f\left(x\middle|g,\widehat{x}\right) = \int_M g(x|\mu)\pi\left(\mu|\widehat{x}\right)d\mu \tag{5}$$

where $\pi(\mu|\widehat{x})$ is the conditional probability density function of μ when $\widehat{x}$ is known. However, we know that, when $\widehat{x}$ has been observed, both $\widehat{x}$ and μ are deterministic values. Thus, $\pi(\mu|\widehat{x})$ is simply a deterministic function $\mu(\widehat{x})$. Formally, we insert $\pi(\mu|\widehat{x}) = \delta(\mu - \mu(\widehat{x}))$ into (5), where δ is the Dirac delta function and $\mu(\widehat{x})$ is a deterministic value. This gives $f(x|g,\widehat{x}) = g(x|\mu(\widehat{x}))$.

To find the function $\mu(\widehat{x})$ we estimate μ in (4) using the maximum likelihood method with one observation $\widehat{x}$. Consequently, we have

$$\ln g(x|\mu) = -\ln\sqrt{2\pi}\sigma - \ln x - \frac{1}{2\sigma^2}(\ln x - \mu)^2.$$

The maximum of this function with respect to μ is for

$$\mu\left(\widehat{x}\right) = \ln\widehat{x},$$

Inserting this value into (4) we finally get

$$f\left(x\middle|g,\widehat{x}\right) = \frac{1}{\sqrt{2\pi}\sigma x}\exp\left[-\frac{\left(\ln\frac{x}{\widehat{x}}\right)^2}{2\sigma^2}\right], \quad x > 0. \tag{6}$$

As $\widehat{x} = e^{\mu}$, then $\widehat{x}$ is the median of the above distribution.

Although $\widehat{x}$ seems to be a natural value to be taken as the amount of CER, the question arises as to whether another value might be more profitable from the seller's point of view. Let us introduce the probability $\alpha \in [0,1]$ and denote by x_α the quantile of order α of the distribution, compare also Fig. 2. The true value of the amount of methane is lower than x_α with probability α. In other words, α expresses the probability that the terms of the CMM project, with the amount of CER equal to x_α, may not be fulfilled due to an insufficient amount of methane. To avoid reference to specific values, in the following we use the ratio $r(\alpha) = \frac{x_\alpha}{\widehat{x}}$, which is a non-dimensional value.

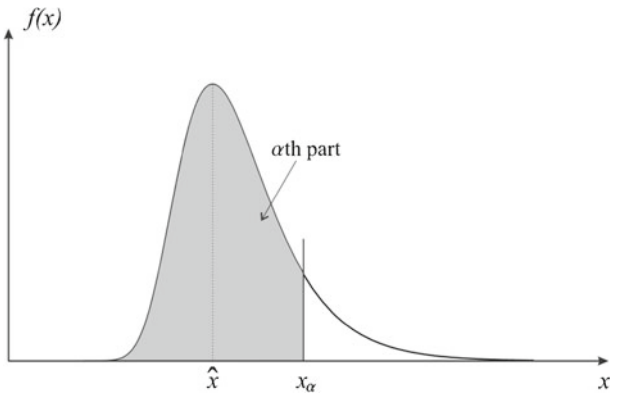

Fig. 2 A distribution of uncertainty underlying methane calculations $f(x)$, a calculated methane amount $\widehat{x}$, and an amount of methane x_α corresponding to the probability α

Since the function $f(x|g,\widehat{x})$ follows the lognormal distribution, its cumulative distribution function (cdf) is

$$F(x_\alpha) = \varphi\left(\frac{\ln x_\alpha - \mu}{\sigma}\right) = \alpha,$$

where φ is cdf of the standard normal distribution. We obtain

$$x_\alpha = \exp\left[\mu + \sigma\varphi^{-1}(\alpha)\right].$$

In our case $\mu = \ln\widehat{x}$, therefore it follows

$$r(\alpha) = \frac{x_\alpha}{\widehat{x}} = \frac{\exp[\mu + \sigma\varphi^{-1}(\alpha)]}{\widehat{x}} = \exp\left[\sigma\varphi^{-1}(\alpha)\right], \tag{7}$$

and $r(\alpha)$ does not depend on $\widehat{x}$.

2.3 Modelling beliefs on parameters of bargaining model

Any change of the amount of CER is to the detriment of both parties. Due to the highly attractive commercial benefits of CDM projects, a project buyer is in pursuit of high volumes of CERs. Obviously, the higher the CER amount is, the more valuable a project becomes. However, if the amount of methane actually generated is lower than the amount considered in a negotiation period, it affects the buyer's benefit, due to the favourable conditions a buyer might have given to a seller during the negotiations.

In this subsection, we aim to incorporate the risk into the extended Rubinstein-Ståhl negotiation model, so that the seller's belief on a buyer's negotiation position reflects the uncertainty of calculating the amount of methane. It is assumed that the uncertainty of assessing the amount of CER is known to the buyer. So, both the estimates of the buyer's discount rates (δ_l,δ_h) and the probability p are affected by this risk, which we express with respective functional dependences. For this, a set of common sense assumptions are taken and possibly the simplest relationships that satisfy them are constructed.

Discount factors δ_l,δ_h. Let us denote the lower and upper estimates of a low discount factor δ_l by δ_{ll} and δ_{lh}, respectively. Similarly, let δ_{hl} and δ_{hh} stand for the lower and upper estimates of a high discount factor δ_h. Assuming a linear positive relationship between the uncertainty α and buyer's unknown discount factors δ_l and δ_h

$$\delta_l(\alpha) = \delta_{ll} - \alpha(\delta_{ll} - \delta_{lh}) \tag{8}$$

$$\delta_h(\alpha) = \delta_{hl} - \alpha(\delta_{hl} - \delta_{hh}). \tag{9}$$

The above expressions approximate the main relations in the simplest way. Greater uncertainty α of the CER amount estimation strengthens the buyer's position, and this is reflected in their higher discount factors.

Probability p. We model the probability p that the buyer is weak as a third order polynomial of α. It is the simplest polynomial satisfying the following conditions

$$p(0) = 1 \qquad p(1) = 0,$$

which are assumed to be approached slowly

$$p'(0) = p'(1) = 0,$$

where $p'(\cdot)$ denotes the first derivative. The conditions provide the following function $p(\alpha)$

$$p(\alpha) = 2\alpha^3 - 3\alpha^2 + 1, \quad \alpha \in [0, 1]. \tag{10}$$

The function is monotonically decreasing, expressing the intuition that the higher the uncertainty of methane calculations is, the stronger is the buyer's position, and thus the lower is the probability that they are weak.

3 Case study

3.1 Introductory information on the Huainan project

The considered CMM capture and utilization project is located in Huainan, Anhui Province of East China. The coal mine belongs to Huainan Coal Mining Group Co., Ltd., situated in the north central part of Anhui Province. Although coal resources of the Huainan mining area are very rich, the geological conditions are complex. Many of the mines experience a high content of explosive mine gas, largely composed of methane and, thus, extremely hazardous to miners.

Within the initiated project, installed technologies capture the CMM and enable its use as a fuel source. This prevents methane from being released into the atmosphere, and increases the safety of coal extraction at the same time. As a result, emission reductions were achieved through combustion of the extracted CMM, which replaced conventional coal usage in more than 15,000 households and was also used in the generation of electricity in the industry sector (Project Document Description 2006).

As mentioned before, division of the margin between the buyer's highest CER unit price and the seller's (Huainan Coal Mining Group Co., Ltd.) lowest price is negotiated at the ERPA stage. In the following we assume that a broker function is incorporated into either the buyer's or seller's side.

3.2 Negotiating CER price: no uncertainty case

In this subsection we consider the negotiation of the CER price, taking no account of the uncertainty of the methane content. To apply the bargaining theory, proper discount factors should be selected for both parties. In practice, this becomes a challenging task. This is particularly true for a buyer's discount rate, which remains basically unknown.

In this case study, to set the values of discount factors (or, in the following, their upper and lower limits) expert assessments were used that were based on the project's documentation. Below we list the most important factors influencing the negotiation positions of the CMM project parties. First of all, there is the costs of communication between parties. Usually English is the working language, so a seller (the Chinese side) needs to hire some interpreters. On the other hand, a buyer also needs to hire some local experts or establish an agency in China to facilitate negotiations. Secondly, collating information comes at a cost for both buyer and seller and acts as a further drain on their discount rates. Before a buyer gives an initial price, they must verify the information on the project from various channels; not only those limited to formal documents and local information, but also from the authorized third parties.

In the current conditions of the Chinese CDM market, the sellers are more concerned to sell the CERs than the buyers are to buy them. This is due to the numerous other opportunities available to the buyers to find a more profitable option. Big international buyers usually possess extensive knowledge of the international CDM market, which besides China, also includes India, South America and others.

Obviously, both sides hope to reach an agreement (i.e. sign ERPA) as soon as possible. The buyer's patience is closely related to the international carbon market price and its domestic environmental policy. That is, when the international carbon market price is decreasing, a buyer will have a lower discount factor. On the other hand, the Chinese side is usually unfamiliar with the international carbon market along with environmental policy of a buyer's country. Therefore, from the seller's point of view, the buyer's discount rate is assumed to be unknown. The seller's discount factor is mainly decided upon by the project's risk factor.

Here, the seller estimates that the buyer is either a weak player with a discount rate δ_l=0.91, or that they are a strong player with a discount rate δ_h=0.975. Furthermore, the seller assumes that these two situations have equal probabilities, i.e. p=0.5. The seller's discount factor δ^S=0.94 remains common knowledge.

For a case with no account of uncertainty, we analyse a real bargaining situation from the past, and therefore use the costs and prices from that period of time. The aim is to check whether the prices calculated from the model are comparable with the actual negotiated ones. When the Huainan project was negotiated, the floor CER price demanded by the Chinese authorities for CMM projects was set at 8 Euro (approximately 70 Yuan/ton); we treat this value as the seller's conservative price. The buyer set his conservative price at 170 Yuan/ton, which yielded a surplus k=100 Yuan/ton to be divided among the players.

Negotiations started with the seller's offer. From (3) we calculate p^*=0.45, and since $p>p^*$, we follow case (i) of the Theorem. The seller proposed that their benefit is

$$k * x^p = k\frac{(1-\delta_l)\left(1-\left(\delta^S\right)^2(1-p)\right)}{1-\left(\delta^S\right)^2+\delta^S\left(\delta^S-\delta_l\right)p} = 38.49 \quad (\text{Yuan/ton})$$

from where the CER price is 108.49 (Yuan/ton). The weak buyer accepted this offer, whereas the strong one rejected it. Then, in the next step, the strong buyer offered to the seller a benefit of

$$k * y^p = k\frac{\delta^S(1-\delta_l)p}{1-\left(\delta^S\right)^2+\delta^S\left(\delta^S-\delta_l\right)p} = 32.41 \quad (\text{Yuan/ton}),$$

yielding the CER price of 102.41 (Yuan/ton). Comparing these results to the CER price negotiated for the Huainan project, the actual buyer was a weak one.

3.3 Estimating uncertainty of methane content assessment

High risk of CER estimation in CMM projects is related to the selection of the project site. It determines such factors as methane reserves, geological mining conditions, gas quality, local demand, gas prices on the local market or currency exchange rate, etc. (Xu 2007b). These uncertainties and risks, although important for both the seller and buyer, are not considered in the study. Here we assume that the project site is known and we focus on an uncertainty of CER originating from inaccuracies in the assessment of the amount of methane for an already selected project site.

For CER assessment, typically the ACM0008 methodology is applied, see ACM (2010) and UNECE (2010). According to this methodology, the annual (Certified) Emission Reductions *ER* of a CDM project are calculated as

$$ER = BE - PE - LE$$

where *BE* are the baseline emissions, saved due to the implementation of the project; *PE* are the project emissions; and *LE* are the leakage emissions. In the CMM case study under consideration, the baseline emissions are represented by the mined methane, which replaces the use of other fuels. Uncertainty of emission reduction is mainly due to baseline emissions *BE*, since project emissions *PE* can be estimated with much better accuracy and leakage emissions *LE* are minor. Therefore, the two latter sources of uncertainties are neglected, and it is assumed that uncertainty of the overall emission reduction is caused by the baseline emissions, which is strictly related to the methane content in the coal bed.

For the Huainan project, uncertainty of methane emission estimation is characterized with two indices: the highest methane content in the coal bed seam and relative methane emission, both measured in m^3/t. The former index is typically used in China to estimate future CER production, while the latter accounts for the technology that has been adopted and provides a more accurate estimation.

Figure 3 shows the positively skewed distributions of these two indices, based on data from 25 coal mines, which extract coal from beds of a similar nature in the region. Thus, the histograms show distributions of the indices in Chinese coal mines of the type similar to the one considered in the case study. We fit the lognormal distributions to the data for both indices, and test the results with the Kolmogorov-Smirnov test, see Table 1A of the supplementary material. Apart from the lognormal distributions, other density functions have also been considered (see the supplementary material). The lognormal distribution provided the best results out of the considered functions.

For the considered indices of the highest and relative methane content, the ratio $r(\alpha)$, calculated with Eq. (7), will be considered in the following. This is shown in Fig. 4b. We determine $r_{min}=r(\alpha=0)=0$, and due to the fact that the support of lognormal distribution is unbounded from above, we set $r_{max}=r(\alpha=0.995)$, which provides $r_{max}=2.79$ for the highest methane content and $r_{max}=6.27$ for the relative methane content. Note that $r(\alpha=0.5)=1$, i.e. when $x_\alpha = \widehat{x}$. This is a consequence of the fact that $\widehat{x}$ is the median of the distribution $f(x|g,\widehat{x})$. The scale parameters have been estimated as $\sigma=0.399$ for the highest methane content and $\sigma=0.713$ for the relative methane content.

4 Simulating negotiation outcome under uncertainty

In this section, the influence of the uncertainty of methane calculations on the negotiated CER price is analyzed. The resulting CER prices are presented in terms of the seller's share of the surplus. To calculate a final CER unit price, a seller's share has to be multiplied by *k* and added to their conservative price.

We begin with modelling the unknown buyer's discount factors δ_l and δ_h, as well as the probability that a buyer is weak, see Fig. 4. The following lower and upper limits of discount factors were assigned: $\delta_{ll}=0.88$, $\delta_{lh}=0.94$, $\delta_{hl}=0.96$, $\delta_{hh}=0.99$. Note that the previously assigned values δ_l and δ_h were fixed as the middles of the discount rates δ_{ll},δ_{lh} and δ_{hl},δ_{hh}, respectively. As before, the seller's discount factor $\delta^S=0.94$ is adopted.

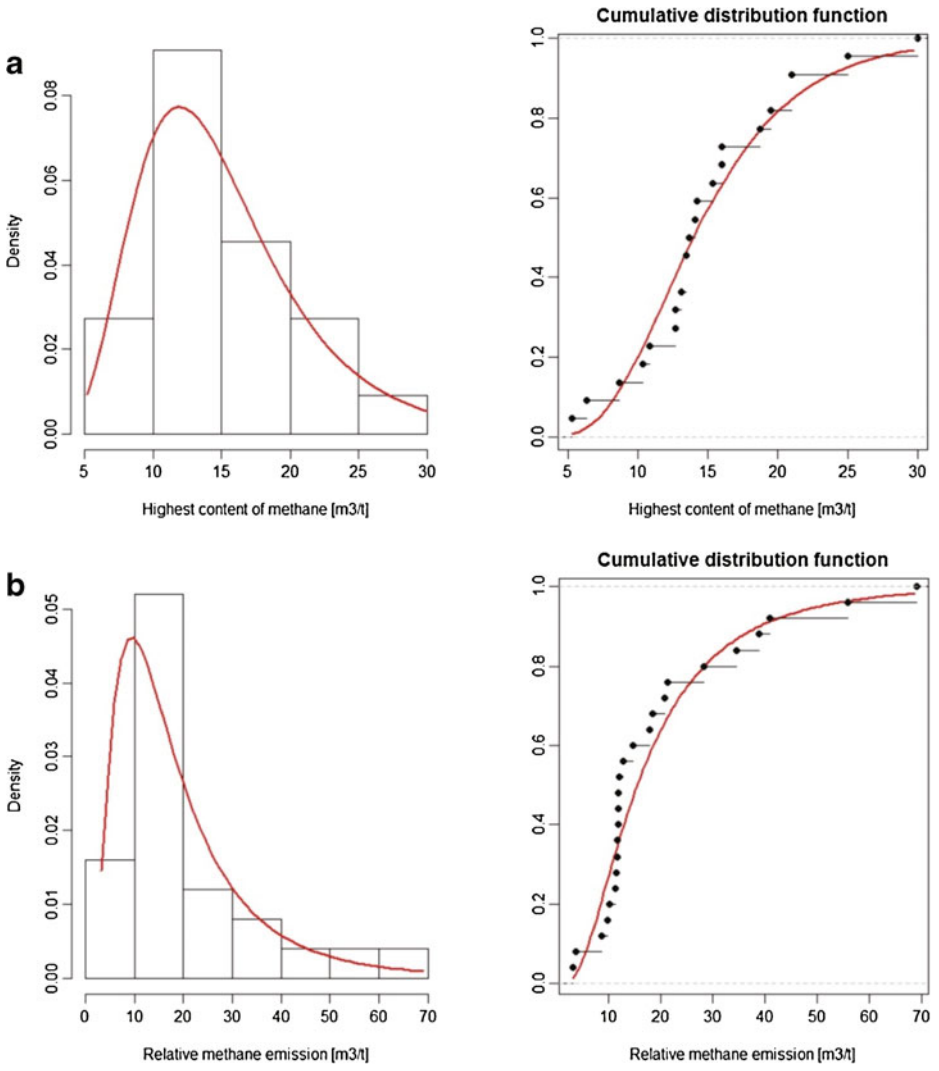

Fig. 3 Distributions of **a** highest methane content and **b** relative methane content with fitted lognormal density functions

Figure 4a depicts the boundary point $p^*=p$ distinguishing between the cases (i) and (ii) of the theorem (here, for $\alpha=0.56$), and Fig. 4c presents the optimal share of a surplus for a range of α values. The difference between the shares accepted by a strong and a weak buyer is about 5 % of the surplus, and note that it is practically independent of α (as long as $\alpha<0.56$). Naturally, the higher the uncertainty α is, the lower share of a surplus the seller gets, and this value is decreasing from 0.69 down to 0.14.

Figure 4c also provides comparison with the previously considered no-uncertainty case, depicted with red lines. For the values of discount factors under consideration, these two instances provide the same results for $\alpha=0.5$, as indicated with a dotted vertical line. Recall that $\alpha=0.5$ may be interpreted that the uncertainty is neglected, upon which the estimated value $x_\alpha = \widehat{x}$ is taken. There $r=1$, compare Fig. 4b.

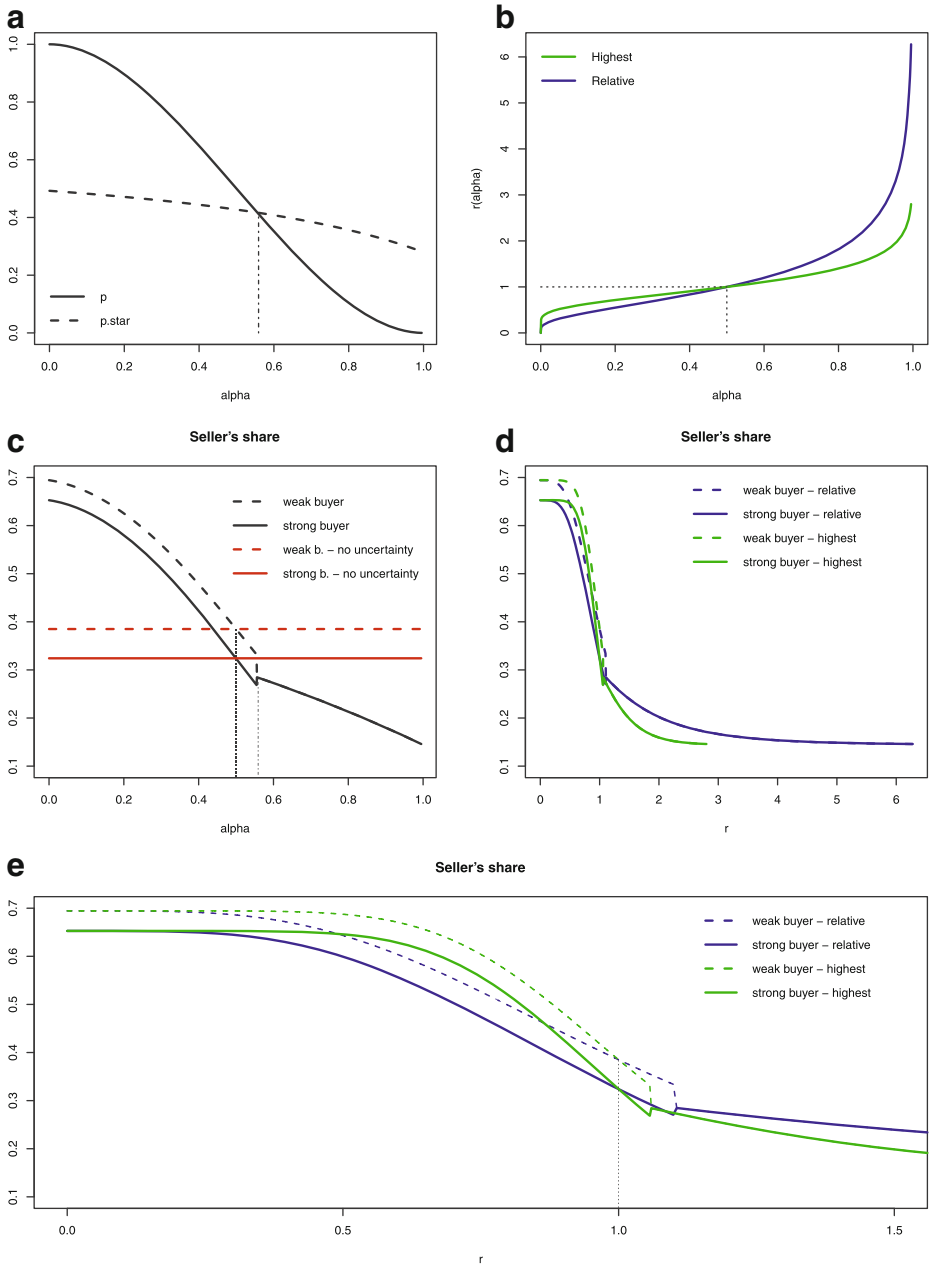

Fig. 4 Negotiation outcome: both p and δ_l, δ_h modelled

Figure 4d depicts the negotiated share of a surplus as a function of the ratio r, illustrating the difference between two methane content indices. Figure 4e provides a more detailed version of the same graph, although for a limited range of r. As shown in this figure, as long as $r<1$, the seller is better off when the highest methane content index is considered, regardless of a buyer's type (weak or strong). This fact is in accordance with our intuition, because the

uncertainty distribution of the highest methane content has a lower dispersion. It should be also noted that the highest methane content index is more often used in China. The situation changes when $r>1$. Then the reduction is less credible and it is better for the seller to consider the relative methane emission index. Technically, this is the effect of its higher dispersion. For a given value of $r>1$, the probability of not fulfilling the project is smaller for the relative methane emission index than for the highest methane content one. Overall, the consideration of the CER price in the function of r expresses a seller's trade-off between gaining a better unit price which, however, requires assuring more credible emission reductions.

The proposed approaches for modelling discount factors δ_h and δ_l, as well as for modelling probability p, do not need to be applied jointly. Each of these can be used as a separate part of an analysis. Figure 5 presents the negotiation outcome for the case of a constant $p=0.5$ (Fig. 5a), and for the case of a constant buyer's discount factors $\delta_l=0.91$, $\delta_h=0.975$ (Fig. 5b). In general, when either the discount factors or probability p are modelled, the situation for a seller is less restrictive as compared with the previous results. In particular, for α close to 1, i.e. when almost the whole of the uncertainty distribution is accounted for, their share of a surplus does not drop below 0.24, while it was 0.14 in the previous setting. Note that in the case of a constant $p=0.5$ (Fig. 5a), for the whole range of uncertainty parameter α the case (i) of the theorem applies, and the seller receives a different share depending on the type of the buyer.

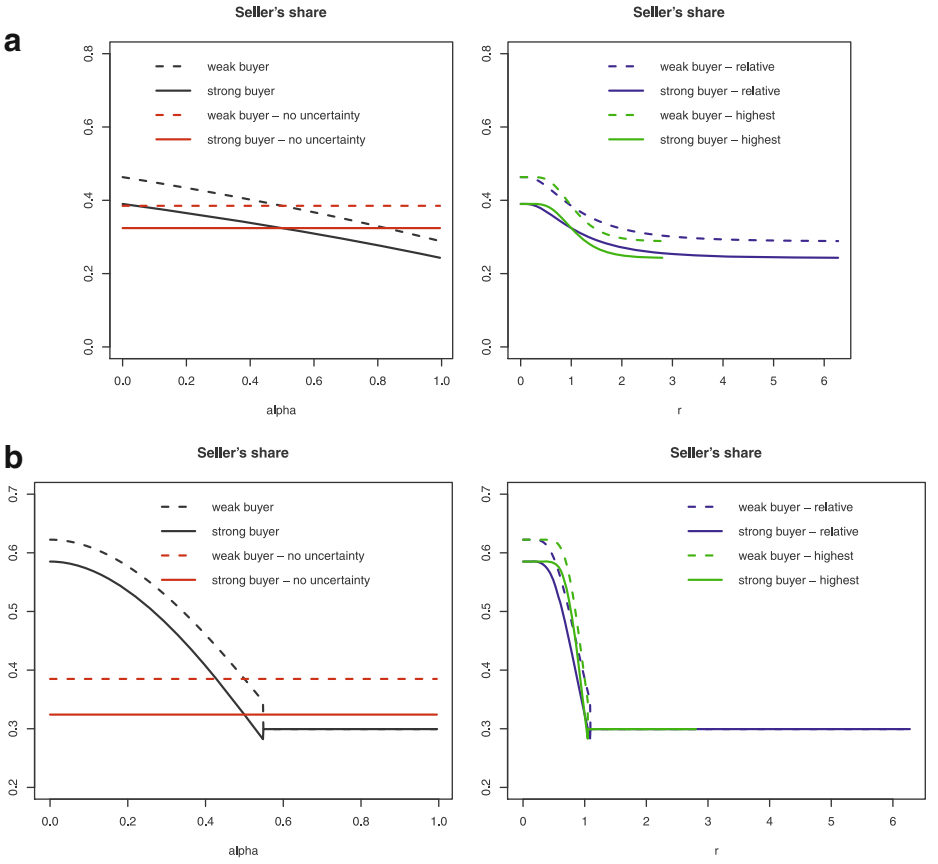

Fig. 5 Negotiation outcome for **a** constant $p=0.5$ and **b** constant $\delta_l=0.91$, $\delta_h=0.975$

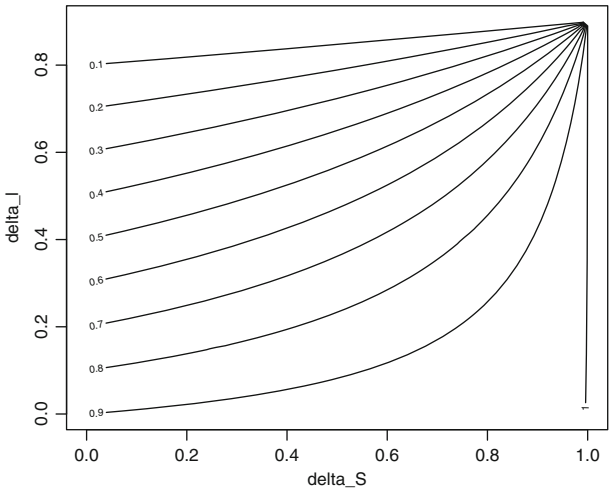

Fig. 6 Optimal seller's share for different discount factors; p=0.5, $\delta_h=\delta_l+0.1$

The applied Rubinstein-Ståhl bargaining game hinges upon assigned values of the discount factors. While the above analysis assumed a constant value of the seller's δ^S=0.94, Fig. 6 presents the optimal seller's share for different values of discount factors for both negotiating parties. To this end, a simplified assumption was made $\delta_h=\delta_l+0.1$, and, furthermore, constant p=0.5 was assigned. The difference in results between the case of a weak and strong buyer was negligible, and therefore is not presented. The figure illustrates that for a high range of discount factors, e.g. higher than 0.7, a negotiation outcome is highly sensitive to small changes in these values. This is not the case for a low range of discount factors.

5 Summary and conclusions

This paper addresses the problem of uncertainty in methane content for CMM projects, and its impact on a negotiated CER price. The Rubinstein-Ståhl bargaining model—in the case of incomplete information—is used to simulate negotiations concerning CER price. The bargaining model has been extended by introducing dependence of its three parameters on a distribution of methane content uncertainty, and more precisely on its quantile of order α, where α is the probability of failure to fulfil the contract due to insufficient methane content in the coal bed. The lower and upper discount factors of a buyer have been chosen as simple linear functions in a predefined range of values. The probability that a buyer is a weak negotiator was designed as a third order polynomial, satisfying a few intuitive conditions.

The proposed methodology was applied for a CMM project implemented in the Huainan coal mine, the Anhui Province in Eastern China. Uncertainty distribution of the methane content was estimated using data on two types of indices, which were gathered from 25 Chinese coal mines with similar geological conditions.

The investigations revealed a few interesting results, fully compatible with those that were predicted as well as fitting in with current negotiation practise.

The uncertainty highly impacts the negotiation results and the parties' shares of the surplus. The dependence of the seller's share on the amount of methane adopted for the project is quite high, particularly for the values of $\alpha<0.5$ or $r<1$, that is for more credible methane contents. There, along

with the decreasing probability of noncompliance the seller's share rises fairly rapidly. The gain of the seller's share, when negotiated with a weak buyer instead of a strong one is about 5 % of the surplus, almost independent of the uncertainty parameter α. This result indicates that a seller can earn a considerable amount of money by being presented with the chance to negotiate with a weak buyer.

Although the analysis covers the full range of the probability $0 \leq \alpha \leq 1$, it is rather unreasonable for the seller to consider either very small or very high values of α. Still, the analysis of this paper presents only a partial answer to the choice of α. Other aspects should also be taken into account, such as the gains achieved when the declared CER amount is satisfied as well as the costs of failing it. To solve these questions the CER price has to be known. In this respect, an analysis of the price bargaining, like that which is presented here, must be an essential part of a comprehensive project planning.

Acquisition of the discount factor values is a difficult part of the analysis. Intuition and experience as well as some intelligence methods may help to assign them. For instance, in their case study Kerachian et al. 2010 utilize the fuzzy set theory to better define uncertainty in utility functions, which, together with discount factors, define the preferences of parties. Another approach would be to introduce the learning stimuli in the bargaining strategies based on the information gathered, but this requires longer sequences of negotiation periods.

In this study simple models of the buyer's reaction to uncertainty have been assumed. More advanced modelling requires wider analysis of the buyer's incentives in the project, accounting also for other factors, such as the project's size.

Acknowledgements The study was conducted within: (i) the Joint China-Poland Intergovernmental Science and Technology Cooperation project No.33-2, (ii) the National Science Foundation of China project No.70941035, and (iii) the Humanities and Social Sciences Research Program of Ministry of Education of the People's Republic of China, No.12YJA630161. Joanna Horabik acknowledges support from the Foundation for Polish Science under International PhD Projects in Intelligent Computing; a project financed by The European Union within the Innovative Economy Operational Programme 2007–2013 and European Regional Development Fund.

The authors thank the reviewers for their stimulating comments, which helped to shape the final version of the paper.

Open Access This article is distributed under the terms of the Creative Commons Attribution License which permits any use, distribution, and reproduction in any medium, provided the original author(s) and the source are credited.

References

ACM (2010) Approved consolidated baseline and monitoring methodology ACM0008. Consolidated methodology for coal bed methane, coal mine methane and ventilation air methane capture and use for power (electrical or motive) and heat and/or destruction through flaring or flameless oxidation. UNFCCC/CCNUCC. ACM0008/Version 07.Sectoral Scope: 08 and 10. EB 55. http://cdm.unfccc.int/methodologies

Bikhchandani S (1992) A bargaining model with incomplete information. J Econ Stud 59:187–203

Brown KA, MacCarthy J, Watterson JD, Thomas J (2010) Uncertainties in national inventory emissions of methane from landfills: A UK case study. In: Proceedings of the 3rd International Workshop on Uncertainty in Greenhouse Gas Inventories. Lviv Polytechnic National University, Lviv, pp 21–30

Hovi J (2001) Decentralized enforcement, sequential bargaining, and the clean development mechanism. CICERO Working Papers 12. https://www.duo.uio.no/bitstream/handle/10852/32764/1617.pdf?sequence=1 Cited 6 Aug 2013.

IPCC (2007) IPCC fourth assessment report: climate change. http://www.ipcc.ch/publications_and_data/publications_and_data_reports.shtml#1

Kerachian R, Fallahnia M, Bazargan-Lari MR et al (2010) A fuzzy game theoretic approach for groundwater resources management: application of Rubinstein bargaining theory. Resour Conserv Recycl 54:673–682

Magalhães G, Espirito Santo Filho F, Alves JW, Kelson M, Moraes R (2010) Reducing the uncertainty of methane recovered (R) in greenhouse gas inventories from waste sector and of adjustment factor (AF) in landfill gas projects under the clean development mechanism. In: Proceedings of the 3rd International Workshop on Uncertainty in Greenhouse Gas Inventories. Lviv Polytechnic National University, Lviv, pp 165–176

Nahorski Z, Horabik J, Jonas M (2007) Compliance and emission trading under the Kyoto protocol: rules for uncertain inventories. Water Air Soil Pollut Focus 7(4–5):539–558

Nahorski Z, Stańczak J, Pałka P (2014) Simulation of an uncertain emission market for greenhouse gases using agent-based methods. Clim Chang. doi:10.1007/s10584-013-1039-2

Oh S-H, Heo G, Woo J-Ch (2010) Uncertainty of site-specific FOD for the national inventory of methane emission. In: Proceedings of the 3rd International Workshop on Uncertainty in Greenhouse Gas Inventories. Lviv Polytechnic National University, Lviv, pp 207–218

Project Document Description (2006) Huainan Panyi and Xieqiao coal mine methane utilization project. http://www.dnv.com/focus/climate_change/Upload/PDD_Huainan%20Panyi%20and%20Xieqiao%20CMM_2006-01-01.pdf. Cited 10 Jan 2012

Rubinstein A (1982) Perfect equilibrium in a bargaining theory. Econometrica 50(1):97–109

Rubinstein A (1985) A bargaining model with incomplete information about time preferences. Econometrica 53(5):1151–1172

Shimada S, Funahashi Y, Li H et al (2005) Economic assessment of enhanced coal bed methane recovery in China. In: Proceedings of the 5th International Symposium on CBM/CMM in China. November 30–December 12005:267–276

Srivastava J (2001) The role of inferences in sequential bargaining with one-sided incomplete information: some experimental evidence. Organ Behav Hum Decis 85(1):166–187

UNECE (2010) UNECE group of experts on coal mine methane. Comments on the ACM. http://cdm.unfccc.int/methodologies/DB/OA37XAW7EI9WHJVZ97RGH2EZ5S9E93/view.html

UNFCCC (2011) Project cycle search database. http://cdm.unfccc.int/Projects/projsearch.html. Cited 1 March 2011

Utaki T (2010) Development of coal mine methane concentration technology for reduction of greenhouse gas emissions. Sci China Tech Sci 53(1):28–32

Vannetelbosch VJ (1997) Wage bargaining with incomplete information in an unionized Cournot oligopoly. Eur J Polit Econ 13:353–374

Xu X (2007a) Investigation in the Huainan coal mining area. Unpublished notes

Xu X (2007b) Risk analysis and control for potential coal bed methane CDM projects of China. China Min Mag 16:1–4 (in Chinese)

Zhang J, Wang H, Qian K et al (2004) Progress of CBM exploration research. China Coalbed Methane 1(1):13–16 (in Chinese)

Zhang M, Ma G, Deyin Y et al (2005) Drainage technologies and utilization prospects of CMM in Hebi coal mining area. China Coalbed Methane 2(3):34–37 (in Chinese)

DOI 10.1007/978-3-319-15901-0_13
Reprinted from *Climatic Change* Journal, DOI 10.1007/s10584-013-0824-2

Uncertainty, cost-effectiveness and environmental safety of robust carbon trading: integrated approach

T. Ermolieva · Y. Ermoliev · M. Jonas · M. Obersteiner · F. Wagner · W. Winiwarter

Received: 7 January 2013 / Accepted: 13 June 2013 / Published online: 22 August 2013
© Springer Science+Business Media Dordrecht 2013

Abstract Carbon markets, like other commodity markets, are volatile. They react to stochastic "disequilibrium" spot prices, which may be affected by inadequate policies, speculations and bubbles. The market-based emission trading, therefore, does not necessarily minimize abatement costs and achieve emission reduction goals. We introduce a basic stochastic model integrating emissions reduction, monitoring and trading costs allowing us to analyze the robustness of emission and uncertainty reduction policies under environmental safety constraints asymmetric information and other multiple anthropogenic and natural uncertainties. Explicit treatment of uncertainties provides incentives for reducing them before trading. We illustrate functioning of the robust market with numerical results involving such countries as the US, Australia, Canada, Japan, EU27, Russia, Ukraine. In particular, we analyze if the knowledge about uncertainties may affect portfolios of technological and trade policies or structure of the market and how uncertainty characteristics may affect market prices and change the market structure.

1 Introduction

The paper aims to analyze cost-effective and environmentally safe carbon trading systems operating under uncertainty about emissions and their abatement and monitoring cost functions, asymmetric information, and irreversibility. For analyzing robust emission trading schemes, we introduce an integrated multiagent emission reduction model under multiple natural and human-related uncertainties. The model pursues the goal that all trading parties jointly achieve individual emissions targets at minimum costs by investing in emissions

This article is part of a Special Issue on "Third International Workshop on Uncertainty in Greenhouse Gas Inventories" edited by Jean Ometto and Rostyslav Bun.

T. Ermolieva (✉) · Y. Ermoliev · M. Jonas · M. Obersteiner · F. Wagner · W. Winiwarter
International Institute for Applied Systems Analysis, Schlossplatz 1, 2361 Laxenburg, Austria
e-mail: ermol@iiasa.ac.at

W. Winiwarter
Institute for Systems Sciences, Innovation & Sustainability Research (ISIS), University of Graz, Merangasse 18, 8010 Graz, Austria

abatement, uncertainty reduction and by redistributing the emissions permits through trading. Safety constraints imposed on the trades require that the reported emissions plus uncertainty are below the targeted level (cap) with a given probability, therefore this creates incentives for parties to invest into uncertainty reduction prior to compliance. Proposed mutually beneficial bilateral trading scheme corresponds to a special distributed optimization method. The implementation of this trading scheme is discussed in section 4 using a computerized multiagent trading system avoiding irreversibility of real trades and asymmetric information of partners.

Different uncertainties affect emission trading in different ways, which may cause market crashes and instabilities similar to financial markets. To limit the role of uncertainties, advocates of regulated trades argue in favor of uncertainty indicators distinguishing sources by their uncertainty levels (Kerr 2000; Godal et al. 2003), which is usually their private information. Therefore, the use of these indicators is similar to the ideas of "signaling" well known in treating the asymmetric information (see e.g. Milgrom and Roberts 1986). Market regulators may set restrictions on source category to be included in trading, and trading scheme may demand a party to set source-specific targets depending on the level of uncertainty.

Emissions cap and trade programs (de Jong and Walet 2004; Kerr 2000) are economic instruments for environmental regulations which become popular both among policy-makers and scientific communities (Stavins 2010). These programs are now a key element in climate change policy negotiations establishing carbon prices as a "new currency" and emission permits as a new asset type (Kerr 2000).

In theory, the market price of tradable emissions permits (allowances) should set up the marginal cost of emissions reductions to meet the cap. In reality, the market prices exhibit periods of high volatility which may be a result of political decisions, information disclosure, speculations. The short-term information about spot prices in different periods may be contradictory and cause parties to revise their "myopic" decisions which, however, may not be reversible. As studied by Potsdam Institute for Climate Impact Research (Roos 2011), immaturity of the existing market policies triggered a major "dash for coal setting out on the construction of dozens of new coal plants. …". Also, in the Netherlands, "… CO2 emissions trading is a marginal consideration in the choice of fuel. Evidently, electricity producers are not too bothered about the price they pay for carbon emissions. The vast majority still favors coal, the worst carbon polluter. The reason is simple: the expected costs of emission rights are negligible compared to other investment outlays." The building of coal-fired plants now will lock-in energy decisions for about 40 years (Stikkelman et al. 2010).

Lessons learned from the existing emission trading (Betz and Sato 2006) point out the need for market safety regulations to smoothen its performance.

In this paper, we propose a computerized multiagent trading system (COMATS) which may function as a prototype of a real decentralized emission trading market under uncertainty without revealing the private information of parties about costs and emissions. The system may enhance real markets by analyzing conditions for strategic robust trades and stable market's performance avoiding potential irreversibility and "lock-in" equilibriums. COMATS is designed as a multicomputer network of traders and can be viewed as a device for decentralized collective regulation of trades towards their cost-effectiveness under safety constraints.

The paper is organized as follows. Section 2 reviews the classical approach to emission trading and discusses its shortcomings in situations with uncertainty. In section 3 the integrated stochastic multiagent model is introduced and analyzed. Section 4 outlines the structure of the COMATS and summarizes numerical results on trading involving such countries as US, Australia, Canada, Japan, EU27, Russia, Ukraine, etc. In this section we show how the knowledge about uncertainties may affect structure of the market, e.g., turn buyer into seller,

and how new participants may improve or destabilize market's performance. Conclusions are presented in section 5.

2 Emission trading under uncertainties

Emission trading as an economic instrument for environmental regulations has been analyzed e.g. by Dales (1968). The author assumed that environmental agency requires each regulated source to submit permits (also known as quotas, credits, or allowances), which are transferable. Each source reduces its emissions until the cost for one more unit of emissions reduction is higher than to buy a permit. If the permit market is perfectly competitive, then marginal abatement costs will be equal to the permit price and therefore equal across all regulated sources.

The equality of marginal abatement costs is a necessary condition for any given level of environmental quality to be achieved at the lowest overall cost, a condition known as cost-effectiveness. Putting a price on carbon was a crucial step towards market-based regulations of climate policies. Montgomery (1972) showed that market instruments may achieve their environmental objectives at lower information requirements than conventional command-and-control systems. Therefore, encouraged by economists (Stavins 2010; Kerr 2000; Baumol and Oates 1975; Dales 1968), the idea of carbon trading markets becomes increasingly popular for global climate change control. The theoretical conclusion of the cost effectiveness is based upon assumption that emissions can be measured objectively and that noncompliance to environmental goals may be verified and penalized (de Jong and Walet 2004).

Unfortunately, the existence of various exogenous and endogenous inherent uncertainties violates traditional pricing concepts and raises serious concerns regarding the ability of existing carbon trading markets to fulfill their main purpose–to control climate change–without creating world-wide irreversible socio-economic and environmental disruptions.

Emissions uncertainties vary in shape and duration depending on their origin (see de Jong and Walet 2004 and discussion in Ermolieva et al. 2010b). Large variability of emissions may easily cause their underreporting requiring regulations as in the following section. A comprehensive discussion of uncertainties and their implications can be found in the volume by Lieberman et al. (eds.) (2007) and in Gillenwater et al. 2007. Some characteristics of uncertainties can be derived after revisions of the historical emissions time series following "The Good Practice Guidance" report of the IPCC (2000). In particular, Winiwarter and Muik (2010) explore uncertainties for total emissions in Austria 2005. Figure 1 shows probability density distribution which is most strongly influenced by the lognormal distribution of the uncertainty in N2O (in CO2 equivalent) emissions. Non-normal character of this distribution illustrates the need for new regulations avoiding standard mean-variance analysis suitable only for normal distributions.

Although data improve and the requirements for measuring emissions are being clarified, some source characteristics are inherently uncertain to be measured with accuracy. There will always be different levels and shapes of uncertainties in their estimates. This raises a fundamentally important issue about developing proper approaches to emission trading under uncertainty providing endogenous forces for uncertainty reduction.

3 Stochastic model for robust emission trading

In the following section, we introduce a distributed optimization model incorporating uncertainty and risk-based regulations into emission trading system. The model imposes

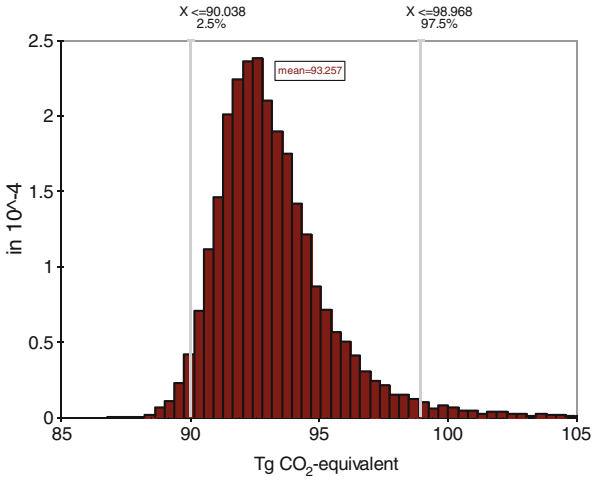

Fig. 1 Probability density distribution of total emissions in Austria, 2005. (*Source:* Winiwarter and Muik 2010)

stability requirement by using appropriate safety constraints to control the level of admissible uncertainty which would guarantee with desirable probability the necessary emissions reduction targets (e.g., post-Kyoto pledge targets).

This type of safety constraints is used in pollution control, financial applications, stability regulations in the insurance industry, reliability theory, and catastrophic risks management (see, e.g. discussion in Ermolieva and Ermoliev 2005; Ermolieva et al. 2010a). In a sense, they reduce the reported emissions reductions to a verifiable level with a given probability.

The model is decomposed into interdependent submodels: individual parties' models and a social planner model. First, for a fixed amount of permits, each party solves its individual problem by defining how much resources to spend on abating emissions and uncertainty reduction to satisfy safety constraints on emissions targets with desirable probability. This problem does not require information on other parties. Second, the social planner decides on the redistribution of permits minimizing the total (social) cost, which involves the knowledge of costs functions of all parties. This information is private and therefore the specific methodology of decentralized (distributed) optimization is applied. The model can be viewed as a prototype to simulate an emission trading market that is regulated in a decentralized way (Ermoliev et al. 2000).

3.1 Party's model

Let us denote the uncertainty of reported emissions x_i as random variable $\xi_i(x_i, \omega_i)$, where ω_i is a vector of all uncertainties (scenarios) affecting emissions of party i. The uncertainty $\xi_i(x_i, \omega_i)$ can be reduced by investments in new production technologies and monitoring mechanisms under additional safety constraints, which can be written as

$$P[x_i + \xi_i(x_i, \omega_i) \leq K_i + y_i] \geq Q_i, \tag{1}$$

for all parties i. Here Q_i denotes a required safety level ensuring the probability of emissions x_i and uncertainties $\xi_i(x_i, \omega_i)$ do not exceed emission target K_i adjusted by tradable (positive or negative) permits y_i, $\sum_{i=1}^{n} y_i = 0$. Safety level Q_i is imposed by regulatory agency to ensure robust performance of the market. In this paper we don't consider verification mechanisms. We assume that Q_i corresponds to varifiable level of $\xi_i(x_i, \omega_i) \leq K_i + y_i - x_i$. Quantile-based constraint

(1) is typicaly used for regulating varifiable standards, when it is impossible to evaluate monetary losses from their violations that would allow to use penalty functions. Convex CvaR risk measures implicitly induce these constraints. The discussion of these issues is beyond the scope of the paper, Yet, necessary detailes can be found in (Ermoliev and von Winterfeldt 2012; Rockafellar and Uryasev 2000).

Safety constraints (1) can be also written in the form of equivalent deterministic nonlinear constraints. Let us define quantile $z_i(x_i)$ as the minimal z such that

$$P[\xi_i(x_i, \omega_i) \le z] \ge Q_i.$$

Then the following equivalent constraints can be substituted for the safety constraint (1):

$$x_i + u_i \le K_i + y_i, u_i \le z_i(x_i), \tag{2}$$

where variable u_i is associated with the level of uncertainty remaining after investing in monitoring and other technologies that may reduce the uncertainty $\xi_i(x_i, \omega_i)$ of emissions. Let us note that indicator u_i corresponds to probabilistic versions of "signaling" used for coping with asymetric information (see e.g. Milgrom and Roberts 1986). Equation (2) show that safety constraints induce risk-related upper bounds $z_i(x)$ on uncertainty dependent on reported emissions level x_i and characteristics of uncertainty ω_i.

For the individual optimization problem, we define the least costs function $f_i(y_i)$ for party i, $i = 1, \ldots\ldots, n_i$, (to comply with imposed safety requirements (2) with fixed permits y_i and the target K_i) as the minimum of expected total emission reduction costs $c_i(x_i, \omega_i)$ and uncertainty reduction costs $d_i(u_i, \omega_i)$ for a given permit y_i:

$$\min_{x_i u_i} E[c_i(x_i, \omega) + d_i(u_i, \omega)] := f_i(y_i). \tag{3}$$

Let us note that in general costs of emissions reductions and monitoring costs are not separable, i.e., instead of $c_i(x_i, \omega) + d_i(u_i, \omega)$ we have to consider a total cost function of the form $C_i(x_i, u_i, \omega)$ that does not affect the following analysis. In fact, similar functions are used in section 4. Cost functions $C_i(\cdot,\cdot,\cdot)$ have a complex structure usually defined implicitly by solving specific nested optimization models (similar to the definition of function $f_i(y_i)$). In section 4 we use for this purpose the GAINS model (Amann 2009; Wagner and Amann 2009; Wagner et al. 2012).

The main issue now concerns cost-effective allocation of permits y_i under asymmetric information about cost functions $f_i(y_i)$, i.e. solution of the following problem.

3.2 Social planner model

The social planner (environmental agency) needs to find the permit vector $y = (y_1, \ldots, y_n)$ or distribution of permits among parties minimizing the total (social) cost

$$F(y) = \sum\nolimits_{i=1}^{n} f_i(y_i) \tag{4}$$

subject to

$$\sum\nolimits_{i=1}^{n} y_i = 0. \tag{5}$$

This means that the total allocation of permits remains the same as at the initial state, i.e., $\sum_{i=1}^{n}(K_i+y_i)=\sum_{i=1}^{n}K_i$.

The optimization model (4)–(5) could be easily solved by the social planner if private information on cost functions and uncertainties is available. The absence of information on

total cost function $F(y)$ requires developing specific decentralized optimization procedures which can be viewed as sequential bilateral emission trading processes.

The convergence study of these processes is based on the following market equilibrium conditions. Assume that $f_i(y_i)$, $i=1, \ldots, n$, is continuously differentiable and strongly convex function. Then, from the Lagrangian minimization $L(y,\lambda)=\sum_{i=1}^{n} f_i(y_i)-\lambda\sum_{i=1}^{n} y_i$, a trade equilibrium is defined as the vector $y = (y_1, \ldots, y_n)$satisfying the following equations:

$$f_i'(y_i) = \lambda, i = 1, \ldots, n, \lambda\sum_{i=1}^{n} y_i = 0. \quad (6)$$

From condition (6) it follows that the marginal value of a permit in equilibrium is equal to a λ same for all parties. Unlike the standard optimization models, the optimality conditions (6) cannot be directly used because parties don't reveal private information about functions f_i, i.e. function $F(y)$ is not known.

3.3 Bilateral negotiations

Our procedure resembles bilateral trades negotiation process when any two parties exchange emissions permits in a mutually beneficial way. Before presenting a step-by-step algorithm let us briefly outline theoretical background of this procedure, more details can be found in Ermolieva et al. 2010a. The convergence of this procedure requires $f_i(y_i)$ to be strongly convex continiously differentiable functions which can be often achieved by slight, practically equivalent, modifications of $f_i(y_i)$. Let $y^k=(y_1^k,\ldots,y_n^k)$ be the vector of emission permits after $k=1, 2, \ldots$ steps (trades). Pick up (say, at random) two parties i and j with permits y_i^k and y_j^k. According to (6), if parties i and j have different marginal costs $f_i'(y_i^k)\neq f_j'\left(y_j^k\right)$, then the permit vector $y^k=(y_1^k,\ldots,y_n^k)$ is not cost-effective. Assume that $f_i'(y_i^k)-f_j'\left(y_j^k\right) < 0$. Constraint (5) requires that the feasible exchange of permits does not change the total allocation of permits, i.e. it has to be such that $y_i^{k+1}+y_j^{k+1}= y_i^k+y_j^k$. If we take $y_i^{k+1}=y_i^k+\Delta$ and $y_j^{k+1}=y_j^k-\Delta$, $\Delta > 0$, then the new feasible vector of permits y^{k+1} for proper Δ reduces the total costs of parties $f_i(y_i^k)+f_j(y_j^k)$ and hence the total cost $F(y^k)$ because:

$$\begin{aligned} F\left(y^{k+1}\right)-F\left(y^k\right) &= f_i\left(y_i^{k+1}\right) + f_j\left(y_j^{k+1}\right)-f_i\left(y_i^k\right)-f_j\left(y_j^k\right) \\ &= \Delta_k\left(f_i'(y_i^k)-f_j'\left(y_j^k\right)\right) + o(\Delta) < 0, \end{aligned} \quad (7)$$

for small Δ. This equation demonstrates that bilateral trade reduces the aggregate costs for sources i and j. From (7) for small Δ we also have important inference:

$$f_i\left(y_i^{k+1}\right)-f_i\left(y_i^k\right) < f_j\left(y_j^k\right)-f_j\left(y_j^{k+1}\right) \quad (8)$$

i.e., the new distribution of permits reduces costs of j more than increases the cost of i. Hence j is able to compensate i for the increased costs in a mutually beneficial way, what is discussed in the next section.

For the convergence of the outlined procedure the value Δ at each step k, $\Delta = \Delta_k$, must equalize marginal costs of parties i and j, i.e., $f_i(y_i^k+\Delta_k)=f_j\ (y_j^k-\Delta_k)$.

Let us summarize the corresponding procedure more precisely in a step-by-step way:

Step 0: Let $y^0=(y_1^0,\ldots,y_n^0)$ be any initial vector of permits, $\sum_{l=1}^{n} y_l^0=0$.

Step k: Let $y^k=(y_1^k,\ldots,y_n^k)$ be the vector of permits y^k at step k. Pick up two parties i and j (at random) with different marginal costs, e.g., $f_i'(y_i^k) < f_j'\left(y_j^k\right)$. Party i sequentially

increases amount $\varepsilon\nu$ of buying permits from party j for a small δ and ν=1, 2, …, ν_k, for some ν_k such that $f_i'\left(y_i^k+\delta\nu_k\right)$ is practically equal $f_j'\left(y_j^k-\delta\nu_k\right)$, i.e.

$$f_i'\left(y_i^k+\Delta_k\right)\approx f_j'\left(y_j^k-\Delta_k\right) := \lambda_k, \delta\nu_k = \Delta_k. \quad (9)$$

Step k+1: Calculate y^{k+1}=(y_1^{k+1},…,y_n^{k+1}), i.e., y_l^{k+1}=y_l^k, $l \neq i, j$, y_i^{k+1}=y_i^k +Δ_k, y_j^{k+1}=y_j^k–Δ_k, and so on, until marginal costs of all parties become practically equal each other, i.e. the equilibrium price λ^* as in (9).

This algorithm operates by using marginal values of publically unknown at each iteration function $F(y)$ and values y_l=y_l^k. Essential assumption is the reversibility of trades that is addressed in section 4.

The value λ_k can be viewed as an equilibrium price at step k. Let us note that price process λ_k is driven endogenously by total (emissions and uncertainty reduction, and trading) cost-minimizing decisions of meeting parties, what is fundamentally different from standard models of financial markets with instanteniously observable prices.

During the process, marginal costs and prices will differ between the sequential trades, but finally the trading system converges to an equilibrium y^*=(y_1^*,…,y_n^*), λ^* with marginal costs of all parties equal to equilibrium price as in (6). The proof of the convergence is for example in (Ermolieva et al. 2010a).

Formally, the algorithm converges in the following sense. Assume that $f_i(\cdot)$, i=1, 2, …, n, are strongly convex functions. Then for any ε>0, there is a δ_ε>0 such that the distance $\|(\lambda_k,y^k)-(\lambda^*,y^*)\|$ between (λ_k, y^k) and the equilibrium (λ^*, y^*) is less than ε for large k.

3.4 Redistribution schemes

From (8) it follows that at each step k trading parties i, j can redistribute joint cost by using some variables φ_i^{k+1} and φ_j^{k+1} reducing initial costs of these parties in mutually beneficial manner:

$$f_i\left(y_i^{k+1}\right)+f_j\left(y_j^{k+1}\right)=\varphi_i^{k+1}+\varphi_j^{k+1}, \varphi_i^{k+1}<f_i\left(y_i^k\right), \varphi_j^{k+1}<f_j\left(y_j^k\right).$$

Therefore at the equilibrium y^*=(y_1^*,…,y_n^*) parties will deal actually with payments φ_i^*<$f_i(y_i^0)$ such that the following equation is satisfied:

$$\sum_{i=1}^n \varphi_i^* = \sum_{i=1}^n f_i\left(y_i^*\right) := F_I,$$

where I = {1, …, n}. From this equation follows the Pareto efficiency of φ^*=$(\varphi_i^*)_{i=1,\ldots,n}$, i.e., a value φ_i^* cannot be decreased without increasing some other value φ_j^*, $i \neq j$, to satisfy this equation. An important question is whether the grand coalition I of parties is stable, i.e., the following equation is also satisfied:

$$\sum_{i\in C} \varphi_i^* \leq F_c$$

for any other coalition $C \subseteq I$. Accordingly, a distribution of payments φ^* is a core solution if it satisfies these two equations.

This is a well-known game-theoretic concept (see e.g., McCain 2010), where F_c corresponds to a coalition function. In the case of bilateral trades the core solution reflects the following intuitively evident fact: if new parties join a coalition C creating a larger coalition

I, parties from C would be able to proceed with the trading process and reduce their costs further. Formally speaking, the bilateral trading procedure for coalition I allows to find the equilibrium price λ^* and a vector $y^*=(y_1^*,\ldots,y_n^*)$ minimizing the Lagrangian $L(y, \lambda^*)$ with $L(y^*,\lambda^*)=\sum_{i=1}^{n}(f_i(y_i^*)-\lambda^* y_i^*)=F(y^*)$. Therefore, if function $F(y)$ is convex, then it is evident that the payment redistribution scheme

$$\varphi_i^* = f_i(y_i^*)-\lambda^* y_i^*, i = 1,\ldots,n, \tag{10}$$

is a core solution, i.e. it minimizes any partial sum of $L(y^*, \lambda^*)$. In nonconvex cases, if the function $F(y)$ is globally Lipschitz continuous, then the core solution remains the same (see discussion in Evstigneev and Flam 2001). Unfortunately, the bilateral trading procedure of section 3.3 will not, in general, converge to a global solution. For this, we need to use an appropriate global distributed optimization approach.

3.5 Price-based scheme

Let us compare the proposed bilateral trading scheme with a market price-based scheme. This section discusses high sensitivity of price-driven markets to uncertainties restricting to achieve cost-effective and environmentally safe solutions even in convex cases and reversible trades.

A cost-effective and environmentally safe price is a solution of the model which is dual to the primal model (4)–(5). The dual model derives the equilibrium price λ^* maximizing the following concave and, in general, non-differentiable (continiously) function

$$g(\lambda) = \min_y \sum\nolimits_{i=1}^{n}(f_i(y_i)-\lambda y_i) \tag{11}$$

A given market price signal λ decentralizes the solution of internal minimization problem into individual subproblems of parties: find solutions $y_i(\lambda)$ minimizing functions $f_i(y_i)-\lambda y_i$ for each i. In general, solutions $y_i(\lambda)$ don't satisfy the balance Eq. (5), i.e. $\sum_{i=1}^{n} y_i(\lambda)\neq 0$, therefore the price λ has to be adjusted towards the desirable balance.

To ensure the balances, current λ_k at time k=0, 1, … is adjusted proportionally to the imbalance, $\sum_{i=1}^{n} y_i(\lambda)$, that is a kind of gradient (subgradient) $g'(\lambda)$ for continuously non-differentiable $g(\lambda)$:

$$\lambda_{k+1} = \lambda_k-\rho_k \sum\nolimits_{i=1}^{n} y_i(\lambda_k) \tag{12}$$

with a step-size ρ_k. From the convergence results of quasi-gradient methods (see, e.g., discussion in Ermoliev and Wets 1988) it follows that with $\rho_k = const/k+1$, the sequence λ_k converges to the equilibrium price maximizing $g(\lambda)$. Unfortunately, this type of procedures requires the private information of parties for tracking imbalances $\sum_{i=1}^{n} y_i(\lambda_k)$. Uncertainties of markets make problematic achieving cost-effective and environmentally safe allocations of permits by using price-based process (12) even under unrealistic assumption that values $\sum_{i=1}^{n} y_i(\lambda_k)$ can be exactly calculated. The convergence of this process to equilibrium price requires rather sophisticated mechanisms for smoothing observable random prices consistently with step-size ρ_k (see e.g. Ermolieva et al. 2010a). In addition to these shortcomings, the main issue for emission trading schemes is the irreversibility of trades restricting to achieve global cost-effective and environmentally safe solutions. For bilateral trades, this is discussed in the following section.

4 Computerise multi-agent trading system: numerical experiments

The available computing technology allows us to organize a Decentralized COMATS based on model (1)–(5) and bilateral trading procedure of subsection 3.3. A distributed computers network connects computers of parties with the computer of a central agency. Using a graphical user interface, parties store private information on cost functions and other characteristics of the model defined by Eqs. (1)–(5) including specific probability distributions and scenario generators characterizing uncertainties of emissions and other parameters.

The central agency imposes market regulations in the form of safety constraints on environmental targets. Following the procedure in section 3.3, the computer of the central agency "picks up" at random, a pair of parties i, j and in anonymous manner, as it is discussed in subsection 3.4, "negotiates" with computers of parties Δ_k and vector y^k solving (9). Then, another pair of parties is picked up and the negotiations are repeated. These calculations can be easily organized without revealing private information of parties, in particular, due to distributed among different computers data of parties. The process goes on until equilibrium (λ^*, y^*) is reached. The equilibrium solution can then be analyzed and implemented in reality using redistribution schemes discussed in subsection 3.4. Therefore at the first stage COMATS evaluates equilibrium prices and permits, whereas at the second stage the equilibrium tradable permits y^* are implemented. The information about the equilibrium price λ^* identifies also the core solution (section 3.4.) defining stable coalition of parties. It means that no party has the incentive to leave the coalition or terminate participation at any intermediate step. COMATS is of benefit both for parties and for the market. For parties, the prototype emission trading enables the analysis of the balance between robust cost-efficient and environmentally safe trades and emissions abatements. For the market, it allows to impose safety regulations ensuring stability and fair functioning without shocks.

In what follows, we discuss the implications of uncertainties on market structure by using COMATS. To analyze performance of COMATS numerically, we use relevant to (1)–(5) data on the costs of emissions reduction from the GAINS model (Amann 2009; Wagner and Amann 2009; Wagner et al. 2012) for the following countries and groups of countries Australia, Canada, EU27, Japan, Norway, Russia, Ukraine, USA. The marginal cost curves (of emissions reduction as a percent of pledge targets) are displayed in Fig. 2.

Table 1 shows reported emissions levels in 1990 and 2009. Projected (baseline) country-specific emissions levels in 2020 are derived from the GAINS model, and the pledge emissions reduction targets in 2020 are set according to (Wagner and Amann 2009). The data on emissions uncertainties and costs of reducing uncertainties are compiled from IPCC, Nahorski et al. 2007, 2010; Obersteiner et al. 2000; Godal et al. 2003; Winiwarter and Rypdal 2001; Winiwarter 2007; Wagner and Amann 2009; Wagner et al. 2012. We employ uncertain emissions level in the year 2020 as percentage of the reported business as usual emissions level in 2020.

Table 2 illustrates the results of emission permit trades among seven countries ignoring uncertainties. In equilibrium, the cost of reducing reported emissions (also optimal price of emissions permit) is about €13 per tC, which is consistent with existing market trends (www.pointcarbon.com). Total costs of emissions reduction to targeted levels without trades are defined by "Costs for mitigation without trades", while "Costs after trades" stands for optimal costs for emissions abatements and trades. Financial advantages of trading are estimated by comparing the two alternatives. Optimal total ("core") costs of parties are calculated according to formula (10). In these experiments, no emission uncertainties are included, therefore no costs are spent on uncertainties reduction, i.e. "unc. reduction" equals 0. Russia

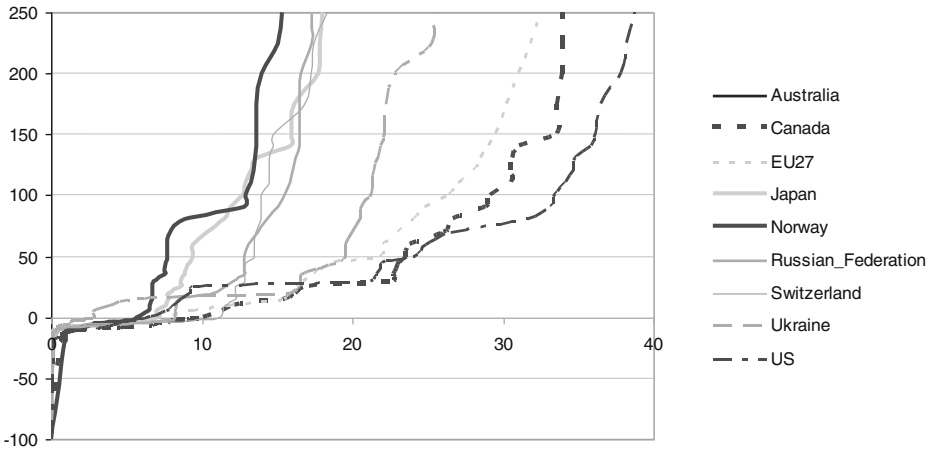

Fig. 2 Marginal cost of emissions reduction as percent of pledge targets, € per tC

and Ukraine are major permits' sellers (negative values of trades), and it is explained by their emissions levels in 2020, which are lower than pledge targets.

Results of a scenario involving uncertainties are presented in Table 3. Optimal marginal cost of reducing unit reported emissions equals the cost of reducing unit uncertain emissions and is about € 25 per tC, which is almost twice higher than in the case when uncertainties are not included in calculations. The higher costs are due to more abatements as the uncertainties are now accounted for in the verification of targets compliance according to (2). Optimal marginal costs also increase because in this case Russia and Ukraine invest in uncertainties reduction and therefore can offer less traded permits at zero price than in the scenario without uncertainties.

In the scenario when uncertainties are explicitly included in the trading, the US turns to a permit supplier. This is due to two reasons. First, the US marginal cost curve is a flatter slope than other countries. Second, because the assumed uncertainties in the US are relatively low. In this scenario, as Table 3 also shows, Russia and Ukraine invest in monitoring to reduce the uncertainties around targets and, therefore, supply less permits than in the case without uncertainties. Although the results have illustrative purpose, the conclusion is that the equilibrium price of emissions permits highly depend on uncertainties.

Table 1 Baseline and pledge targets

	Emissions 1990	Emissions 2009	Baseline 2020	Pledge target 2020	Unc. (% baseline)
USA	5069	6006	6641	4815	15
Australia	278	391	418	264	10
Canada	456	558	693	433	15
EU27	4399	4241	4677	4321	15
Japan	1143	1270	1316	1086	15
Russia	2499	1583	1945	2374	25
Ukraine	716	339	374	680	25

(Wagner and Amann 2009)

Table 2 Trades ignoring uncertainty

	USA	Austr	Can	EU27	Japan	Rus	Ukr
Em opt (MtC)	5017	397	643	4401	1274	1900	340
Unc opt	0	0	0	0	0	0	0
Trades opt	202	133	210	80	188	−474	−340
Marginal cost (€ per tC)	13	13	13	13	13	13	13
Costs after trades (million €)							
Em reduction	11091	261	650	2969	392	1270	200
Unc reduction	0	0	0	0	0	0	0
Trades	2596	1637	2540	958	2231	−5739	−4046
Total (core)	13687	1898	3190	3927	2622	−4469	−3845
Costs for mitigation without trades (million €)							
Em reduction	13839	16992	29341	4221	23959	0	0
Unc reduction	0	0	0	0	0	0	0
Total	13839	16992	29341	4221	23959	0	0
Financial advantages of trading	152	15095	26152	294	21336	4469	3845
Total profits							71342

In both scenarios, with and without uncertainties treatment, the "core" solution derived at equilibrium makes all parties better off. Total profits from trades equal about 71.3 and 213 Billion €, in case without and with uncertainty, respectively, which is 19 % and 23 % higher, for without and with uncertainties, than in the situation without trading.

Distortions to the emissions trading system may be caused by individual characteristics of market players. For example, as Table 4 indicates, participation of the US in EU ETS is of major

Table 3 Trades with uncertainty

	USA	Austr	Can	EU27	Japan	Rus	Ukr
Em opt (MtC)	3519	385	606	4138	1229	1803	327
Unc opt	249	37	59	988	150	331	153
Trades opt	−1047	157	232	805	293	−240	−200
Marginal cost (€ per tC)	25	25	25	25	25	25	25
Costs after trades (million €)							
Em reduction	38735	666	1733	9157	1259	3686	500
Unc reduction	5031	344	626	2704	558	207	142
Trades	−25181	3782	5579	19360	6645	−5772	−4219
Total (core)	18586	4792	7939	31221	8462	−2293	−3577
Costs for mitigation without trades (million €)							
Em reduction	21712	30087	59560	37598	90418	0	0
Unc reduction	2925	4756	8204	8587	13354	71	0
Total	24637	34843	67764	46185	103772	0	0
Profits/financial advantages of trading	6051	30051	59825	14965	95310	2325	3577
Total profits							212104

Table 4 Trades with uncertainty, US excluded

	USA (excluded)	Austr	Can	EU27	Japan	Rus	Ukr
Em opt	3519	336	518	3589	1165	1577	293
Unc opt	249	35	58	989	154	295	149
Trades opt	−1047	107	142	257	233	−502	−237
Marginal cost	25	75	75	75	75	75	75
Costs after trades (million €)							
Em reduction	38735	3860	8702	49011	6587	19884	3040
Unc reduction	5031	1148	2003	8359	1680	690	356
Trades	−25181	7974	10665	19233	17556	−37469	−17901
Total (core)	18586	12983	21370	76603	25823	−16895	−14505
Costs for mitigation without trades (million €)							
Em reduction	21712	30087	59560	37598	90418	71	0
Unc reduction	2925	4756	8204	8587	13354	−38	0
Total	24637	34843	67764	46185	103772	33	0
Profits/financial advantages of trading	6051	21860	46394	−30417	77949	16928	16996
Total profits							153270

benefit. The market without the US has much higher marginal cost (if compared to Table 3) due to rather steep cost curves and high demands in permits (except for Russian and Ukraine) of the other traders.

5 Concluding remarks

In theory, the emission price of tradable permits should establish the marginal cost of emissions reductions to meet the cap. In reality, the existence of various exogenous and endogenous inherent uncertainties violates this traditional deterministic pricing concept. Lessons learned from the existing emission trading schemes point out the need for the market's safety regulations smoothing its performance.

Proposed in this paper multi-agent approach integrating regulations of carbon emissions and uncertainties with redistribution of emissions through emission trading under safety constraints allows us to design a computerized multiagent trading system that may function as a prototype of a robust emission trading market. The model explores conditions of market's stability with respect to uncertainty by using appropriate safety constraints controlling verifiable uncertainty reductions which would guarantee cost efficiency of trades and safety levels of emission reduction targets (e.g., post-Kyoto pledge targets). We illustrate functioning of the robust market with numerical results involving such countries as the US, Australia, Canada, Japan, EU27, Russia, Ukraine, etc. Explicit treatment of uncertainties may significantly affect portfolios of technological and trade policies, market prices and change the market structure. We conclude also that exclusion or inclusion of additional players may have dramatic effects on the market.

Acknowledgments The authors are grateful to the anonymous reviewers for valuable comments that helped us to improve the manuscript. We also thank Guest Editor Dr. Jean P. Ometto for his suggestions.

References

Amann M (2009) Integrated assessment tools: the greenhouse and air pollution interactions and synergies (GAINS) model. Pollut Atmosph Special Issue 73–76

Baumol W, Oates W (1975) The theory of environmental policy. Cambridge University Press, Cambridge, New York, Sydney

Betz R, Sato M (2006) Emissions trading: lessons learnt from the 1st phase of the EU ETS and prospects for the 2nd phase. Clim Pol 6:351–359

Dales JH (1968) Pollution property and prices: an essena in policy-making and economics. University of Toronto Press

De Jong C, Walet K (eds) (2004) A guide for emission trading: risk management and business implications. Risk Books, London

Ermoliev Y, von Winterfeldt D (2012) Systemic risk and security management. In: Ermoliev Y, Makowski M, Marti K (eds) Managing Safety of heterogeneous systems. Springer, Berlin, pp 19–49

Ermoliev Y, Wets R (eds) (1988) Numerical techniques of stochastic optimization. Computational mathematics. Springer Verlag, Berlin

Ermoliev Y, Michalevich M, Nentjes A (2000) Markets for tradable emission and ambient permits: a dynamic approach. Environ Res Econ 15:39–56

Ermolieva T, Ermoliev Y (2005) Catastrophic risk management: flood and seismic risks case studies. In: Wallace SW, Ziemba WT (eds) Applications of stochastic programming. MPS-SIAM Series on Optimization, Philadelphia

Ermolieva T, Ermoliev Y, Fischer G, Jonas M, Makowski M (2010a) Cost effective and environmentally safe emission trading under uncertainty. In: Marti K, Ermoliev Y, Makowski M (eds) Coping with uncertainty: robust solutions. Springer, Heidelberg, pp 79–99

Ermolieva T, Ermoliev Y, Fischer G, Jonas M, Makowski M, Wagner F (2010b) Carbon emission trading and carbon taxes under uncertainties. Clim Chang 103(1–2)

Evstigneev I, Flam S (2001) Sharing nonconvex cost. J Glob Optim 20:257–271

Gillenwater M, Sussman F, Cohen J (2007) Practical policy applications of uncertainty analysis for national greenhouse gas inventories. In: Lieberman D, Jonas J, Nahorski Z, Nilson S (eds) Accounting for climate change: uncertainty in greenhouse gas inventories–verification, compliance, and trading. Springer Verlag

Godal O, Ermoliev Y, Klassen G, Obersteiner M (2003) Carbon trading with imperfectly observable emissions. Environ Res Econ 25:151–169

IPCC (2000) Good practice guidance and uncertainty management in national greenhouse gas inventories. Intergovernmental Panel on Climate Change, National Greenhouse Gas Inventories Programme, Hayama

Kerr S (ed) (2000) Global emissions trading: key issues for industrialized countries. Edward Elgar, Cheltenham, UK, Northampton, MA, US

Lieberman D, Jonas M, Nahorski Z, Nilsson S (2007) Accounting for climate change: uncertainty in greenhouse gas inventories—verification, compliance, and trading. Springer Verlag, Berlin

McCain R (2010) Game theory: a nontechnical introduction to the analysis of strategy. World Scientific Publishing, ISBN-13 978-981-4289-65-8

Milgrom P, Roberts J (1986) Price and advertising signals of product quality. J Polit Econ 94:796–821

Montgomery DW (1972) Markets in licenses and efficient pollution control programs. J Public Econ 75:273–291

Nahorski Z, Horabik J, Jonas M (2007) Compliance and emissions trading under the Kyoto protocol: rules for uncertain inventories. In: Lieberman D, Jonas M, Nahorski Z, Nilsson S (eds) Accounting for climate change: uncertainty in greenhouse gas inventories–verification, compliance, and trading. Springer Verlag 119–138

Nahorski Z, Stanczak J, Palka P (2010) Multi-agent approach to simulation of the greenhouse gases emission permits market. In: Proceedings of the 3rd International Workshop on Uncertainty in Greenhouse Gas Inventories, 22–24 September 2010, Lvov, Ukraine, 183–195

Obersteiner M, Ermoliev Y, Gluck M, Jonas M, Nilsson S, Shvidenko A (2000) Avoiding a lemons market by including uncertainty in the Kyoto protocol: same mechanism–improved rules. Interim report IR-00-043. International Institute for Applied Systems Analysis, Laxenburg

Rockafellar T, Uryasev S (2000) Optimization of conditional value at risk. J Risk 2(3):21–41

Roos J (2011) EU emissions trading triggered dash for coal. The Breakthrough Institute, http://breakthrougheurope.org/

Stavins R (2010) The problem of the commons: still unsettled after 100 years. Discussion paper RFF DP 10–46. Resources for the Future. Washington DC, www.rff.org

Stikkelman R, Dijkema G, Chappin E (2010) Emissions trading fails to reduce CO2 emissions. Delft University of Technology. Faculty of Technology, Policy and Management

Wagner F, Amann M (2009) GAINS contribution to ETMA request #2B-v1, International Institute for Applied Systems Analysis (IIASA)

Wagner F, Amann M, Borken-Kleefeld J, Cofala J, Höglund-Isaksson L, Purohit P, Rafaj P, Schöpp W, Winiwarter W (2012) Sectoral marginal abatement cost curves: implications for mitigation pledges and air pollution co-benefits for Annex I countries. Sustain Sci 7:169–184

Winiwarter W (2007) National greenhouse gas inventories: understanding uncertainties versus potential for improving reliability. Water Air Soil Pollut 7:443–450. doi:10.1007/s11267-006-9117-3

Winiwarter W, Muik B (2010) Statistical dependence in input data of national greenhouse gas inventories: effects on the overall inventory uncertainty. Clim Chang 103:19–36. doi:10.1007/s10584-010-9921-7

Winiwarter W, Rypdal K (2001) Assessing the uncertainty associated with national greenhouse gas emission inventories: a case study for Austria. Atmos Environ 35:5425–5440

DOI 10.1007/978-3-319-15901-0_14
Reprinted from *Climatic Change* Journal, DOI 10.1007/s10584-013-1039-2

Simulation of an uncertain emission market for greenhouse gases using agent-based methods

Zbigniew Nahorski · Jarosław Stańczak · Piotr Pałka

Received: 23 December 2012 / Accepted: 19 December 2013 / Published online: 7 February 2014
© The Author(s) 2014. This article is published with open access at Springerlink.com

Abstract The paper presents the problem of a simulation of the greenhouse gases emission permits market where only low accuracy emission amounts are known. An organization of the market with uncertain emissions is proposed and trading rules for individual market participants are discussed. Simulation of the market is based on a multi-agent system. Negotiation of purchase/sale prices between the parties are introduced, where the trading parties adopt one of two options: (i) bilateral negotiations, and (ii) sealed bid reverse auctions. Results of simulation runs show trajectories of transaction prices, as well as probability distributions of learning agents' bidding prices.

1 Introduction

Markets for emisions of greenhouse gases (GHG) were designed to lower the costs of GHG emission abatement. In GHG markets every party is allocated an emission quota, otherwise known as permits (usually smaller than the actual emissions). At the end of the trading period, a party has either to keep its emissions within the allowed quota, or buy permits for superfluous emissions. In this context, we either use the term on trading emisions or trading emission permits.

Some existing markets, such as the EU ETS (IETA 2005), trade only these gases, whose amount can be adequately defined. However, a market covering all anthropogenic emissions, like that covered by the Kyoto Protocol, must also include very poorly assessed emission amounts, such as those connected with agriculture or land-use change. Then the question

This article is part of a Special Issue on "Third International Workshop on Uncertainty in Greenhouse Gas Inventories" edited by Jean Ometto and Rostyslav Bun.

Electronic supplementary material The online version of this article (doi:10.1007/s10584-013-1039-2) contains supplementary material, which is available to authorized users.

Z. Nahorski (✉) · J. Stańczak
Systems Research Institute, Polish Academy of Sciences, Newelska 6, 01-447 Warsaw, Poland
e-mail: Zbigniew.Nahorski@ibspan.waw.pl

P. Pałka
Institute of Control and Computation Engineering, Warsaw University of Technology, Nowowiejska 15/19, 00-665 Warsaw, Poland

arises, does trading such emissions actually ensure their reduction as hoped and planned for? And, should a tonne of poorly estimated and well defined emissions be priced equally?

Markets are often analyzed by either using a static or dynamic optimization or a game-theoretic approach. With full information on the parties, these approaches allow for analytical analysis of markets. Recently, agent-based models have been used to investigate market behavior dynamics using a simulation approach. Parties are represented by intelligent programming agents which negotiate and trade goods according to given market rules and the partial information they possess. This approach is much more flexible as to any assumptions made on the market information and tries to better mimic real market behaviours, including also their transients. It is applied in this paper to simulate a GHG emission permits market.

The method proposed does not assume an ideal market. Neither the equilibrium prices are assumed to be known in the trading, nor is an approach made without trading prices, Ermoliev et al. (1996) or Ermolieva et al. (2010), considered. A more sophisticated market model is introduced, with price negotiations and price influenced agent behavior, similar to that in Bonatti et al. (1998). Each successive transaction moves the market toward an equilibrium.

In simulations, a multi-agent platform for multicommodity exchange (Kaleta et al. 2009) has been used. Each agent minimizes its own objective function, which is the cost of emission reduction plus any expenditure for the permits. The permit purchase/sale prices have an influence upon the profitability of transactions and the decision to buy/sell permits, i.e. whether it is better to reduce emissions or to buy permits. Two trading mechanisms are considered: a bilateral trade and a sealed-bid reverse auction (a tender).

Trade negotiations are the way to solve uncertainty in selling/buying prices, whichever trading mechanism is used. However, as mentioned earlier, uncertainties in emission amounts also characterize GHG markets, as well as some other markets designed for trading environmental quantities. These uncertainties have not influenced the prices in any of the previous and existent markets. In the solution that is presented in this paper emission uncertainties are taken into account in the simulation by using effective permits, as proposed in Nahorski et al. (2007). This brings the problem of trading uncertain emissions to that of usual trade with a perfectly known amount of the good being traded. The goal of this paper is to simulate a market using the rules proposed in earlier papers, and particularly in Nahorski et al. (2007) and Nahorski and Horabik (2012).

Only a few methods have been proposed to solve the trade in uncertain environmental goods, and in particular goods with very differentiated uncertainties, say 2–5 % as against 80–100 % uncertainty. Apart from that which is described in Nahorski et al. (2007), the present authors are only aware of that described by Ermolieva et al. (2013). Our method is simple in implementation and does not demand far reaching changes in the trading rules. Knowledge of the uncertainty parameters is necessary, but it is also needed in other methods.

2 Market with known emissions

Before presenting the method, we should like to start with a short presentation of an analytical solution of the market with fully known variables. Let us consider a market with N parties P_n, $n=1,\ldots N$, trading the emission permits. Each party has been allocated K^{P_n} permits. K^{P_n} are called the targets. Their distribution, in the form of emision permits, is supported by computer simulations and is conducted during political negotiations to reduce the harmful enviromental effect of total emissions. At the compliance time a party must not emit more than the number of permits they possess. However, it may freely sell or buy permits to achieve the target. We

denote by x^{P_n} the emission of the n-th party and by E^{P_n} the traded permits. Emission must be nonnegative, $x^{P_n} \geq 0$. In this section, the number of traded permits E^{P_n} may be positive, when bought, or negative, when sold.[1] At the starting time, the total emission is greater than the number of permits

$$\sum_{n=1}^{N} x^{P_n} > \sum_{n=1}^{N} K^{P_n}, \tag{1}$$

which necessitates its reduction. It is quite common to refer to percent emission reduction, i.e. to express the targets as $K^{P_n} = \left(1-\delta^{P_n}\right)x_0^{P_n}$, where $100\delta^{P_n}$ is the percent of reduced emissions. In this paper we shall deal with absolute reductions, but any recalculations in both ways are obvious.

If the abatement cost functions $c^{P_n}(x^{P_n})$ of market participants are known to the central planner, the total cost optimization can be calculated and marginal cost λ at the equilibrium that are equal for all participants, can be found, see supplementary material. However, the cost functions are known only to the respective parties, so, consequently, prices of permits are set at the market. During trading, the n-th party is looking to minimize its cost of reducing the emission and buying/selling the permits E^{P_n}, i.e. to minimize the function

$$f^{P_n}\left(x^{P_n}, E^{P_n}\right) = c^{P_n}\left(x^{P_n}\right) + \lambda_t E^{P_n}, \tag{2}$$

subject to

$$x^{P_n} \leq K^{P_n} + E^{P_n}, \tag{3}$$

with known targets K^{P_n}. Above, $\lambda_t \geq 0$ is the price of one unit of permits in the transaction t. Typically, λ_t is different from the unknown optimal equilibrium price λ, as trade is continuing in time. The parties simply have to live with the uncertainty in earning/loosing money during trading.

In the market considered in this paper, emission amounts are also not precisely known. The market for uncertain inventories has been already discussed in Nahorski et al. (2007), Nahorski and Horabik (2008), Bartoszczuk and Horabik (2007), Ermolieva et al. (2010, 2013). It was formulated as an optimization problem (the central planner's view), with a minimization of the total cost to achieve the common limit on emissions, subject to compliance with a fixed risk α. It focused on the equilibrium solution, and the time evolution of the prices on the market was not considered. In the real market, the parties make decisions on trading prices in a process of price negotiation. Some negotiations in simulating GHG trading were considered in Nahorski et al. (2012), but emission uncertainty were not dealt with. The organization of the market presented here follows the ideas presented in Nahorski and Horabik (2010, 2012).

In Ermoliev et al. (2000), an approach to simulating a bilateral exchange of permits was proposed. The idea is that two parties meet randomly and exchange their permits if the transaction is feasible for both parties, i.e. the marginal costs of the parties differ. Each such transaction makes the social cost function smaller, see Ermolieva et al. (2010). As the cost function is constrained from below by 0, and the sequence of cost function values is decreasing with each transaction, then it will eventually converge to a minimum. In the original paper by Ermoliev et al. (1996) it is assumed that the number of exchanged permits reaches zero (albeit not hastily) and then it is proved that the sequence converges to the global minimum with a probability of 1, as in the stochastic approximation method. The prices of the permits are not taken into account.

[1] In further sections E^{P_n} will be always nonnegative; the minus sign is used for negative values.

Prices were included in simulation by Stańczak and Bartoszczuk (2010). As before, only feasible transactions are considered. The price p of the transaction is drawn at random from the interval constrained by the marginal costs of the trading parties. The number of trading permits is also drawn randomly.

In the present paper the transaction price is set through bilateral negotiations or through auctions (tenders). No central institution is needed, except for the purpose of designing the market rules. This differs from the solution proposed in Ermolieva et al. (2013), where a central institution helps to set prices of bilateral contracts at the point of equal marginal costs for both trading parties.

3 A market with uncertain emissions

3.1 Basic notions

We assume here that any lack of exact knowledge is expressed by the uncertainty interval

$$\widehat{x}-d^l \le x \le \widehat{x}+d^u, \tag{4}$$

where $\widehat{x}$ is the reported emission (inventory) and d^l and d^u are the lower and upper spreads of the uncertainty interval of a party. For the sake of simplification, the indices P^n which identify parties have been omitted. The graphical interpretation of the derivations below can be found in Figure S1 in the supplementary material. To be absolutely certain that a party fulfills the limit K, the full uncertainty interval should be below the limit (Figure S1(a)). However, a weaker condition will be used in this paper. Following Nahorski et al. (2007) we will state that a party is *compliant with the risk* α, if its emission inventory satisfies the condition

$$\widehat{x}+d^u \le K+\alpha\left(d^l+d^u\right). \tag{5}$$

This condition means that the α-th part of the uncertainty interval of the party's emission volume estimate (inventory) is allowed to lie above the limit K (Figure S1(b)). The condition (5) can be also written as

$$\widehat{x}+\left[1-\left(1+\frac{d^l}{d^u}\right)\alpha\right]d^u \le K. \tag{6}$$

Thus, a part of the upper spread of the uncertainty interval is added to the emission estimate before compliance is checked. This can be also interpreted in such a way that an unaccounted emission, due to uncertainty, is included in the condition to reduce the risk of non-compliance. Let us introduce *the relative upper and lower spreads* of the uncertainty intervals and denote them as

$$R^l=\frac{d^l}{\widehat{x}} \quad \text{and} \quad R^u=\frac{d^u}{\widehat{x}}, \tag{7}$$

respectively. Denoting *the fraction of the unaccounted emission* in the emission estimate as

$$u(\alpha)=\left[1-\left(1+\frac{d^l}{d^u}\right)\alpha\right]R^u, \tag{8}$$

the compliance with the risk α of equation (6) can be also written as

$$\widehat{x}[1+u(\alpha)] \le K. \tag{9}$$

The value on the left hand side is called *the expanded emission*, and this value

$$\widetilde{K} = \frac{K}{1+u(\alpha)} \tag{10}$$

is called *the corrected limit*.

3.2 Effective emissions

The above compliance-proving policy can be used to modify the rules of emission trading. The main idea, as presented in the earlier papers by Nahorski et al. (2007); Nahorski and Horabik (2008; 2010), involves transferring the uncertainty of the seller's emission volume to the buyer's emission volume together with the volume of traded emissions, and then including it in the buyer's emission balance. We use superscript ^{S} and ^{B} to distinguish between the seller and the buyer respectively in such a transaction.

Let us denote by $\widehat{E}^S$ the amount of estimated seller emission allocated for trade, in tonnes. This emission is associated with the lower and upper spreads of the uncertainty intervals $\widehat{E}^S R^{lS}$ and $\widehat{E}^S R^{uS}$, respectively. The value

$$E_{eff} = \widehat{E}^S\left[1-u^S(\alpha)\right] \tag{11}$$

is called *the effective emission* (Nahorski et al. 2007). To interpret this notion, let us be aware that the buyer subtracts the purchased emission permits from their initial number of permits. Thus, to check the buyer's condition of compliance with the risk α, after having purchased $\widehat{E}^S$ units of emissions, the following expression has to be considered

$$\widehat{x}^B - \widehat{E}^S + \widehat{x}^B u^B(\alpha) + \widehat{E}^S u^S(\alpha) = \widehat{x}^B - E_{eff} + \widehat{x}^B u^B(\alpha) \le K^B. \tag{12}$$

It can also be written as

$$\widehat{x}^B + \widehat{x}^B u^B(\alpha) \le K^B + E_{eff}. \tag{13}$$

Put simply, buying effective emissions is equivalent to directly increasing with their added value the buyer's compliance limit with the risk α. Consequently, the transaction helps the buyer to achieve their limit.

3.3 Basic relations in trading

The observation (13) is used below to organize a market with uncertain emissions, with the effective emissions as the trading good. The rules of trading are given for the individual participant of the market. The initial values before starting the trade are denoted by the subscript $_0$, and those after the transaction number $t \ge 1$ by the subscript $_t$.

Let us assume that the amount of $\widehat{E}_t^S \ge 0$ is sold by the seller S to the buyer B. The lower e_t^{lS} and the upper e_t^{uS} uncertainty spreads related to this amount are

$$e_t^{lS} = R_0^{lS}\widehat{E}_t^S = \frac{\widehat{E}_t^S}{\widehat{x}_0^S} d_0^{lS} \quad \text{and} \quad e_t^{uS} = R_0^{uS}\widehat{E}_t^S = \frac{\widehat{E}_t^S}{\widehat{x}_0^S} d_0^{uS}, \tag{14}$$

where $d_0^{lS}=d^{lS}$, $d_0^{uS}=d^{uS}$, $R_0^{lS}=R^{lS}$, and $\widehat{x}_0^S = \widehat{x}^S$. Thus, after the transaction we have

$$\widehat{x}_t^S = \widehat{x}_{t-1}^S + \widehat{E}_t^S \quad \text{and} \quad \widehat{x}_t^B = \widehat{x}_{t-1}^B - \widehat{E}_t^S, \tag{15}$$

with $\widehat{x}_0^B = \widehat{x}^B$. According to the rules of interval algebra we have for the uncertainty spreads

$$d_t^{lS} = d_{t-1}^{lS} + e_t^{lS} \qquad d_t^{uS} = d_{t-1}^{uS} + e_t^{uS} \tag{16}$$

$$d_t^{lB} = d_{t-1}^{lB} + e_t^{lS} \qquad d_t^{uB} = d_{t-1}^{uB} + e_t^{uS}\,. \tag{17}$$

Estimated emissions of parties not involved in the transaction do not change, and $\widehat{E}_t^S = 0$ is taken to stand for them.

Let us notice that the effective emissions in the transaction can be expressed as

$$E_{eff,t}^S = \widehat{E}_t^S \left\{ 1 - \left[1 - \left(1 + \frac{e_t^{lS}}{e_t^{uS}} \right) \alpha \right] \frac{e_t^{uS}}{\widehat{E}_t^S} \right\} = \widehat{E}_t^S \left[1 - u^S(\alpha) \right], \tag{18}$$

where the last equality stems from (14). The quantity of effective emissions is smaller than those that are estimated, unless precise knowledge of the inventory is known or α zeros $u^S(\alpha)$. The more uncertain the inventory is, and the smaller α, the less effective are emissions allocated to the party.

3.4 Organization of the market

Now, we shall outline a market in effective emissions, acting according to the following principles.

- When trading, the effective emissions (11) and corrected limits (10) are used.
- After the *t*-th transaction, the seller adjusts their accumulated estimated emission according to the rule

$$\widehat{x}_t^S = \widehat{x}_{t-1}^S + \frac{E_{eff,t}^S}{1 - u^S(\alpha)}. \tag{19}$$

- After the *t*-th transaction, the buyer adjusts their accumulated estimated emission according to the rule

$$\widehat{x}_t^B = \widehat{x}_{t-1}^B - \frac{E_{eff,t}^S}{1 + u^S(\alpha)}. \tag{20}$$

By adopting the above rules, a party is compliant with the risk α after transaction t if its accumulated estimated emission is not greater than its corrected limit

$$\widehat{x}_t \leq \widetilde{K}. \tag{21}$$

Evidence to substantiate this assertion is given in the supplementary material.

The bounds below show a reasonable amount of effective emissions to be traded in a transaction and reflect the requirement for lacking permits by the buyer and the possibility to spend exceeding permits by the seller, respectively. They are

$$E^S_{eff,t} \le \min\left\{ \left[1 + u^B(\alpha)\right]\left(\widehat{x}^B_{t-1} - \widetilde{K}^B\right), \left[1 - u^S(\alpha)\right]\left(\widetilde{K}^S - \widehat{x}^S_{t-1}\right) \right\}. \quad (22)$$

A derivation of this formula can be found in Nahorski and Horabik (2012). In the simulations, the parties generally conform to this condition, but a party may find it profitable to abate emissions and in this way increase its bounds (a seller) or decrease them (a buyer). The decision on abatement may be taken at each stage of the negotiations. The seller abates if it is profitable for them to sell any additional permits. The buyer purchases permits, if it is unprofitable for them to abate.

In conclusion, the organization of the market is as follows.

1. Before starting, all the limits are recalculated to the corrected limits $\widetilde{K}$, according to (10).
2. The parties negotiate the trading condition, taking into account the effective emissions E_{eff}, which are used in the negotiation of the selling/purchasing price. The maximum amount of effective emissions for selling is $[1-u^S(\alpha)]\left(\widetilde{K}^S - \widehat{x}^S_{t-1}\right)$. The maximum amount of effective emissions required by the buyer is $[1 + u^B(\alpha)]\left(\widehat{x}^B_{t-1} - \widetilde{K}^B\right)$.
3. Having terminated the transactions, the seller and the buyer adjust their accumulated estimated emissions according to (19) and (20), respectively.
4. To check the compliance, the current accumulated estimated emissions are compared with the corrected limits.

The trade above is in effective emissions, which is the common exchanged "good". However, to compare the prices of the effective emissions with the marginal costs of reducing the emissions, it is necessary to recalculate the prices for effective emissions to those of estimated emissions. As for the seller it holds that $E_{eff} = [1-u^S(\alpha)]\widehat{x}^S$, one unit of the estimated emissions $\widehat{x}^S_t$ is equivalent to $1-u^S(\alpha)$ units of the effective emissions $E_{eff,t}$. Similarly, for the buyer, one unit of the estimated emissions is equivalent to $1+u^B(\alpha)$ units of the efficient emissions. Therefore, the following holds.

5. The price of one unit of efficient emissions $p_{eff,t}$ and one unit of estimated emissions p^S_t for the seller are related as follows

$$p_{eff,t}\left[1-u^S(\alpha)\right] = p^S_t. \quad (23)$$

6. The price of one unit of efficient emissions $p_{eff,t}$ and one unit of estimated emissions p^B_t for the buyer are related as follows

$$p_{eff,t}\left[1 + u^B(\alpha)\right] = p^B_t. \quad (24)$$

In any successive transaction it holds that

$$\frac{p^S_t}{1-u^S(\alpha)} = \frac{p^B_t}{1 + u^B(\alpha)}.$$

So, the smaller the uncertainty of a party inventory is, the higher is its estimated emission price when it is a seller, and the smaller is the price when it is a buyer.

4 Simulation system

4.1 Trading mechanisms

Two trading mechanisms are considered: the bilateral trade and the sealed bid reverse auction. In the bilateral trading, agents split randomly into pairs. Once this is done the paired agents negotiate independently of on another. If an offer is received that lowers an agent's cost, it is accepted; if not, it is not accepted. The next splitting occurs after this running negotiation has been terminated. This is repeated iteratively. Each negotiation may terminate in an agreement or not, depending on the negotiator's expected profits. The transaction costs are neglected.

In the sealed bid reverse auction one participant takes on the role of an auction operator, while the others assume the role of bidder. The operator is chosen randomly using the bully election algorithm (Mamun et al. 2004). To ensure equal opportunities for each participant to become the operator, a priority is chosen randomly at the beginning of each auction. All other participants may submit a bid for trading a number of permits with a specified price. The operator chooses the most profitable bid, taking into account its preference. Afterwards, a new operator is chosen and the process is repeated iteratively. The operator calls either for selling or buying emissions, depending on their requirements.

4.2 Multi-agent system

To retain asymmetric information of the trading parties an agent-oriented paradigm (Shoham 1993. Shoham and Leyton-Brown 2009; Woolridge 2009) is applied. Individual parties interact there by interchanging messages, which ensures separation of their data. Each entity (or group of entities) in such a multi-agent system is represented by a piece of software, called an agent. Agents are embedded in an environment that allows them to communicate by using a protocol, in which some of the frequent communication patterns are designed.

A multi-agent system is a system composed of two or more autonomous software agents communicating with each other and working towards their own individual ends. Such a system is designed to achieve some overarching objectives and to operate in accordance with the intentions of the system designer. These goals are not implemented directly, but rather through the individual objectives of each of the agents and their interactions. Each agent represents a single party, which is guided by its own interests. In our case, an individual agent is motivated by the desire to achieve certain gains from the exchange of permits, i.e. to reduce its costs. The overarching goal of the system is that of the central planner, i.e. to minimize the total cost of fulfilling the emission limits. To achieve their goals, agents cooperate and compete (so called coopetition, Bengtsson and Kock (2000)). The coopetition is modeled by the strategic behavior of the agents. For a general discussion of the negotiations between programmable agents see Lopes et al. (2008).

A widely used standard for the description of multi-agent systems is the ODD-protocol, Grimm et al. (2010). A detailed description of the system prepared that uses the ideas of the ODD-protocol can be found in the supplementary material.

4.3 Non-learning agents

To prepare an offer the agents use knowledge stored in their state. Two kinds of agents are considered, learning and non-learning ones. A non-learning agent state consists of its emission, its emission reduction cost, the bought/sold permits and their costs. Using this knowledge, an agent is able to assess whether the coming offer is profitable or not.

Negotiation in the bilateral trading arena commences with establishment of the number of permits offered for negotiation by a trading agent. A prototype number is drawn randomly according to a uniform distribution on an interval extending from zero to a determined empirically upper value in order to ensure the stable behavior of the market. Once this is done the minimum of the number of permits lacking to achieve the limit given by (22) and the prototype number, is computed. Finally, the minimum from the numbers submitted by both parties is taken. The number of permits is not changed during any bargaining over the price. An offer price of an agent is computed randomly using a given (see Section 5.3 for details) probability distribution defined by the agent's price interval, which extends from the agent's marginal cost to the last most favorable price of an accepted offer. In this way, starting prices for negotiations are formed. Then the parties try to reach the final price, step by step, by successive incrementation (by a buyer) or decrementation (by a seller) of any previous offers with a constant predetermined step value. The negotiations succeed when both parties agree upon a price. If one side has reached its limit of profitability and the other refuses to accept the actual price, the negotiation fails and no transaction is performed. An exchange of offers takes place until the end of negotiations. Only then may the agents become engaged in any successive negotiations.

A similar random mechanism is used to form an offer price in the tender. Having gathered the offers, the auction operator chooses the most favorable one, and the transaction is concluded. The parties taking part in the tender are not engaged in any other negotiations during this period.

4.4 Learning agents

Agents' actions modify the agents' state. This is used by learning agents to improve the selection of transactions and any subsequent bidding and/or negotiating, through setting and modifying the probabilities of their execution. For example, if a bid price in an auction is too low when buying, it is very likely that some other party overbids it. If it is unnecessarily high, the gain will be small. Agents use a variant of the reinforcement learning method, see Brenner (2006). More precisely, a learning agent state is augmented with additional variables, which store information on transactions concluded by the agent, separately for selling and buying. This is used to form and adapt probability distributions of succeeding in a transaction. The interval of possible offers is divided into ten subintervals. Having concluded a transaction, the value in an appropriate subinterval is increased. The initial distribution is uniform. Any predicted gain is calculated by multiplying the experimental probability of profiting from the potential gain in the middle of the corresponding subinterval. These expected gain distributions are used for generating successive bids, which are selected using a roulette wheel method. This way better bids are employed more frequently.

5 Simulation results

5.1 Case considered

The simulation was carried out using the case study described in Horabik (2007) and Nahorski et al. (2007). Five trading parties: the USA, the EU, Japan, CANZ (Canada, Australia, New Zealand) and the EEFSU (East European and Former Soviet Union), indexed $n=1,\ldots,5$, respectively, are assumed to take part in the Kyoto Protocol trade agreement. We assume that all these parties conform to the Kyoto Protocol regulations to reduce CO_2 equivalent

emissions. The parties have been specified emission limits K^{P_n}, BAU (business as usual) emissions $\widehat{x}_0^{P_n}$, and the cost reduction functions c^{P_n}. As set forth in Horabik (2007), the cost of reduction can be well approximated by a square function of the size of the reduced emissions

$$c^{P_n}\left(\widehat{x}_0^{P_n}-\widehat{x}^n\right)=\begin{cases} a^{P_n}\left(\widehat{x}_0^{P_n}-\widehat{x}^{P_n}\right)^2 & \text{for} \quad \widehat{x}^{P_n}<\widehat{x}_0^{P_n} \\ 0 & \text{for} \quad \widehat{x}^{P_n}\geq\widehat{x}_0^{P_n} \end{cases}. \tag{25}$$

The variable $\widehat{x}^{P_n}$ stands for the current accumulated emission permits. The marginal cost of the emission permit λ^{P_n} is the derivative of the function c^{P_n}. Symmetric uncertainty distributions are considered, for which better estimates of uncertainty can be given. The data for the problem are given in the Table S1 in the supplementary material.

5.2 Learning agents

Results obtained in all simulations are quite similar. The values of final emissions, numbers of traded permits, final marginal costs and the reduction cost are almost identical. The equilibrium results obtained are also similar to the results for the centrally planned market (Horabik 2007; Nahorski et al. 2007; Bartoszczuk and Horabik 2007). Bigger differences can be noticed in the values of permit costs, caused by the different ways of reaching contracts in the methods under consideration.

In Fig. 1a and b a few exemplary trajectories of transaction prices are depicted, while in Fig. 1c and d examples of trajectories of consecutive prices in a trade between only two individual parties are shown. In both cases, the tender trade (operated only by sellers in this case) gives smoother trajectories, because selection of the best price filters out the outlying higher ones.

In the sealed bid reverse auction trade, final marginal costs do not converge precisely to the same value. This is caused by the competition among parties. Less profitable transactions are rejected and some parties are unable to win transactions that would lead them to the equilibrium point. This fact is more visible for smaller α. When ignoring uncertainty, for $\alpha = 0.5$, the final marginal costs are almost equal. In the bilateral case marginal costs tend to the equilibrium because the contracting parties are selected randomly, and if the transaction is profitable for both parties, it is concluded, even if more profitable transactions could be made, Fig. 1a. In the tender case more profitable transactions are prefered by seller or buyer operators and some parties actually finish the simulation with worse results.[2]

The curves depicted in Fig. 2 present the experimental probability densities of bids, dependent on either call prices or final transaction prices, and expressed as a percentage of its actual marginal costs (100 % corresponds to the marginal cost and 900 % corresponds to 9 times the marginal cost when selling,[3] while 0 % corresponds to the marginal cost, and 100 % corresponds to the lowest price when buying). The data are recorded from 1,000 simulations. Generally, market participants buy permits at prices close to their marginal costs, with distributions similar to exponential ones. Selling is more complicated, because the EEFSU sells permits with almost equal probability for all possible bid prices. But for the final transaction prices the distribution is much closer to an exponential one. This effect is caused by the fact that high bid prices in bilateral trade are negotiated to much lower prices in any

[2] Only selected examples of extended simulations are included.

[3] EEFSU has most time the marginal cost 0 due to excessive permits ("hot air"). But in this case a small value *min* was introduced to keep more realistic conditions in the price calculation.

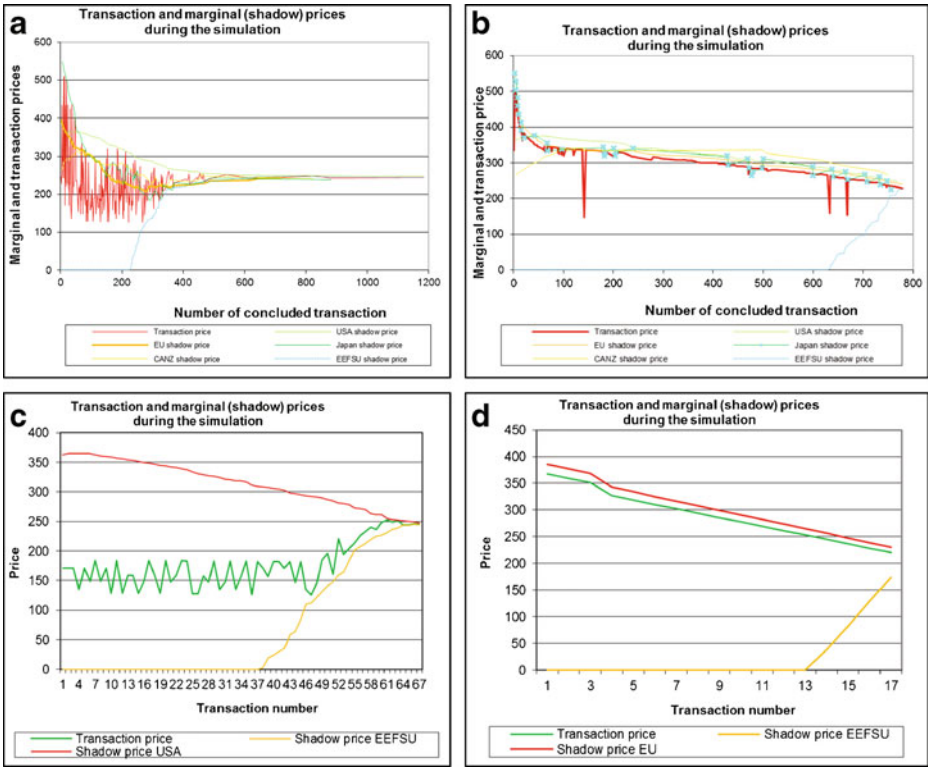

Fig. 1 Trajectory of prices in consecutive contracts, in USD/MtC/y, in a single simulation, with α=0.3, for: **a**, **c** bilateral negotiations, and **b**, **d** sealed bid reverse auctions (operated only by sellers), **a**, **b** for all market participants, **c** only transactions between the USA and the EEFSU are shown, **d** only transactions between the EU and the EEFSU are shown

concluded transactions. Still, the EEFSU was able to sell a big share of permits at much higher prices.

5.3 Non-learning agents

Non-learning agents have a fixed probability distribution of bidding. After experiments with cut-normal and cut-lognormal distributions, the empirical distributions which have been gathered in learning-agent simulations, have finally been used to generate prices offered by non-learning agents. In Fig. 3 the trajectories of consecutive transaction and marginal costs during single simulations are depicted, with α=0.3. Figure 3a presents the results for the bilateral negotiations, and Fig. 3b for the sealed bid reverse auction. In both cases, the marginal costs of the parties converge to the final equal marginal cost. The transaction prices are located inside the marginal costs, so they converge as well. They gather mostly in the upper part, close to the upper marginal costs. This is particularly visible for the bilateral negotiations (Fig. 3a), and in the later part of the sealed bid reverse auctions (Fig. 3b). The auctions are mostly won by the EEFSU, due to its possession of the most competetive selling prices.

Analyzing the parties' behaviours, let us first consider Japan for the sealed bid reverse auction model (see Fig. 3b). To begin with, Japan is prompt in its purchase of permits; it lowers

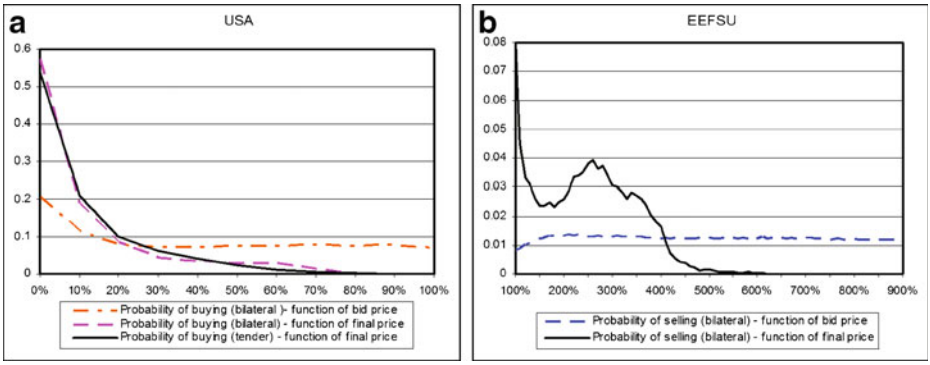

Fig. 2 Probabilities of concluded transactions for selected market participants as a function of a bid or final price expressed as a marginal cost percentage: **a** bilateral and tender the USA, **b** bilateral trade the EEFSU

its marginal cost equally quickly. When the marginal cost reaches the level of the prices of other countries, Japan begins selling the permits. The same process, on a smaller scale, can be observed for the EU and CANZ. The USA, in turn, is mostly buying the permits while conditions are favorable, and EEFSU is generally selling permits: initially its "hot air" permits, and then from reducing its emissions.

In the bilateral trade (see Fig. 3a) CANZ, the EU and Japan are energetic in their purchase or sale of permits. As in the previous case, the USA is mostly buying and the EEFSU is mostly selling. The transaction prices, agreed randomly, are much higher than in the sealed bid reverse autions. Nevertheless, they tend to decrease in time. Hence, the overall profit for the seller (the EEFSU) is greater, and for the buyer (the USA) it is smaller than in the sealed bid reverse auction trade. Japan profits more in the tender trade.

Equilibrium results, averaged after 5 simulations, are presented in Table S2 in the supplementary material. In all cases the market converges to a point of (almost) equal marginal costs, which is a necessary condition of optimality. The marginal costs and traded permits are close to those obtained by central optimization of the market. There are differences between emission reduction and permit cost distributions among parties for the bilateral and tender trade, as a result of different ways of reaching the equilibrium.

The emission reduction costs are almost equal for both trade mechanisms. They rise when the uncertainty parameter α decreases. The same is for the overall costs for each party. Thus, for a smaller α, it may be profitable to invest in a decreasing uncertainty of the inventory. For a smaller α, more parties reduce their emissions and sell their permits. For α=0.1, every party globally sells more emissions than buys. This is due to the specific features presented by the trading of uncertain emissions, which balances the traded effective emissions but imbalances the estimated ones.

5.4 Comparison and discussion of results

Equilibrium results of all methods are similar, see Figure S2 in the supplementary material. For a parameter α larger than 0.2, values of final marginal costs are almost identical for all cases. For one that is smaller than 0.2, the results slightly differ. Larger marginal costs are for the learning and the smaller are for the non-learning agents. The results obtained indicate that the marginal cost $\lambda(\alpha)$ in the equilibrium and the total final emission $x(\alpha)$, for a given α, can be well approximated by the following linear function

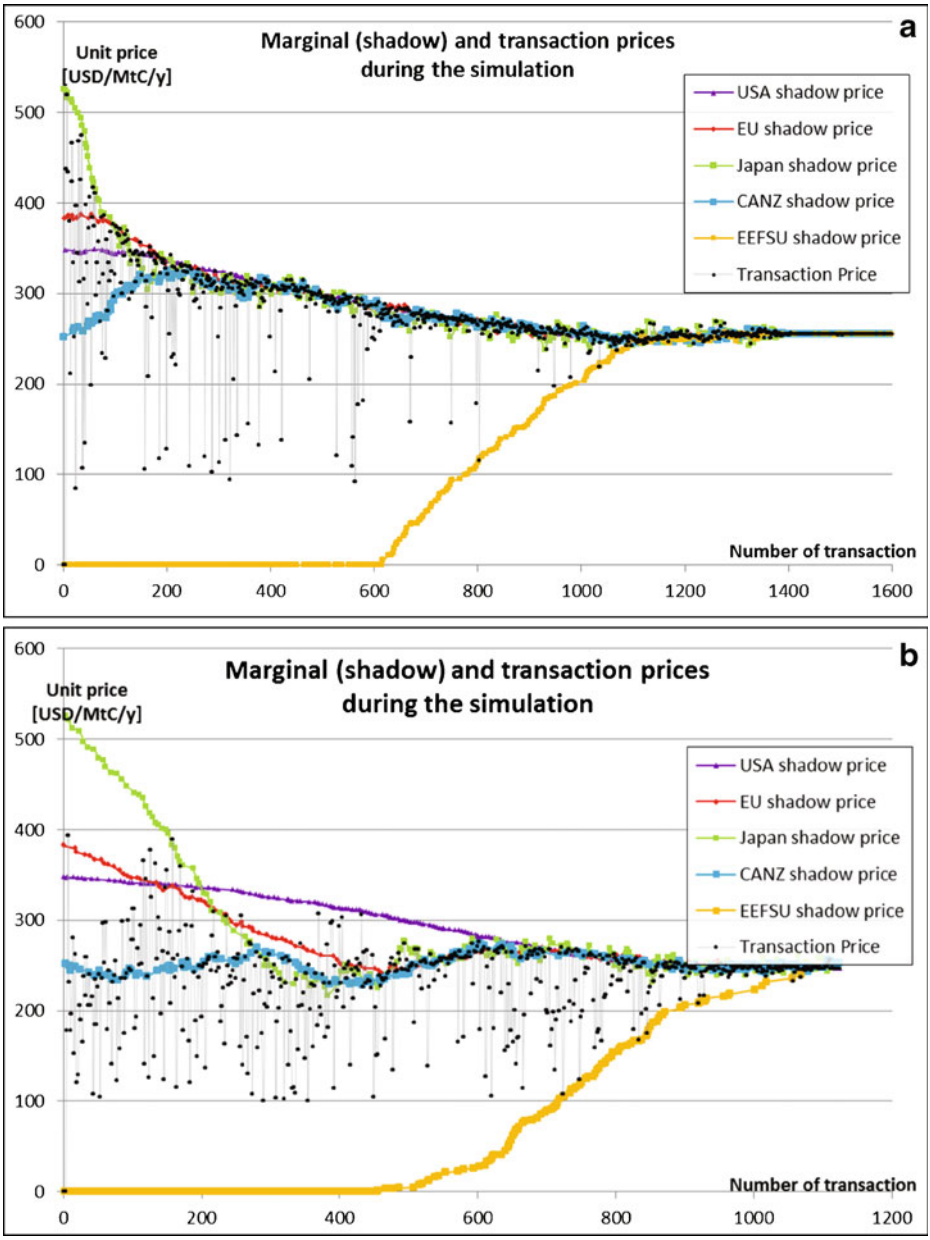

Fig. 3 Trajectory of unit prices in consecutive contracts, in USD/MtC/y, in a single simulation, for α=0.3; **a** with bilateral negotiations, **b** with sealed bid reverse auction

$$\lambda = -3.6502x + 4418.7.$$

This suggests the possibility of anticipating the final marginal cost for a given final emission. Also, knowing the marginal cost functions and the equilibrium price, the total final emissions can be determined. These dependencies may be helpful for the market designer.

During trading, the prices tend to keep close to the buyers' marginal costs. This is partly due to the rapidly converging marginal costs of most parties, except for the EEFSU and the fact that transaction prices between the parties fall between their marginal costs. Parties are aware of this tendency as is shown in the distribution for the USA in Fig. 2a. In bilateral negotiations the transactions are concluded far more often when they start with offers close to the buyer's marginal costs. The distribution for the final prices are close to the buyer's marginal costs both in bilateral negotiations and auctions. But the EEFSU often successfully finalizes its bilateral negotiations for different initial prices, Fig. 2b, and gets prices accepted that are often much higher then its marginal costs. This is an effect of the monopoly of the EEFSU, which is the main seller, while other participants have to compete to buy permits. The effect of transaction prices gathering close to the buyer's marginal costs is also evident in Fig. 3.

As the buyer's marginal costs decrease in time, the prevailing prices on the market also decrease. It is particularly visible for the bilateral negotiations, Fig. 3a, but also in the final stage of the auctions, Fig. 3b. This effect has been also observed in the real markets. The decrease is rather slow, which is in part due to the severe limitation of the traded volumes in our simulation. Greater volumes cause, however, bigger difficulty in their precise convergence to the equilibrium.

6 Conclusions

This paper concentrates on presenting the possibility of using agent-based computation tools to simulate trading of goods, which can not be quantified with satisfactory accuracy. A conservative compliance rule approach is considered, dependent on an accepted risk (probability) of not fulfilling an emission limit. The smaller the risk is, the more emissions have to be reduced. The market is designed to guarantee that the reductions are introduced, but a distinct feature is that the uncertainty of emissions influences their market prices. Those that are more uncertain are cheaper than those that are more certain. A specially designed muli-agent system was constructed to simulate trading with the two market mechanisms mentioned above. Multi-agent methods are used for market simulations, mainly because they are able to deal with complicated multi-interaction systems. The applied multi-agent approach seems to be a suitable tool for analyzing the economic phenomena of a market with uncertainties in prices, which appears in the GHG emissions market that is considered in this paper. Consequently, it was possible to observe the behavior of the market and its participants alongside a growing number of concluded transactions. The approach is also suitable for investigating the strategies of participants in the market as well as other market mechanisms than those considered in the paper, bilateral negotiations or tenders.

The results obtained are recognised as being preliminary ones, as rather simple assumptions have been taken in the simulations. Firstly, a simple negotiation of prices is assumed, in which the agents do not apply sophisticated strategies, and do not take into account any contract prices in other transactions. This is connected with the market mechanisms considered in the paper. In both the final transaction prices can remain secret.

The simulations provided phenomena which resembled real trade. A particularly interesting fact is that of grouping the transaction prices nearer the buyer's marginal costs, which has the effect of decreasing the prevailing transaction prices in time, with a corresponding rise in the number of concluded transactions. This result has been obtained for five parties (groups of states) active on the market. Five participants form a very small market in comparison with the

real market's dimensions. However, any simulation of bigger markets presents a difficulty in the acquisition of the participants' emission abatement cost curves.

Acknowledgments Partial financial support from the Polish State Scientific Research Committee and National Scientific Center under the grants N N514 044438 and N N516 375736 is gratefully acknowledged. Preparation of the final version has been supported by the statutory fund of the Systems Research Institute, PAS.

Open Access This article is distributed under the terms of the Creative Commons Attribution License which permits any use, distribution, and reproduction in any medium, provided the original author(s) and the source are credited.

References

Bartoszczuk P, Horabik J (2007) Tradable permit systems: considering uncertainty in emission estimates. Water Air Soil Poll: Focus 7:573–579

Bengtsson M, Kock S (2000) "Coopetition" in business networks – to cooperate and compete simultaneously. Ind Mark Manag 29(5):411–426

Bonatti M, Ermoliev Y, Gaivoronski A (1998) Modeling of multi-agent market systems in the presence of uncertainty: the case of information economy. Robot Auton Syst 24(3–4):93–113

Brenner T (2006) Agent Learning Representation: Advice on Modelling Economic Learning. In: Tesfatsion L, Judd K.L (eds) Handbook of Computational Economics, vol 2. Elsevier, 895–947

Ermoliev Y, Klaasen G, Nentjes A (1996) Adaptive cost-effective ambient charges under incomplete information. J Environ Econ Manag 31:37–48

Ermoliev Y, Michalevich M, Nentjes A (2000) Markets for tradeable emission and ambient permits: a dynamic approach. Environ Resour Econ 15:39–56

Ermolieva T, Ermoliev Y, Fischer G, Jonas M, Makowski M (2010) Cost effective and environmentally safe emission trading under uncertainty. In: Marti K, Ermoliev Y, Makowski M (eds) Coping with Uncertainty. LNEMS 663. Springer, 79–99

Ermolieva T, Ermoliev Y, Jonas M, Fischer G, Makowski M, Ren H, Wagner F, Winiwarter W (2013) Uncertainty, cost-effectiveness and environmental safety of carbon trading: integrated approach. Interim Report IR-13-003. International Institute for Applied Systems Analysis, Laxenburg

Grimm V, Berger U, DeAngelis DL, Polhill JG, Giske J, Railsback SF (2010) The ODD protocol: a review and first update. Ecol Model 221:2760–2768

Horabik J (2007) On the costs of reducing GHG emissions and its underlying uncertainties in the context of carbon trading. Interim Report IR-07–036, IIASA

IETA (2005) Emission trading master agreement for the EU scheme. In: Version 2.1 as of 13 June. International Emission Trading Association (IETA), Geneva, Switzerland. http://www.ieta.org/ieta/www/pages/getfile.php?docID=1001

Kaleta M, Pałka P, Toczyłowski E, Traczyk T (2009) Electronic trading on electricity markets within a multi-agent framework. In: Computational Collective Intelligence. Semantic Web, Social Networks and Multiagent Systems. LNAI 5796. Springer, 788–799

Lopes F, Woolridge M, Novais AQ (2008) Negotiation among autonomous computational agents: principles, analysis and challenges. Artif Intell Rev 29:1–44

Mamun QEK, Masum SM, Mustafa MAR (2004) Modified bully algorithm for electing coordinator in distributed systems. WSEAS Trans Comput 3(4):948–953

Nahorski Z, Horabik J (2008) Greenhouse gas emission permit trading with different uncertainties in emission sources. J Energ Eng - ASCE 134(2):47–52

Nahorski Z, Horabik J (2010) Compliance and emission trading rules for asymmetric emission uncertainty estimates. Clim Chang 103(1–2):303–325

Nahorski Z, Horabik J (2012) A market for pollution emission permits with low accuracy of emission estimates. In: Kaleta M, Traczyk T (eds) Modeling Multi-Commodity Trade: Information Exchange Methods. Springer, 151–165

Nahorski Z, Horabik J, Jonas M (2007) Compliance and emission trading under the Kyoto protocol: rules for uncertain inventories. Water Air Soil Poll: Focus 7(4–5):539–558

Nahorski Z, Stańczak J, Pałka P (2012) Application of multi-commodity market model for greenhouse gases emission permit trading. In: Kaleta M, Traczyk T (eds) Modeling multi-commodity trade: information exchange methods. Springer, 137–149

Shoham Y (1993) Agent oriented programming. Artif Inteligence 60(1):51–92
Shoham Y, Leyton-Brown K (2009) Multiagent Systems: Algorithmic, Game-Theoretic, and Logical Foundations, Cambridge University Press
Stańczak J, Bartoszczuk P (2010) CO_2 emission trading model with trading prices. Clim Chang 103(1–2):291–301
Woolridge M (2009) An Introduction to Multi-Agent Systems, Wiley

DOI 10.1007/978-3-319-15901-0_15
Reprinted from *Climatic Change* Journal, DOI 10.1007/s10584-013-1006-y

Economic, institutional and technological uncertainties of emissions trading—a system dynamics modeling approach

Irina Dolgopolova · Bo Hu · Armin Leopold · Stefan Pickl

Received: 5 January 2013 / Accepted: 7 November 2013 / Published online: 8 January 2014
© Springer Science+Business Media Dordrecht 2013

Abstract System dynamics models are employed for analyzing the impact of different uncertainties on carbon emission trading–both on national and business levels. Economic, institutional and technological uncertainties significantly influence any country's benefits from emission permit trading. If a country participates in trading on the international market then the possible price range becomes the source of additional uncertainty. In the case of business investment decisions for implementing resource-saving technology, our system dynamics model shows that the first-mover investor will get significantly fewer advantages than his followers, which leads to delay in primary investment to the sector.

1 Introduction

Reducing greenhouse gas (GHG) emissions is one of the global challenges of environmental protection which belongs to the unanimous aims of the international community next to others like overcoming poverty and promoting development (see, e.g., United Nations Web Services Section, Department of Public Information 2008). "[International] emissions trading, as set out in Article 17 of the Kyoto Protocol, allows countries that have emission units to spare–emissions permitted them but not 'used'–to sell this excess capacity to countries that are over their targets. Thus, a new commodity was created in the form of emission reductions or removals" (UNFCCC 2009, Mechanisms | Emissions Trading). This concept is considered to be one of the most effective ways to harness the power of market to mitigate income losses caused by the reduction of GHG emissions, and thus to push the efforts addressing the global climate challenge.

However, there are substantial economic, technological and even institutional uncertainties each of which may influence the development of the emissions trading market. In this paper we attempt to use system dynamics models to estimate these uncertainties. Our considerations

This article is part of a Special Issue on "Third International Workshop on Uncertainty in Greenhouse Gas Inventories" edited by Jean Ometto and Rostyslav Bun.

I. Dolgopolova
Baikal National University of Economics and Law, Irkutsk, Russia

B. Hu (✉) · A. Leopold · S. Pickl
Universität der Bundeswehr München, Neubiberg, Germany
e-mail: bo.hu@unibw.de

show that an uncertain emissions trading market may jeopardize the international GHG reduction commitment.

In the following section 2 we will provide an overview of recent developments. In a former approach (Pickl et al. 2010) a so-called TEM (Technology-Emission-Means) model was used to simulate the behavior of several agents intending to reduce their CO_2 emission within an international market situation. Therefore, the time-discrete TEM model provides scenarios which are the basis for a decision support process which will be extended in the present article via comfortable system dynamic techniques.

Section 3 introduces a system dynamics model to estimate the marginal economic utility of CO_2 emissions for a national economy and thus the possible permits price for an international emissions trading. Based on model simulations we then discuss how economic, technological and institutional uncertainties may result in uncertainty of permits price in an international emissions trading.

In section 4 we present a further system dynamics model describing two competitors trying to find their optimal point of time to adopt certain resource-saving technology for their production process. Such an approach is related to the game-theoretic approach in (Deissenberg and Pickl 2004; Pickl 2008) where a so-called Kyoto game is used to characterize several allocation principles. Here, we integrate the uncertainty aspect within such an allocation process. Since this optimum depends strongly on the increasing price of the resource to be saved our model simulations show that an uncertainty of price may make decision-makers postpone their resource-saving projects for years for the sake of a higher financial performance.

We conclude that system dynamics can be seen as a useful approach to simulate and to handle different aspects of uncertainty of emissions trading, economic and technological development. At the end an outlook for further extensions of system dynamics techniques is described.

2 Recent developments

Two basic approaches for reducing CO_2 emissions–carbon tax and cap-and-trade–were debated among scientists over the years before and after the commencement of the Kyoto protocol. Despite all the advantages of carbon tax (see, e.g., Avi-Yonah and Uhlmann 2009; Wittneben 2009; CPA Australia 2009) emissions trading scheme is considered to be the most effective way to provide economic incentives for companies to invest in resource-saving technologies.

However, cap-and-trade systems appear to have major disadvantages–a significant number of exogenous and endogenous uncertainties that overlap existing benefits.

Uncertainties like volatile market prices of electricity and fuels influencing the carbon emissions market have been indicated in the work of (Laurikka and Koljonen 2006). Additionally, the auxiliary uncertainty originates from the behavior of emission permits market.

It has also been stated that uncertainty in climate protection policies introduces additional risks to the investment decisions "…through its effects on inducing greater optionality considerations in the behavior of investors" (Yang et al. 2008, p.1934). Furthermore the macroeconomic impact of government policies is presented by their influence on domestic production and exports and imports of clean and conventional energy (Alexeeva-Talebi and Anger 2009).

Very few publications have been made recently on the subject of the role of uncertainties that arise from emissions trading. In most of them this question is also seen in a long-term investment perspective. Generally speaking, policy uncertainties and price volatility are major

concerns for the firms investing in energy related projects. Due to the long-term and irreversible character of investment projects, investors prefer to postpone their decisions until they have additional information about the ongoing project performance. The analysis with the help of stochastic dynamic computable general equilibrium model with an extended energy sector employing Chinese data shows that uncertainties are beneficial for the environment while still unfavorable for the welfare (Schenker 2011).

In the work of (Blyth and Bunn 2011) the three-dimensional perspective of policy, market and technological risks is presented, indicating that actually all the commitments and goals set by European Union (EU) are sources of uncertainty. Policy risks are provided by the level of the cap, the level of technology support, and the energy efficiency target. More specifically market risks are: uncertainty in the level of demand for electricity and fuel prices. Technology based risks incorporate the price and the quantity of the abatement available. These risks exist and co-evolve in a complex way which requires detailed modeling to identify their importance in various scenarios.

Furthermore investment decisions for long-term projects significantly depend on the level of risk. Although built to provide the most cost-effective approach to reducing CO_2 emissions, emissions trading may create uncertainties that limit different kinds of investment opportunities and distract most investors from entering projects related to renewable energy. This is crucial since existing technological uncertainties by themselves are enough for switching "the timing competition […] in a fundamental way from a preemption game to a waiting game" (Hoppe 2000, p.331).

The models described in this paper are aimed to present the economical, technological and institutional uncertainties at different levels of decision-making. They are based on the TEM model (Pickl 1998) which can be seen as a first approach to simulate the relationship between technologies, emissions and (financial) means. Key element of the TEM model is the matrix of effectiveness which characterizes the effect of financial investments on reductions of CO_2. As mentioned above the TEM model provides first scenarios which can be the basis for further optimization approaches. In (Pickl 2001) several scenarios are introduced. As the matrix of effectiveness consists on empirical parameters its estimation is crucial. These parameters are analyzed under uncertainties in (Pickl et al. 2010).

Here, we employ system dynamics models to demonstrate the range of possible outcomes at supra-national and national level. At the end of the paper we combine the system dynamics approach with the so-called Kyoto game which was invented to characterize certain allocation procedures (Pickl 1998; Deissenberg and Pickl 2004).

3 Economy, energy consumption and emissions trading

3.1 System dynamics model for dependency between economy, energy consumption and emissions

From a very general perspective, the correlation between energy supply and national economy can be depicted in a Causal Loop Diagram shown in Fig. 1, left. Beginning on the right side of the model, economic strength and energy demand are directly correlated through the energy efficiency factor (see Chontanawat et al. 2006). Furthermore, energy shortage, in the centre of the model, inhibits the development of the economy as observed in numerous developing nations as well as in developed countries during energy crises.

Each energy supply is in fact a combination of both clean energy and conventional energy which both react to energy shortages. While a market driven growth in the

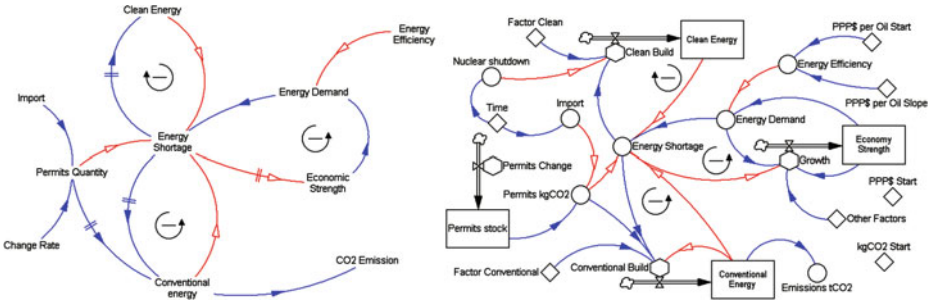

Fig. 1 Left: causal loop diagram, right: stock and flow diagram (Hu and Pickl 2010)

provision of clean energy can be evaluated positively from the point of view of economic development and of emission reduction, the target of emission reduction can be acquired when the market authority controls the feedback loop for conventional energy by the way of limiting emission permits. The assignment of the total amount of emission permits confines the total amount of conventional energy on the market and thus inhibits its growth respectively enforces a reduction of conventional energy by constantly diminishing the amount of emission permits. For more details of the model see (Hu and Pickl 2010).

On the basis of the Causal Loop Diagram shown above we create a new Stock and Flow model (Fig. 1, right) which allows to understand the development of a country regarding its economic strength and its energy supply within a given period of time using numerical simulations. This means in detail, that this system dynamics model shows the interconnectivities between essential stocks and different real parameters and additionally visualizes three main negative feed-back loops within the model. Generally speaking, the results of the simulation concerning the growth of economy, energy consumption and quantity of emission may be compared to published statistical data.

Therefore it has to be said at this point that in the following two subchapters, this system dynamics model will be used for calculating different aspects of uncertainty of economic and technological development. Finally this system dynamics model about dependency between economy, energy consumption and emissions tries to support the understanding for the uncertainty caused by international emissions trading.

In Table 1, the most important variables used in Fig. 1 are listed. The starting and fitting parameters are used to describe the reality as closely as possible, while different scenarios in the future can be simulated using the scenario parameters. Notice that in the sense of CO_2 emissions nuclear energy is roughly seen as a part clean energy supply.

Real economic and CO_2 emissions data (see Gapminder Foundation 2008) are used to calibrate the model presented above. In Fig. 2, the real economic (red squares) and emissions (black squares) data of China, meanwhile the largest CO_2 emitter of the World, between 1990 and 2005 are depicted. Based on our calibrated model, the CO_2 emissions are also calculated and shown as the grey line. The correlation between the economic and emissions data can nicely be described by the model.

Using the same model and calibrated parameters both a so-called business as usual (BAU) scenario and a scenario of certain reduced CO_2 emissions can be simulated. The area between the BAU (black line) and the reduced CO_2 emissions (light blue line) represents the CO_2 abatement per capita within 15 years (2005–2020), while the

Table 1 Variables used in the system dynamics model shown above

Type	Variable	Explanation	Unit of measure
Starting parameters using real data	PPP$ start	Purchasing Power Parity (PPP) at the beginning of a given period of time	PPP$/capita·year
	KgCO2 start	CO_2 emission at the beginning of a given period of time	kg/capita·year
	PPP$ per oil start	PPP$ per consumed energy in kg oil equivalent (energy efficiency) at the beginning of a given period of time	PPP$/kg
	PPP$ per oil slope	Annual growth rate of energy efficiency	PPP$/kg·year
Fitting parameters	Factor clean; factor conventional	Speed of reaction of energy suppliers egarding a given shortage of clean energy or conventional energy	1/year
	Other factors	External, not ascertained factors, which promote economic development	1/year
Scenario parameters	Permits change	Change of national emission permits	kg/capita·year
	Import	Imported emission permits	kg/capita·year
Important indicators	Economic strength	Purchasing Power Parity in a given year	PPP$/capita·year
	Emission	CO_2 emission in a given year	kg/capita·year

area between the BAU (red) and reduced (blue) economic development shows the total per capita income loss during the same period of time. In this way the marginal utility of CO_2 emissions can be estimated for each country as a function of targeted CO_2 reduction based on BAU. In addition, "Other Factors" can be changed to model different economic growth rates in the future while "PPP$ per Oil Slope" and "Factor

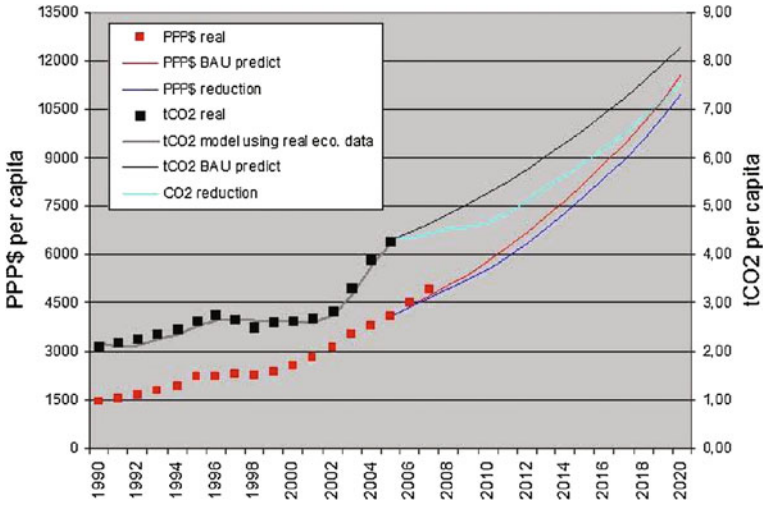

Fig. 2 The development of GDP per capita and CO_2 emission for China under different emission schemes

Clean" are used in different scenarios to reflect different speeds to achieve higher energy efficiency and higher capacity of CO_2 neutral energy supply.

3.2 Uncertainty of economic and technological development

Using the system dynamics model described in section 3.1 we are able to estimate the influence of economical and institutional uncertainties on a country's benefits from emission permits, for example, for USA, the largest CO_2 emitter of the World not long ago. In details the following Fig. 3 shows the marginal utility as a function of economic growth and targeted emissions reduction. Economic uncertainties are presented as changes in the rate of economic growth. Institutional uncertainties–are various targets for emissions reduction. Given different levels of economic performance, and diverse institutional constraints, the U.S. economy becomes open to a significant number of possible scenarios (marginal utility curves) or price uncertainties that influence investments in emissions reduction.

Technological uncertainty mostly arises from unclear perspectives about the implementation and future performance of new sustainable technologies. We include technological uncertainties, such as speed in building clean energy capacities and energy efficiency into the list of different scenarios. According to Fig. 4 technological factors are sources of additional uncertainty that can make the marginal utility of CO_2 emissions and thus the permits price in a possible trading in the future even less predictable.

3.3 Uncertainty caused by international emissions trading

If we look at the uncertainties in emissions permits price in the context of international trading scheme, then the pricing mechanism becomes even more complicated. Figure 5 shows the case of trading between USA and China under economical and institutional uncertainties. If economic growth in the USA during the period of 2005–2020 will be at the same rate as in 1990–2005, then different conditions of total permits increase in China will result in a difference in permits price from 84 $ (Price 1) to 209 $ (Price 2).

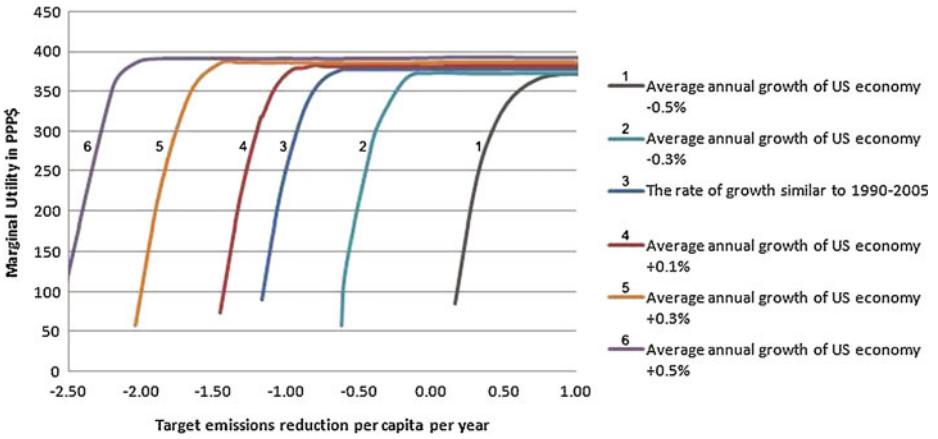

Fig. 3 Marginal utility as a function of economic growth and targeted emissions reduction per capita in USA

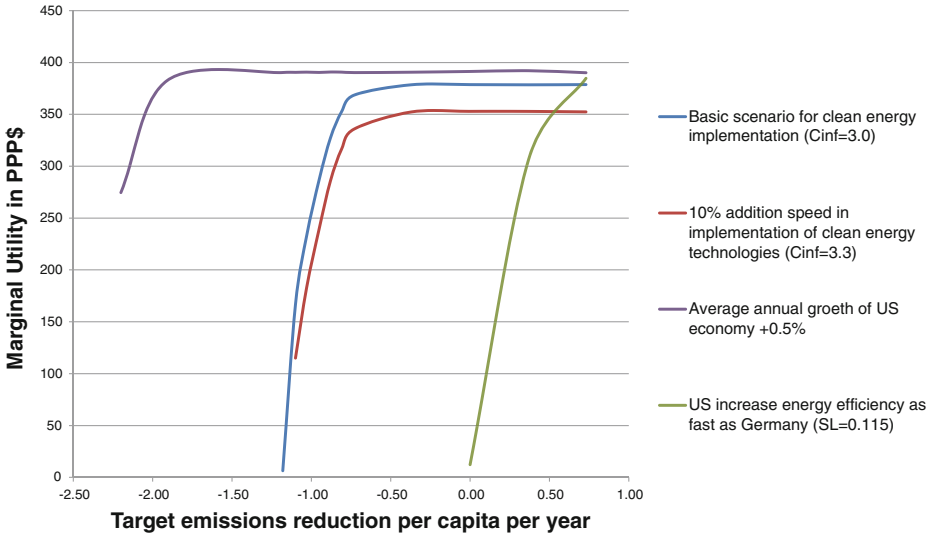

Fig. 4 Marginal utility as a function of energy efficiency and speed of implementation of CO_2 neutral energy supply

4 Implementation of resource-saving technology under the conditions of increasing resource price and uncertainty

4.1 Timing competition in adopting resource-saving technology

Closely connected to Section 3, we develop in this section a new system dynamics model to explain the situation of the implementation of resource-saving technology under the conditions of increasing resource price and uncertainty. This system dynamics model describes two competing participants (a first mover and a follower) with different strategies regarding new resource-saving technology.

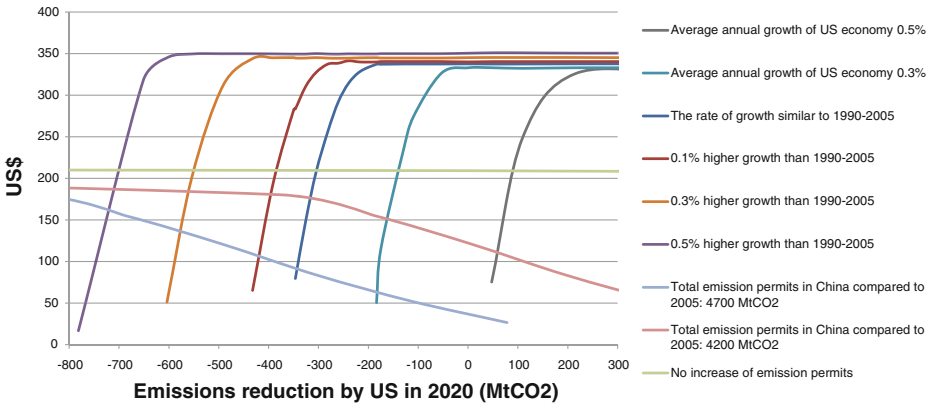

Fig. 5 Uncertainty caused by emissions trading between USA and China

As already mentioned in the beginning, the Kyoto protocol and the international emissions trading should encourage each company to invest in resource-saving technologies to reduce its GHG emissions. From a business point of view, the decision is made on the basis of an expected positive profit from such an investment. In our model, the price for resources to be saved is rising and therefore the average costs for resources for production are also increasing. To stay profitable, the companies need to reduce the amount of non-regenerative energy needed for the production by implementing resource-saving technology. The following iterative method of the system dynamics model is aimed to explain the complexity finding the right moment in time for adopting and furthermore investing in resource-saving technology.

As defined in our system dynamics model shown in Fig. 6 the revenue of a company achieved through a resource-saving project is given by the sum of investment and production incomes, while the spending consists of costs for installation and maintenance. The model takes into account that the development of "Unit Cost" obeys an internal learning curve. The decision problem is to find the optimal timing to start the installation of resource-saving capacity to maximize the stock "Money" within in a longer period of time, say 20 years.

To install resource-saving capacity one does not only need internal but also external services and purchased parts. This leads us to the model depicted in Fig. 7. We assume that purchased parts (and services) consist of business sector specific ones on the one hand and commodities on the other hand. The costs of the business sector specific parts (and services) obey a business sector specific learning curve. We assume that the price of the resource to be saved and the prices of commodities are independent from the behavior of the actor under consideration.

A deciding input parameter of this model is the price development of the resource to be saved. While uncertainty of price development remains, in contrast to the conventional concept of the time-based competition (Stalk 1988) in which a moment of time as early as possible is desired, this model shows that, under certain conditions, there exists an optimal timing to start the installation of the resource-saving capacity (Fig. 8).

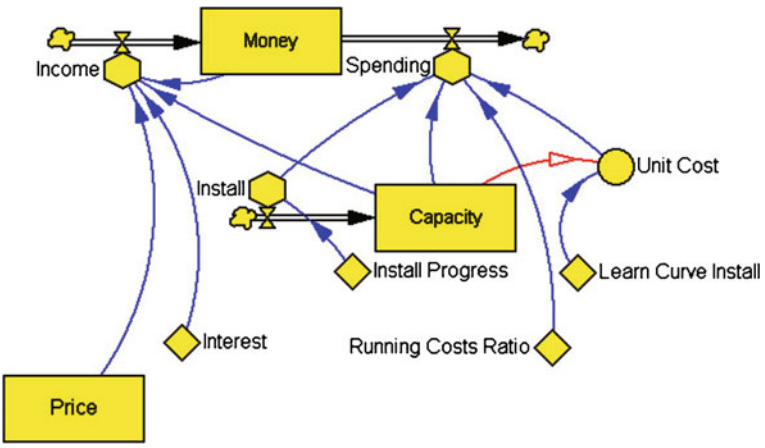

Fig. 6 Profit calculation for investment in resource-saving capacity

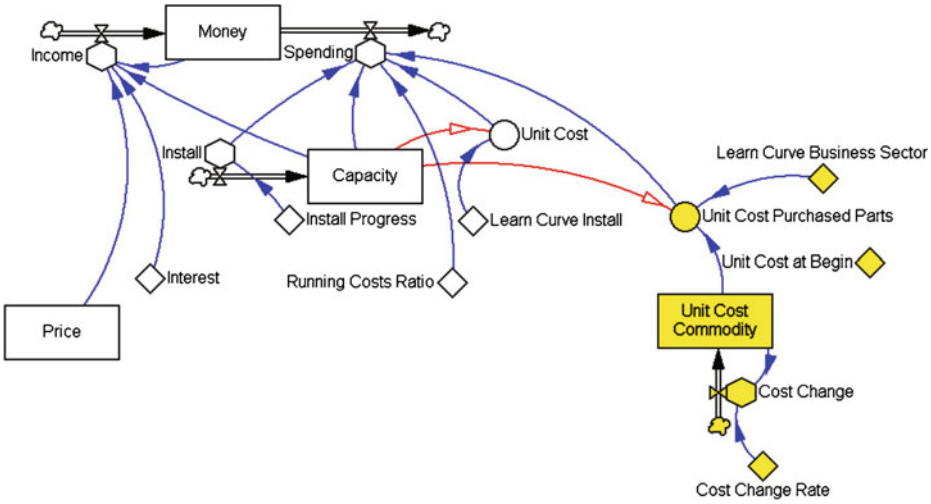

Fig. 7 Commodities and business sector specific parts and services

The last extension to the model is to take a follower ("Money F") in the same business sector into account. After the first-mover company started its resource-saving project, there always exists an optimal moment of time, when a follower company producing same products can start its project in the same way. Because the first-mover and the follower share the same learning curve of business sector the supply market for the purchased parts and services will become cheaper for the follower than for the first-mover (Fig. 9). This system dynamics model will be used in the following chapter for further explanations of the existence of different kinds of uncertainty, which arise not only on a macro-economic but especially on a micro-economic level.

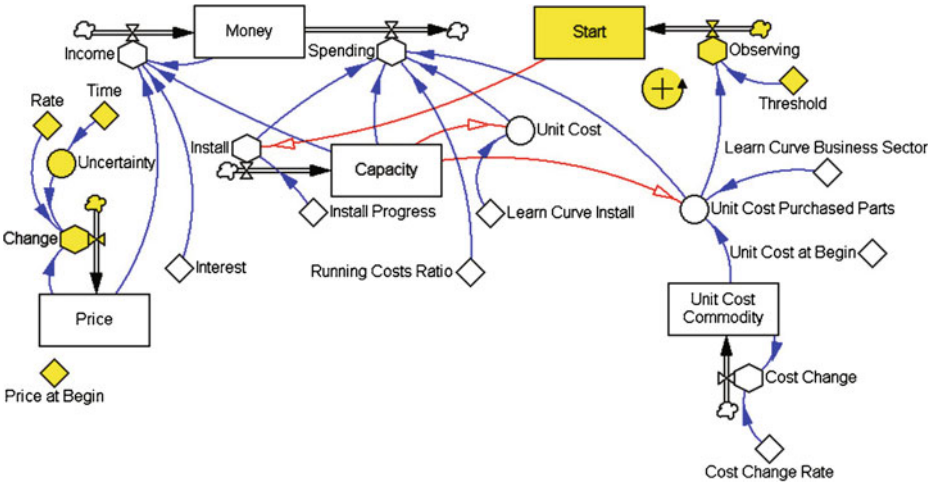

Fig. 8 Price development of the resource to be saved

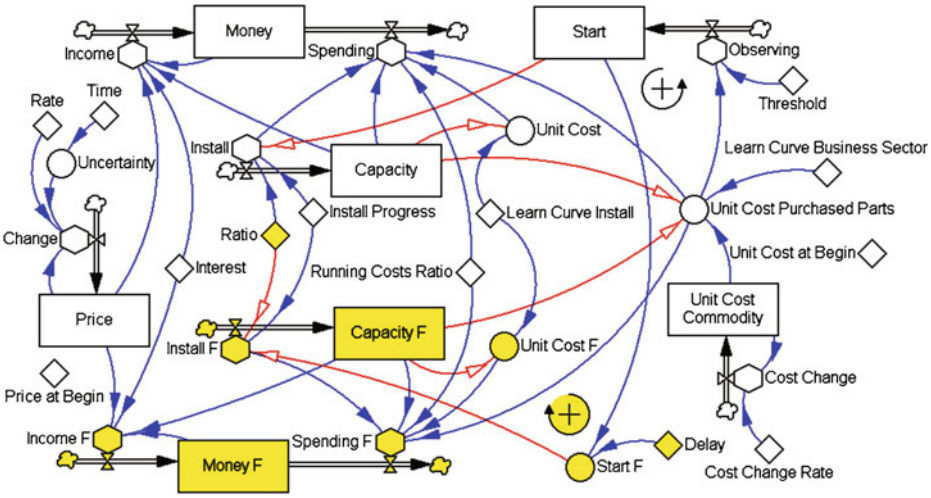

Fig. 9 Two competitors in a business sector

4.2 Uncertainty and follower advantage

According to the model presented in section 4.1 time is the crucial point when investing in resource-saving capacities under the condition of the existing uncertainty and increasing resource price. In a former approach certain allocation principles were characterized from a more static point of view (Pickl 2001, 2008). Here, we extend this characterization in a dynamic way.

Our model simulations show that there exists an optimal point of time for the start of resource-saving capacity project by the first-mover since the resource price increases while the costs for resource-saving capacities decrease. However, it is possible for a follower to start later to have a higher financial performance and lower investment volume. Uncertainty of price development can make the position of the follower even more comfortable. This in turn causes that a potential first-mover will postpone his resource-saving project for years to evade competitive disadvantages. The final result is a significant delay in implementation of resource-saving capacity in the whole business sector.

Figure 10 shows a possible scenario using model simulation: both the annual increase rate of the price of the resource to be saved and the annual interest rate are assumed to be 5 %. The decrease rate of the price of purchased parts increases as the first-mover and the follower start their resource-saving implementations respectively in the 3rd and 6th year. Notice that the first-mover has to make a much higher financial effort than the follower but at the end of the time period under consideration only a slightly higher financial performance. Under certain conditions the follower can even have a higher financial performance than the first-mover.

The next two figures show how price uncertainty can further influence first-mover and follower investment outcomes. In Fig. 11 the increasing rate of resource price is slowing down. In this case, first-mover and follower have equal financial performance, but first-mover investment project requires higher investments.

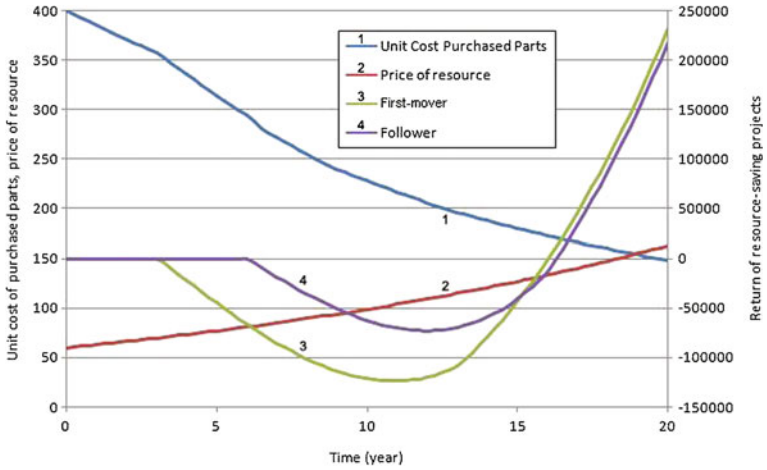

Fig. 10 Simulated development

If the follower follows the first-mover with optimized timing the first-mover does not only have a slightly lower financial performance but also a much higher risk of bankruptcy than the follower (Fig. 12).

Figure 13 shows the financial advantage of such a follower as a function of time delay before the follower starts his resource-saving project. In our model simulation we assume that interest and the annual increase rate of the resource to be saved are both 5 %. The follower has an advantage of 1.2 % in financial performance even if there is no uncertainty of resource price development. In the case when −1 % slowdown in resource price increase occurs after the first-mover starts investment (from 5 % to 4 %), the follower may achieve about almost 6 % higher

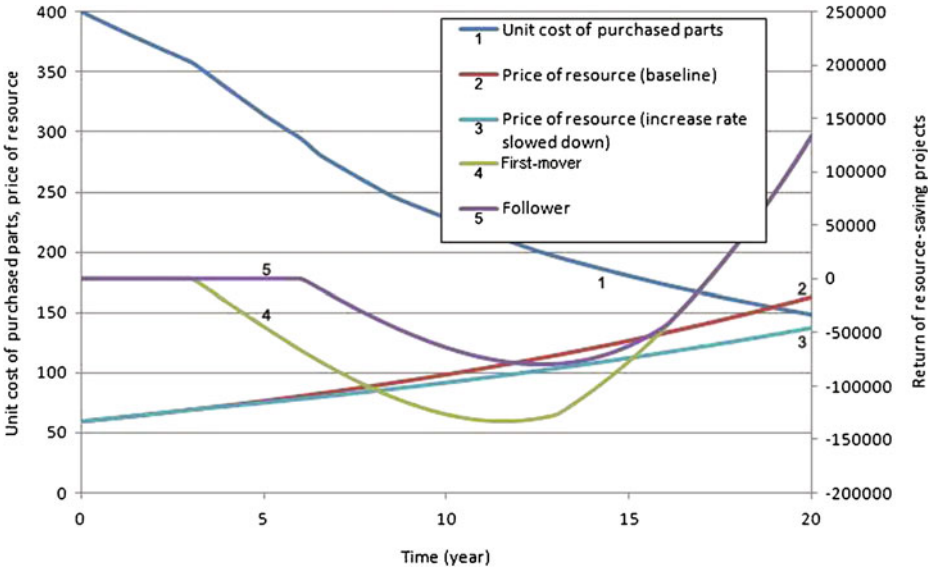

Fig. 11 Price development slows down

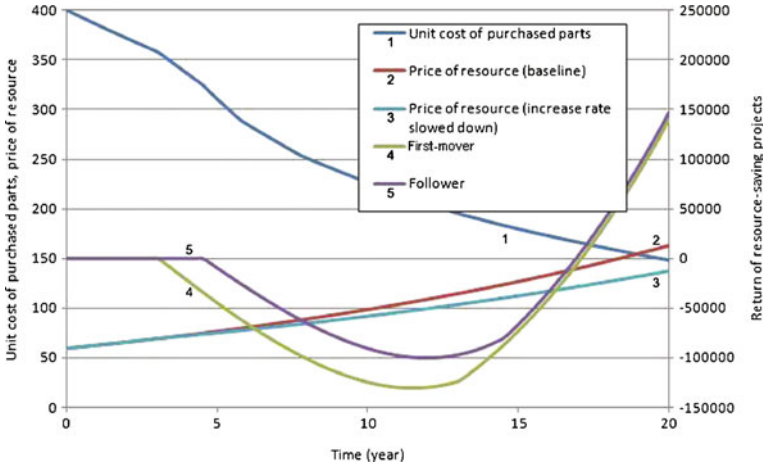

Fig. 12 The development of the prices and financial performance

financial outcome if he starts his investment about 1.5 years later then the first-mover. Consequently, the advantages of the follower under multiple uncertainties interfere with the first-mover investments in resource-saving technologies. As mentioned above, these follower advantages may make a potential first-mover and thereby the whole business sector postpones its resource-saving investments significantly.

5 Conclusions

We introduce two system dynamics models to estimate economical, institutional and technological uncertainties of emissions trading and their consequences for the effectiveness of emissions trading as a climate protection instrument.

The interdependence between economy, energy consumption and emissions is shown by using the first model which gives the opportunity to work with real economic data. We use this model to calculate income loss that occurs due to CO_2 reduction and thereby the possible price of emission permits for different countries. Sensitivity analyses

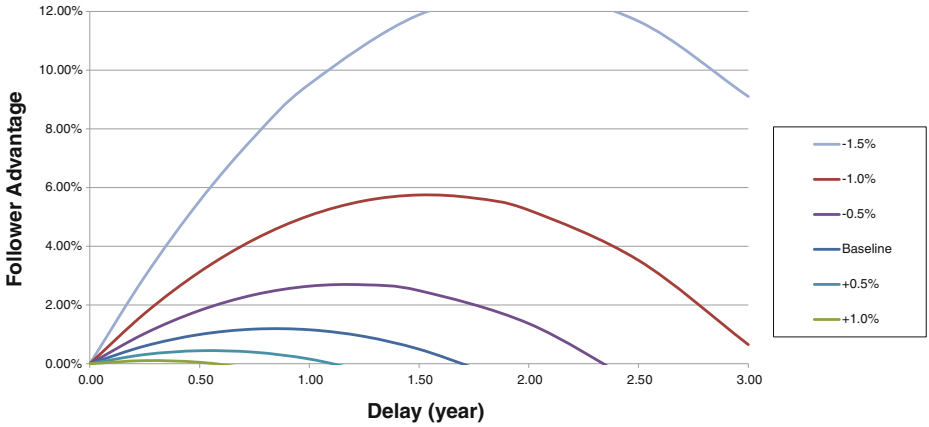

Fig. 13 Uncertainties influencing the follower decision

indicate that all three types of uncertainties–institutional (targeted emissions reduction), economical (the rate of economic growth) and technological (speed of energy efficiency improvement and clean energy implementation)–influence the price of emission permits significantly. The range of possible price options is very broad and leaves possible investors with very risky investment projects. To demonstrate uncertainties in emissions trading between two countries we use an example of USA and China, the both largest CO_2 emitters of the world. Different levels of economic development and different policies towards emissions reduction result in a significant difference in permits price between these two participants. Consequently, international interactions add even more uncertainty to pricing mechanism of emission permits.

The second model in this paper describes the behavior of specific decision-makers who are interested in investing in resource-saving technologies. Our system dynamics model indicates that there exists an optimal point of time for a potential first-mover to start a resource-saving capacity project under the condition of increasing price of the resource to be saved. However, our scenario simulations also show that a competitor in the same business sector can start his resource-saving project at a later moment of time to achieve higher financial outcome with lower investments, especially when uncertainties exist. This follower advantage is a substantial obstacle for a potential first-mover and thereby for a whole business sector to start investments in resource-saving projects.

Using system dynamics model simulations we find evidences that emissions trading appears to be able to provide invalid signals for decision-makers. Investors are facing wide range of permits price simultaneously being open to numerous economic, technological and institutional uncertainties. The authors state that system dynamics is a useful modeling tool to deal with uncertainty. Finally, the financial performance index can be seen as an important orientation measure which should be extended in further approaches.

References

Alexeeva-Talebi V, Anger N (2009) Developing supra-european emissions trading schemes: an efficiency and international trade analysis. Conference on the International Dimensions of Climate Policies, University of Bern, Bern, Switzerland, 21–23 January 2009

Avi-Yonah R, Uhlmann D (2009) Combating global climate change: why a carbon tax is a better response to global warming then cap and trade. Stanford Environment Law Journal, No 3, 28, University of Michigan Law School

Blyth W, Bunn D (2011) Coevolution of policy, market and technical price risks in the EU ETS. Energy Pol 39: 4578–4593, Elsevier

Chontanawat J, Hunt L, Pierse R (2006) Causality between energy consumption and GDP: evidence from 30 OECD and 78 non-OECD countries. Surrey Energy Economics Centre (SEEC), Department of Economics Discussion Papers (SEEDS), 113, Department of Economics, University of Surrey, Surrey, UK, Jun 2006

CPA Australia (2009) Climate change policy: carbon tax versus an emissions trading scheme–the debate between experts. ISBN 978-1-876874-23-0

Deissenberg C, Pickl S (2004) An algorithmic solution to the Kyoto game. In: Sachkov YL (ed) Generalized solutions in control problems IFAC. Fizmatlit, Moscow, pp 343–351

Gapminder Foundation (2008) Gapminder. http://www.gapminder.org/ (24.02.2009)

Hoppe H (2000) Second-mover advantages in the strategic adoption of new technology under uncertainty. Int J Ind Organ 18:315–338

Hu B, Pickl S (2010) Analysis and design of international emission trading markets applying system dynamics techniques. Daniel M. Dubois (Hrsg.): Computing Anticipatory Systems: CASYS '09: Ninth International Conference on Computing Anticipatory Systems, AIP Conference Proceedings, Volume 1303, 408–415

Laurikka H, Koljonen T (2006) Emissions trading and investment decisions in the power sector—a case study in Finland. Energy Pol 34:1063–1074, Elsevier

Pickl S (1998) Der τ-value als Kontrollparameter–Modellierung und Analyse eines Joint-Implementation Programmes mithilfe der dynamischen kooperativen Spieltheorie. Shaker Verlag, Aachen, 198 pages

Pickl S (2001) Optimization of the TEM Model–co-funding and joint international emissions trading. Operations Research Proceedings 2000 (Selected Papers). Springer, Berlin, Heidelberg, pp 113–118

Pickl S (2008) Climate change, sustainable development and risk: realizing a financial fonds within the TEM model as an economic and business opportunity. In: Hansjürgens B, Antes R (eds) Climate change, sustainable development and. Physica Publishers, pp 145–156

Pickl S, Kropat E, Hahn H (2010) The impact of uncertain emission trading markets on interactive resource planning processes and international emission trading experiments. Clim Chang 103(1–2):327–338, Springer

Schenker O (2011) How uncertainty reduces greenhouse gas emissions. Research Paper, Universität Bern, http://mpra.ub.uni-muenchen.de/29591/1/MPRA_paper_29591.pdf (01.07.2011)

Stalk G Jr (1988) Time–the next source of competitive advantage. Harv Bus Rev 66(4):41–51

UNFCCC (2009) Kyoto protocol. 14.01.2009, http://unfccc.int/kyoto_protocol/items/2830.php (02.03.2009)

United Nations Web Services Section, Department of Public Information (2008) Image & reality: questions and answers. About the United Nations, http://www.un.org/geninfo/ir/index.asp (22.02.2009)

Wittneben B (2009) Exxon is right: let us re-examine our choice for a cap-and-trade system over a carbon tax. Energy Pol 37:2462–2464

Yang M, Blyth W, Bradley R, Bunn D, Clarkk C, Wilson T (2008) Evaluating the power investment options with uncertainty in climate policy. Energy Econ 30:1933–1950, Elsevier

DOI 10.1007/978-3-319-15901-0_16
Reprinted from *Climatic Change* Journal, DOI 10.1007/s10584-014-1076-5

Accounting for uncertainties and time preference in economic analysis of tackling climate change through forestry and selected policy implications for Scotland and Ukraine

Maria Nijnik · Guillaume Pajot

Received: 3 January 2013 / Accepted: 2 February 2014 / Published online: 21 February 2014
© Springer Science+Business Media Dordrecht 2014

Abstract The paper discusses the development of economic techniques for dealing with uncertainties in economic analysis of planting trees to mitigate climatic change. In consideration of uncertainty, time preference and intergenerational equity, the traditional cost-benefit analysis framework is challenged with regard to the discounting/non-discounting of carbon uptake benefits, and because it usually uses a constant and positive discount rate. We investigate the influence of various discounting protocols on the outputs of economic analysis. The idea of using the declining discount rate is also considered. Several numerical examples dealing with the analysis of afforestation for carbon sequestration in Scotland and Ukraine are provided. We show that the choice of discounting protocols have a considerable influence on the results of economic analysis, and therefore, on the decision-making processes related to climate change mitigation strategies. The paper concludes with some innovative insights on accounting for uncertainties and time preference in tackling climate change through forestry, several climate policy implications of dealing with uncertainties, and a brief discussion of what the use of different discounting protocols might imply for decision making.

1 Introduction

An important social function of forests is their role in climate change mitigation (CCM). Numerous recent studies have addressed the cost-effectiveness of terrestrial carbon sink (Newell and Stavins 2000; van Kooten 2004; Stavins and Richards 2005; Nijnik and Bizikova 2008; Moran et al. 2008; Brainard et al. 2009; Nijnik et al. 2013). These studies suggest that the extent to which the mitigative role of forests can be enhanced is mediated by externalities, uncertainties, and complexities. These are shaped by a range of environmental, economic and policy drivers; market signals; institutional arrangements; and by public attitudes and behavioural patterns.

This article is part of a Special Issue on "Third International Workshop on Uncertainty in Greenhouse Gas Inventories" edited by Jean Ometto and Rostyslav Bun.

M. Nijnik (✉) · G. Pajot
The James Hutton Institute, Aberdeen, UK
e-mail: maria.nijnik@hutton.ac.uk

Forestry can contribute to CCM in many ways, including the establishment of tree plantations; increasing (i) carbon density (e.g. low thinning or long rotations), (ii) carbon storage in soils and (iii) wood products; and implementing renewable energy projects. Some of these measures are contested in the literature, e.g. long rotations (enhancing carbon storage in trees) on the one hand, and short rotation forestry, combined with the use of bio-energy, on the other (when, in addition to terrestrial carbon sequestration, the substitution of wood for fossil fuel is considered as a CCM measure); however, support for afforestation[1] is widespread.

Carbon sequestration through afforestation is usually considered to be a cost-efficient and synergistic option: when incorporated in multi-functional forestry (Nijnik and Miller 2013) it can co-deliver a variety of ecosystem services (Nijnik et al. 2012), at the same time as providing economic incentives for sustainable forest management. Afforestation is technically feasible; and many countries have a legacy of tree-growing (Nijnik and Bizikova 2008). It has been proved as effective for carbon sequestration, and effects are almost immediately apparent when trees are planted. Afforestation is also considered to be a low resource- and energy-consuming climate policy measure (Binkley et al. 2002).

Despite this, when van Kooten et al. (2004) carried out a meta-analysis of 68 studies, including a total of 1,047 observations worldwide, they identified huge variability across estimates of carbon sequestration costs. Baseline estimates of costs through forest conservation (based on analysis of 981 observations from 55 studies) ranged from US$46.62–US$260.29 per tonne C.[2] Although such variation across marginal cost estimates of carbon sequestration is partly due to the different methods and assumptions used, it also indicates that terrestrial carbon sequestration involves a great deal of uncertainty.

How to account for uncertainties in the economic analysis of natural resource use has long been debated. The uncertainties are largely associated with scenarios, data, and modelling. Scenario uncertainties primarily concern the assumptions made (e.g. on time preference). Data uncertainties are concerned with the reliability of information. Model-related uncertainties (i.e. a combination of the uncertainty in the parameter estimates and in the model structure itself) also need to be identified, quantified and accounted for. The IPCC (2007) provides recommendations for uncertainty assessment, including the notion that tackling climate change through forestry should involve consideration of the discounting to be applied.

In this paper, accounting for uncertainties and time preference is limited to discounting. We investigate the influence of discount settings on the economics of carbon sequestration through forestry in Scotland and Ukraine and the consequent policy implications.[3] The countries are selected to illustrate how the economics of tackling climate change is sensitive to discount settings, regardless of the context of such investigation. The countries provide different contexts of policies, institutional capacities and forest management practices. According to FAO (2010), Scotland (in the North-West of Europe) and Ukraine (in the South-East of Europe) are both sparsely wooded, each with approximately 16 % of total area invested in forestry. However, Scotland's forests are primarily managed for timber production; this is not the case in Ukraine where nearly 50 % of forests are natural vegetation. In Scotland, publicly owned forests account for approximately 50 % of the total wooded area. In Ukraine, public forestry prevails.

[1] In this paper, the terms afforestation and reforestation are considered to be synonymous.
[2] The conversion factor from CO_{2e} to C is 3.67 (i.e. 44/12).
[3] Because of the social science focus and the national level of this research, trade-offs between the accuracy and scale of the analysis were unavoidable. Therefore, a number of generalised assumptions and simplifications had to be made. These should not undermine the purpose and main results of this paper.

We analyse the economics of establishing forest plantations, investigating carbon storage in trees biomass[4] (for Scotland and Ukraine); and also the energy and wood product policy options (for Ukraine).[5] Selected cost-effectiveness estimates (under various discounting protocols) are provided. We discuss the implications of the findings, showing that the discounting protocol selected exerts considerable influence on carbon sequestration decision making processes. The main conclusion is that choice of discounting protocol has a dramatic impact on the economic acceptability of an afforestation project; and accounting for uncertainties in tackling climate change through forestry merits further investigation by applied interdisciplinary scientists.

2 Theoretical overview

Ecosystem services (ES) provided by forests (Nijnik and Miller 2013) are often long-lived, with some benefits being felt far into the future. This means that uncertainties faced by decision makers relate to both current and future demand and supply of ES, i.e. to their stock and flow. Difficulties in estimating the future benefits of carbon sinks are also due to uncertainties about the dynamics of carbon. Added to these are uncertainties linked to a number of factors: ecological (i.e. ecosystems' related), and technological (i.e. developments in science, technique and innovation); economic (i.e. related to development trajectories); environmental (e.g. connected to land quality and the state of environment); and social (i.e. concerned with tenure rights; changes in policies, markets and social norms). In Ukraine, a great deal of uncertainty is associated with property rights (particularly, with land markets), institutional settings and managerial aspects of forestry. Cost-benefit (CBA) and cost-effectiveness analyses (CEA) of planting trees for CCM, therefore, run into a wide range of uncertainties, and the extent to which mitigation strategies can be justified on efficiency grounds largely depends on the discount rate (DR) employed.

From a social science perspective, discounting has two basic sources. The first represents social time preference: we have to discount benefits arising in the future because of diminishing marginal utility of consumption. The second source is the productivity of capital or its social opportunity cost; if resources are invested instead of being consumed now, they could provide a higher level of consumption in the future (Pearce and Turner 1990). Given perfectly functioning markets, the social rate of time preference would equal the social opportunity cost of capital: there is no logic in investing unless future benefits offset the social rate of time preference.

In the actual world, the situation is different (particularly, in emerging market economies, such as Ukraine); and in the absence of perfect information, a choice has to be made. There are many justifications for using one or another discount setting. In addition to time preference, or as a measure of alternative investments, a positive inflation rate and uncertainty over future earnings could be used to justify selection of a DR.

[4] The storage option (van Kooten 2004) presumes planting and growing of trees without considering future use of wood and land. Such a simplified assumption can only be made together with the assumption that by harvesting the trees, using the revenues to cover future costs of establishing new forests and storing carbon, both the gains and losses in physical and monetary values are well balanced.

[5] Woody biomass is being recognised as a renewable energy source with low GHG emissions (Matthews and Robertson 2003; Galbraith et al. 2006). Also, the building of more timber-rich houses and increasing the service life of wood products are considered to be valuable contributions to reducing carbon impacts (Read et al. 2009). However, the wood products sink may not be strong and/or last long, while energy substitution effects are debatable in the literature. These policy options, therefore, require further exploration (Bottcher et al. 2012).

In forest economics, justification of one as opposed to another discount setting relies above all on the uncertainty of upcoming events and their outcomes. Because economies are affected by random shocks, uncertainty about income growth induces people to invest more for the future. This precautionary effect underpins the argument for reducing DRs (Gollier 2001). The concept of intergenerational equity, Clark's (1973) consideration of risk related to depletion of natural resources, and Ramsey's (1928) idea of ethical indefensibility underpin arguments for non-discounting (or using low discount settings) in forestry.

However, financial returns in forestry are commonly low, and investment risks are high due to both the long rotation periods of timber, and the risk of losses, through forest fires, pest invasions or storm damages. Disturbance dynamics are complex, varying with disturbance type, intensity, frequency, extent, and scale.[6] In private forestry, therefore, because of long-term investments under risks and uncertainties, and to secure income generation sooner rather than later, support is usually given to positive (and even rather high) discount rates (Samuelson 1961).

Particular difficulties arise in the choice of DRs for climate related economic analysis. Firstly, this is because marginal damages from atmospheric carbon are not certain over time. Secondly, there is uncertainty about the benefits of carbon control strategies for future generations. Ecological economists argue that even if the preferences of upcoming generations for CCM measures were to be taken into account, it would be impossible to accurately reflect these, because future preferences are unknown. Uncertainty in climate change economics is exceptionally high (Shvidenko et al. 2010); and there is no agreed method for adjusting the DR for risk in the present valuing of uncertain future benefits and losses (Hanley and Spash 1993).

Nordhaus (1991) argues that the efficient degree of control of carbon concentrations should be minimal where there are high costs, low damages and high discounting, and maximal where there are low costs, high damages and low discounting. The current costs of mitigation strategies are often high, and if we believe that future technology will enable carbon emission reductions at almost no cost, an infinite DR could be applied. The opposite assumption results in the reverse conclusions. Overall, largely because of uncertainties, discounting (including of carbon uptake benefits) becomes an important question when using CEA of CCM.

On the one hand, it is probable that marginal damages caused by climate change will not worsen in the long run. Such probability might increase over time, provided there is ongoing technological progress. We may also rely on the increasing stock of knowledge; the development of human and social capital, and of innovation that will enable future generations to solve problems which cannot be solved today. On the other hand, even if the most extensive damages and losses occur in the far future, their discounting at a positive rate assigns them insignificant present values (PV), ultimately advocating little immediate action to alleviate climate change. Therefore, for decision making to favour the resilience-to-climatic-changes scenario, the more rapidly CO_2 concentrations in the atmosphere are projected to increase over time (increasing the risk of future damages and losses), the less future carbon benefits should be discounted.

Ecological economists, in particular, have acknowledged this complexity and questioned the traditional notion of using constant and positive DRs (Cyriacy-Wantrup 1942; Harrod 1948). Increasing attention is being given to ethical considerations about the welfare of future generations and safeguarding good environment status (Brainard et al. 2009; Hepburn and Koundouri 2007). The traditional framework of CBA and CEA has been challenged because the use of a constant and positive DR reduces the weight of future benefits and costs

[6] Carbon leakages (Dyer and Nijnik 2013) could be accounted for through risk analysis, insurance policies, deductions, and buffer pools, where discounting for risk has an important role (Chomitz 2002).

(Chichilnsky 1997; Price 2005). We acknowledge these concerns, and in the following section, along with the traditional framework, use a declining discount setting.

3 Effects of using different discount settings on the decision-making processes of tackling climate change through afforestation in Scotland

The methodology-in-use is of Stavins and Richards (2005) which is adapted by Nijnik et al. (2013). We assess the benefits of forestry over one rotation, i.e. the 'Fisher rotation'[7], and assume that forestry generates timber sales income through thinning and clear fell harvesting. A simplified form of the net present value ($NPV_{Forestry}$) is:[8]

$$NPV_{Forestry} = -c + pve^{-rT} \quad (1)$$

where:

p is the timber price
c is the plantation cost
v is the timber volume
T is a temporal variable
r is the discount rate.

We calculated the cost per tonne of carbon sequestration, as an expression of cost effectiveness (CE), by dividing an estimate of the opportunity costs of land conversion to forests by the number of tonnes of carbon sequestered:

$$CE = \frac{NPV_{Forestry} - NPV_{Farmimg}}{\Delta C} \quad (2)$$

where:

$NPV_{Forestry}$ is the NPV of forestry
$NPV_{Farming}$ is the NPV of farming
ΔC is the carbon stock gain over one rotation (i.e. 'benefits' of the project).[9]

Carbon sequestration rates were derived from Bateman and Lovett (2000). Yield tables from the Forestry Commission (FC) (2010) were used to analyze timber volumes and estimate the costs and benefits of forestry operations in Scotland. Timber prices were taken from the FC's website. Land market values (Savills Research 2010) were used to account for the opportunity cost of land. We analysed the costs of carbon sequestration for converting low, medium and good quality land to forests, assuming that woodlands would initially displace land with a low agricultural potential.

[7] For the most important species in Scotland (Sitka spruce YC14), the maximized $NPV_{Forestry}$ is equivalent to £732.75 per ha in 49 years, i.e. the nominal length of a commercial rotation.
[8] Although thinnings are not included in the simplified Eq. 1, they were considered in calculations.
[9] Several assumptions were made on our computation of $NPV_{farming}$. Land price represents a capitalization of future net benefits. However, using of gross margins from farming activities as the measure probably overestimates the costs of carbon sequestration, since it only deducts variable costs from gross farm earnings. We therefore used an approach (Nijnik et al. 2013) based on land market values. We presumed a one-time tree planting (see endnote 4), considering that the carbon stock of the initial land use is small, and that the carbon stock in forestry is the 'benefit' used to calculate the cost-effectiveness.

Firstly, only financial variables were discounted. We paid particular attention to planting Sitka spruce (relatively fast growing and the most common tree species in Scotland), and in line with Moran et al. (2008) assumed a private DR of 7 %, and a social DR of 3.5 %. Then, we followed the HM Treasury (2003) guidelines for declining discount rate (DDR) protocol, so that incomes occurring in the years beyond 30 were discounted at a lower rate.

It is possible to simulate what the carbon sequestration rate of a plantation could be. However, fires, storms, pests and diseases can threaten a forest's potential to sequester carbon. Also, different forests exhibit different sequestration patterns: slow growing species provide distant benefits; and fast growing species generate almost immediate carbon sequestration benefits (e.g. hybrid poplar, as shown in Section 4). A tree plantation would offset the effect of carbon emission activities while new technologies with low carbon intensity are developed. In a 'buying time' option, it would be appropriate to encourage high sequestration rates plantations (consisting of fast growing species).

To take the temporal dimension into account, it also seems sensible to discount carbon uptake benefits, making it possible to compare CCM projects that exhibit different sequestration patterns (e.g. fast growing versus slow growing plantations). In that case, the comparison is made on the basis of carbon sequestration in trees. However, the wood product stocks are also going to be a function of the type of trees planted; slow growing species will provide sawtimber used in construction and in the supply of long lived products, whereas fast growing species will be allocated to bio-energy or to short lived products, such as paper.

These differences (occurring post-harvest) could also be taken into account through discounting. Other comparisons could be made: projects aiming at sequestering carbon in the biomass versus projects aiming at sequestering carbon in soils, or projects reducing emissions versus carbon sequestration projects. Also, with discounting of carbon removals (when costs are compared to benefits on an identical basis, van Kooten and Sohngen 2007) the methodology (Richards and Stokes 2004; Nijnik 2005) becomes suitable for considering the use of wood in products, or as a substitute for fossil fuel (shown in the following section):

$$B = \int_0^{T1} S'(t)e^{-rt}dt - \int_0^{T2} S'(t)e^{-rt}dt \tag{3}$$

where:

B describes the benefits of the project;
S′ describes annual carbon flow (change in carbon)
T_1 is the rotation length implemented in the first project, and
T_2 is the rotation length implemented in the second project.

Results showing the influence of various discounting protocols for Sitka spruce plantations in Scotland are given in Fig. 1.

As seen in Fig. 1, costs per tonne of carbon sequestration are higher with a constant 7 % DR (for economic variables) as compared to using the DR of 3.5 %. The DDR protocol favours long term projects because incomes occurring in the far future are discounted at a lower rate. Therefore, DDR reduces the costs of carbon sequestration in forestry (giving more weight to future financial flows of income compared to current ones). Further, discounting carbon fluxes (at the same rate of 3.5 % as the economic variables) has severe impacts on costs: they are almost doubled.

The results provide evidence that afforestation with Sitka spruce on low grade agricultural land (currently used for low density sheep grazing) may be a cost effective option of CCM,

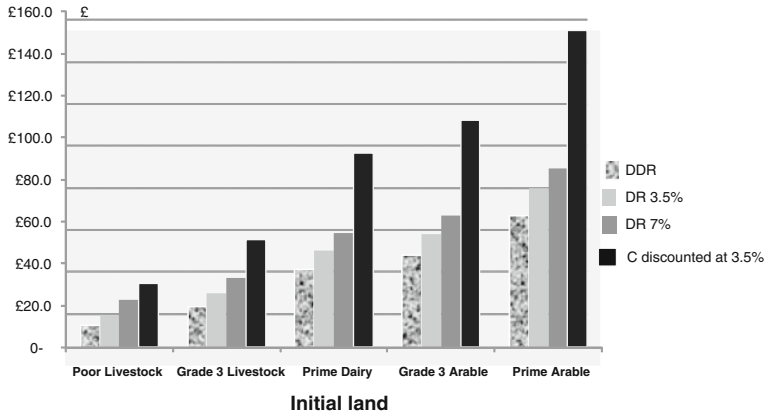

Fig. 1 Estimates for the costs per tonne of carbon sequestration: an example for creation of Sitka spruce plantations in Scotland under different discount rate (DR) settings, including declining discount rates (DDR)

ranking the costs in some regions of Scotland below the shadow price of carbon estimated by DEFRA (2008). The results also show that the choice of discounting protocol in CEA has a significant effect on the economic acceptability of an afforestation project. Clear cutting is distant in time, and is more affected by a high DR than agricultural annual income flows.

4 Influence of different discount settings on the results of economic analysis of carbon sequestration: policy implications for Ukraine

In the analysis of afforestation for carbon uptake in Ukraine (i.e. the storage option) the methodology allowing for the discounting of carbon removals (see Section 3) was used; with its milestones (by Nijnik 2005) presented in Table 1.[10]

Three discount settings for carbon removal are used. The first presumes no discounting of carbon, assuming that the value of marginal carbon damages in the future will increase at the real rate of discount. This assumption implies that the carbon sequestered is valued equally, no matter when it is captured. However, because non-discounting is a very specific assumption, particularly in long-term projections, and to make an initial appraisal of sensitivity of the results to discounting, positive settings of 2 % and 4 % for carbon removal have also been used.

Discounting of carbon benefits at a social rate (4 %) presumes that marginal damages from emissions are constant over time. This is a reasonable assumption since we have no evidence to predict any other scenario. As a 4 % discount rate was applied to the discounting of financial variables in our analysis for Ukraine, it was logical to use the same rate for the discounting of carbon uptake benefits. The discounted carbon per ha across forestry zones, for the storage option under different discount rates assigned for carbon benefits is shown in Table 2.

The highest estimates of carbon uptake over 40 years are for hybrid poplar in the Wooded Steppe. The estimates for Ukraine are comparable with corresponding estimates for the UK (Read et al. 2009), the Netherlands (Slangen et al. 1997; Nabuurs et al. 1999), Finland

[10] Due to the variety of conditions, there would be a decrease of soil carbon in some areas, and an increase in some others. It was assumed, therefore, that on average soil carbon would remain unchanged. The litter pool, which in Ukraine accounts for a small proportion of the total pool, was not reflected in this research.

Table 1 Milestones of the methodology for the estimation of the above and below ground biomass in forest and of the stored carbon

	Ukraine
Selection of lands suitable for afforestation	The Ukraine's Forestry Spatial Classification by Gensiruk and Nizhnik (1995) was used as the framework for assessing the possibilities to enlarge forest cover (by 2289.3×10^3 ha, in total)
Baseline land-use in the selected areas	Marginal agricultural land, and bare land (belonging to forestry)
Units for which the above-ground biomass was analyzed	Across 5 forestry zones: the Polissja, the Wooded Steppe, the Steppe, the Carpathian Mountains and the Crimea
Given the tree-growing conditions, the following tree species were selected	Hybrid poplar *Populus robusta*—in the Wooded Steppe; 30 % hybrid poplar, 20 % alder, *Alnus glutinosa*, etc. hardwoods and 20 % pine, *Pinus sylvestris*, etc. softwoods—in the Polissja; pine—in the Steppe and the Crimea, and spruce *Picea sitchensis*—in the Carpathians
Estimation of biomass	Growth functions were estimated by Nijnik (2004). The best fit e.g. was achieved using the functional form for stand growth of spruce (V) related to (t) the age of trees (first site classes): $V(t)= 0.159\ t^{2.240}\ e^{-0.018t}$ (parameter estimates statistically significant at $P= 0.05$).
Translation of the stem biomass to total above ground biomass	Stem wood was multiplied by 1.51 for coniferous and by 1.69 for softwood species (following Lakida et al. 1995)
Carbon content in the above-ground biomass	Multiplying by the coefficient of $0.2 tC/m^3$ (Jessome 1977)
Carbon sequestered in roots	0,2317 relates R to G for spruce; for pine: $R(V)=0.146\ (V)^{-0.519}$, where V=growing stock (Lakida et al. 1995); for all other species: $R(G)= 1.43319G^{0.639}$ (van Kooten and Bulte 2000)

(Pussinen et al. 1997) and other countries. However, while carbon estimates are comparable with those elsewhere in Europe the costs per tonne of carbon removed in Ukraine are relatively lower (Table 3).

As seen in Table 3, the estimates depend significantly on the DR applied; at discount rates lower than 2 %, the costs are covered by the returns in the majority of Ukraine's regions. However, the results also indicate that in the Polissja zone and particularly in the Steppe, afforestation for carbon sequestration alone[11] is cost-inefficient at 2 % and higher DRs.

We also considered the option of harvesting trees when their growth decelerates, so that carbon is stored in wood products or is burned instead of fossil fuel. In the wood products option, carbon sink duration is equivalent to the life of the products. An assumption was that wood products release carbon back into the atmosphere after 40 years' storage.[12] In both the wood-for-coal-substitution and in bio-energy scenarios[13], the rotation ages of poplar and

[11] Multi-functional afforestation in Ukraine is analysed in (Nijnik et al. 2012).

[12] This is a simplified assumption. In reality, much of carbon returns to the atmosphere almost immediately after timber harvesting; and the rest of the carbon release follows a negative exponential curve, with cumulative loss over time. Carbon release paths largely depend on tree species; with oxidation rates for wood products being roughly 0.02 per year (van Kooten and Bulte 2000).

[13] Energy required for harvesting and processing of wood, costs of converting power plants to wood, production costs of coal, and changes in transportation costs were ignored. Also, given the purpose of this paper, the technological aspects of wood vs. coal, e.g. combustion techniques, efficiency of burners, or emissions from non-CO_2 gases etc., were beyond the scope. The costs considered included: opportunity cost of land; tree planting, care, protection and replanting costs and those of timber harvesting.

Table 2 Cumulative carbon sequestered per ha, under the storage scenario

Carbon (t C ha^{-1})	Polissja	Wooded Steppe	Steppe	Carpathians	Crimea
0 %	203.2	236.3	37.3	178.6	99.6
2 %	91.29	106.19	16.76	80.26	44.75
4 %	41.0	47.7	7.5	36.0	20.1

Including in the root pool

mixed species were assumed to be of 20 years. Coniferous trees were considered ready for harvesting when they reach 40 years of age.

In calculating estimates for a fossil fuel substitution, i.e. a bio-energy policy scenario, we considered that the wood (above ground biomass) is burned to generate energy, replacing an energy equivalent of fossil fuel. When wood is used, carbon stored in wood biomass is released as CO_2 upon burning. Using timber for energy production is therefore in itself largely a carbon neutral process (so long as the energy required for harvesting and processing wood is not taken into account, van Kooten 2004). The net gain here is the amount of CO_2 that would have been released by burning fossil fuel if this had not been replaced by the burning of woody biomass.

The estimates shown in Table 4 (which do not reflect changing prices over time) provide evidence that under the wood-for-fuel substitution and wood products sink policy options, the DRs used in the analysis are again important factors influencing the results.

The time horizon considered is also very important (as shown by van Kooten 2004): the longer the period investigated, the more useful the results, because the effects (e.g. through the replacement of non-timber materials) are repeatable, and social benefits are expected to be higher in the long run of multiple rotations.

5 Discussion

The immediate consequence of positive discounting is that future benefits (costs) are worth less than present benefits (costs). This notion (or concern) was recognised long before climate change was considered as a problem. Ramsey (1928) argued that discounting is an ethically indefensible practice. Cyriacy-Wantrup (1942) recommended the use of zero or negative DRs, when valuing health, education or defence services. Heal (1981) admitted that the DR is something we choose, and that this choice is largely a political issue. Harrod (1948) defined

Table 3 Present value of carbon sequestration costs, € per tonne C

Forestry zones	€ per tonne at the discount rates of		
	0 %	2 %	4 %
Polissja	5.8	7.1	8.7
Wooded Steppe	4.6	5.9	7.2
Steppe	78.5	120.0	173.3
Carpathians	8.7	12.7	17.9
Crimea	16.2	15.6	32.0
The Ukraine	9.5		18.1

C is in permanent tonnes for the above-ground biomass

Table 4 Costs of carbon sequestration over 80 years per forestry zone, alternative scenarios

Scenario	Discount rate for carbon	Polissja	Wooded Steppe	Steppe
Energy	0 %	16.5	16.2	153.4
	4 %	405.3	397.1	3764.4
Product	0 %	33.0	32.4	215.8
	4 %	69.1	67.7	1035.9

Only for the above-ground biomass

discounting as a polite expression for rapacity. His argument was based on ethical and environmental grounds; it appears that the consequences of discounting are significant when the economic valuation process deals with environmental issues occurring in the distant future.

By contrast, some authors (Price 2005) consider that high DRs reduce the number of viable investment projects. Given that some projects (particularly under uncertainties) might be a threat to good environmental status, the use of high DRs can be seen as positive. Another positive effect of high DRs is that investments are directed towards the most efficient projects, so that revenues earned will provide future generations with the economic means to adapt. Acknowledging the will to give more weight to future costs and benefits, some scientists have advocated the use of declining discount rates (Groom et al. 2005). Hepburn and Koundouri (2007) provide the following justifications for using DDRs in economic analyses:

- Time preference: experiments show that people tend to use higher DRs in their everyday lives for present trade-offs rather than for more distant ones;
- Pessimism about the future: hyperbolic discounting, with the DR being formally a function of consumption growth; if consumption is expected to fall, or if this is probable, then we should use DDRs;
- Uncertainty: in the face of uncertain futures with several likely discount rates, taking an average of discount factors corresponding to likely DRs is called the certainty equivalent discount factor. It is possible, working backwards, to find the certainty equivalent DR; this rate appears to be a declining one.

Some other theoretical developments (Chichilnsky 1997; Li and Lofgren 2000) show that DDRs are necessary to achieve intergenerational equity. Also, policy makers, such as the UK and French governments, recognise these justifications, and recommend the use of DDRs for economic appraisal (HM Treasury 2003; Lebegue 2005).

As shown in the case of tree-planting in Scotland, the use of DDRs (for economic variables) tends to favour long term projects. The DDRs applied to both forestry and agriculture work in favour of forestry. We show that DDRs considerably improve the projected profitability of forestry, and reduce the cost estimates of carbon sequestration (Fig. 1). Nevertheless, there are situations when short term benefits are preferred. Climate change is characterized by thresholds beyond which irreversible effects may appear. If a threshold is close, we might prefer a short term strategy of sequestering carbon quickly, or drastically reducing carbon emissions.

Thus, the choice of discounting protocol, with justifications for the settings (including a zero and/or a DDR considered) has a significant impact on the economic acceptability of an afforestation project. Among the consequences of using a DDR in economic analysis is that more projects would pass the CBA test. Environmental strategies generating long term benefits would also be favoured, which would be particularly relevant in the case of CCM (under uncertainties) because costs would be spread over centuries.

We have explained the accounting for uncertainties and time preference in economic analysis of tackling climate change through forestry showing a high sensitivity of cost-effectiveness of afforestation to the discount settings applied (including the discounting of carbon uptake benefits, specifically shown in Ukraine). Results also add to the evidence suggesting that an important factor influencing the costs of carbon sequestration through forestry is the opportunity cost of land, which in Scotland (and some regions in Ukraine) is relatively high. It suggests that tree-planting for carbon sequestration should be focused on the less productive land rather than considering larger scale afforestation.

In Scotland, the decline of hill farming (because of CAP reforms and other drivers) may create space for new economic activity on abandoned farmland, among which it could be forestry.[14] In Ukraine, large-scale agriculture under the previous regime supported the conversion of forest or grassland to agricultural land. Currently, the decreasing agriculture will likely cause the increase of abandoned land; a rising role of forestry could then be predicted (Nijnik et al. 2012).

This paper considers carbon forestry alone. However, terrestrial carbon sequestration projects are likely to be implemented if they are consistent with the wider programmes of sustainable development (especially in remote rural areas). A multi-purpose afforestation is often seen as a sustainable way of land reclamation and increasing productivity of abandoned land, whilst utilization of biomass from plantations can provide employment opportunities and create new options for land development, being also a sustainable energy alternative (Nijnik et al. 2012).

Policy measures supporting these activities in Scotland aim for "win-win" situations to benefit rural development, people, the economy and environment (Read et al. 2009). In Ukraine (facing institutional challenges and affected by regional socioeconomic disparities) afforestation is seen as a means to increase economic gains to forestry through an enlarged wood production, and to the agricultural sector by using soil protection and hydrological forest functions. It also deemed to be beneficial through the mitigation of climate change; and to Ukraine, specifically and possibly, in view of accumulating financial assets through carbon trading (Nijnik et al. 2011), and providing opportunities for deliberative processes and pro-market reforms.

6 Conclusions

The traditional practice of using a positive and constant discount rate in CBA and CEA has been challenged; and our findings contribute to suggesting that a positive and constant discount setting is not the only solution. Declining discount rates have been proposed as a way to deal with uncertainty, and also to enhance intergenerational equity.

The estimation protocol also includes provision for discounting carbon removals. However, the benefits of carbon sequestration are highly uncertain; and also because of time preference, future carbon reductions may decrease in value rapidly (at DRs of 5 % and higher, the PV of any amount of carbon sequestered some 50 years from now rapidly approaches zero).

In this paper, the consequences of using various discounting protocols on the costs of carbon sequestration in forestry are revealed and explained. Despite that the conditions (e.g.

[14] Institutional changes and future cash flows for and responses of farming enterprises merit attention but are beyond the scope of this paper. Also, shifting to forestry would depend on whether agricultural subsidies continue to hold up land prices and whether cultural values would affect the propensity to develop forest-based activities on private land, including those of tree-planting (Nijnik et al. 2013).

natural, social, and economic) in Ukraine are very different from those in Scotland, the research has provided quite similar results for the uncertainty issues, which are important in decision making on tackling climate change through afforestation.

The general conclusion is that choice of discounting protocol has a dramatic impact on the economic acceptability of an afforestation project; and innovative insights into the accounting for uncertainties in tackling climate change through forestry (including the consideration of uncertainty on carbon sequestration and carbon stocks changes) merit further investigation through applied interdisciplinary research. In particular, elaboration of the theoretical and ethical rationales for various carbon forestry discounting protocols, and their links to the real world situations and decision making processes, are needed (and these are complex, case specific, context sensitive and scale dependent).

There is also an understanding that using the most appropriate discount setting is only one way to account for uncertainties in tackling climate change through forestry. Many other options (going beyond the scope of this paper) exist. Such options include building on bottom-up (local scale) and top-down (wider scale) actions, therefore, connecting science, policy and participation, and moving beyond narrowly-focused technical approaches towards more holistic innovative strategies of strengthening resilience to climate change.

To conclude, accounting for risks and uncertainties in tackling climate change through forestry could be enhanced by developing skills and mutual learning across relevant stakeholder groups, and through interactive capacity-building on an ongoing basis.

Acknowledgments The support from the Scottish Government (RESAS) Research programme is gratefully acknowledged. We are grateful for the reviewers of this paper for their helpful comments and to Sue Morris for the help with proofreading.

References

Bateman IJ, Lovett AA (2000) Estimating and valuing the carbon sequestered in softwood and hardwood trees, timber products and forest soils in Wales. J Environ Manag 60:301–323

Binkley D, Ryan M, Stape J, Barnard H, Fownes J (2002) Age-related decline in forest ecosystem growth: an individual-tree, stand-structure hypothesis. Ecosystem 5:58–67

Bottcher H, Freibauer A, Scholz Y, Gitz V, Ciais P, Mund M, Wutzler T, Schulze E-D (2012) Setting priorities for land management to mitigate climate change. Carbon Balance Manag 7(5)

Brainard J, Bateman IJ, Lovett AA (2009) The social value of carbon sequestered in Great Britain's woodlands. Ecol Econ 68:1257–1267

Chichilnsky G (1997) What is sustainable development? Land Econ 73:467–491

Chomitz KM (2002) Baseline, leakage and measurement issues: how do forestry and energy projects compare? Clim Pol 2(1):35–49

Clark C (1973) The economics of over-exploitation. Science 181:630–634

Cyriacy-Wantrup SV (1942) Private enterprise and conservation. J Farm Econ 24:12–21

DEFRA (2008) Climate change act http://www.defra.gov.uk/environment/climatechange/uk/

Dyer G, Nijnik M (2013) Implications of carbon forestry programs on local livelihoods and leakage. Ann For Sci. doi:10.1007/s13595-013-0293-9

FC Forestry Commission (2010) Forestry facts and figures. Forestry Commission, Edinburgh

Food and Agricultural Organization of the United Nations (2010) http://www.fao.org/forestry

Galbraith D, Smith P, Mortimer N, Stewart R, Hobson M, McPherson G, Matthews R, Mitchell P, Nijnik M, Norris J, Skiba U, Smith J, Towers W (2006) Review of greenhouse gas life cycle emissions, air pollution impacts, economics of biomass production and consumption in Scotland. SEERAD FF/05/08 Project Report

Gensiruk S, Nizhnik M (1995) Geography of forest resources of Ukraine. Svit Publishers, Lviv

Gollier C (2001) The economics of risk and time. Massachusetts Institute of Technology, USA

Groom B, Hepburn C, Kondouri P, Pearce D (2005) Discounting the future: the long and short of it. Environ Resour Econ (31)
Hanley N, Spash C (1993) Cost-benefit analysis and the environment. Edward Elgar Publishers, Cheltenham, UK
Harrod RF (1948) Towards the dynamic economy. St Martin's Press, London
Heal (1981) Economics and resources. In: Butlin (ed) Economics of the environmental and natural resource policy. Westview Press, Boulder
Hepburn CJ, Koundouri P (2007) Recent advances in discounting: implications for forest economics. J For Econ 2–3(13):169–189
HM Treasury (2003) The green book: appraisal and evaluation in central government. London
IPCC (2007) Climate change 2007 mitigation. In: Metz B, Davidson OR, Bosch PR, Dave R, Meyer LA (eds) Cambridge University Press
Jessome A (1977) Strength and related properties of woods grown in Canada. Forestry Tech. Rep. 21, Ottawa, Canada
Lakida P, Nilsson S, Shvidenko A (1995) Estimation of forest phytomass for selected countries of the former European USSR. WP-95-79 IIASA, Laxenburg
Lebegue D (2005) Révision du taux d'actualisation des investissements publics. Rapport pour le Commissariat General du Plan
Li C, Lofgren KG (2000) Renewable resources and economic sustainability: a dynamic analysis with heterogeneous time preferences. J Environ Econ Manag 40:236–250
Matthews R, Robertson K (2003) Forest products and bioenergy. In: Karjalainen T, Apps MJ (eds) Carbon sequestration in the global forest sector. IUFRO Task Forces on Environmental Change state of the art report
Moran D, MacLeod M, Wall E, Eory V, Pajot G, Matthews R, McVittie A, Barnes A, Rees B, Moxey A, Williams A, Smith P (2008) UK marginal abatement cost curves for the agriculture and land use, land use change and forestry sectors out to 2022 with qualitative analysis of options to 2050. Report to the Committee on Climate Change, RMP4950
Nabuurs G, Dolman A, Verkaik E et al. (1999) Resolving issues on terrestrial biospheric sinks in the Kyoto Protocol. Dutch National Research Programme on Global Air Pollution and Climate Change. Report 410 200 030, 100
Newell RG, Stavins RN (2000) Climate change and forests sinks: factors affecting the costs of carbon sequestration. J Environ Econ Manag 40(3):211–235
Nijnik M (2004) To an economist's perception on sustainability in forestry-in-transition. For Policy Econ 6:403–413
Nijnik M (2005) Economics of climate change mitigation forest policy scenarios for Ukraine. Clim Pol 4:319–336
Nijnik M, Bizikova L (2008) Responding to the Kyoto Protocol through forestry: a comparison of opportunities for several countries in Europe. Forest Policy and Economics 10:257–269
Nijnik M, Miller D (2013) Targeting sustainable provision of forest ecosystem services with special focus on carbon sequestration. In R Matyssek, N Clarke, P Cudlin, T Mikkelsen, J-P Tuovinen, G Wiesser, E Paoletti (eds) Climate change, air pollution and global challenges: understanding and perspectives from forest research. Elsevier, pp 547–565
Nijnik M, Slee B, Pajot G (2011) Opportunities and challenges for terrestrial carbon offsetting and marketing, with some implications for forestry in the UK. South-East Eur For J 1(2):69–79
Nijnik M, Oskam A, Nijnik A (2012) Afforestation for the provision of multiple ecosystem services: a Ukrainian case study. Int J For Res 1–12
Nijnik M, Pajot G, Moffat A, Slee B (2013) An economic analysis of the establishment of forest plantations in the UK to mitigate climate change. Forest Policy and Economics 26:34–42
Nordhaus W (1991) To slow or not to slow: the economics of the greenhouse effect. Econ J 101:920–938
Pearce D, Turner R (1990) Economics of natural resources and the environment. Hertfordshire
Price C (2005) How sustainable is discounting? Economics, sustainability and natural resources. In: Kant, Berry (eds) (1), p 6
Pussinen A, Karjalajnen T, Kellomaki S, Makipaa R (1997) Potential contribution of the forest sector to carbon sequestration in Finland. Biomass Bioenergy 6(13):377–387
Ramsey FP (1928) A mathematical theory of saving. Econ J 38:543–559
Read DJ, Freer-Smith PH, Morison JIL, Hanley N, West CC, Snowdon P (2009) Combating climate change—a role for UK forests. An assessment of the potential of UK's trees and woodlands to mitigate and adapt to climate change. The Stationery Office, Edinburgh
Richards K, Stokes C (2004) A review of forest carbon sequestration cost studies: a dozen years of research. Clim Chang 63:1–48
Samuelson P (1961) The evaluation of social income: capital formation and wealth. In: Lutz and Hague (eds) The theory of capital. New York, USA
Savills Research (2010) http://www.savills.co.uk/research/

Shvidenko A, Schepaschenko D, McCallum I, Nilsson S (2010) Can the uncertainty of full carbon accounting of forest ecosystems be made acceptable to policy makers? Clim Chang 103:137–157

Slangen L, Van Kooten G, Van Rie PF (1997) Economics of timber plantations on CO_2 emissions in the Netherlands. Tijdschr van de Landbouw 4(12):318–333

Stavins RN, Richards K (2005) The costs of US forest-based carbon sequestration. Report for the Pew Center on Global Climate Change, Arlington VA

van Kooten GC (2004) Climate change economics. Edward Elgar, Cheltenham

van Kooten GC, Bulte E (2000) The economics of nature: managing biological assets. Blackwell Publ, Oxford

van Kooten GC, Sohngen B (2007) Economics of forest carbon sinks: a review. Int Rev Environ Resour Econ 1: 237–269

van Kooten GC, Eagle AJ, Manley J, Smolak T (2004) How costly are carbon offsets? A meta-analysis of carbon forest sinks. Environ Sci Policy 7:239–251